



Michigan Technological University
Create the Future Digital Commons @ Michigan Tech

Dissertations, Master's Theses and Master's
Reports - Open

Dissertations, Master's Theses and Master's
Reports

2011

Comparative study of anchorage strengths of epoxy coated hooked bars

Paul W. Koning
Michigan Technological University

Follow this and additional works at: <https://digitalcommons.mtu.edu/etds>



Part of the [Civil and Environmental Engineering Commons](#)

Copyright 2011 Paul W. Koning

Recommended Citation

Koning, Paul W., "Comparative study of anchorage strengths of epoxy coated hooked bars ", Master's Thesis, Michigan Technological University, 2011.
<https://doi.org/10.37099/mtu.dc.etds/246>

Follow this and additional works at: <https://digitalcommons.mtu.edu/etds>



Part of the [Civil and Environmental Engineering Commons](#)

A COMPARATIVE STUDY OF ANCHORAGE STRENGTHS OF
EPOXY COATED HOOKED BARS

By

Paul W. Koning

A THESIS

Submitted in partial fulfillment of the requirements for the degree of

MASTER OF SCIENCE

CIVIL ENGINEERING

MICHIGAN TECHNOLOGICAL UNIVERSITY

2011

© 2011 Paul W. Koning

This thesis, “A Comparative Study of Anchorage Strengths of Epoxy Coated Hooked Bars,” is hereby approved in partial fulfillment of the requirements for the Degree of MASTER OF SCIENCE IN CIVIL ENGINEERING.

Department of Civil and Environmental Engineering

Signatures:

Thesis Advisor

Theresa M. Ahlborn

Committee Member

George R. Dewey

Committee Member

Nilufer Onder

Department Chair

William M. Bulleit

Date

Table of Contents

List of Figures	v
List of Tables	viii
Abstract	ix
1 Introduction	1
1.1 Use of Hooked Bars in Reinforced Concrete	1
1.2 Objectives	2
1.3 Scope	3
1.4 Organization	4
2 Previous Work	5
2.1 Bond and Confinement	5
2.1.1 Rebar	5
2.1.2 Hooked Rebar	6
2.1.3 Surface Conditions	8
2.2 History of Hooked Rebar	10
2.3 Historical Research Data Summarized	21
2.4 ACI Code 318 Historical Progression	22
2.4.1 ACI 318-77	22
2.4.2 ACI 318-89	23
2.4.3 ACI 318-95	24
2.4.4 ACI 318-99	24
2.4.5 ACI 318-02	24
2.4.6 ACI 318-05	25
3 Experimental Program	27
3.1 Concrete	27
3.1.1 Mix	27
3.1.2 Water	28
3.1.3 Air Entrainment and Cement	28
3.1.4 Coarse and Fine Aggregate	28
3.2 Reinforcement	29
3.2.1 Steel	29
3.2.2 Layout	30
3.3 Specimens	32
3.3.1 Coating	32
3.3.2 Displacement Wires	33
3.3.3 Casting	37
3.3.4 Concrete Cylinders	38
3.3.5 Loading System	39

3.3.6	Loading Procedures	40
3.3.7	Failure	42
4	Results and Discussion	43
4.1	Variables	43
4.1.1	Gage Location	43
4.1.2	Rebar Yield Stress.....	43
4.1.3	Exact Load Level / Slip measurements.....	43
4.1.4	Dial Gage Reading.....	44
4.1.5	Cross-Sectional Area of Rebar.....	45
4.1.6	Modulus of Elasticity of Steel in Rebar	45
4.1.7	Coating Thickness.....	45
4.1.8	Rebar	46
4.1.9	Concrete	47
4.1.10	Variables Summary.....	48
4.2	Tensile Strength Testing	48
4.2.1	Coating Thickness Measurements, Cracks, Spots and Thickness Limits...	50
4.2.2	Concrete Strength.....	57
4.3	Pullout Testing.....	62
4.3.1	Phase 1	62
4.3.2	Phase 2 and Phase 3	63
4.3.3	Sample Calculations.....	69
4.3.4	Effect of Tie Spacing	80
4.3.5	Effect of Coating Hooked Rebar.....	84
4.3.6	Effect of Coating Type.....	89
5	Conclusions.....	92
5.1	Review of Program	92
5.2	General Discussion	93
5.3	Discussion Regarding Objectives	94
5.4	Suggestions For Future Work	95
5.4.1	Data Gathering.....	95
5.4.2	Program Setup.....	96
6	References.....	99
Appendix A.	Aggregate Distribution.....	101
Appendix B.	Additional Rebar Information	102
Appendix C.	Data Plots	103
Appendix D.	Crack Patterns	113

List of Figures

Figure 1.1: Corner and wall face as example beam-column joints.....	1
Figure 2.1: Deformed rebar cross-section.....	5
Figure 2.2: Types of bond failure	6
Figure 2.3: General forces reacting to loaded hook.....	7
Figure 2.4: Concentration of reaction stresses in concrete	8
Figure 2.5: Angle reduction of primary reaction forces	9
Figure 2.6: Specimen design by Minor and Jirsa (1975).....	10
Figure 2.7: Specimen design by Marques and Jirsa (1975).....	12
Figure 2.8: Specimen design by Pinc et al. (1977)	14
Figure 2.9: Load frame setup by Pinc et al. (1977)	15
Figure 2.10: Specimen design by Hamad et al. (1993).....	17
Figure 2.11: Load frame setup by Hamad et al. (1993).....	18
Figure 2.12: Test setup by Hamad et al. (2006).....	20
Figure 3.1: Reinforcement arrangement for specimens.....	29
Figure 3.2: Elevation view of specimen and load frame	31
Figure 3.3: Plan view of load frame.....	32
Figure 3.4: Displacement wire attached to hook	34
Figure 3.5: Displacement wire and tube layout	35
Figure 3.6: Spring loaded clamp without and with guide sleeve.....	36
Figure 3.7: Camera position.....	37
Figure 4.1: Rib angle with respect to rebar.....	47
Figure 4.2: Rebar fracture planes.....	50
Figure 4.3: Manufacturer coating thickness data for A934 hooked rebar	53
Figure 4.4: Manufacturer coating thickness data for miscellaneous rebar	53
Figure 4.5: A775 epoxy coating thickness for hooked rebar	54
Figure 4.6: A934 epoxy coating thickness for hooked rebar	55
Figure 4.7: A934 coated rebar missing coating	56
Figure 4.8: A775 broken coating	57
Figure 4.9: Concrete compression testing for Phase 2.....	59
Figure 4.10: Concrete compression testing for Phase 3.....	60
Figure 4.11: Strength progression across sets for Phase 2.....	61
Figure 4.12: Strength progression across sets for Phase 3.....	62
Figure 4.13: 3EA77b - load progression without load drops.....	65
Figure 4.14: 3EA77f - load progression with load drops.....	66
Figure 4.15: 3EA77f - slip progression with load drops.....	67

Figure 4.16: 3EA77f - middle gages stress VS slip	68
Figure 4.17: +/- One standard deviation from mean for the top & mid gage	80
Figure 4.18: +/- One standard deviation from mean for the mid gage	81
Figure 4.19: Slip ratios for tie spacing for all stress values	83
Figure 4.20: Slip ratios for ties spacing at the 60 ksi stress level	84
Figure 4.21: Slip ratios against black bar across all stress values	85
Figure 4.22: Slip ratios against black bar for 60 ksi stress level.....	86
Figure 4.23: Bottom gage at max stress.....	88
Figure 4.24: Bottom gage at max stress plus one load increment	89
Figure 4.25: Slip ratios for coating type across all stress values	90
Figure 4.26: Slip ratios for coating type for 60 ksi stress level	90
Figure 4.27: Exact (raw) slip ratios for coating type for 60 ksi level	91
Figure A.1: Fine aggregate Distribution	101
Figure A.2: Coarse aggregate distribution	101
Figure B.1: Rib angle and spacing for all specimens.....	102
Figure C.1: Phase 2 +/- one standard deviation from mean for the top & mid gage	103
Figure C.2: Phase 2 +/- one standard deviation from the mean for the mid gage	104
Figure C.3: Phase 2 +/- one confidence interval from the mean for the top and mid gage	105
Figure C.4: Phase 2 +/- one confidence interval from the mean for the mid gage	106
Figure C.5: Phase 2 raw data for rebar slip at max rebar stress as recorded at the bot gage	107
Figure C.6: Phase 2 raw data for rebar slip at maximum rebar stress plus one load step as recorded at the bottom gage.....	108
Figure C.7: Phase 3 95% confidence interval from mean for effect of tie spacing at the top gage (7db & 3db in pairs)	109
Figure C.8: Phase 3 95% confidence interval from mean for effect of tie spacing at the mid gage (7db & 3db in pairs)	110
Figure C.9: Phase 3 95% confidence interval from mean for effect of tie spacing at the top gage (775, 934 & uncoated in sets).....	111
Figure C.10: Phase 3 95% confidence interval from mean for effect of tie spacing at the mid gage 9775, 934, & uncoated in sets).....	112
Figure D.1: Phase 2 specimen 3db_a.....	115
Figure D.2: Phase 2 specimen 3db_b.....	116
Figure D.3: Phase 2 specimen 5db_a.....	117
Figure D.4: Phase 2 specimen 5db_b.....	118
Figure D.5: Phase 2 specimen 7db_a.....	119
Figure D.6: Phase 2 specimen 7db_b.....	120

Figure D.7: Phase 2 specimen 9db.....	121
Figure D.8: Phase 3 specimen 9.....	122
Figure D.9: Phase 3 specimen 10.....	123
Figure D.10: Phase 3 specimen 11.....	124
Figure D.11: Phase 3 specimen 12.....	125
Figure D.12: Phase 3 specimen 13.....	126
Figure D.13: Phase 3 specimen 14.....	127
Figure D.14: Phase 3 specimen 15.....	128
Figure D.15: Phase 3 specimen 16.....	129
Figure D.16: Phase 3 specimen 17.....	130
Figure D.17: Phase 3 specimen 18.....	131
Figure D.18: Phase 3 specimen 19.....	132
Figure D.19: Phase 3 specimen 20.....	133
Figure D.20: Phase 3 specimen 21.....	134
Figure D.21: Phase 3 specimen 22.....	135
Figure D.22: Phase 3 specimen 23.....	136
Figure D.23: Phase 3 specimen 24.....	137
Figure D.24: Phase 3 specimen 25.....	138
Figure D.25: Phase 3 specimen 26.....	139
Figure D.26: Phase 3 specimen 27.....	140
Figure D.27: Phase 3 specimen 28.....	141
Figure D.28: Phase 3 specimen 29.....	142
Figure D.29: Phase 3 specimen 30.....	143
Figure D.30: Phase 3 specimen 31.....	144
Figure D.31: Phase 3 specimen 32.....	145
Figure D.32: Phase 3 specimen 33.....	146
Figure D.33: Phase 3 specimen 34.....	147
Figure D.34: Phase 3 specimen 35.....	148
Figure D.35: Phase 3 specimen 36.....	149
Figure D.36: Phase 3 specimen 37.....	150
Figure D.37: Phase 3 specimen 38.....	151
Figure D.38: Phase 3 specimen 39.....	152
Figure D.39: Phase 3 specimen 40.....	153
Figure D.40: Phase 3 specimen 41.....	154
Figure D.41: Phase 3 specimen 42.....	155

List of Tables

Table 2.1: Minor and Jirsa 1975 Data Summary	21
Table 2.2: Marques and Jirsa 1975 Data Summary	21
Table 2.3: Hamad et al. 1993 Data Summary	22
Table 3.1: Concrete Mix Properties	27
Table 3.2: Fine And Course Aggregate Charateristics	28
Table 3.3: Number Of Epoxy Coating Measurement Locations	33
Table 4.1: Rib Patterns.....	46
Table 4.2: Tensile Testing Data	49
Table 4.3: Coating Thickness Statistics For Rebar	51
Table 4.4: Pullout Testing Day Concrete Cylinder Compression Data	58
Table 4.5: Current Program Data Summary	64
Table 4.6: Raw Data From Specimen 3EA77e	72
Table 4.7: Data From Series 3EA77	73
Table 4.8: Summary Of Statistics Across All Series	74
Table 4.9: Statistical Analysis Output For All Series	78
Table 4.10: Full Set Of Series Ratios.....	79
Table 4.11: Reduced Set Of Series Ratios	79

ABSTRACT

Hooked reinforcing bars (rebar) are used frequently to carry the tension forces developed in beams and transferred to columns. Research into epoxy coated hooked bars has only been minimally performed and no research has been carried out incorporating the coating process found in ASTM A934. This research program compares hooked rebar that are uncoated, coated by ASTM A775, and coated by ASTM A934.

In total, forty-two full size beam-column specimens were created, instrumented and tested to failure. The program was carried out in three phases. The first phase was used to refine the test setup and procedures. Phase two explored the spacing of column ties within the joint region. Phase three explored the three coating types found above. Each specimen included two hooked rebar which were loaded and measured independently for relative rebar slip. The load and displacement of the hooked rebar were analyzed, focusing on behavior at the levels of 30 ksi, 42 ksi and 60 ksi of rebar stress. Statistical and general comparisons were made using the coating types, tie spacing, and rebar stress level. Many of the parameters composing the rebar and concrete were also tested to characterize the components and specimens.

All rebar tested met ASTM standards for tensile strength, but the newer ASTM A934 method seemed to produce slightly lower yield strengths. The A934 method also produced coating thicknesses that were very inconsistent and were higher than ASTM maximum limits in many locations. Continuity of coating surfaces was found to be less than 100% for both A775 and A934 rebar, but for different reasons. The many comparisons made did not always produce clear conclusions. The data suggests that the ACI Code (318-05) parameter of 1.2 for including epoxy coating on hooked rebar may need to be raised, possibly to 2.5, but more testing needs to be performed before such a large value change is set forth. This is particularly important as variables were identified which may have a larger influence on rebar capacity than the Development Length, of which the current 1.2 factor modifies.

Many suggestions for future work are included throughout the thesis to help guide other researchers in carrying out successful and productive programs which will further the highly understudied topic of hooked rebar.

1 Introduction

1.1 Use of Hooked Bars in Reinforced Concrete

Hooked bars are used every day on reinforced concrete projects all over the world. In many cases they are used in locations where a straight bar cannot be designed with adequate development length. The hooked bar's primary role is to provide a tensile anchorage for resistance to structural loading. Three locations exist where hooks are common used: the edge of slabs, the end of bridge piers, and in beam-column joints.

Many beam-column joints are in the building's interior where hooks are not needed, but at the outside wall of a building hooks are employed to anchor the beams to the columns. Along the face of the wall these hooks are fairly heavily confined by the combination of column ties and transverse reinforcement running in the edge beams. At the corner of the building, the hooks are confined by the column stirrups, any additional stirrups required by the designer and the standard code specified concrete cover.

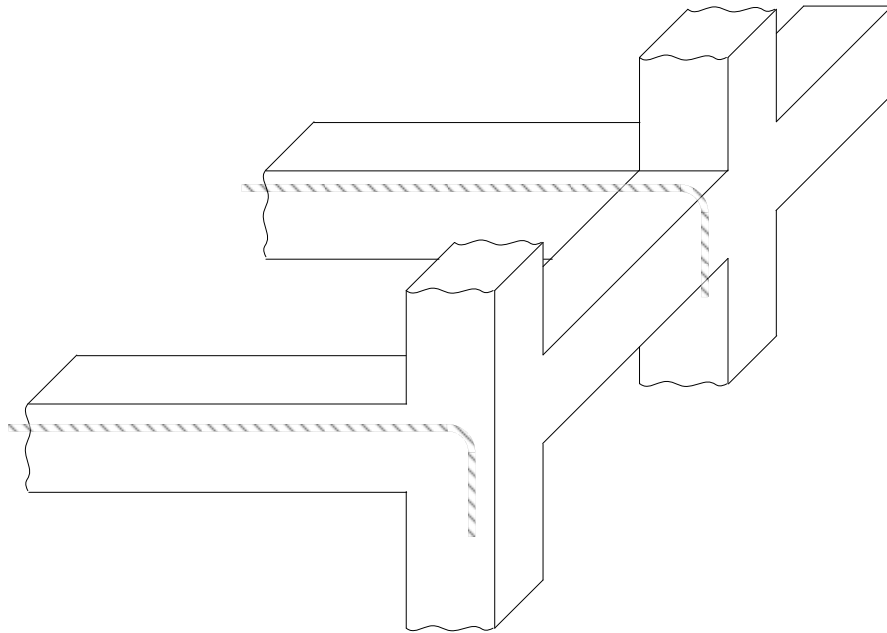


Figure 1.1: Corner and wall face as example beam-column joints.

Although hooks are used frequently and serve an important role, there has been relatively little research conducted to determine the impact of tie spacing and bar coating effects on the anchorage strength of the standard hook. In the 1970's epoxy coated bars

began to be used more widely and research programs were conducted to determine what effect the epoxy coating had on straight bar bond characteristics. In 1990, a research program by Hamad et al. further investigated straight bars with epoxy coating but also looked at the effects of the epoxy coating on hooked bar bond characteristics. Since that time, 15 plus years, only a couple of subsequent test programs have been conducted involving hooked bars with an epoxy coating, and repeat experiments to verify the results of the original research have not yet been completed. The research herein describes an experimental test program and results of hooked bar strength for variable column tie spacing and coating type.

1.2 Objectives

The idea of testing hooked bars that have been epoxy coated by ASTM A934 lead to other questions and possibilities regarding the many variables that are found in a beam column joint. To limit the size of the test program, many of the variables have been held constant (as much as practical). This includes concrete strength, size of rebar, position and orientation of rebar, radius of bend on hook, length of tail on hook, dimensions of column, and rate of loading. To keep the project realistic in terms of what actually might happen during field conditions, some procedures have been altered from laboratory research norms. Further discussion regarding variables can be found in Chapter 3 and Chapter 4.

The first objective of this research is to compare the pullout strength of hooked bars that have been epoxy coated using two different ASTM methods (A775, A934). This will make sure the old ASTM and the new one create hooked bars with reasonably similar capacity.

The second objective is to compare the epoxy coated pullout strengths to that of uncoated hooked bars (referred to as black bar).

The third objective is to determine what level of lateral confinement is necessary to cause yielding of the hooked bars before failure of the column or total loss of bond occurs.

1.3 Scope

The research was carried out in three dependent phases. This meant that the next phase could not fully begin until the testing results of the previous phase could be evaluated. In total, 42 specimens were created and tested to failure.

Phase 1: A single black bar specimen was made for the purpose of working out any bugs in the testing setup and procedures. Specifically, it was unknown whether or not the method for attaching wires to the hooks would be effective.

Phase 2: Seven more specimens were tested to investigate the influence of tie spacing in the hook region for black bar hooks. Pairs of specimens were made using joint region ties spaced at $3d_b$, $5d_b$, $7d_b$, and $9d_b$. Phase 2 answered to the third objective and resulted in using $3d_b$ and $7d_b$ as tie spaces in Phase 3. “ d_b ” is the hooked bar’s diameter.

Phase 3: Thirty-four specimens were constructed according to the Experimental Layout in Figure 1.1. The effects of the epoxy coating method on hook anchorage strength are studied here using the previously chosen tie spaces and three different coating types. This phase answered to the first and second objectives of the research project which is reflected by the increased number of specimens tested for each type of configuration.

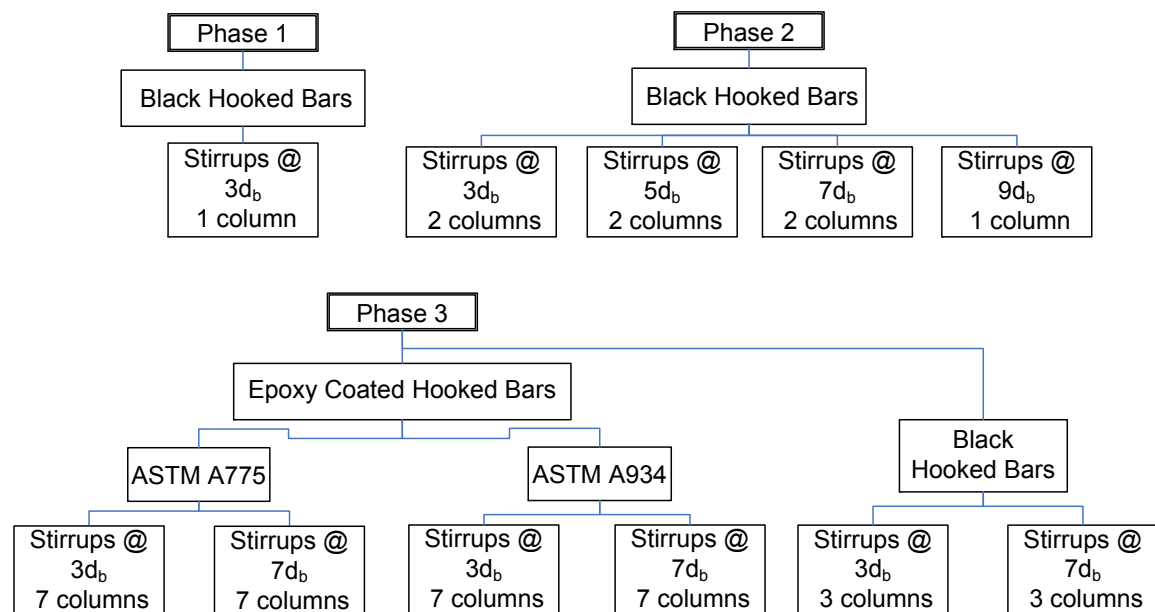


Figure 1.2: Experimental layout

1.4 Organization

Chapter 2 presents a history of related testing and what ACI has issued as design requirements. A short review of rebar/concrete interaction, commonly called “bond”, is included. Chapter 3 outlines the experimental program, including materials, equipment and procedures used. Chapter 4 presents a discussion of many of the variables involved, the results from the many different tests that were run and a related statistical comparison of the data. Chapter 5 summarizes various variable data, presents conclusions related to the project objectives and provides recommendations for future work.

2 Previous Work

2.1 Bond and Confinement

2.1.1 Rebar

Plain rebar is round with a flat and essentially smooth surface. Deformed rebar is also round, but it has both ribs and flats. The height, slope, orientation, and spacing of ribs can vary by manufacturer, but the inclusion of ribs on rebar is an industry standard. The interaction between concrete and rebar is commonly called bond.

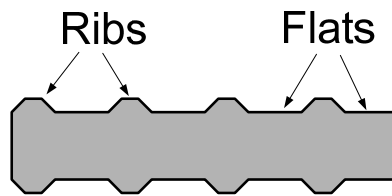


Figure 2.1: Deformed rebar cross-section

There are four different ways in which tensile load causes bond failure. Figure 2.2 shows the rebar-concrete interaction as the result of a load in the direction indicated by the solid arrow.

Type A is a plain rebar that will slip out of the surrounding concrete with minor to no damage to the surrounding concrete. Only surface friction keeps the plain rebar from slipping (ignoring the very minor chemical bond between steel and concrete).

Type B is a ribbed rebar that has been heavily confined within the concrete, but the concrete is weak relative to the steel. The result is a shear plane connecting the tops of the ribs and the rebar pulls out, taking the surrounding concrete with it.

Type C is a ribbed rebar that is well confined, but the angle of the ribs is high. The concrete directly in front of the ribs will crush first due to the high contact pressure. Next, cracks will form radiating outward as the surrounding concrete is compressed forward and the concrete's tensile strain limit is reached. Final failure potentially causes severe damage to the surrounding concrete.

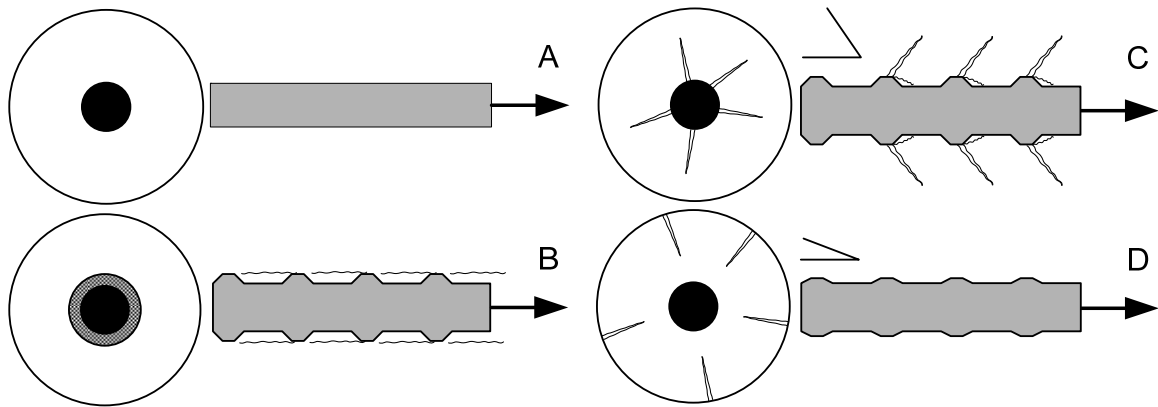


Figure 2.2: Types of bond failure

Type D is a ribbed rebar that is well confined, but the angle of the ribs is low. The concrete surrounding the rebar is more uniformly compressed, but the direction of the reaction stress is mostly perpendicular to the direction of the tensile force applied to the bar. Eventually the stress levels at the exterior concrete surface exceed the concrete tensile limit and cracks form. The rebar slips forward as the cracks widen. Cracks progress deeper more quickly as tensile capacity of the concrete is lost by deepening cracks. Final failure is most damaging to the nearest exterior concrete surface and could result in spalling.

2.1.2 Hooked Rebar

Standard hooked rebar are only used as tensile reinforcement so the reaction forces are a result of the bar being pulled on from an outside force. The hook itself is broken into three components, labeled in Figure 2.3 as Sections 1, 2, and 3. The development length of a hook, l_{dh} , is measured from the right side of Section 1, the critical face, horizontally left to the furthest extreme of Section 2.

Section 1 is the straight portion before the curve starts. This section is also referred to as the lead embedment length or the straight lead length. It acts in the same manner as any other straight rebar anchorage. The ribs create a mechanical interaction with the surrounding concrete as well as a friction component. The flats only create a surface friction interaction.

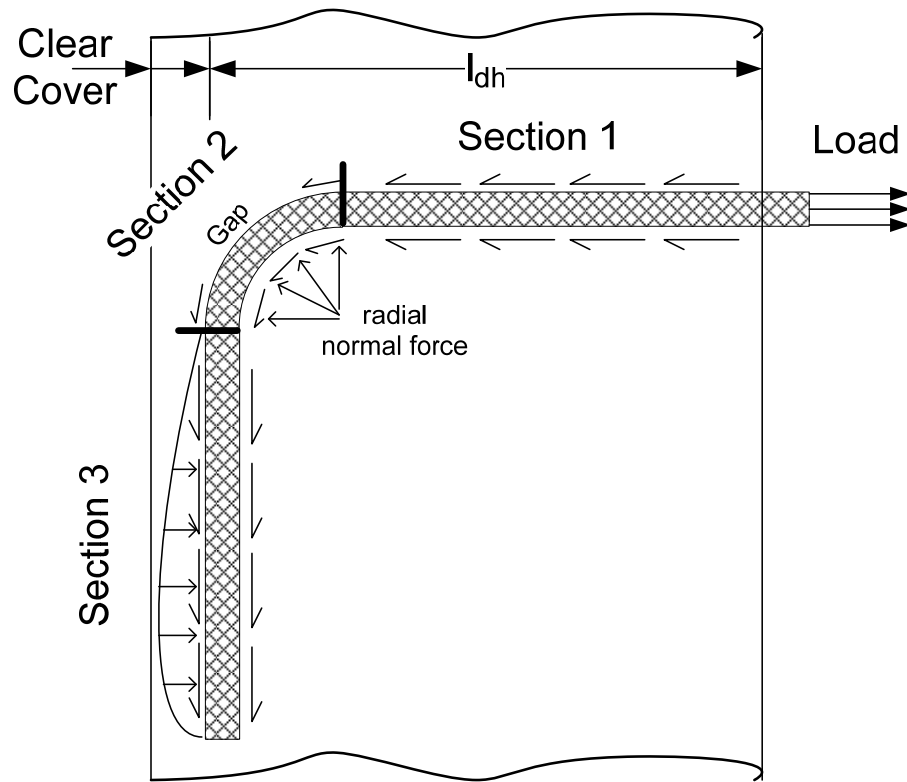


Figure 2.3: General forces reacting to loaded hook

Section 2 is the curved portion of the hook. The tensile load on the bar causes direct compression forces in the concrete on the inside of the curve. The ribs have a direct interlock and friction component with the concrete. The flats have surface friction, but there is a normal pressure created by the curve which increases the value of the friction component. It has been reported by Marques and Jirsa (1975) and Hamad et al. (1993, 2006) that side concrete cover spalling occurs most heavily in this region. The reason is not due to the increased level of reaction load per unit length along the bar, but is caused by the path that the load is directed. The curve causes overlapping regions of reaction loads which highly increases the stress burden on the concrete. An illustration of these overlapping regions is offered in Figure 2.4. The shaded boxes represent the angle at which reaction stresses are distributed away from the rebar. Notice the stress regions heavily overlap on the inside of the curve, concentrating the reaction stresses near the middle of the curve and spreading them out again closer to Sections 1 and 3. The result is higher occurrences of spalling if inadequate side confinement is provided by steel and/or

concrete. The outside surface of the curve acts similar to Section 1 under low load levels, primarily before bar slip begins. Soon after the bar slips the bar pulls away from the outside concrete surface. A gap forms and negligible rebar-concrete interaction is present.

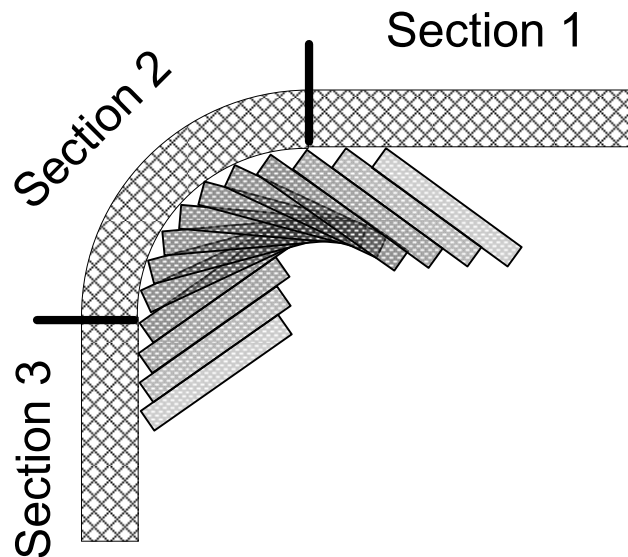


Figure 2.4: Concentration of reaction stresses in concrete

Section 3 is the tail of the hook. It primarily acts the same as Section 1, but has an additional component caused by the curve. As the bar slips, even a little, the curve wants to straighten out. This includes the end of the curve near Section 3. The result is a normal force generated by the tail pushing on the concrete cover. This doesn't result in a gap on the inside of Section 3, but it has been reported by Hamad et al. (1993) to produce enough stress to cause horizontal cracking in the concrete cover. Higher levels of confinement can eliminate these cracks. The normal force acting on the flats in Section 3 is not sufficient per unit length to significantly increase the friction component of the bond between rebar and concrete.

2.1.3 Surface Conditions

Uncoated rebar, or black bar, is relatively rough and often has some amount of oxidation (rust) by the time it has been sealed within concrete. The placement of concrete around rebar could even produce some rust due to the presence of both water and a small amount of entrained air. When the concrete cures, there can be a combination of chemical

adhesion and frictional interlock between the two surfaces. Evidence of this interlock has been found when spalling cover is removed to find some patches of concrete and concrete residue still adhered to the rebar surface. Ultimately, the friction component of bond is not normally significantly large and is often ignored.

Coated rebar, epoxy coated in the current study, is very smooth. The rebar is cleaned very thoroughly to remove all rust before it is coated and the finished coating becomes glassy smooth on the surface after it has hardened. When spalling cover is removed from over coated rebar, the epoxy surface is barren of adhered concrete. This indicates that even on a chemical level, there is no concrete adhesion visible to the naked eye. The frictional component on the flats of rebar is nearly zero without additional normal forces. Even with normal forces the coating can slip on the underlying surface of the bar. Sliding on the coating would effectively make the epoxy act as a lubrication layer between the rebar and concrete.

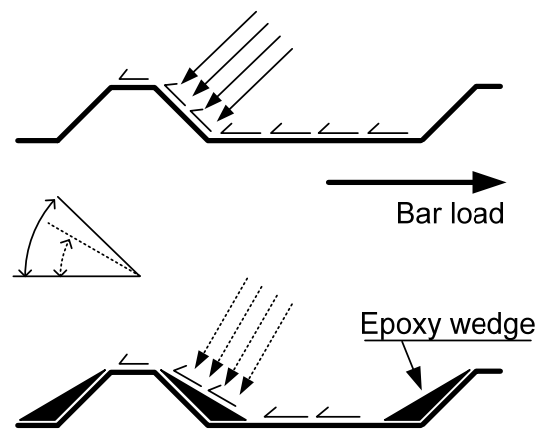


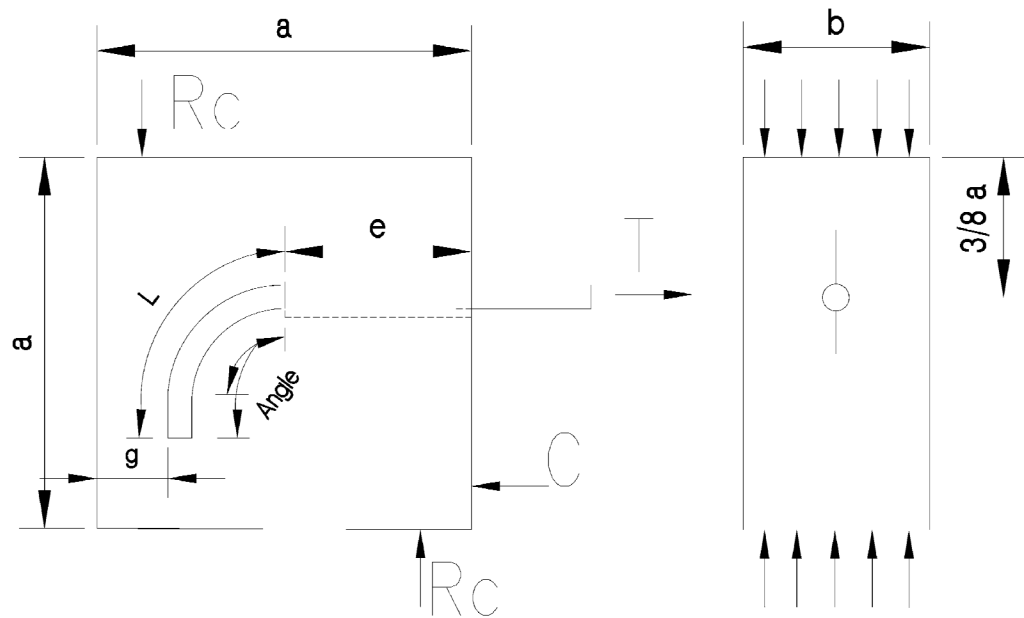
Figure 2.5: Angle reduction of primary reaction forces

On the ribs, the epoxy coating reduces the small friction component, but there is a physical barrier present also. The epoxy is often thicker near the base of the rib than the top. This makes the rib angle smaller relative to the direction of bar slip (Figure 2.5) and so reduces the intensity of mechanical interlock normally present. The reduced hooked rebar tensile capacity as a result of epoxy coating was the focus of Hamad et al.'s (1993) work using rebar coated by ASTM A775. However, the effect of the newer ASTM A934

method for applying epoxy coating to rebar has not previously been studied for standard hooked rebar.

2.2 History of Hooked Rebar

Minor and Jirsa (1975) studied the general variables involved with determining the anchorage capacity of a hooked bar. Eighty pullout tests were conducted using 37 different specimen configurations. Hooked rebar sized No.5, No.7 and No.9 were tested. Other variables examined were the bond length before curve, the radius of the bend, and the angle of the bend in the curve. Each specimen was set up according to Figure 2.6. The length of rebar denoted as “e” in the figure was debonded using a plastic sleeve to help create results based on pullout failures rather than rebar yielding failures.



Bar Size	Dimensions (inches)					
	a	b	e	g(min)	L	Angle
No. 5	12	8	6	2-7/8	Var	Var
No. 7	16	8	8	4-1/8	Var	Var
No. 9	16	12	7-1/2	2-7/8	Var	Var

Figure 2.6: Specimen design by Minor and Jirsa (1975)

The criteria of load verses slip was used to compare results so the specimens were instrumented with slip wires. This was accomplished by drilling a small hole at a location

of interest on the back side (left for Figure 2.6) of the rebar. A 0.059 inch diameter music wire was then inserted into the hole. A small diameter plastic tube was slipped over the remaining wire to protect it and allow it to later slide through the hardened concrete. As the rebar slipped through the concrete, so would the wire. A dial gage resting on the end of the wire and attached to the face of the specimen would display the movement of the embedded wire.

The test procedure for most specimens called for applying the load then resting for 1 minute before applying more load. At every 4th load interval the load was held for 5 minutes to allow the slip wire to stabilize. Generally, 30 to 40 load increments were conducted before the test finished.

Each test was terminated if one or more of three failure conditions occurred; a bar stress of 60 ksi was reached, the bar pulled out of the concrete block, or the concrete block fractured.

Analysis of data from testing by Minor and Jirsa (1975) was used to form several conclusions.

1. For equal bond length to bar diameter ratios, if the bend angle was greater, then the slip would be greater for any given bar stress. For the same bond length to bar diameter ratio, when a smaller ratio of radius of bend to bar diameter existed then there would also be greater slip for a given bar stress.
2. In a hooked bar connection, if there are both straight and curved sections in the joint, then most of the slip is found in the curved section of the rebar.
3. There was not a large difference in strength between straight bar and hooked bar connections when considering practical construction applications.

Additionally, it was suggested that 90 degree hooks are preferred compared to 180 degree hooks and that the radius of the bend should be as large as possible to reduce slip.

Marques and Jirsa (1975) tested full scale beam-column joints to investigate the effects of variables for joint confinement. Tie spacing and cover requirements were of main concern, but the size of the hooked rebar, the hook geometry, lead embedment

length, and column axial load were also varied. Many different specimen configurations resulted from the numerous variables. Figure 2.7 shows the placement of reinforcement and the column sizes used. The rebar was not debonded at the free face (right side for Figure 2.7) as Minor and Jirsa (1975) had done.

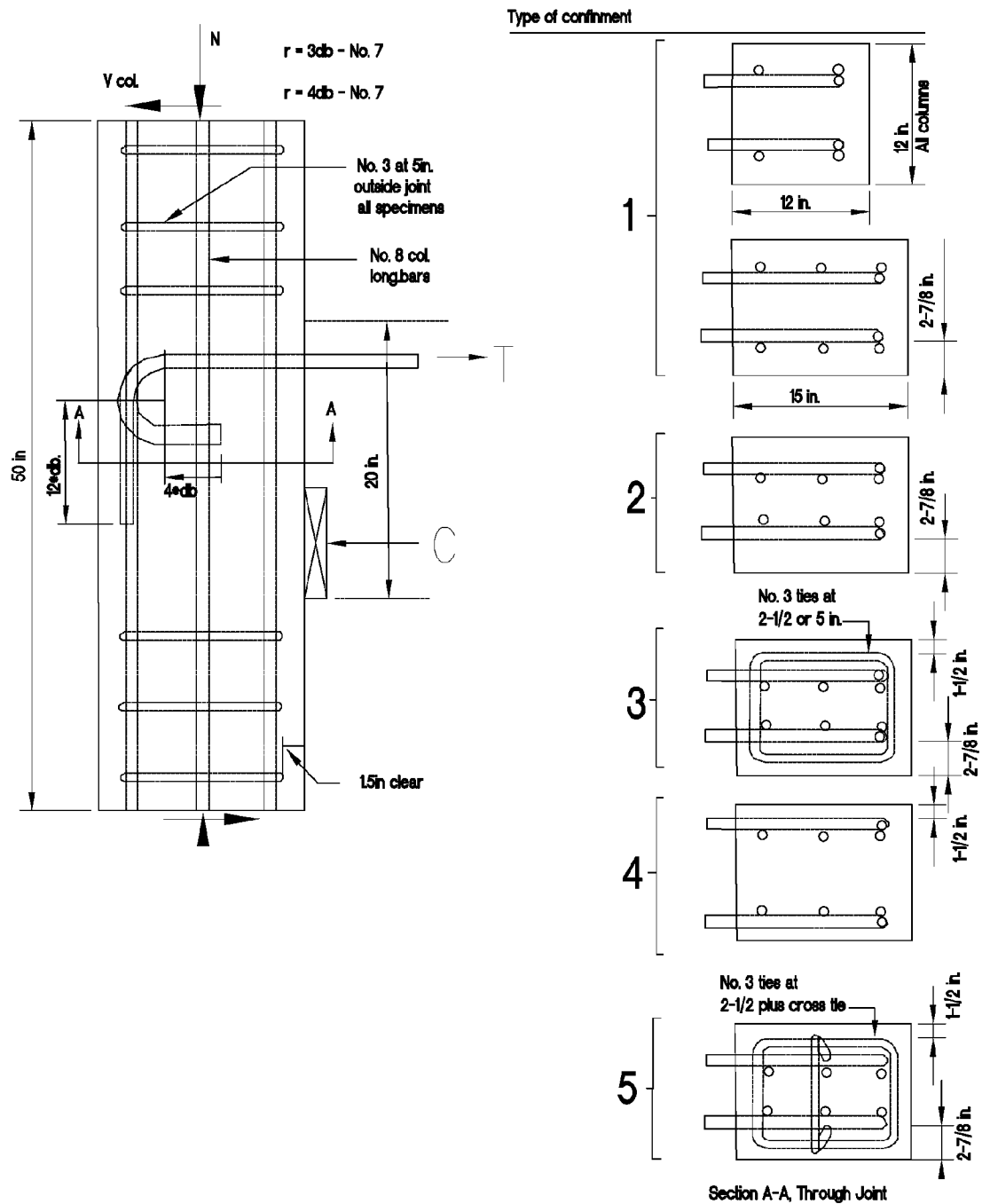


Figure 2.7: Specimen design by Marques and Jirsa (1975)

The slip measurement method developed previously by Minor and Jirsa (1975) was applied by Marques and Jirsa (1975). The dial gage readings were measured to the nearest 0.001 inch. Loading proceeded in rebar stress increments of roughly 2000 psi with 2 minute rest periods between loads. Each test was terminated when one of the two rebar either pulled out of the column or stopped holding load.

It was reported that “failure was fairly sudden and resulted in the entire side face of the column spalling.” The region of heaviest spalling was near the inside radius of the curved portion of the hook forward to the free face. The back side of the column usually did not have the same level of damage as the sides and free face.

Marques and Jirsa (1975) concluded that:

1. 90 and 180 degree hooks were not significantly different in anchorage capacity.
2. Ties were most effective if placed in the joint region spaced at equal to or less than the hook radius and recommended a center to center tie spacing of $3*d_b$, where d_b is the nominal diameter of the hooked rebar.
3. Anchorage strength was higher with higher levels of confinement. Both tie spacing and cover thickness affect the degree of confinement.
4. A minimum lead embedment length before the curve of the hook is necessary to achieve higher anchorage strengths.

Pinc et al. (1977) conducted 16 tests on beam-column joints to investigate the effect of lead embedment length and lightweight concrete on the anchorage capacity of hooked rebar. The test specimens and reaction frame were modeled after the work done by Marques and Jirsa (1975) so that a direct comparison of data could be used.

Specimens varied in cross-section from 12x12 to 12x24 inches and were all 50 inches tall. Progressively deeper sections were used to change the development length. The hooks were No.9 and No.11 bars for all testing except the series that used lightweight concrete; there, No.7 bars were used. Similar to Marques and Jirsa (1975), a specific axial load was applied to each test specimen.

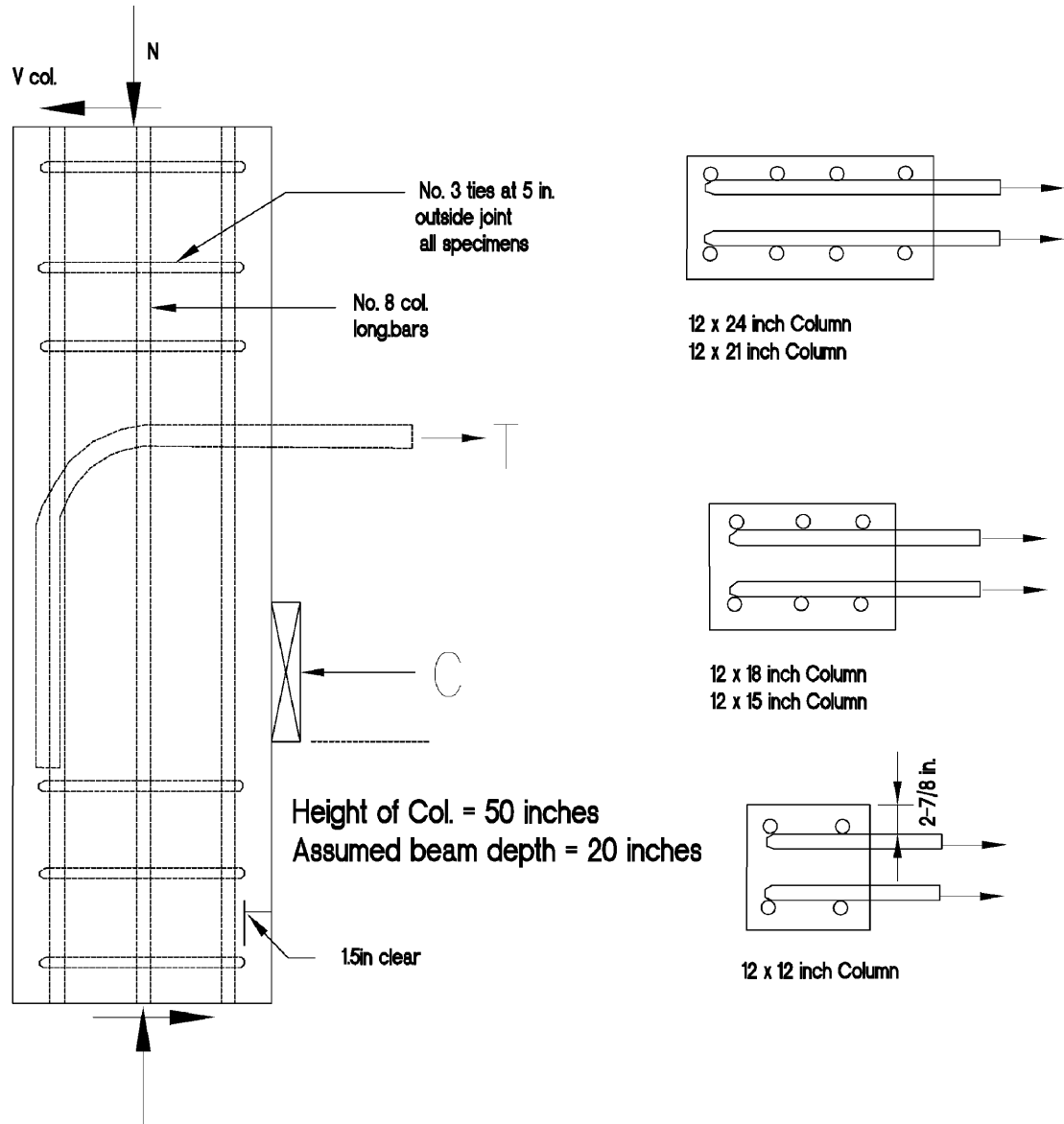


Figure 2.8: Specimen design by Pinc et al. (1977)

It is noted that no column ties are present in the hook region in Figure 2.8. There is an unidentified object in Figure 2.9. It appears to be a hydraulic cylinder between the top of the concrete column and the steel frame. It is unknown whether it was used as a method of measuring pressure while holding the top of the column in place or if it was intended to set a controlled distance to which the top of the column could rotate.

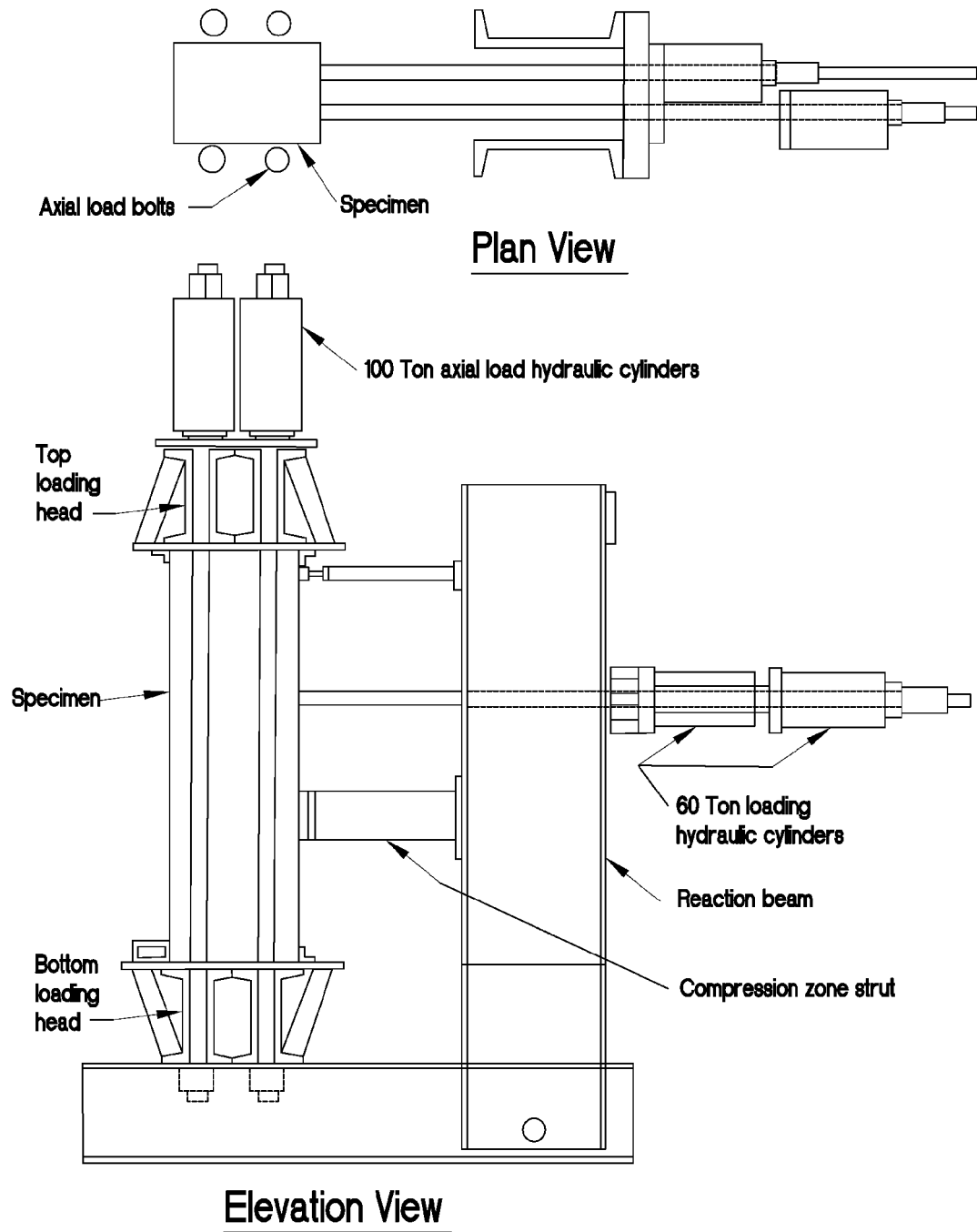


Figure 2.9: Load frame setup by Pinc et al. (1977)

The hooks were instrumented using the same method as Marques and Jirsa (1975) for both bar slip and strain. Loading proceeded in rebar stress increments of 2000 psi with 2 minute rest periods between loads. The test was stopped when either the specimen

failed or the hooked bars yielded. Additionally, after each test reached its failure condition, load was added until the maximum stroke of the hydraulic rams was reached, which was about 3 inches.

The report provides a failure hypothesis which says that the strength of a hooked bar anchorage is governed by the level of confinement that is present and not by the pullout strength as would be the case for a straight bar anchorage. Confinement is defined as concrete cover by Pinc et al. (1977). Using data from both this test and previous tests, it was deemed that the length of embedment and level of confinement were the primary factors for determining the strength of the hooked rebar anchorage. Measurements of stress during testing indicated that at the level of load necessary to fracture the concrete there was little stress being transferred from the lead embedment length to the surrounding concrete.

Hamad et al. (1993) studied several variables that affect the anchorage capacity of epoxy coated hooked bars when used in beam-column joints. The effect of epoxy coating on hooks was previously untested and at the time the most current ACI Code (318-89) did not address the issue. The study was setup as a direct comparison between uncoated (black) hooked bars and epoxy coated (by ASTM A775) hooked bars. The other elements of the study were the affects of rebar diameter, concrete compressive strength, concrete cover thickness, tie spacing in the joint region, and the hooked rebar's geometry.

The specimens were 48 inches tall and 12 inches wide but varied between 12 inches deep for No.7 bars and 15 inches deep for the No.11 bars. Column longitudinal reinforcement for the No.7 bars was four No.8 bars located in the corners just inside the column ties. The hooked rebar were located on the inside of the longitudinal bars. Two hooks were used in each column; one hook was uncoated and the other was epoxy coated. Figure 2.10 is an example of what Hamad et al.'s (1993) specimen looked like for the No.7 bar tests. The development length (l_{dh}) used was purposely chosen to be shorter than the ACI 318 Building Code specified so that a bond failure would be more likely to occur than rebar rupture.

Bar slip was measured using the same technique that Minor and Jirsa (1975) had developed. The test setup shown in Figure 2.11 was designed to have the column act as a cantilevered beam to simulate the reaction forces at a beam-column joint. After the first series of tests, the setup was adjusted by the addition of a bearing plate between the top of the concrete column and the steel frame. The plate was added to restrict excessive column rotation which resulted from the high moment loads. Additionally, anchorage plates were welded to the longitudinal reinforcement at the base of the column to resist the applied load.

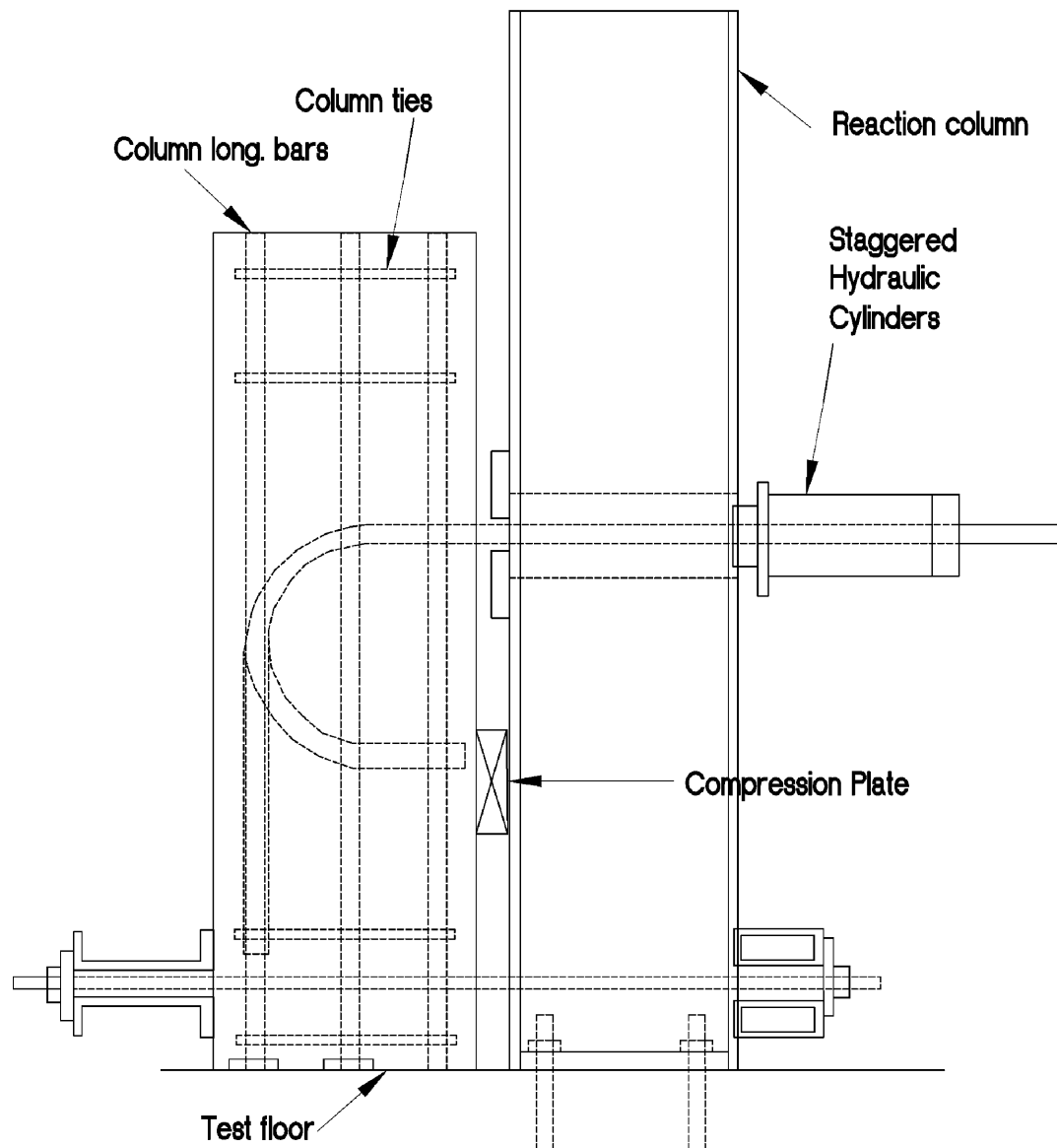


Figure 2.11: Load frame setup by Hamad et al. (1993)

Loads were applied in tension to the No.7 hooked bars in increments of 1 kip to 2 kips. There is no mention of how long load levels were held between load stages so the rate of increasing stress and stress dispersal time are unknown. The loading time could be important when trying to compare data created from separate research programs. The test was stopped when either bond failure or rebar yielding occurred.

For most of the specimens, failure was sudden and resulted in a large loss of load. No large area spalling is reported as was the case for Marques et al. (1975), but a series of crack patterns were present on the column surface stemming from several locations. One crack pattern of interest was found near the tail of the 90 degree hooks on the back of the column (left side for Figure 2.11) and extended horizontally at high levels of loading. It was suggested that at high loads the curve of the hook was trying to straighten out as the bar slipped through the concrete. This straightening pushed the tail outwards against the back wall of the column, splitting the concrete cover.

After removing the concrete cover on several specimens it was found that on uncoated rebar there were patches of adhered concrete, mostly in front of ribs, while the epoxy coated bars were free of any concrete residue.

The bond ratio, of coated over uncoated, across the test series ranged from a low of 0.76 to a high of 0.94 and the average was 0.837. This average is roughly equal to 1/1.20 or a 20 percent decrease in bond for epoxy coated hooked rebar.

Hamad et al. (1993) concluded that:

1. More ties (more confinement) in the joint region produced higher anchorage loads before failure and allowed for larger slip values at high loads.
2. 90 degree hooks produced higher anchorage loads and less slip than 180 degree hooks.
3. Epoxy coated hooks consistently had lower anchorage loads and higher slip values than uncoated hooks.
4. The relative anchorage and slip values between uncoated and epoxy coated bars were not dependent on any of the other variables being tested.

5. A 20 percent increase in the development length of the epoxy coated hooks should be incorporated into future designs.

The State-of-art report by the **International Federation for Structural Concrete (2000)** regarding “Bond of reinforcement in concrete” cites Hamad et al.’s (1993) research on the influence of epoxy coating on hooked rebar.

Hamad et al. (2006) performed a series of tests to investigate the performance of bonded-in reinforcement compared to cast-in reinforcement. The loading scenario was a cantilevered beam anchored into a wall with the load applied on the end of the cantilever. A few of the specimens used uncoated standard hooked bars of 12mm and 14mm for the tensile anchorage. Figure 2.12 shows an example of how the test was set up. For simplicity, most of the reinforcement details have been left out.

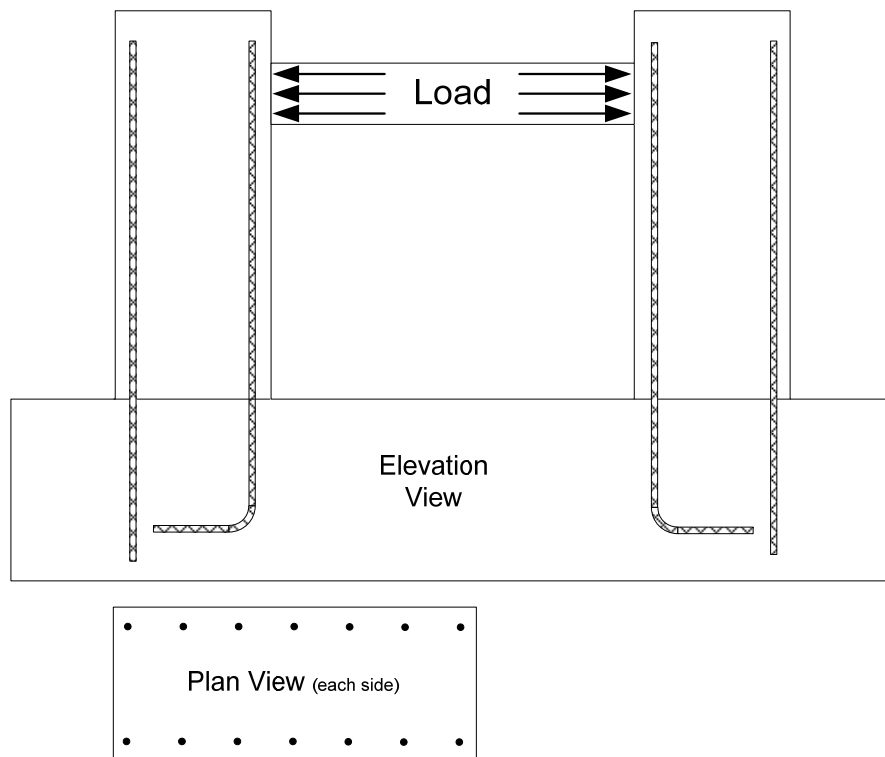


Figure 2.12: Test setup by Hamad et al. (2006)

The side concrete cover on the hooks should show the effects of being anchored in mass concrete because the tensile anchorages are embedded into the wall element. This

would be similar to a beam column joint on the interior of a building where the side concrete cover would be much greater than minimum code requirements. The tensile anchorage for the beam element in these tests consisted of a row of several hooked bars. The row of hooks creates a plain of parallel stresses which effectively undo the beneficial aspect of being anchored into mass concrete. At the edge of the specimens with hooked anchorages there was spalling near the hook's tail and at the curve.

2.3 Historical Research Data Summarized

Data was pulled from reports, theses and journal articles created by past research programs. These data are summarized below. Caution should be applied when making comparisons between the summarized programs as each of the many variables can cause adjustments to results. For this same reason, these data sets will not be compared here to the data from the current program. The specimens used by Pinc et al. (1997) and Hamad et al. (2006) were deemed too different from the current program to make meaningful comparisons of the data.

Table 2.1:
Minor And Jirsa 1975 Data Summary

	f _c (ksi)		Failure Type		Rebar Stress at Failure (ksi)		Slip at 60 ksi Lead Stress (inches)		Stress at 0.01 inch Lead Slip (ksi)	
	A	B	A	B	A	B	A	B	A	B
7-8.5-90-2.0	3.8	4.7	T	F	63	68	0.037	0.032	30	23
7-6.4-90-3.0	3.5	4.4	P	F	61	68	0.078	0.047	17	19
7-6.4-90-2.0	5.5	6.4	F	F	67	61	0.037	0.041	21	20
7-4.3-90-2.0	5.0	6.2	F	F	57	66	--	0.033	34	30

Notation: (1) bar size, (2) bond length, (3) bend angle, (4) bend radius.

F-fracture of concrete, P-bar pullout, T-terminated at high stress or large slip

Table 2.2:
Marques And Jirsa 1975 Data Summary

	f _c (ksi)		Axial Column Load (kips)	Tie Spacing Through Joint (inches)	Lead Embedment (inches)	Stress (ksi) at Lead Slip of			Stress at failure (ksi)	Approx. Slip at Failure (inches)
	Top batch	Bot batch				0.005	0.016	0.05		
J7-90-15-3-H	4.5	4.8	555	5	9.5	37	65	80	104	0.21
J7-90-15-3a-H	3.9	3.6	535	2.5	9.5	37	63	80	98	0.22

Table 2.3:
Hamad et al. 1993 Data Summary

	f'_c (ksi)	Tie Spacing Through Joint	f_{su} (ksi)	Lead Embedment (inches)	Lead Slip (inches)
7-90-U*	5.4	--	61.2	4.375	--
7-90-C*	5.4	--	47.2	4.375	--
7-90-U-T4	3.7	No.3 @ 4in.	Yielded bar	4.375	0.075
7-90-C-T4	3.7	No.3 @ 4in.	Yielded bar	4.375	0.090
7-90-U	2.57	--	43.33	4.375	0.024
7-90-C	2.57	--	35.0	4.375	0.050

* slip measurements were unreliable

2.4 ACI Code 318 Historical Progression

Using the ACI 318 Building Code, there are two places where provisions are found directly describing design requirements for standard hooks. Chapter 7 – Details of Reinforcement specifies the required shape of the hooks and Chapter 12 – Development and Splices of Reinforcement specifies how much tensile load can be applied to the hooks. The following sections highlight the progression of changes to Chapter 7 and Chapter 12 that are relevant to the current study. It is not intended to be a comprehensive review of all ACI Code changes and additions.

For all years of the ACI Code presented below the following variables are unchanged:

d_b = Diameter of hooked rebar, in.

f_y = Yield stress of rebar, psi

f'_c = Concrete compressive strength, psi

l_{hb} = Basic Development Length, in.

l_{dh} = Development Length, in.

2.4.1 ACI 318-77

7.1(b) One option for a standard hook is to have “a 90 degree bend plus an extension of at least $12*d_b$ at free end of bar...”

Table 7.2 of ACI 318-77 specifies that the minimum diameter of bend for a No.7 rebar is $6*d_b$.

12.2.5 No development length shall be less than 12 inches.

12.5.1 “Standard hooks shall be considered to develop a tensile stress in bar reinforcement of f_h .”

$$f_h = \xi * \sqrt{f'_c}$$

Where ξ is not greater than the values in Table 12.5.1 of ACI 318-77, for Top bars of No. 7 size $\xi = 360$.

A footnote states “Values of ξ may be increased 30 percent where enclosure is provided perpendicular to plane of hook. Enclosure may consist of external concrete or internal closed ties, spirals, or stirrups.” The footnote does not suggest how much cover or how many ties would be necessary to make a 30 percent increase in strength legitimate.

12.5.2 The designer may use Section 12.2.2 for computing an embedment length equivalent to that of a straight bar.

2.4.2 ACI 318-89

7.1.2 Unchanged from 1977 ACI Code Section 7.1(b)

12.5 The Development Length (l_{dh}) is the Basic Development Length (l_{hb}) multiplied by the applicable adjustment factors.

$$l_{hd} = \frac{1200 * d_b}{\sqrt{f'_c}}$$

12.5.1 No development length (l_{dh}) shall be less than $8*d_b$ nor less than 6 inches.

According to the commentary for Section 12.5, the ACI Code (318-83) was heavily revised in regards to hooks. One of the key changes was to include a (0.8)

modifier in Section 12.5.3.3 regarding the inclusion and spacing of ties or stirrups in the hook region. The reasons given in the commentary for this change reflect the insights and conclusions found in the research done by Pinc et al. (1977). The specified tie spacing across the region is $3*d_b$ for the equation modifier to be used.

2.4.3 ACI 318-95

7.1.2 Unchanged from 1977 ACI Code Section 7.1(b)

12.5 A new provision, Section 12.5.3.6, is added to the modification factors of the basic development length formula. The provision gives a (1.2) modifier if epoxy coated reinforcement is used.

2.4.4 ACI 318-99

7.1.2 Unchanged from 1977 ACI Code Section 7.1(b)

12.5 Unchanged from 1995 ACI Code Section 12.5

2.4.5 ACI 318-02

7.1.2 Unchanged from 1977 ACI Code Section 7.1(b), but 7.1.4 is added to address seismic design.

12.5 Revised following notation changes in the ACI Code. The new formula for the development length is

$$l_{dh} = \left(\frac{0.02 * \beta * \lambda * f_y}{\sqrt{f'_c}} \right) * d_b$$

Where : β = modifier for epoxy coated reinforcement, 1.2

λ = modifier for lightweight aggregate concrete, 1.3

12.5.3 (b) Expanded to allow ties and stirrups to be placed either perpendicular or parallel to the hooked bar being developed. To use the 0.8 modifier a tie spacing of $3*d_b$ is still required, but the first ties must be spaced no further than $2*d_b$ from the top of the hook to the center of tie.

Details in the Section 12.5 Commentary have been added to help illustrate proper tie design around a standard hook when the tie modifier (0.8) is used.

2.4.6 ACI 318-05

7.1.2 Unchanged from 1977 ACI Code Section 7.1(b)

12.5 Revised to reflect notation changes in the ACI Code, but the formula for the development length has not effectively changed. The new formula is

$$l_{dh} = \left(\frac{0.02 * \psi_e * \lambda * f_y}{\sqrt{f'_c}} \right) * d_b$$

Where : ψ_e = modifier for epoxy coated reinforcement, 1.2

λ = modifier for lightweight aggregate concrete, 1.3

It is interesting to note that if a designer does not wish to use the allowable modification factors then there is no requirement to provide sufficient concrete cover or ties of any particular spacing in the hook region. Minimum concrete cover requirements provided in the Code do apply, but have been shown by previous research to not be adequate to resist spalling at the location just inside the curve of the hook for cases of high loads. Ties may be present in the hook region as required for minimum tie and stirrup spacing for columns and beams, but this does not guarantee sufficient concrete reinforcement to confine the standard hooked rebar.

Across all presented versions of the ACI 318 Building Code, standard hooks have never been allowed to be considered effective for developing reinforcement in

compression. There are many circumstances where this provision seems obvious, but this author has been unable to find research to back up the 'no compression' theory.

3 Experimental Program

3.1 Concrete

3.1.1 Mix

The experimental program was carried out at Michigan Technological University's Benedict Laboratory, in Houghton, Michigan, United States of America.

The concrete is a standard Michigan Department of Transportation (MDOT) mixture supplied by ready-mix truck from a local supplier. The mix is designated as MDOT Grade D and is labeled as a 4500 psi, 28 day compressive strength. More information about the mix design can be found in Table 3.1.

The concrete mix design was chosen on the basis that at a design strength of 4500 psi it would be a fair representation of what any randomly selected ready-mix supplier could provide. There are suppliers in the United States that can regularly produce 10,000 psi concrete, but there are also places where achieving 3000 psi without the aid of admixtures can be a struggle. Additionally, because the ready-mix supplier already had a mix designed for this strength, there was no need to create and verify strength on a new mix design.

Table 3.1:
Concrete Mix Properties

	Phase 2	Phase 3	
Load Size	2.0	6.5	cubic yards
Coarse Agg. - 6A	3780	12040	lbs
Moisture Content	0.3	1.0	%
Fine Agg. - 2NS	2240	7500	lbs
Moisture Content	3.5	5.0	%
Cement - Type 1	1320	4285	lbs
Water	50	127	gal
Air Entrainment	16	44	oz
Air Content	8.0	6.5	%
Slump	5.0	4.5	inches
Temperature	71	70	degrees F

3.1.2 Water

The water and aggregate come from local sources while the cement and air entrainer are commercially available ingredients. No additional water was added to the concrete once it reached the casting site.

3.1.3 Air Entrainment and Cement

The incorporation of air entrainer into the concrete mix design was not intentional, but is also not seen as detrimental. The entrained air for the Phase 3 batch was measured at 6.5% using the pressure method, ASTM C231. The air entrainer was MB-AE 90 produced by Master Builders Inc., which is now a division of BASF. The cement was a basic Type 1 with no known Fly Ash or Silica Fume additives.

3.1.4 Coarse and Fine Aggregate

All the aggregate comes from a glacially deposited mixture of sand and gravel that is separated into specific gradations at the quarry, but is not separated by mineral content or shape. This primarily effects the coarse aggregate which contains a random selection of rounded and split stones and originally comes from sources both local and, possibly, hundreds of miles away. The sand has a similar random mineral content. Several tests were run on a sample of the aggregate to better characterize it. ASTM C128 and C136 methods were followed for each test in Table 3.2.

Table 3.2:
Fine And Coarse Aggregate Characteristics

		Fine Agg. - 2NS Sand	Coarse Agg. - 6A Stone
Fineness Modulus		2.60	5.75
Loss by Wash of Mass(%)		1.39	0.71
Bulk Specific Gravity			
	Oven Dry	2.62	2.68
	Sat. Surf. Dry	2.66	2.73
Apparent Specific Gravity		n.a.	2.83
Percent Absorption		1.39	1.81
Angularity of Fine Agg.(%)		36.4	n.a.
Angularity of Coarse Agg. --		% Agg. 2 or more crushed faces	57.7
		-- % Agg. 1 or more crushed faces	64.6
		-- % rounded Agg.	35.4

3.2 Reinforcement

3.2.1 Steel

The steel reinforcement was Grade 60 rebar. No modifications were made to the surface texture or epoxy coating beyond what was necessary to attach the displacement wires. The uncoated rebar used in Phase 2 was rust free while in Phase 3 it was thoroughly surface rusted, but not enough to have an effect on strength. The epoxy coated rebar was coated with epoxy meeting either ASTM A775 or ASTM A934 as was necessary for each test group. All rebar was bent and coated by the manufacturer and incorporated into the current program as delivered.

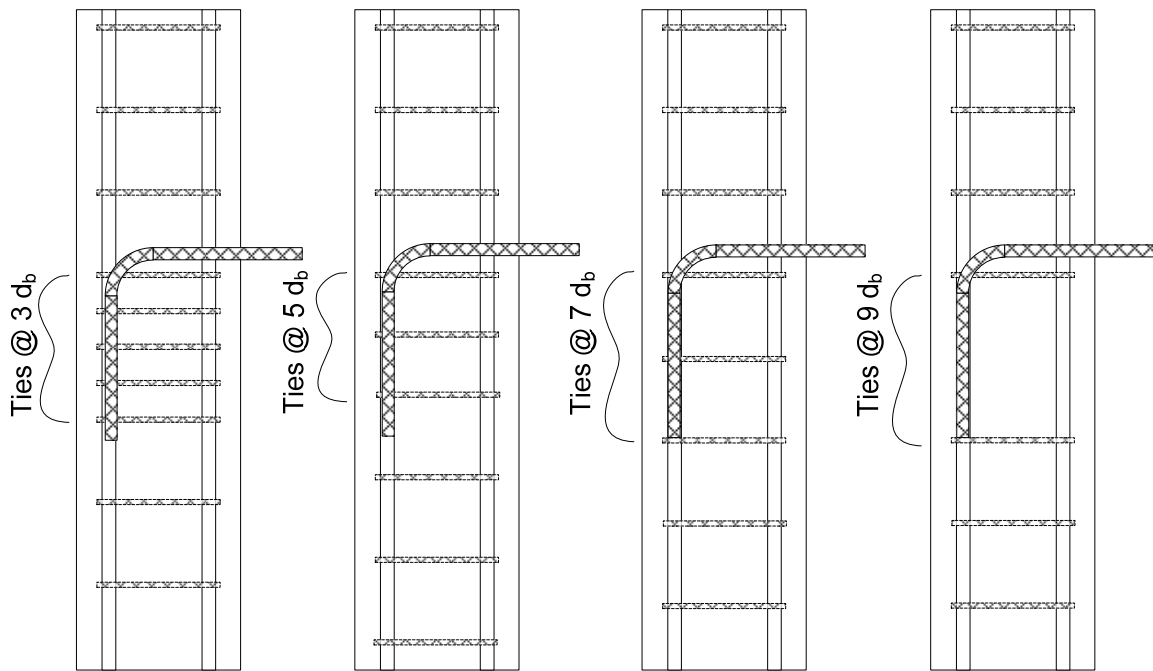


Figure 3.1: Reinforcement arrangement for specimens

The ties placed in the hook region were coated in the same manner as the hooks in that specimen. This includes at least a single tie above the hooked bar and at least one tie past the tail of the hook, see Figure 3.13.1. Efforts were made to only use non-matching ties at the last tie location either at the top or bottom of the specimen. When non-matching ties were used, epoxy coated ties were used to fill in tie spaces on epoxy coated specimens before using uncoated ties. The effect on the hooks from non-matching ties is

minimal as ties outside the hook region are only confining the column longitudinal bars. Tie spacing outside the hook region was set at 6 inches which is the ACI Code (318-05) maximum using half the least dimension of the column, 12 inches. A closer tie spacing was not deemed necessary without an axial load being placed on the column. The location of the closing corner of the ties was alternated between the two back corners of each column. This was done to reduce any possible zippering effect that may be induced from having all the closing corners located down one corner of the column.

The decision to use the size and arrangement of longitudinal bars was not based on designing the column for flexure or compression. Instead, the four No.8 bars were chosen to keep the column reinforcement as similar to previous tests as possible for comparison purposes. The same was true for choosing to use the No.3 ties and the No.7 hooks.

Attempts were made to obtain all rebar for the same test group from the same heat of mill steel. After reviewing the paperwork that accompanied the rebar as it was delivered, it became apparent that not all of the rebar came from the same heat. For this reason, random samples of straight No.7 rebar were tensile tested using a Tinius Olsen 120 kip screw drive machine. ASTM A370 and A615 were followed to test 10 lengths of rebar. The same wedges and rebar chucks used for the pullout testing were used for the tensile testing. Load was applied in displacement control with most tests lasting between 6 and 10 minutes.

3.2.2 Layout

Each specimen is 14 inches wide, 12 inches deep and 48 inches tall, and is made up of 4 longitudinal No.8 bars, 2 hooked No.7 bars, and a specific quantity of No.3 ties. Every connection between longitudinal bar and tie was joined together with a single loop of rebar tie wire. The wire was twisted together at the ends and turned tight by hand. Excess wire was clipped off so that only about $\frac{1}{2}$ to $\frac{3}{4}$ inch of twist was leftover. This helped to reduce the occurrence of cuts and scrapes to those handling the completed rebar cages. The longitudinal bars were located inside the closed loop of the No.3 ties. The hooks were located inside and next to the longitudinal bars. Figure 3.2 illustrates the setup used for the specimens. The hook protruded out of the front of the column at 30.5

inches from the base. The roller supports were spaced 11 inches from the center of the hook protrusion. Similar to Hamad et al. (1993), the development length (l_{dh}) provided was 10 inches for all specimens and purposely made shorter than the ACI Code (318-05) specifies so that the specimens failed in bond instead of yielding of the rebar.

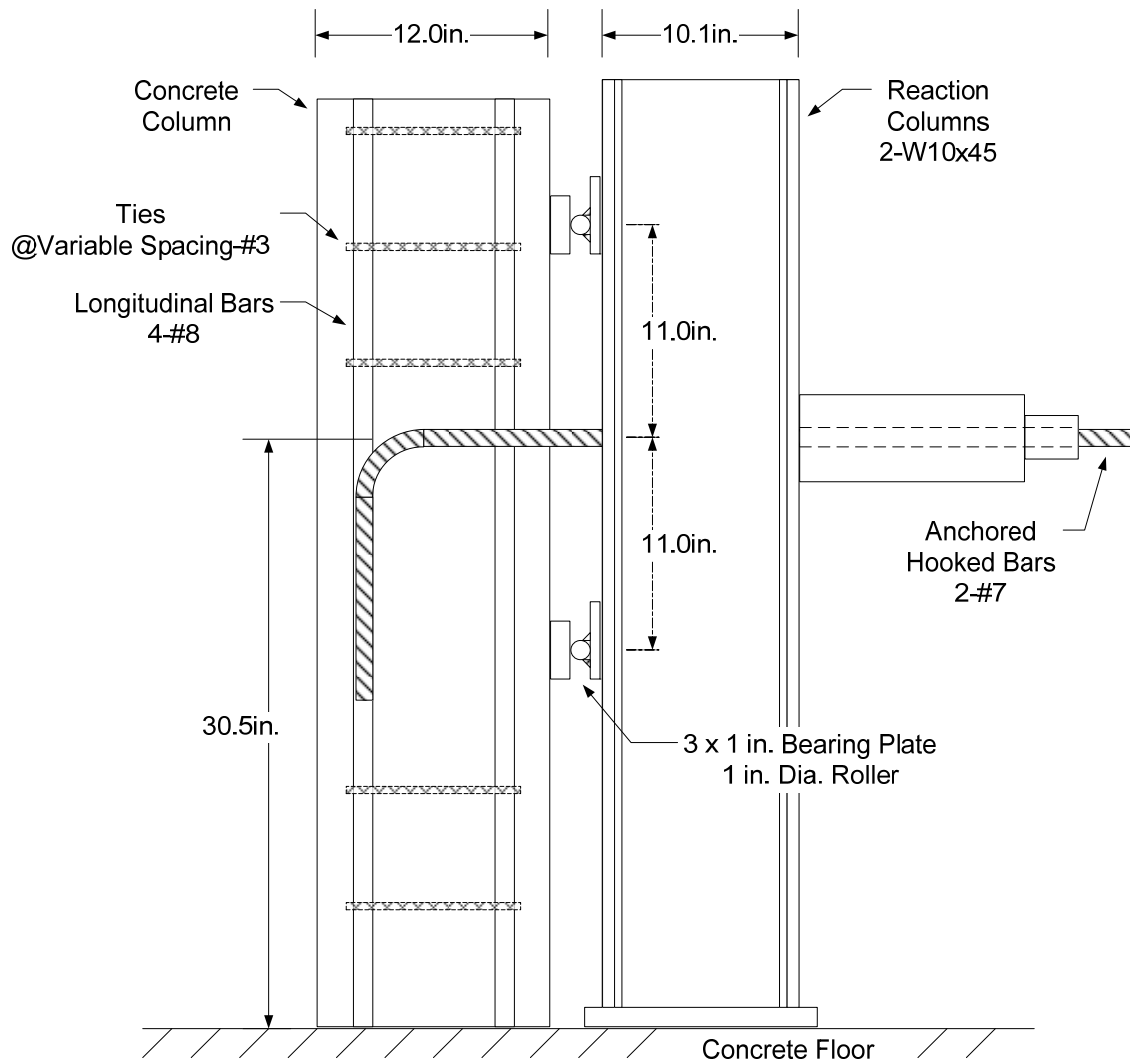


Figure 3.2: Elevation view of specimen and load frame

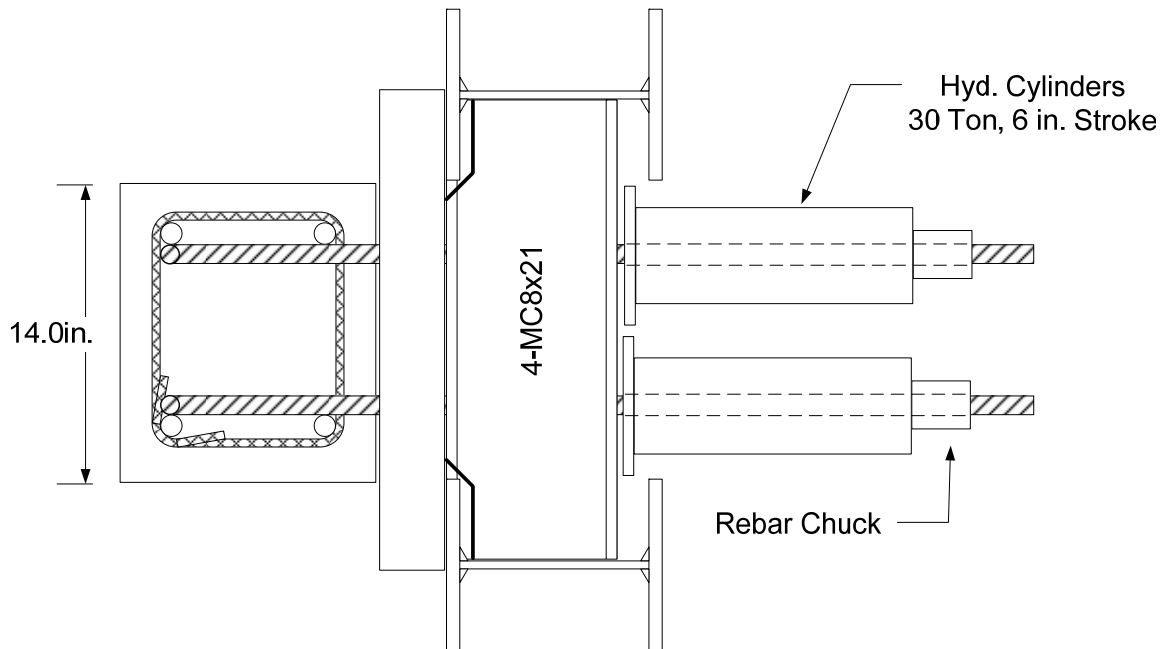


Figure 3.3: Plan view of load frame

3.3 Specimens

3.3.1 Coating

Uncoated (black) rebar was used as it was supplied. No attempt was made to modify the mill scale and surface rust.

There are many proprietary forms of epoxy coating that can be applied to rebar. No particular brand of coating was specified to the rebar supplier. Scotchkote 413 from various production batches was the primary coating supplied with one set of No.3 ties being coated by a Valspar brand epoxy. It was not possible to detect the difference between the two brands visually, but when compared side by side it was possible to determine which bars were coated using ASTM A775 versus ASTM A934.

Epoxy coated rebar came in two forms. Half were coated according to ASTM A775 and the other half by ASTM A934. For both ASTM methods the rebar must be thoroughly cleaned and the rebar is heated before the epoxy coating is applied. The difference is that for ASTM A775 the rebar is coated by machine while straight and then it is cut and bent to shape. For ASTM A934 the bar is cut and bent first, then spray coated

by hand while resting or hanging on a rack. ASTM A775 was originally approved in 1981 and was the object of Hamad et al.'s (1993) research. ASTM A934 was originally approved in 1995, but has not been previously tested on hooked rebar.

A PosiTector 6000-FN2 was used to measure the epoxy coating thickness. This instrument uses a magnetic attraction principle, instead of the less accurate eddy current principle, to determine a coating thickness over a magnetic base metal. ASTM A775 and A934 both include requirements for the epoxy coating thickness measurements, but these were used as a guideline, not as a rule, for lack of perfectly adequate measuring equipment. It is believed that the readings as taken are sufficient for the purpose of the current program. Table 3.3 shows the number of locations each rebar was checked for coating thickness, but each location was also measured at least 3 times to get an average reading. All measurements on the curved section of the hook were made on the outside of the curve. Most measurements on straight sections were made in the wide flat spaces where the rebar designation can be found.

Table 3.3:
Number Of Epoxy Coating Measurement Locations

	A775		A934	
	Curve	Straight	Curve	Straight
Longitudinal Rebar	n.a.	1	n.a.	1
Hooked Rebar	5	6	5	4
Ties	Random		Random	

It was noted during thickness testing that significant coating thickness differences existed between the flat sections and the tops of ribs. These differences could exceed 10 mils.

3.3.2 Displacement Wires

The method for measuring rebar movement inside concrete that was developed by Minor and Jirsa (1975) was modified for this project. The rebar surface was roughed up using a metal file instead of drilling a small hole in the rebar. Braided picture hanging wire 0.05 inches in diameter was used instead of music wire. The end of the wire was split into two bunches and squeezed flat with pliers, then crimped sideways in opposite directions to make a tee. High strength epoxy glue was applied to the split end of the wire

and the roughed up rebar surface. The wire and surface were then meshed together and the epoxy glue surface was smoothed out. Bar surface coverage was between $1/16^{\text{th}}$ and $1/8^{\text{th}}$ of a square inch at this point.



Figure 3.4: Displacement wire attached to hook

One drop of multi-purpose oil was dripped into thin, clear, flexible tubing ($3/32''$ ID, $5/32''$ OD) to act as a lubricant. The tubing was then slipped over the steel wire all the way to the hardened epoxy glue. A small ball of clay was wrapped around the joint between rebar and tubing to seal the two together. For future reference, this was only moderately successful as it was prone to coming apart during casting. It may be better to just glue the tubing straight into the rebar before the epoxy glue has hardened. Rebar surface coverage was about $1/4$ square inch for each finalized attachment location. A finished displacement wire attachment to the top of a hook from Phase 1 is shown in Figure 3.4.

The tubes were slipped through small holes in the wall of the forms. About 3 inches of both wire and tube protruded from the $\frac{3}{4}$ inch thick forms. During casting of Phase 3 specimens, it was necessary to use temporary clamps to hold the topmost wires/tubes in place. Without the clamps the falling concrete would drop on the outstretched tube, bend it, and pull it inside the form leaving it nearly impossible to repair. This is the cause of several missing data series related to the topmost reading position.

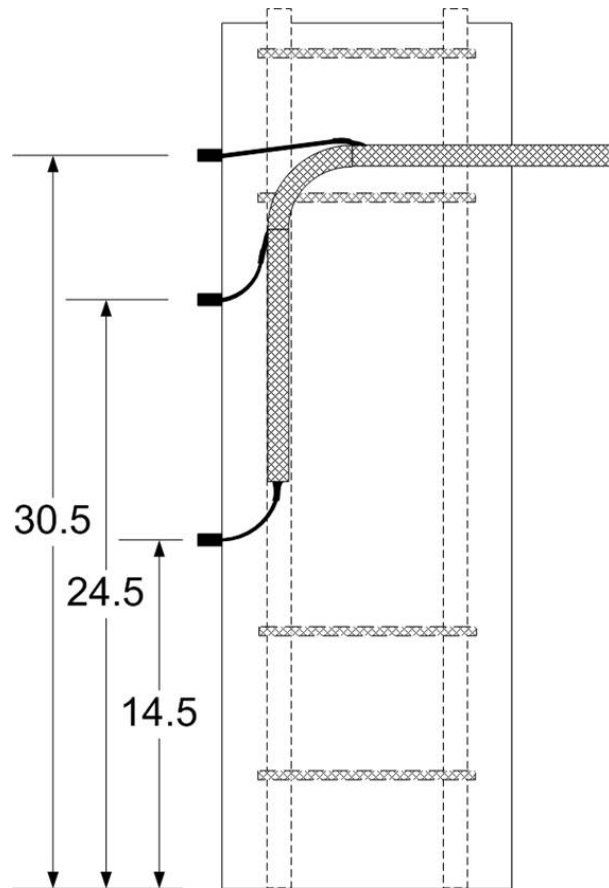


Figure 3.5: Displacement wire and tube layout

During pullout testing the excess tubing was cut off outside of the cured concrete. A spring loaded clamping device was attached to the protruding wire giving it around 3 lbs of tension. In Phase 3 a smooth metal guide sleeve was added to increase the clamping device's stability. Two small shots of hot glue on opposite corners were used to attach the guide sleeve to the concrete surface. The sleeve greatly increased the reliability of the system to produce usable data. Blocks of wood were glued to the concrete using

Heavy Duty Liquid Nails Construction Adhesive. Dial gages accurate to 0.001 inch were then mounted on the wood blocks and positioned onto the flat surface on top of the clamping device.

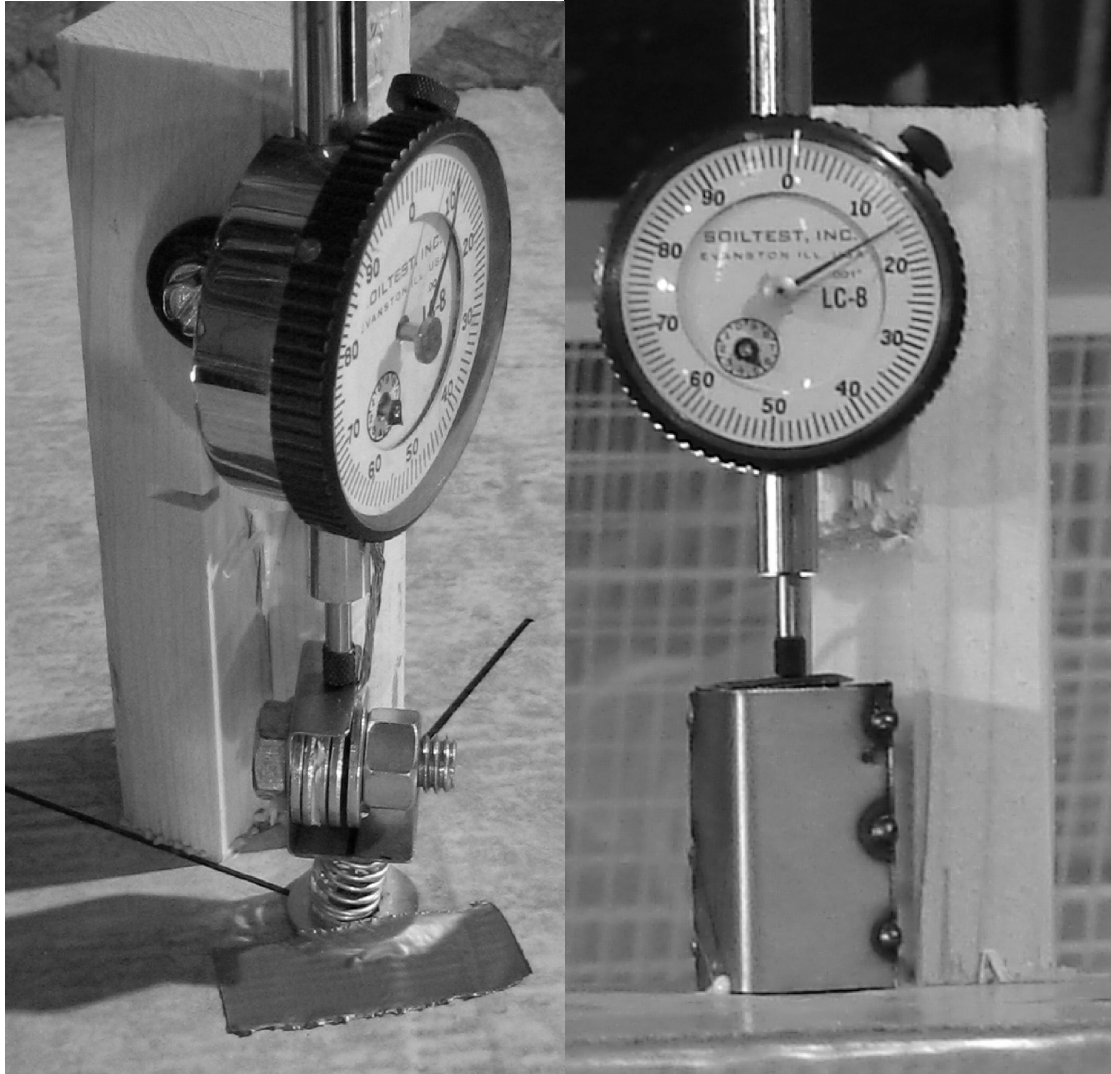


Figure 3.6: Spring loaded clamp without and with guide sleeve

When under load the rebar would slip through the confining concrete, pulling the displacement wire with it. This compressed the spring and allowed the dial gage to change readings. A digital camera was employed to capture the readings of all 6 dial gages simultaneously for data collection. Figure 3.7 shows the position of the camera and

all 6 dial gages that was necessary to ensure a direct line of sight and straight on view of the gages.

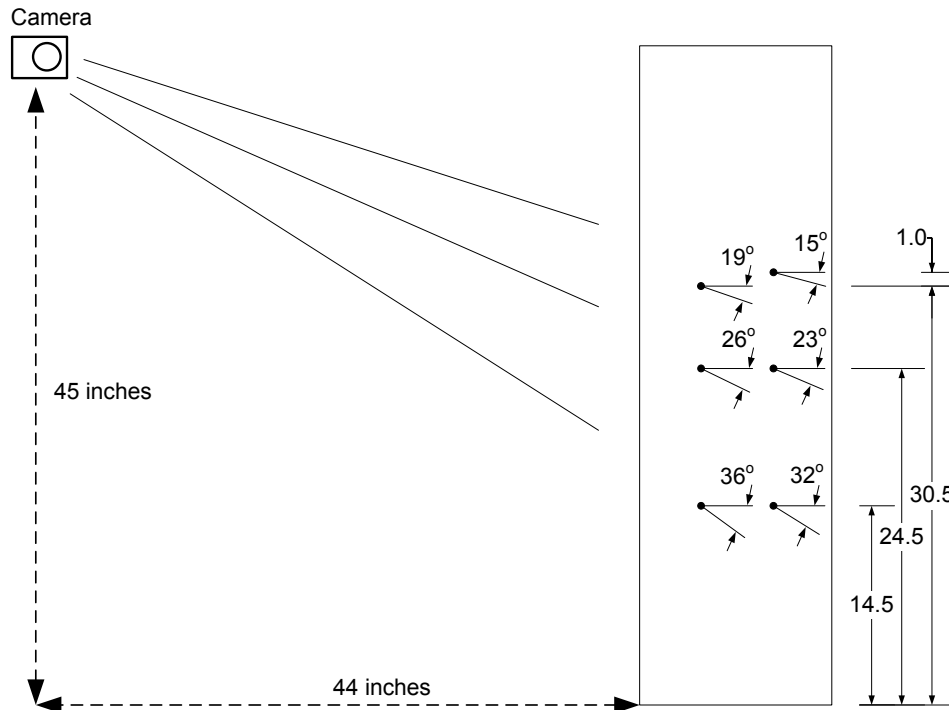


Figure 3.7: Camera position

3.3.3 Casting

The Phase 1 specimen was cast from 5 batches of concrete mixed back to back in a rotatory pan mixer. The mix design was similar to that used in Phases 2 and 3. Two 6x12 inch cylinders were cast from each batch to check later for a uniform compressive strength.

For Phases 2 and 3, the first several feet of concrete to come down the shoot was discarded when the ready-mix truck arrived. Experience has shown that the first couple feet contains relatively more water and the next couple feet contains relatively more coarse aggregate than the rest of the load.

For Phase 2 of the project, all 7 specimens were cast, finished and 24 hour cured without movement. The room on casting day was approximately 65 degrees Fahrenheit with 80% relative humidity. The top of the specimens were left uncovered. Casting took about 75 minutes to complete.

A hand held electric vibrator was used to consolidate the concrete and lift loops were installed in the specimen tops to make moving them easier once cured. At 7 days the forms were removed and the specimens moved to another location in the same room to continue curing. No special curing conditions were used. This was an attempt to simulate field conditions in which the best practical practice is to keep the forms on the concrete for as long as possible to keep the moisture in.

Casting 34 specimens within reach of the ready-mix truck's shoot from the overhead door was not possible. For Phase 3 of the project the specimens were mobilized using pallets and pallet jacks. The concrete was placed in one location and then the pallets were moved 10 to 50 feet to a second location where they stayed for the next 7 days. On casting day the room was still about 65 degrees Fahrenheit and the relative humidity was about 85%. From start to finish casting took 65 minutes. Finishing and curing procedures were the same as in Phase 2.

During casting the internal concrete temperature, air content and slump were checked via ASTM methods C1064, C231, and C143 respectively. Refer back to Table 3.1 for these values.

3.3.4 Concrete Cylinders

A set of five 6x12 cylinders were cast following ASTM C31 for each column in Phase 2. These were tested for compressive strength at 7 days by breaking one cylinder. Pullout testing began at 28 days and the final four cylinders were broken within 20 hours of beam-column testing.

In Phase 3, sets of five 6x12 cylinders were cast for each of the five categories of specimens found in Figure 1.. The two categories of black hooked bars were treated as one for the purpose of cylinders. One cylinder from each category was broken at seven days to check the progression of concrete curing. At 28 days, one more cylinder was broken from each category and three cylinders were broken on each day that pullout testing commenced for that category.

All cylinders were tested using a Baldwin 300 kip hydraulic compression machine. A computer program controlled the rate of loading to meet ASTM C39 and elastomeric pads of 70 duro were used along with the appropriate steel caps.

3.3.5 Loading System

The hydraulic loading system consisted of Enerpac parts pressure rated to 10,000 psi. The hydraulic system starts at a hand operated hydraulic pump. Next is a tee for fluid flow to the two sides of the system. Each side of the system is identical in parts, though one side was noted to often receive a few more psi of pressure during lower levels of load. This difference is attributed to variability in internal spring resistance in the valves. Beyond the tee was two manually operated check valves facing in opposite directions connected by a few feet of hydraulic hose. During normal loading, the valves closest to the hydraulic cylinders were in the closed position so that if side 'A' of the system lost pressure for any reason, then side 'B' would retain pressure. If the pressure loss was permanent, such as a broken rebar, then the valve closer to the tee on side 'A' could be manually closed to isolate that side of the system. Loading could then resume on side 'B'.

Between the second valve and the hydraulic cylinder was a digital readout pressure gage. The gages from both sides 'A' and 'B' were orientated so that they could be viewed from a single location on the side of the pump. When a data point was taken by digital photo of the dial gages, a digital photo was also taken of the two load gages. Most of the time both photos were taken within a couple seconds of each other or less. In this way, both load and displacement was simultaneously recorded for all gages attached to the testing system.

The two center hole hydraulic cylinders are each rated to 30 tons and have a six inch stroke. The manufacturer's literature specifies the effective pressure area as 7.22 in². Calibration in the lab against a certified load cell and against the Enerpac digital pressure gage showed that the effective pressure area was closer to 7.17 in². The lower area was used for all calculations of system loads. Comparison between the load cell and the digital gages showed a difference of around 200 pounds at some load levels. This is less than a 0.5% difference from capacity and not considered significant enough to warrant adjustments of the measured loads during testing.

Rebar chucks and wedges made by Howlett Machine Works and sized for No.7 rebar were used to transfer load from the hydraulic cylinders to the rebar. A heavy spring was clamped into place to reduce initial wedge slip, but otherwise the teeth on the wedges

caused a self seating action into the wedge collar. No modifications were made to the uncoated rebar prior to loading. By the end of most tests the teeth had clenched through the rebar ribs and barely contacted the rebar flats. During initial testing the epoxy was not removed from the coated rebar. The epoxy tended to fill up the wedge teeth which lead to a gripping system failure on test 3EA93e. On subsequent tests the epoxy coating was removed through angle grinder brushing along approximately 3 inches of the wedge region. No further problems were encountered from wedges slipping.

3.3.6 Loading Procedures

An initial preload of 30 psi to 70 psi was generally applied to the rebar chucks to steady and seat the reaction system. Loading progressed in stages of close to 6 ksi bar stress. This corresponded to 500 psi of hydraulic system pressure. To complete a load stage, the hydraulic pressure was quickly brought up to that stage's stop pressure and then slower pumping was used to help steady the pressure near the point desired. When the pressure seemed to mostly steady out, photos were taken and the timer was started for that stage. When the timer ended, pumping for the next stage proceeded.

For the first three stages (up to 1500 psi) the load was held for 30 seconds. Beginning at the 2000 psi level, the load was held for 2 minutes at the 1000 marks and held for 30 seconds at the 500 marks. For most stages it took around 30 seconds to increase and steady the pressure. During the stage when the rebar was yielding it would usually take nearer to 2 or 3 minutes to stabilize the pressure. Close to the end of the test, one side(or the other) would often fail first by high levels of slip. The high slip would cause a significant loss of hydraulic pressure (usually 2000 psi or more) for the side slipping. The failed side would be isolated by closing the appropriate valve and loading would continue for the remaining side. In many cases 3 to 4 data points would be taken after the slip failure to be certain the test was done. Separating these additional data points was usually 5 pushes of the pump for one sided loading or 10 pushes for two sided loading. Resting time for these additional stages was only long enough to capture the gage readings. The additional loading did not follow an exact procedure, but seemed to produce adequate results considering the rebar anchorage system had already failed and the slip measurement system would begin failing at this time anyway. The high levels of

slip that occurred as the joint failed would either strip the measurement wires off the rebar, break the wires in tension, or cause the dial gages to reach their maximum stroke.

For safety reasons, no personnel were allowed to walk in the path of the loaded rebar. Initial tensile testing of sample rebar showed that when rebar breaks it tends to fly great distances and with great force in the direction it was being loaded. During more than one pullout test the highest level of bar stress recorded was higher than the average ultimate rebar stress found during tensile testing.

Pullout testing was never stopped due to rebar breaking. Failure was always caused by excessive rebar slip. When excessive slip occurred, it was a slow process and did not result in full side spalling as previous researchers have reported. This may be a function of the type of loading system being used. When the hydraulic pressure was increased, the rebar would stretch and the pressure would drop due to the resulting hydraulic cylinder extension. At high loads when slip failure occurred it is not known whether the cylinder extension or rebar/concrete movement caused the drop in rebar load. It is suspected that both occurred to some extent, but rebar movement was ultimately the cause of the load drop. This is characterized by the inability to increase the load again by extending the cylinder after failure. Instead, the load would continue to drop with further cylinder extension. Strangely, ultimate loss of load near the 7000 psi level would often result in a new load of nearly 5000 psi. This is still roughly 60 ksi of rebar stress. Sometimes significant cylinder extension was needed to decrease the pressure to 4000 psi, or 48 ksi rebar stress. This leads to unknown numbers of questions regarding post bond failure load capacity.

In load controlled testing systems it is not possible to see the post failure strength because once bond failure occurs the fractured concrete is overloaded and side spalling would be significant. Displacement controlled loading systems are usually favored for research due to their higher level of safety and, usually, higher data quality. The problem is that it does not simulate realistic field conditions. In most cases when a structure is overloaded, past ultimate, the load is not immediately released and so post bond failure slip is entirely unrestricted.

3.3.7 Failure

After reviewing past research programs it became apparent that there was not one single definition to describe failure of the test specimen. This could be a result of the many variations of specimen shape, size, and other variables or maybe a function of exactly what information was deemed most important to acquire at the time. No matter the reason, the question of what defines failure during the destructive testing of the joint specimens became a topic of many discussions during project planning without agreement on a firm answer. Generally, the joint was determined to have failed when the ultimate load was reached, but during actual testing it became apparent that this was not exactly the case. As described in the section Loading Procedures, failure was almost always declared when an attempt to increase the applied load resulted in increased rebar displacement rather than increased rebar stress. This can be seen in the data presented in the Results and Discussion chapter.

4 Results and Discussion

4.1 Variables

This section is intended to describe some of the variables that may have affected the data as it was collected, but it is understood that there are very likely other variables not considered. When possible, included with each variable is the known or assumed range of value so that the reader can make their own decision as to the variable's weight within the testing system in the event that the provided influence and assumption is not agreeable.

4.1.1 Gage Location

The displacement wires were connected to the hooked rebar at a distance of 4 inches from the furthest perpendicular face of the rebar by using a square held on the outside of the curve. The wires were attached to the rebar on the flats between ribs. Due to the uncontrolled location of ribs, the attachment points were up to ± 0.25 inches from the optimal 4 inches. It was not possible to make a more accurate placement without removing ribs to make exact wire placements. The influence of the placement range was unknown and goes unaccounted for in data adjustments.

4.1.2 Rebar Yield Stress

The ACI Code requires a minimum yield stress of 60 ksi. The range of known yield stress was 62.9 ksi to 82.9 ksi. Considering that the ACI Code minimum was met, it was assumed that all the steel was both strong enough and the same. All specimens were pullout tested well beyond the steel rebar's yield stress, but data used for comparison purposes was limited to the generally accepted yield limit of 60 ksi. Because no data from beyond the rebar yield stress was used in the statistical analysis and comparisons, the output data did not need adjustment.

4.1.3 Exact Load Level / Slip measurements

The load level that corresponds to the related slip measurement was used as it was read from the digital pressure gages. Through pre-testing gage calibration, three issues were found. The first issue was that the exact cross-sectional area that the hydraulic fluid

acts on was not known. Through the calibration process it was found most agreeable to use 7.17 in^2 for the pressure area so that load cell readings and gage readings matched up the best at the appropriate load related to 60 ksi of rebar stress. The second issue was that the divergence by the load gages to the load cell's reading caused a load range error of about 400 pounds. This means that any load, as read during testing, could have been +/- 200 pounds with the highest accuracy near 60 ksi of rebar stress. The third issue was that one hydraulic pressure gage sometimes read 3 psi higher than the other gage despite being in the same system. This affect seemed to fall away after a few hundred psi of hydraulic pressure was applied.

During the testing process it was not possible to keep the applied load at exactly the level desired for the load holding part of the load stage. This usually lead to a slightly lower load being held steady than planned.

Corrections for load related issues were attempted via linear interpolation of the raw output data. After changes to a few data points were made it was determined that the interpolation was not changing the slip results by enough to be noticeable in relation to both the value of the original slip measurement and the degree of precision that the dial gages were capable of. It was then deemed unnecessary to do the interpolation and the few changes that had been made were reversed back to the original values.

4.1.4 Dial Gage Reading

Digital photos used for recording the dial and pressure gages were not always perfectly readable. Many instances occurred where the value of a reading was initially guessed. After reviewing the full load slip curve, minor adjustments to the guessed values were made. This would seem like an unscientific approach to precise data collection, but after spending many hours reviewing the numerous load slip curves there is confidence that this method worked. Additionally, the impact of this method is thought to be almost none because only 3 of the 20 data points are used from any one gage.

It is believed that using dial gages with precision as high as 0.0001 inches would be beneficial over the gages used (0.001 inches of precision). This is especially important for the bottom gage where slip values were very small or non-existent. There is an all

encompassing reason that the higher precision gages were not used. Refer to the end of the section for this.

4.1.5 Cross-Sectional Area of Rebar

The cross-section for all No.7 rebar was assumed to be 0.60 in^2 . This value was taken from ASTM A615-06a, Table 1 and is close to the calculated value of 0.601 in^2 . Measurements of individual rebar were not performed as there was no clear way to adjust for any deviations anyway. Potential adjustments are even less clear because the actual rebar diameter could change an infinite number of times along the length of the bar but only a finite number of rebar slip measurements can be taken.

4.1.6 Modulus of Elasticity of Steel in Rebar

Modulus of Elasticity values were not provided by the steel mill with the other metallurgical properties. Values were also not collected during laboratory tensile testing. If various rebar had differing Modulus values then the load distribution along the hooked rebar could be altered. This in turn could change slip values and failure modes. All rebar used was assumed to have similar Modulus of Elasticity values such that they would have no affect on testing.

4.1.7 Coating Thickness

Coating thickness in respect to ASTM thickness values will be discussed more in a later section. As a general variable the coating thickness makes a mess of the data if adjustments were to be made. As it is, information was available to provide guidance for coating thickness on straight rebar, but the information necessary to make data adjustments for hooked rebar was not available. The A775 rebar had fairly consistent coating thickness so no adjustments would be likely. On the other hand, the A934 rebar had wide ranges of coating thicknesses both between bars and within single bars.

There is an additional coating that is often overlooked, the mill scale found on black bar. Chemical adhesion between the concrete and black bar is attributed to one of the benefits of uncoated rebar verses coated rebar, but the concrete is often or always adhering to the mill scale and not to the rebar directly. Mill scale has a wide range of adhesion to rebar. This means that the ‘slippery’ nature of coated rebar could also be

present for black bar to some degree. Thickness measurements of mill scale were not taken and are not accounted for in the final data.

4.1.8 Rebar

The rebar was placed as close to it's intended position as was practical within the rebar cage. The as-built position of rebar for many of the specimens was measured. It was found that rebar locations varied by anywhere from +/- 1/8 inch to +/- 1/2 inch depending on which bar was being measured. The entire rebar cage may have also been moved an unknown distance in any direction during the casting process. Since these many, small non-conformities exist in nearly all specimens and are randomly distributed across the various sets of specimens, it was not possible to make corrections on any individual specimen's data. It is also unknown what effect the offset rebar has on the data for the purpose of making corrections.

The angle and spacing of the rebar ribs was measured for the No.7 hooked rebar. Table 4.1 shows the seven different rib varieties found. It was noted during measuring that the angles 56 degrees and 60 degrees may be the same angle at 58 degrees, but that the accuracy of the measurements makes them look like two separate angles. All rib patterns pass ASTM A615-06a which controls rebar rib size, orientation, and spacing. The angles were measured such that 90 degrees is perpendicular to the longitudinal direction of the rebar. The spacing was measured as the longitudinal length of the flat section between ribs.

**Table 4.1:
Rib Patterns**

Angle	Spacing (inch)	
56	1/4	3/8
60	1/4	3/8
66	1/4	3/8
74	1/4	--

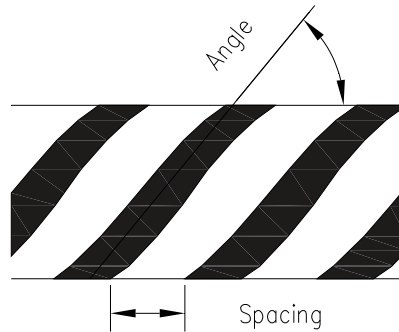


Figure 4.1: Rib angle with respect to rebar

The angle of the rib helps to direct the rebar forces into the concrete. The direction that the angle was facing in relation to the side concrete cover was not noted. In some cases the angle directs the rebar forces to the outside concrete face and on other specimens the forces are directed inward. This could influence the propensity of the rebar to crack the concrete cover prematurely and so reduce the rebar's confinement and load holding capacity.

The slope of the rib also helps to direct forces from the rebar to the concrete. The general effects of a shallow or steep slope were previously discussed. There were at least two slopes present on Phase 2 rebar and another two slopes present on Phase 3 rebar. Rebar with ribs spaced at $\frac{1}{4}$ inch had a shallower slope relative to the rebar with ribs at $\frac{3}{8}$ inch spacing. The height of the ribs was not measured, but visual inspection showed that they were about the same.

In general there are many variables that can be changed on rebar. Some of these variables have been investigated on straight bar tests, but their effects related to hooked rebar are not known. Therefore, no adjustments to the data can be made.

4.1.9 Concrete

It is widely known that concrete is a highly variable material. Even in the strictest laboratory setting it is difficult to produce two batches of concrete with the same compressive strength. Adding to the problem is the variance induced into the strength value by the testing process that creates the value. Further, a larger percentage of concrete strength comes from the natural aggregate. Natural aggregate means more natural variability and less certainty in exact strength.

The concrete used in Phase 2 and Phase 3 of the current program came from two separate ready-mix trucks using the same mix design yet yielded very different strengths. Even the concrete cylinders from one batch produced different strengths and so it is not unreasonable to believe that any one specimen made from that same concrete could have a range of concrete strengths within it. There is no known way to precisely control concrete strength (excluding UHPC) and no way to make corrections for local strength differences. More information about the strength of the concrete used can be found in a later section.

4.1.10 Variables Summary

There is potential that the error induced into the data by any one of the many variables could offset any possible increase in precision from all the other variables combined. This is especially true for the most uncontrollable variables; rebar and concrete. There are an unknown number of small adjustments that could be made in any one part of the entire testing setup that could have some impact on the data that was produced. The solution is to change mindsets.

Instead of running the program as an exacting laboratory experiment, there was consideration at each step in the process on how things would be done on a real construction site. This does not mean that procedures and methods were less carefully performed, but it does mean that when the data was analyzed it was seen at face value. It assumes that all the variation in the random variables that make up each specimen nullify each other to some degree so that the data across a group of specimens can be compared based on the one major variable that makes them similar.

4.2 Tensile Strength Testing

Rebar tensile data was collected from manufacturer documentation and laboratory testing. ASTM A615 requires Grade 60 rebar to have a minimum yield and ultimate tensile strength of 60,000 psi and 90,000 psi, respectively. Table 4.2 shows that all rebar tested meets the minimum criteria. The average ultimate strength of each of the three categories was fairly similar with a range of only 5.4 ksi. The average yield strengths have a wider range, 10.7 ksi, than the average ultimate strength. The Black rebar have a

typical Grade 60 average yield strength of nearly 72 ksi. The A775 rebar has an increased yield strength of 78.5 ksi, while the A934 rebar was the weakest at 67.8 ksi. The low yield of 62.9 ksi comes from a heat of steel that was used to make No.3 ties for both the Black and A934 categories.

**Table 4.2:
Tensile Testing Data**

Type	Yield (ksi)	Ultimate (ksi)
Black	73.3	93.3
	75.0	93.7
	74.1	102.9
	74.2	93.7
	75.3	93.3
	* 66.1	105.3
	* 62.9	96.6
	average	71.6 97.0
A775	77.5	102.5
	77.7	101.5
	78.2	102.5
	* 69.9	109.4
	* 81.0	103.0
	* 82.9	103.8
	* 80.6	101.6
	* 78.2	97.8
	* 80.6	102.0
	* 78.2	100.2
	average	78.5 102.4
A934	66.3	105.0
	66.0	104.8
	* 77.6	95.4
	* 66.1	105.3
	* 62.9	96.6
	average	67.8 101.4

*Data Provided by Manufacturer

Relatively few total rebar were tested and multiple casting heats are present across the sample size. Both of these points make it imprudent to draw a definitive statistical based conclusion on a correlation between the coating method used and actual tensile yield strength. The data does show that rebar coated by the ASTM A934 method needs to be closely monitored for yield strength as an end product.

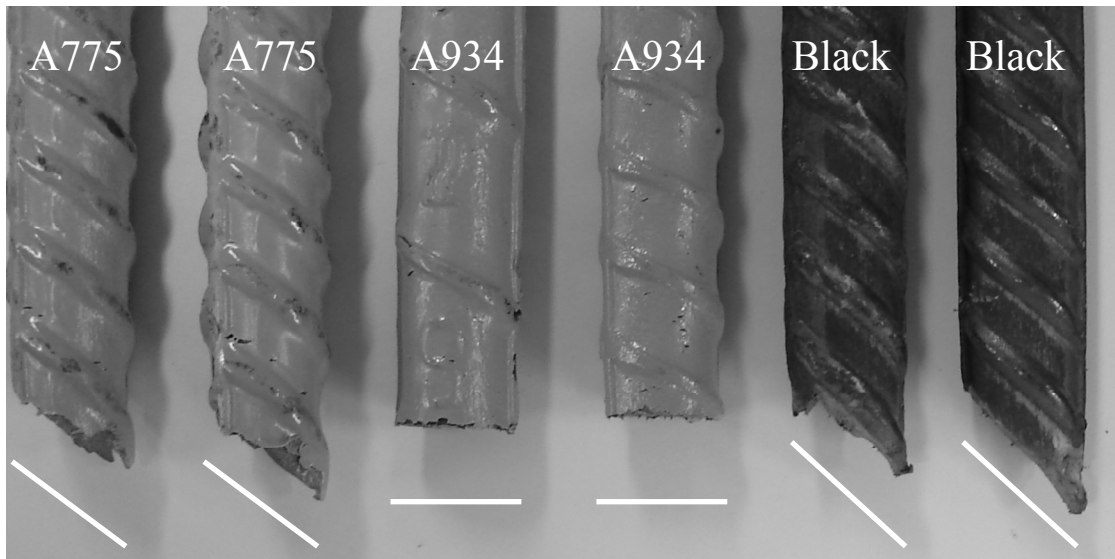


Figure 4.2: Rebar fracture planes

Two rebar from each category were lined up for a side by side comparison of the fracture planes after laboratory tensile testing finished. The white lines in Figure 4.2 are positioned parallel to the broken end of the respective rebar. The A775 and Black rebar show similar fracture planes, but the A934 rebar broke in a definitively different manner. No known differences existed from one test to the next, but the A934 rebar broke very cleanly and nearly perfectly perpendicular to the direction of pulling. Both the A775 and Black rebar broke at a plane of around 45 degrees (similar to the angle of the ribs) and had rough, jagged surfaces. The non-similar fracture plains and lower average yield strengths may be indicators of metallurgical flaws in the A934 rebar, but the rebar did meet ASTM requirements so further investigation into the metallurgy was deemed beyond the scope of the current program.

4.2.1 Coating Thickness Measurements, Cracks, Spots and Thickness Limits

ASTM A934 Section 9.1.1 specifies coating thickness. For a 90 degree curve, or less, the curved sections of a rebar must meet the same limits as the straight sections. So, independent of whether the manufacturer measured the coating thickness on the straight sections or the curved sections, the Upper thickness limit is 12 mils.

ASTM A775 Section 8.1.1 specifies the coating thickness to be 7 to 16 mils for any bar sized No's 6 to 18. The rebar tested in Table 4.3 were No. 7 and No. 8 rebar. Both ASTM A775 and A934 require that "No single recorded coating thickness measurement shall be less than 80% of the specified minimum or more than 120% of the specified maximum thickness."

Table 4.3:
Coating Thickness Statistics For Rebar

A934, Hooked Rebar		Total Measurements: 270			
	Limits:	Minimum	Lower	Upper	Maximum
	mils	< 5.6	< 7	> 12	>14.4
	Cat. 1, #	0	0	235	207
	Cat. 2, %	0	0	87	77
Values:	Minimum	Maximum	Range	Average	St. Dev.
	7.9	43.6	35.7	19.6	6.5

A775, Hooked Rebar		Total Measurements: 306			
	Limits:	Minimum	Lower	Upper	Maximum
	mils	< 5.6	< 7	> 16	>19.2
	Cat. 1, #	0	33	3	0
	Cat. 2, %	0	11	1	0
Values:	Minimum	Maximum	Range	Average	St. Dev.
	5.8	17.9	12.1	9.2	2.0

A934, Straight Rebar		Total Measurements: 56			
	Limits:	Minimum	Lower	Upper	Maximum
	mils	< 5.6	< 7	> 12	>14.4
	Cat. 1, #	10	13	3	1
	Cat. 2, %	18	23	5	2
Values:	Minimum	Maximum	Range	Average	St. Dev.
	3.2	17.6	14.4	7.9	2.9

A775, Straight Rebar		Total Measurements: 60			
	Limits:	Minimum	Lower	Upper	Maximum
	mils	< 5.6	< 7	> 16	>19.2
	Cat. 1, #	0	0	0	0
	Cat. 2, %	0	0	0	0
Values:	Minimum	Maximum	Range	Average	St. Dev.
	7.1	15.4	8.3	10.9	1.9

Cat. 1 ---- Number of measurements in category

Cat. 2 ---- Percent exceeding category limit

1 mil = 0.001 inch, 0.0254 mm

Of the 306 measurement positions on hooked rebar coated by ASTM A775, there were 11% that failed to meet the ASTM Lower limit, but all the bars did meet the

Minimum limit. This means that the coating is being applied a little too thin. A closer look at the data shows that 18 of the 31 hooked bars tested met all thickness requirements. Straight A775 rebar fully conformed to coating thickness requirements which is the reason only zeros are reported for that rebar type.

Of the 270 measurement positions on hooked rebar coated by ASTM A934, no bars fully passed the coating thickness requirements. Additionally, 87% of the hooks had coatings thicker than the ASTM Upper limit and 77% of the hooks did not even meet the ASTM Maximum limit. Straight rebar were measured at one location for each bar. On Straight bars the issue was a coating that was too thin instead, with 18% of the bars not meeting the ASTM Minimum limit.

The coating thickness requested of the manufacturer was 8 mils, +/- 2 mils. The data points in Figure 4.3 show the coating thickness measurements taken at the manufacturing plant for the A934 No.7 hooked rebar. The coating is a little thicker than requested, but still within ASTM requirements. The same is true for a miscellaneous set of thickness measurements taken for other rebar sizes and shapes, shown in Figure 4.4.

In Figure 4.3 through Figure 4.6, the lower heavy black line represents the ASTM Minimum thickness required. The higher heavy black line is the Maximum limit and the two dashed lines are the Lower and Upper limits.

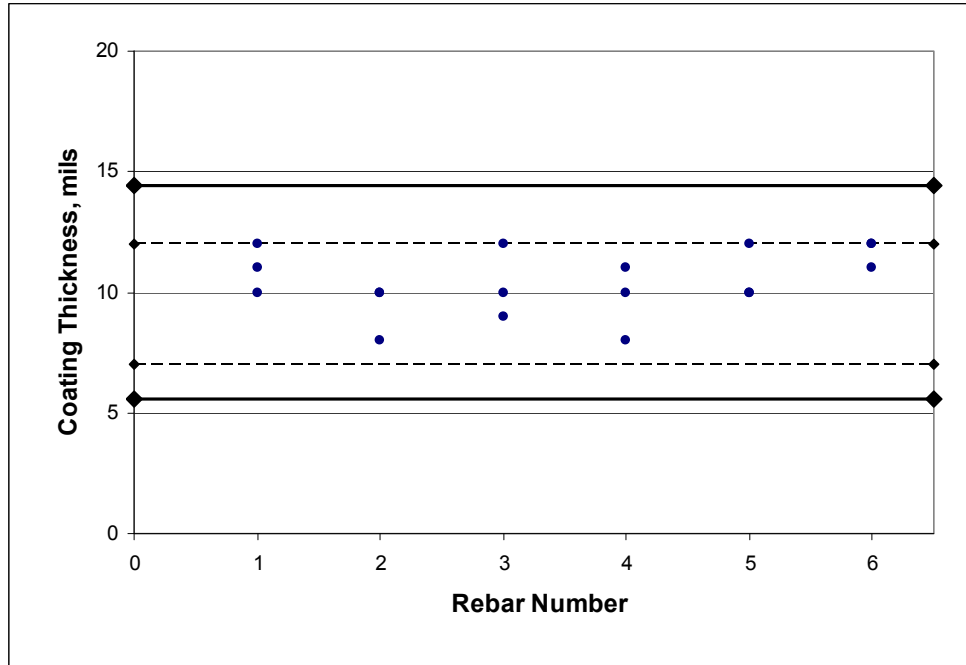


Figure 4.3: Manufacturer coating thickness data for A934 hooked rebar

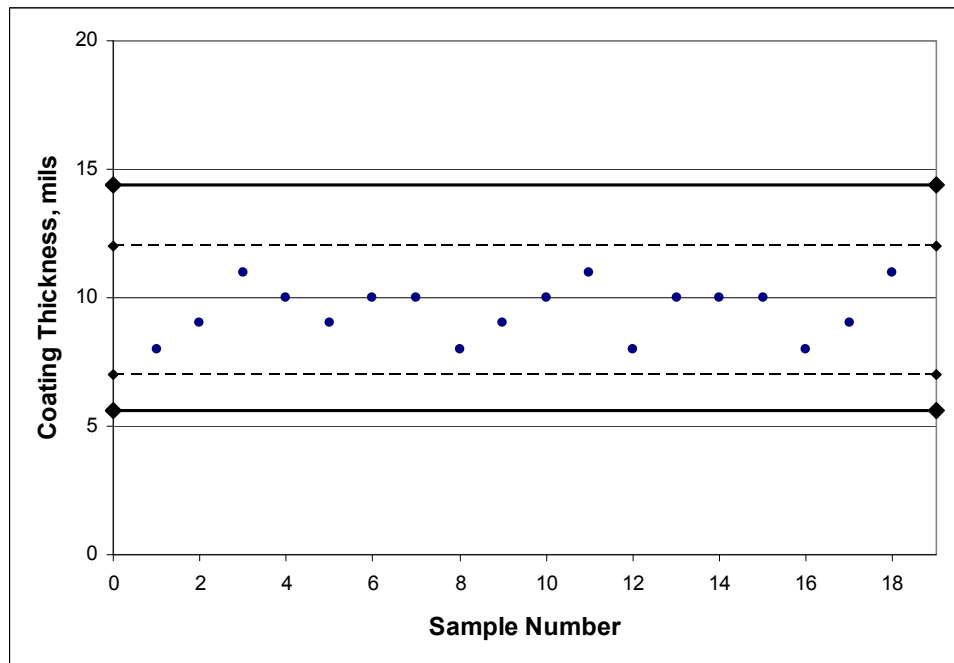


Figure 4.4: Manufacturer coating thickness data for miscellaneous rebar

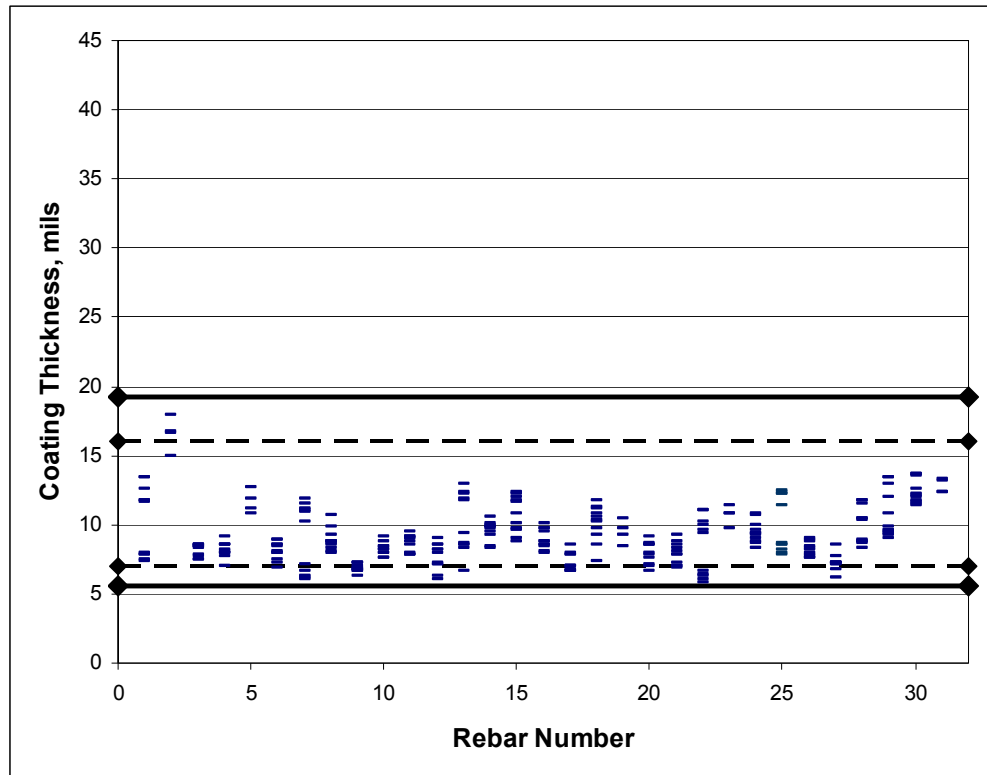


Figure 4.5: A775 epoxy coating thickness for hooked rebar

Figure 4.5 and Figure 4.6 are set to the same scale to clearly illustrate the difference in scatter between the A775 data and the A934 data. No change of equipment, personnel or technique was enacted at any time during the coating thickness testing. The inability of the A934 coating to conform to the ASTM requirements is likely a result of a general manufacturing problem: How to apply a spray coating on rebar after it has been cut and bent to various shapes? The common solution is to apply the coating by hand held electrostatic spray gun instead of by machine. Unfortunately, this brings a human element into the picture. It would be hard to believe that any human can visually make the distinction between a wet coating 10 mils thick verses a coating that is 15 mils thick. It makes it even harder to meet the ASTM that the range of acceptable coating thickness is smaller for the A934 process than the A775 process, as noted previously in Table 4.3.

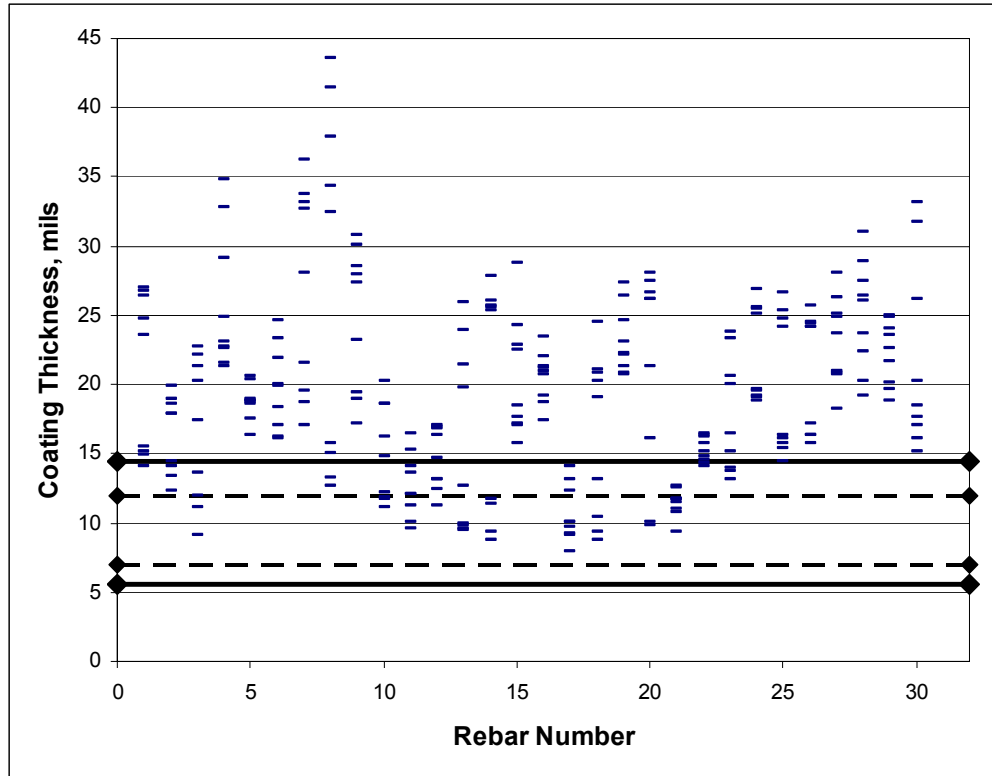


Figure 4.6: A934 epoxy coating thickness for hooked rebar

Another issue with coating after bending is every location where the rebar rests on the spraying rack must be brush coated by hand after the rest of that rebar's coating has hardened. For large high output coating facilities, this can lead to many locations that must be specially touched up and it is easy for one to get missed. Even on the relatively small rebar order used in the current program at least one location went uncoated, as circled in Figure 4.7.

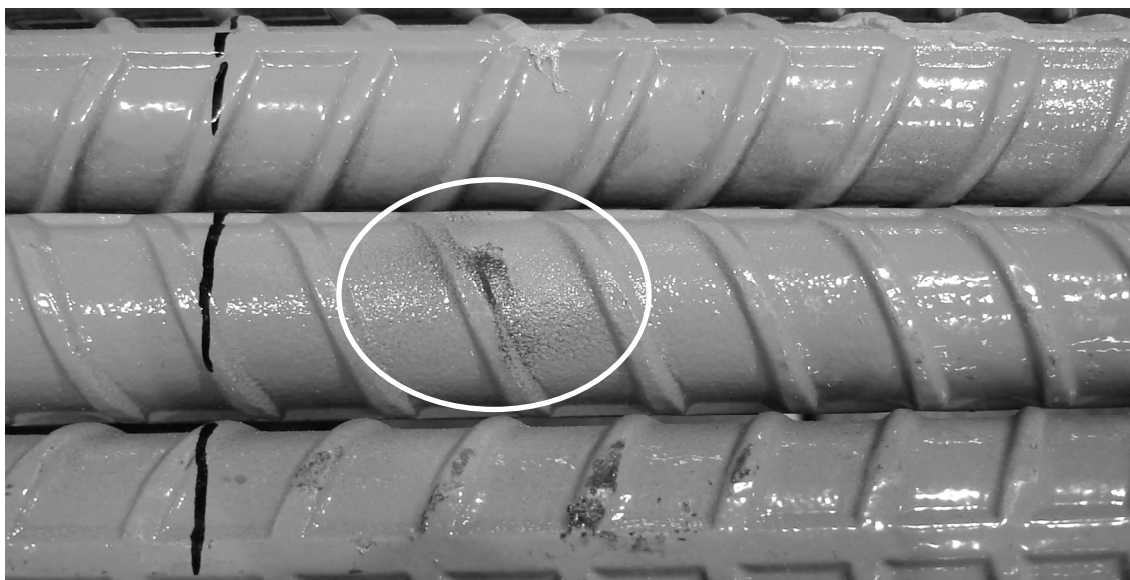


Figure 4.7: A934 coated rebar missing coating

There were no locations found on the A775 rebar where the coating had never been applied. A775 rebar did exhibit two other problems though. The first problem was locations on the outside of bends where either the bending equipment rubbed the coating off the ribs or the coating simply split as a result of excessively high strain or rate of strain. Nearly all the A775 No.3 ties displayed the type of lost coating found on the left side of Figure 4.8. The second problem is certainly one of excessive strain within the coating. The right side of Figure 4.8 shows the outside of the bend on a No.7 hooked rebar. The type of split shown was found on 4 separate hooked rebar several weeks after receiving shipment. It is unknown whether this type of split was present at time of shipment and went unnoticed or if it occurred at a later time. It is known that the split was not initiated by anything in the laboratory that would have sliced or scratched the rebar.



Figure 4.8: A775 broken coating

4.2.2 Concrete Strength

Concrete cylinders were created for all three phases of the program. The average compressive strength for the Phase 1 cylinders on pullout testing day was 4.93 ksi. For information regarding the cylinders tested for Phase 2 and Phase 3, see Table 4.4. The Phase 3 concrete was stronger on average than the Phase 2 concrete. The difference in strength was a result of using two batch sizes and the inherent variability found in ready-mix concrete.

Table 4.4:
Pullout Testing Day Concrete Cylinder Compression Data
Phase 2

Set	Average	Minimum	Maximum	Range	St. Dev.
1	3.96	3.80	4.18	0.38	0.16
2	4.09	3.95	4.23	0.27	0.11
3	4.00	3.78	4.17	0.39	0.17
4	4.29	4.18	4.43	0.26	0.11
5	3.95	3.78	4.22	0.45	0.19
6	4.00	3.91	4.09	0.18	0.08
7	4.08	3.77	4.31	0.54	0.23
Overall	4.05	3.77	4.43	0.66	0.18

Phase 3

Set	Average	Minimum	Maximum	Range	St. Dev.
3EA77	5.38	5.09	5.75	0.65	0.34
3EA73	5.51	5.35	5.64	0.29	0.15
3EA93	6.07	5.89	6.24	0.35	0.17
3EA97	5.81	5.57	6.09	0.52	0.26
3B_3,7	6.39	6.29	6.51	0.22	0.11
Overall	5.83	5.09	6.51	1.41	0.42

All values presented as " ksi "

The Maximum value found in Phase 2 is not even as high as the Minimum value found in Phase 3. This makes it clear that the concrete strengths used in Phase 2 and Phase 3 are not from the same statistical population. It would add an additional variable to the test program if the data from both Phases were to be mixed. For this reason, data from Phase 2 should not be added to the data in Phase 3 related to Black bar pullout testing. A technique of normalizing the concrete strengths to a pre-set value could be applied, but the influence of concrete strength on the anchorage capacity of hooked bars in the specific arrangement and testing setup used in the current program would have to be verified before the data normalizing would be valid. The required information was not available, so concrete strength normalizing was not used in the current program.

For Phase 2 and 3 the average strength of each set of cylinders was used to create data points in Figure 4.9 and Figure 4.10. For Phase 2, one cylinder was tested at seven days for each of the seven sets. Additionally, Sets one through five were tested at 28 days when the respective columns were pullout tested and sets six and seven were tested at 29

days. The spread of average cylinder strengths at seven days was roughly 500 psi, but this spread decreased to 330 psi for the average 28 day and 29 day tests.

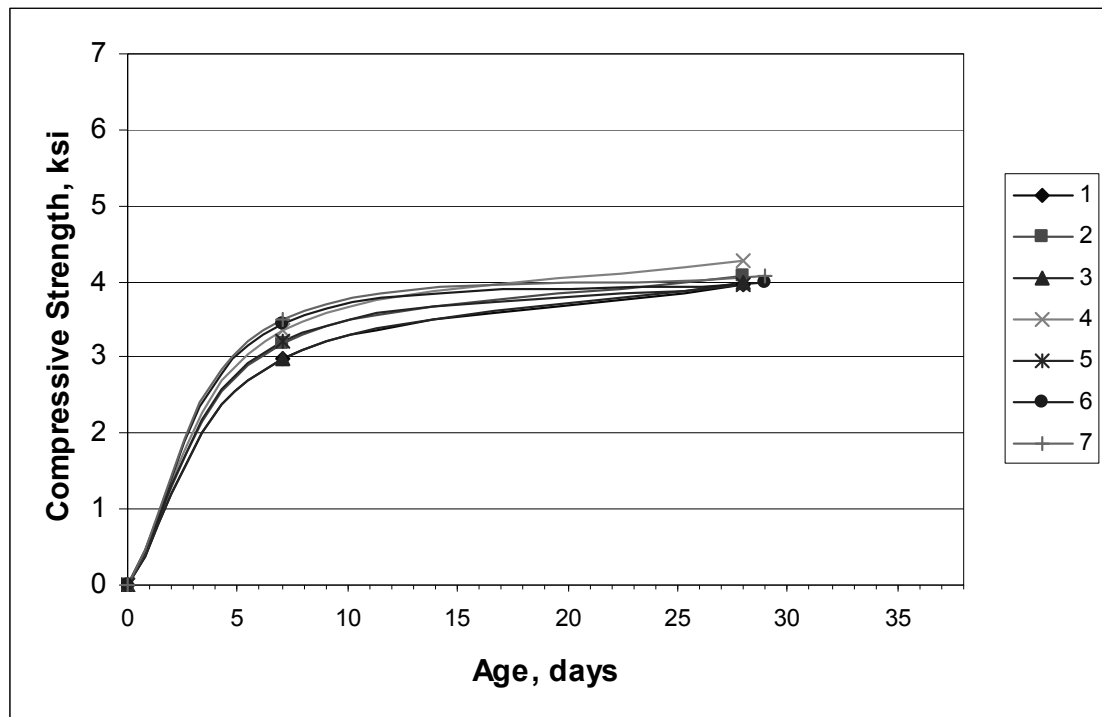


Figure 4.9: Concrete compression testing for Phase 2

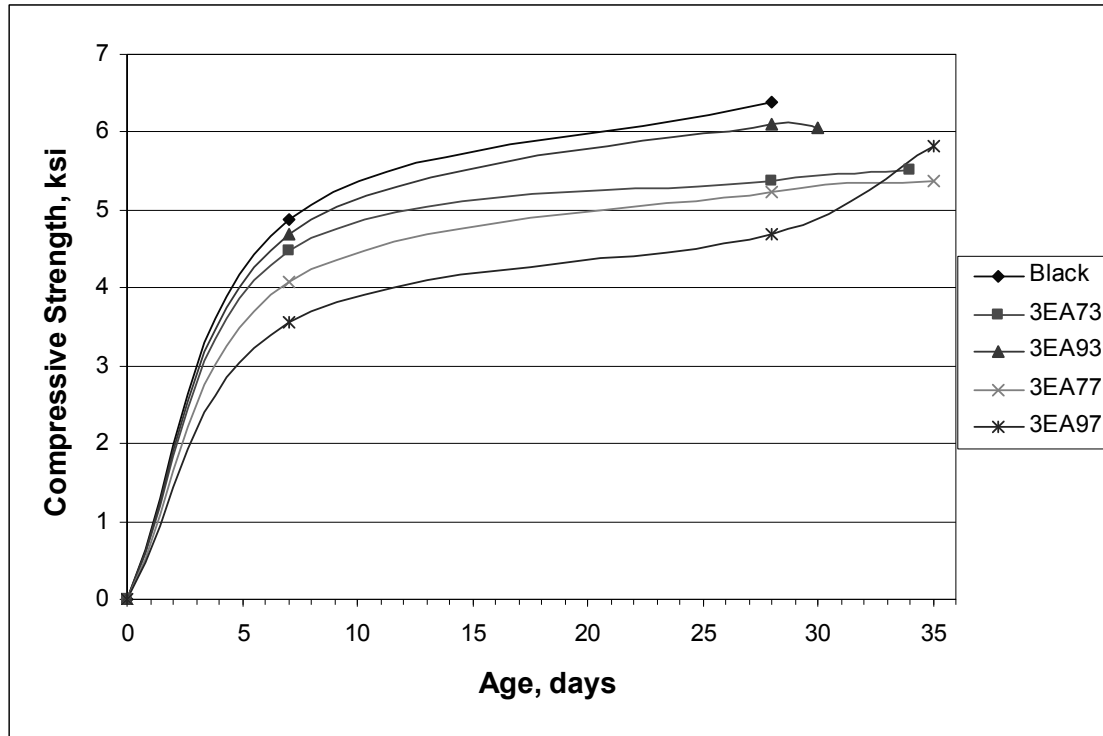


Figure 4.10: Concrete compression testing for Phase 3

In Phase 3, one cylinder was tested at seven days from each of the five sets. At 28 days, one more cylinder was tested from each set and then the remaining cylinders of each set were tested on the same day that the respective columns were pullout tested. A wide range of compression strengths were witnessed at both seven days and 28 days. The strength of cylinders for 3EA97 were the lowest at both the seven and 28 day marks, but the strength appears to have come up quite quickly by day 35 when the corresponding columns were tested. An alternative possibility is that the single cylinder broken at 28 days was a low break. If this was the case and more cylinders had been broken then the average would have likely been more in-line with the value of the other sets at 28 days. The average of all the final strengths was 5.83 ksi. The range of the average cylinder strengths at seven days, 28 days and test day was 1.32 ksi, 1.69 ksi and 0.69 ksi, respectively. A comparison of ranges found in Phase 2 and Phase 3 shows that the larger Phase 3 batch of concrete produced a much wider range on strengths, both initially and at final strength.

The data points in Figure 4.11 and Figure 4.12 are lined up according to the order in which the concrete was cast. For Phase 2, there is a definite progressive increase in seven day strength from the first concrete out of the ready-mix truck to the last. On the contrary, the 28 day strength is nearly steady across the sets.

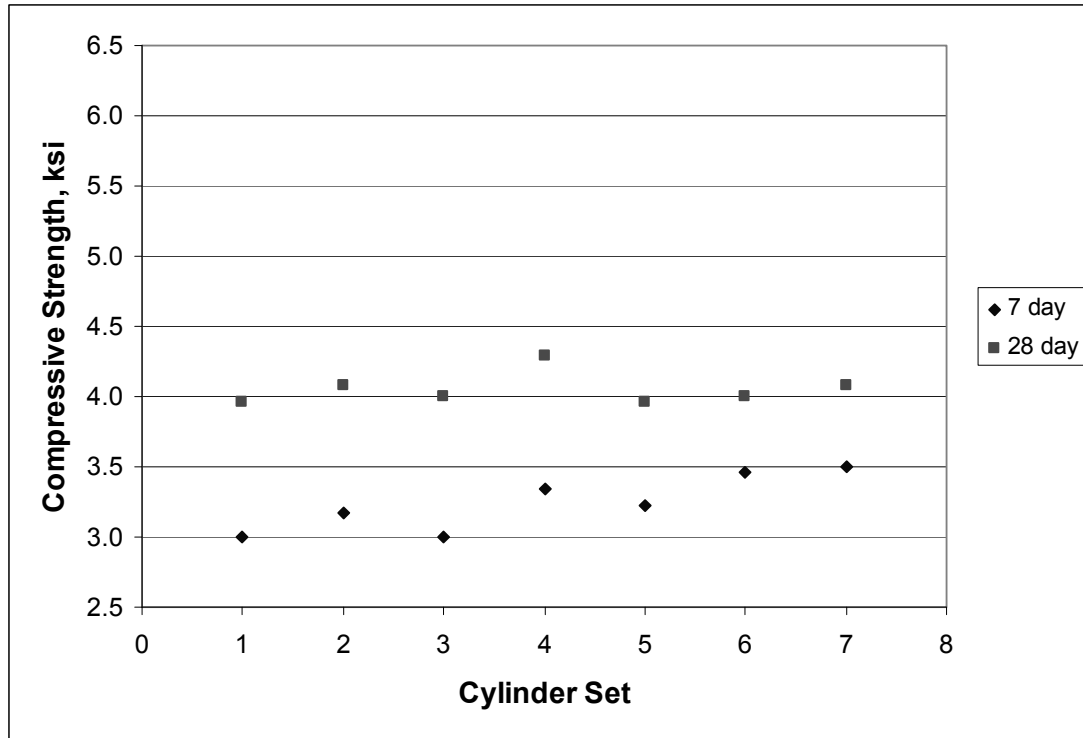


Figure 4.11: Strength progression across sets for Phase 2

The Cylinder Sets in Figure 4.12 refers to the sets 3EA77, 3EA73, 3EA93, 3EA97, and 3B_3,7 in order of one through five. The larger concrete batch used for Phase 3 seems to have increased the spread of seven day strengths. From the first concrete cast to the last, the range of strengths is nearly twice that found in Phase 2. Another difference from Phase 2 is the 28 day and Test day strengths continue to show the casting order by displaying increasing strength for concrete cast later. Set 4 (3EA97) does not follow the pattern suggested here. It is unknown what caused the deviation.

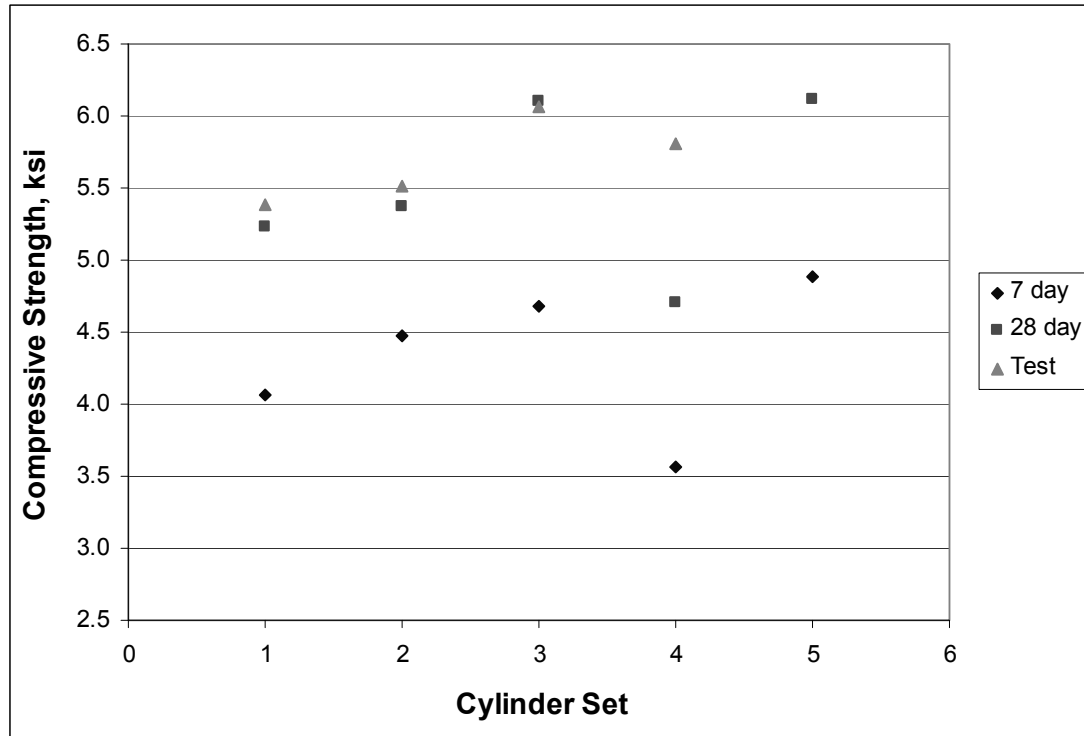


Figure 4.12: Strength progression across sets for Phase 3

The Test day data point for the 3B_3,7 set is not missing. This was the first set to have pullout testing (at 28 days) and so is the same value as the 28 day cylinder tests. This means that four cylinders were broken for this set instead of three. One cylinder test result was omitted from calculating an average strength because its value fell outside the acceptable range of variation as described in ASTM C39-05 Section 10.1.1. This was the only omitted value from all Phase 2 and Phase 3 cylinder tests.

4.3 Pullout Testing

4.3.1 Phase 1

Data resulting from Phase 1 pullout testing was erratic at best. Many of the displacement wires malfunctioned and the loading procedure was not clearly consistent with what was used in Phases 2 and 3. For these reasons, Phase 1 pullout data will not be presented or used for comparison or statistical purposes. Phase 1 was very helpful in refining various techniques and procedures though and so is still considered valuable in those respects.

4.3.2 Phase 2 and Phase 3

A summary of the data collected and calculated in Phase 2 and 3 is presented in Table 4.5. The concrete compressive strength is an average from the samples taken during casting. The rebar tie spacing across the joint varies from 3*db to 9*db depending on the series group. The lead rebar stress was calculated using the nominal rebar diameter and the load being applied by the hydraulic system. The mean slip for each gage location (Top and Mid) is an average of the data from each set of specimens. Lastly, the maximum values for stress and slip are shown for each tie spacing used. The maximum stress and slip values encompass all the data from each set and so are not necessarily from the same set. For example, for set 2B_3 the maximum stress of 81.2 ksi could have been from the first specimen in that set while the maximum slip of 0.029 inches could have been from the third specimen in the same set. These are also the maximum values for all three levels of rebar stress (30, 42, and 60 ksi), not just from the 30 ksi level. A key to the notation composing each set and series identifier is included below the table for convenience.

**Table 4.5:
Current Program Data Summary**

Series	f`c (ksi)	Tie Spacing Through Joint @ _*d _b	Lead Rebar Stress (ksi)	Mean Slip (inches)		Maximum Value *	
				Top	Mid	Stress (ksi)	Slip (inches)
Phase 2							
2B_3	4.04	3	30	0.002	0	81.2	0.0290
2B_5	4.12	5	30	0	0	76.9	0.0070
2B_7	4.04	7	30	0.003	0	82.7	0
2B_9	3.96	9	30	0.001	0	77.3	0
2B_3	4.04	3	42	0.005	0.00025		
2B_5	4.12	5	42	0.005	0.00075		
2B_7	4.04	7	42	0.006	0		
2B_9	3.96	9	42	0.004	0		
2B_3	4.04	3	60	0.017	0.0010		
2B_5	4.12	5	60	0.011	0.00375		
2B_7	4.04	7	60	0.017	0.00125		
2B_9	3.96	9	60	0.014	0.0005		
Phase 3							
3EA77	5.4	7	30	0.003	0	74.0	0.0227
3EA73	5.5	3	30	0.004	0.00029	83.1	0.0154
3EA97	5.8	7	30	0.004	0.00043	76.7	0.0072
3EA93	6.1	3	30	0.004	0	83.1	0.0074
3B_7	6.4	7	30	0.003	0	77.0	0
3B_3	6.4	3	30	0.003	0	82.8	0.0072
3EA77	5.4	7	42	0.008	0.00079		
3EA73	5.5	3	42	0.010	0.00064		
3EA97	5.8	7	42	0.011	0.00093		
3EA93	6.1	3	42	0.011	0.0005		
3B_7	6.4	7	42	0.008	0.00017		
3B_3	6.4	3	42	0.008	0		
3EA77	5.4	7	60	0.027	0.00836		
3EA73	5.5	3	60	0.031	0.0045		
3EA97	5.8	7	60	0.032	0.00743		
3EA93	6.1	3	60	0.034	0.00421		
3B_7	6.4	7	60	0.025	0.00267		
3B_3	6.4	3	60	0.024	0.00167		

Series Notation: (1)Phase, (2)Coating, E-epoxy, B-black

(3)ASTM- A775, A934, (4)Tie Spacing

3*d_b = 2.625 inches, 5*d_b = 4.375 inches

7*d_b = 6.125 inches, 9*d_b = 7.875 inches

* Maximum Stress and Slip Values are not necessarily from same test.

Several graphs were made for every pullout test to help verify that the data was entered correctly and to help visualize the progression of both load and slip during the test. Figure 4.13 shows a typical curve resulting from applying load over time to the free end of the embedded hooked rebar. There are generally three parts to the shape. The first part starts at 0 ksi rebar stress and runs up to about the 25 ksi of rebar stress. When 25 ksi of rebar stress was applied to each of the two hooks under load, the concrete column

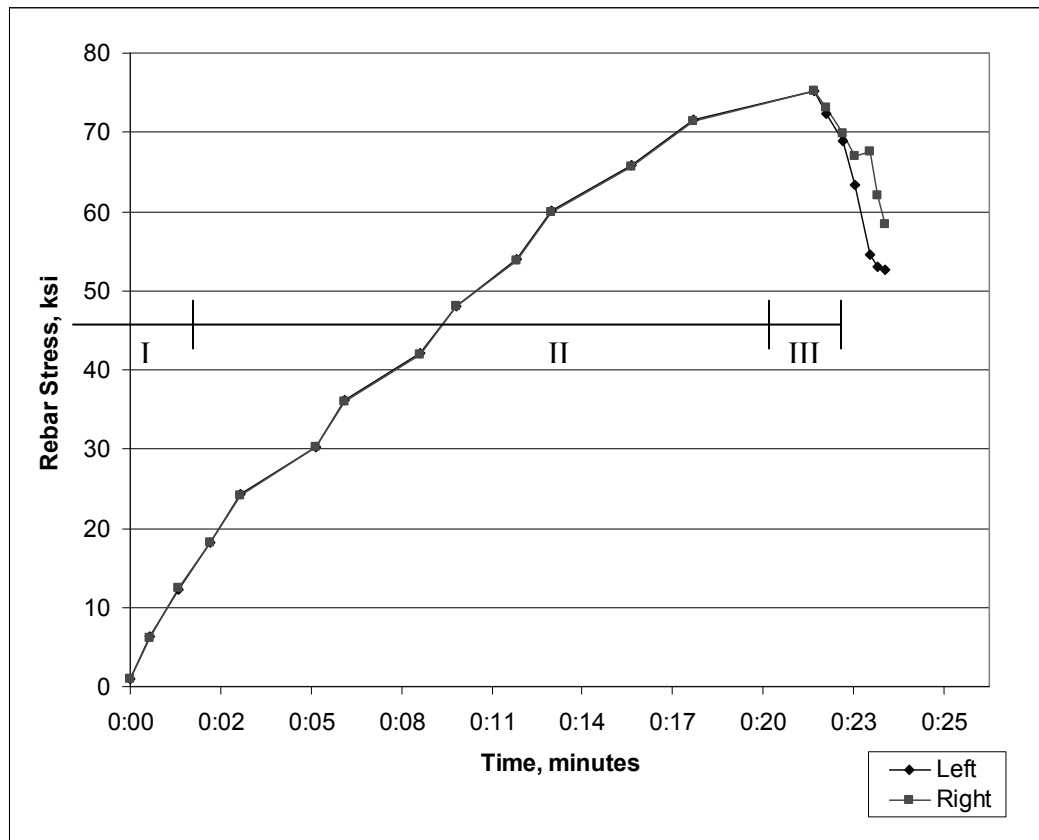


Figure 4.13: 3EA77b - load progression without load drops

cracked on the loaded face. The second part runs from 25 ksi to the ultimate load obtained. The slope is different in part two due to the elastic and plastic stretching of both the hooked rebar and the No.8 longitudinal rebar inside the specimen near the tension face. The third part is the post ultimate stress section. It is clear that even though capacity was rapidly being lost the rebar was still holding a high level of load. Of forty-two pullout tests, there was never a case when the load moved immediately from ultimate to

zero. In fact, after adding several additional increments of displacement on a couple specimens, the rebar stress never dropped below 9 ksi.

One of the lessons learned from Phase 1 testing was that the level of stress being held at a load stage tended to drop before loading commenced for the next stage. To get a better feel for how much the load was dropping, double data points were taken during two runs of pullout tests. Figure 4.14 displays what data from one of those tests looked like. Vertical segments are from when load was being increased and horizontal (or decreasing) segments are from the load holding time. If data points were taken at very small increments of time, such as 2 points per second, then the graph would be similar to Figure 4.14, but many times more jagged on the vertical steps. The overall shape in Figure 4.14 is the same as in Figure 4.13, which is expected as they are both from the 3EA77 series.

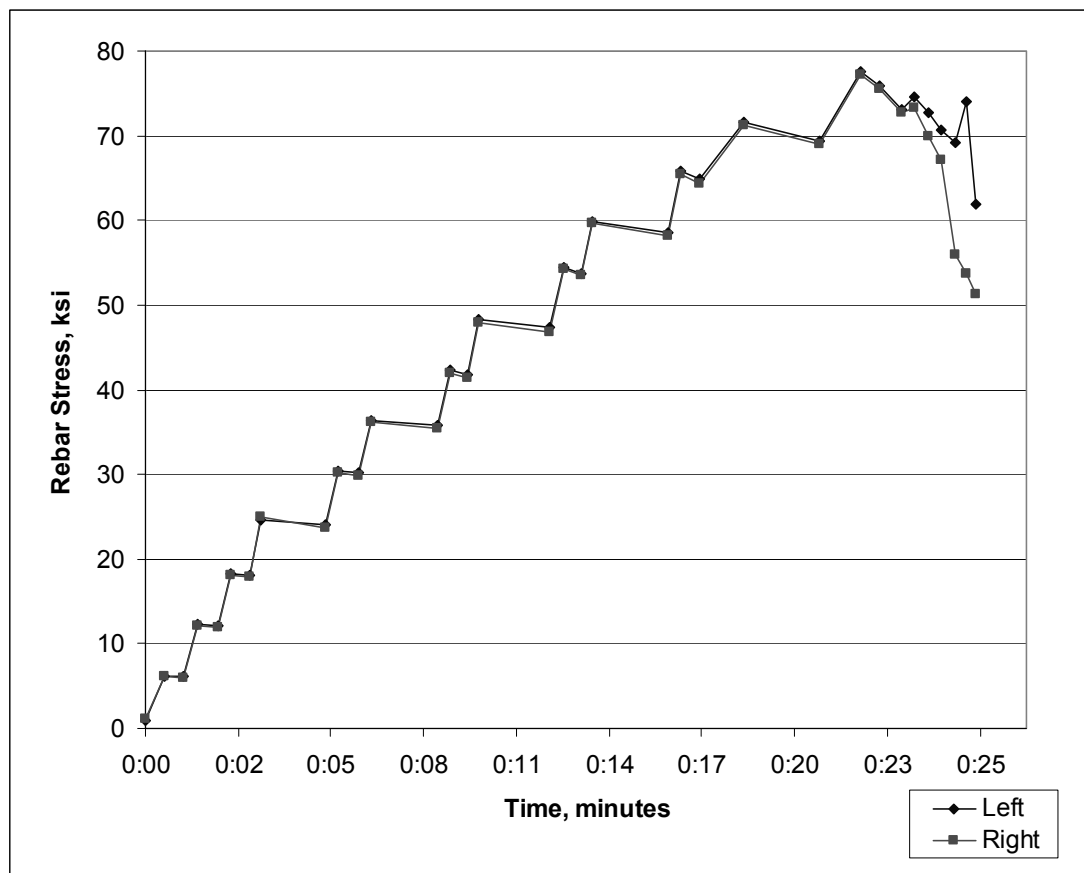


Figure 4.14: 3EA77f - load progression with load drops

To help see the slip data from a different perspective a plot of rebar slip vs. time was plotted and is shown in Figure 4.15. This data also has three parts, corresponding with the three parts from Figure 4.13. In general terms, the first part was horizontal, indicating that the rebar was not moving very much or at all. Part two was when the rebar was moving relative to the adjacent concrete. The movement can be attributed to elastic stretching, rebar slippage through loss of bond, increased concrete cracking, and concrete crushing on rib faces at higher loads. The third part was nearly vertical as a result of the beam column joint failing. High values of slip occurred after a maximum load was reached. In some cases there was minor side face and tension face spalling near the hooked rebar. In most cases there was only widespread cracking with the cracks very quickly getting longer and wider after ultimate load. The same data set was used for both Figure 4.14 and Figure 4.15 which gives a clear picture that despite the quickly increasing values of slip, there is still a significant holding capacity within the joint.

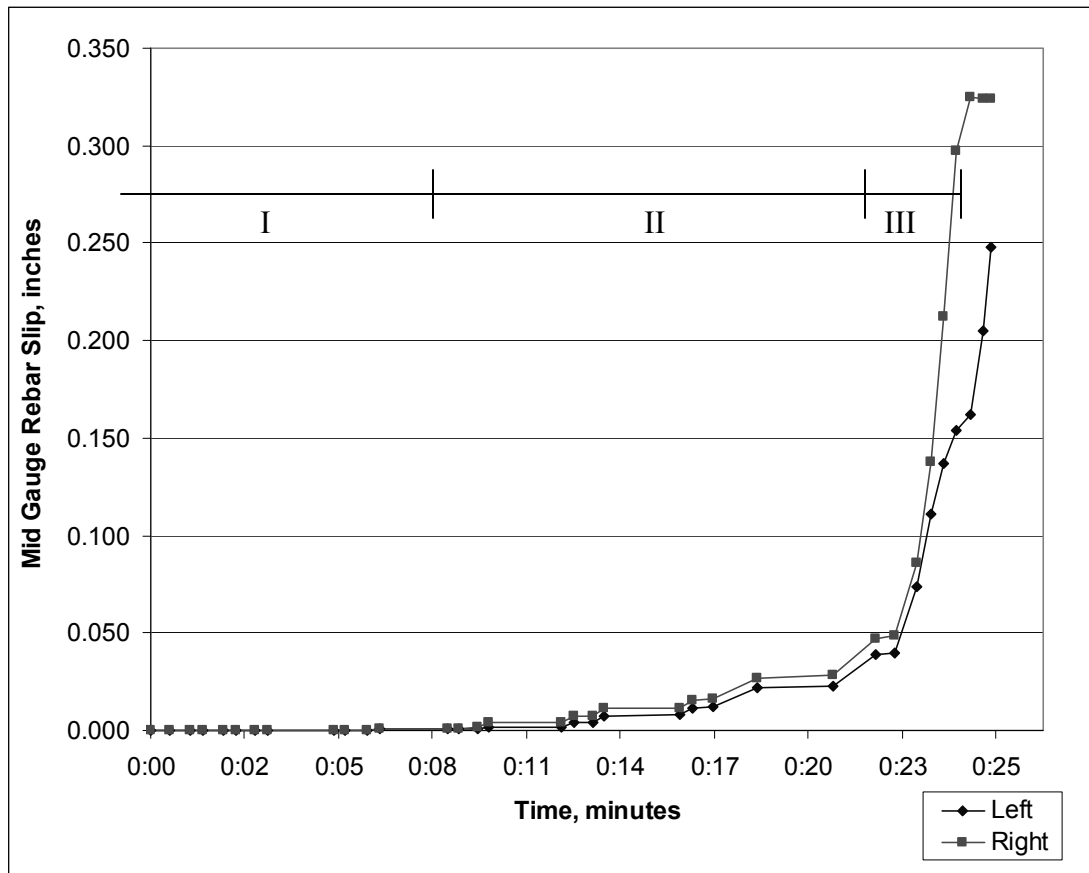


Figure 4.15: 3EA77f - slip progression with load drops

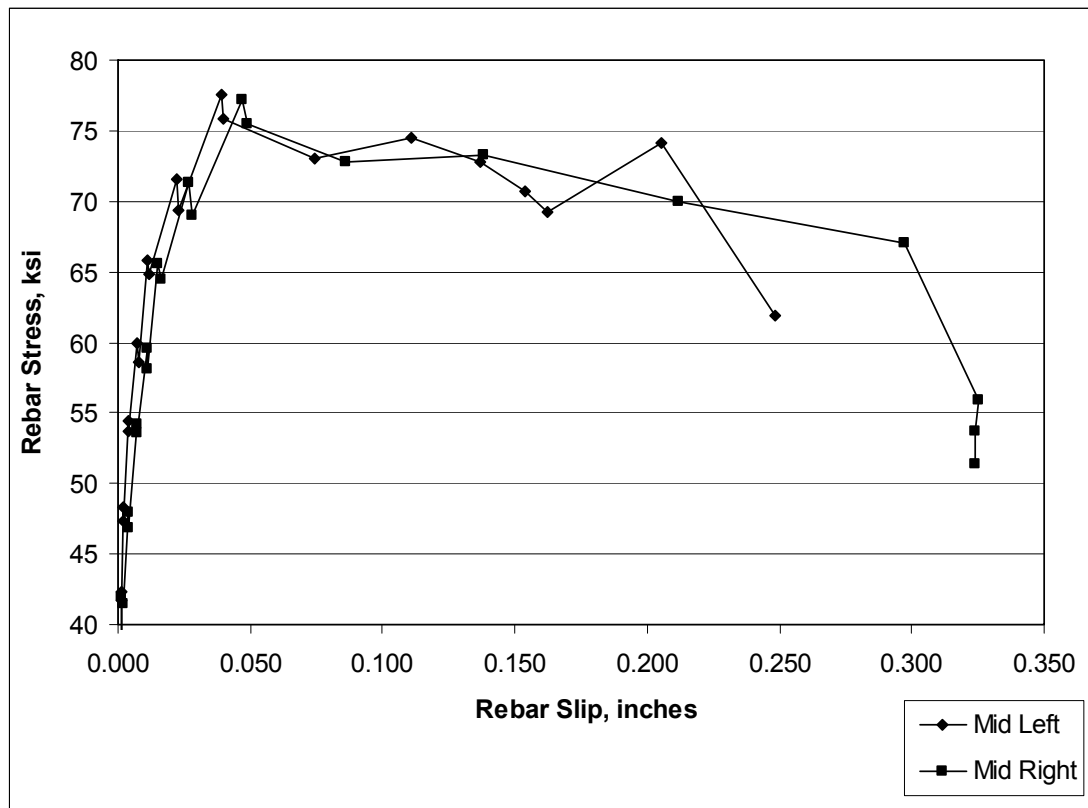


Figure 4.16: 3EA77f - middle gages stress VS slip

Figure 4.16 is a good representation of the stress versus slip curves generated for each specimen. The last three data points of the Mid Right curve show the reduction in applied stress as the Mid Left curve is given additional stress. This is one of the many cases where one side of the hydraulic system was isolated out so that additional stress could be applied to the other side of the system. The second to last data point of the Mid Left curve shows how even after the ultimate stress causes greatly increased rebar slip, the level of stress that can be applied to the joint can still be quite high. This extra capacity was observed on several of the test specimens. The counterpoint is that by re-achieving this high stress level the joint sustains a more sudden and increased level of damage, which causes a greater stress drop and higher slip. This does open a door to the idea that some internal mechanism is present which can sometimes allow stresses to redistribute for an increase in capacity, even if short lived.

4.3.3 Sample Calculations

A single run through the steps between raw data and final statistical ratios is included here. The series 3EA77 is used as an example with the rest of the series included where appropriate. The data reduction steps are presented first, with samples of the intermediate tables following. A set of calculations of the statistics is included as well.

Non-digital dial gages were used for the slip measurements and no effort was made to align them all to zero before testing began. One of the first steps working with the raw data was to zero-out the slip values. The data from each test specimen was then integrated into the master table of results for all series and specimens.

Data Reduction Steps:

1. Record raw numbers from photographs into master data spreadsheet with data separated for each specimen.
2. Create individual spreadsheet for each specimen. Link data from master sheet to individual sheets. This sheet helps identify:
 - a. Raw data entered incorrectly
 - b. Dial gages that recorded values in reverse direction from the other gages
 - c. The testing run time for that specimen
 - d. The key load points: 30ksi, 42ksi, and 60ksi as well as the maximum stable load achieved
 - e. Displacement gages that failed to record any data
 - f. The last displacement gage reading that is accepted is correct
 - g. The displacement gage readings that occurred after the gage had failed
 - h. The absolute maximum load recorded during the test
 - i. The rebar slip values for each key load

The sheet also contains several graphs to help visually identify interesting points within the test. These sheets included:

- a. Load Progression Over Time
- b. Slip Progression Over Time
- c. Rebar Stress VS. Slip curves run to:
 - i. Max Load
 - ii. Max Load plus 1 reading
 - iii. final data before gage failure
- d. Specific location Rebar Stress VS. Slip curves for:
 - i. Left and Right Top Gages
 - ii. Left and Right Mid Gages
 - iii. Left and Right Bot Gages
 - iv. Top, Mid & Bot Left Gages
 - v. Top, Mid & Bot Right Gages

- vi. All data points gathered for specimen
- 3. Create a new Excel file and spreadsheet to facilitate further data handling.
- 4. On sheet 1 the key data is linked from Step 2 to show the Slip values for all six displacement gages at the load values of 30ksi, 42ksi, 60ksi, max load, and max plus 1 step. This sheet also serves as a gathering point for all other sheets within the file and as a working surface for various data explorations further described below.
- 5. For each key load and location the summary data is used to find:
 - a. Mean
 - b. Standard Deviation
 - c. Low value
 - d. High value
 - e. Range
 - f. Number of valid specimens per series
 - g. Confidence Interval (2 sided, 95%)
- 6. Create graphical comparisons across paired series for Slip VS. the following:
 - a. Stirrup Spacing (3db and 7db) for:
 - i. Standard Deviation from (and with) Mean
 - 1. Top location
 - 2. Mid location
 - ii. 95% Confidence Interval from (and with) Mean
 - 1. Top location
 - 2. Mid location
 - b. Coating Type (A775, A934 and Black) for:
 - i. Standard Deviation from (and with) Mean
 - 1. Top location
 - 2. Mid location
 - ii. 95% Confidence Interval from (and with) Mean
 - 1. Top location
 - 2. Mid location
- 7. Create graphs for Slip VS. Bar Stress for the Bot location across all series using raw values for:
 - a. Max Load
 - b. Max Load and Max Load plus 1 reading

Not enough usable data for the Bot location resulted from testing to make meaningful graphical and statistical comparisons as could be done with the Top and Mid locations.
- 8. Extract from the specimen specific spreadsheets the precise load value for the key load points: 30ksi, 42ksi, and 60ksi.
 - a. Find the mean, standard deviation, range, low and high values across each key load category for each specimen arrangement.
 - b. Compare the collected values to see if the extracted loads are acceptably close to the target key load value.
 - c. Compare the exact load ranges recorded to the maximum reading accuracy of the recording system. The maximum reading accuracy was about +/- 200 lbf.

9. Perform statistical analysis
 - a. Determine if compared variances are equal or not equal using f-test
 - b. Determine if compared means are equal or not equal using t-test
 10. Create series comparison ratios
 - a. Series with statistically equal means receive a “1”.
 - b. Not-same series are set to ratio by dividing
 - i. Coated / Uncoated
 - ii. A934 / A775
 - iii. 7*db / 3*db
 - c. Non-comparable series receive a “0” and are excluded from further use
 - d. Find mean for each comparable combination using ratios from each key load point: 30ksi, 42ksi, and 60ksi.
 - i. Top mean slip ratio
 - ii. Mid mean slip ratio
 11. Apply ratios to bar graphs for easier cross comparison and trend identification
- END

Table 4.6:
Raw Data From Specimen 3EA77e

7.17 Left			Right			0.6			
time	lapse	progress	system		picture	left	right	left	right
			pressure ksi			bar load kip	bar load ksi		
1:44:38	0:00:00	0:00:00	55	67	1450	0.394	0.480	0.657	0.801
1:45:14	0:00:36	0:00:36	522	505	1451	3.743	3.621	6.238	6.035
1:46:08	0:00:54	0:01:30	1027	1004	1452	7.364	7.199	12.273	11.998
1:47:05	0:00:57	0:02:27	1529	1505	1453	10.963	10.791	18.272	17.985
1:48:01	0:00:56	0:03:23	2062	2033	1454	14.785	14.577	24.641	24.294
1:50:24	0:02:23	0:05:46	2556	2524	1455	18.327	18.097	30.544	30.162
1:51:25	0:01:01	0:06:47	3046	3023	1456	21.840	21.675	36.400	36.125
1:53:48	0:02:23	0:09:10	3539	3519	1457	25.375	25.231	42.291	42.052
1:54:42	0:00:54	0:10:04	4003	3980	1458	28.702	28.537	47.836	47.561
1:57:05	0:02:23	0:12:27	4496	4482	1459	32.236	32.136	53.727	53.560
1:57:56	0:00:51	0:13:18	5001	4975	1460	35.857	35.671	59.762	59.451
2:00:26	0:02:30	0:15:48	5511	5482	1461	39.514	39.306	65.856	65.510
2:02:08	0:01:42	0:17:30	5952	5935	1462	42.676	42.554	71.126	70.923
2:05:38	0:03:30	0:21:00	5770	5694	1463	41.371	40.826	68.952	68.043
2:06:10	0:00:32	0:21:32	5633	5540	1464	40.389	39.722	67.314	66.203
2:07:03	0:00:53	0:22:25	5491	5352	1465	39.370	38.374	65.617	63.956
2:07:40	0:00:37	0:23:02	5746	4653	1466	41.199	33.362	68.665	55.603
						0.000	0.000	0.000	0.000
MaxValue			6379	6370		45.737	45.673	76.229	76.122

Step	Dial Gages						picture
	top left	top right	mid left	mid right	bot left	bot right	
1	0.000	0.000	0.000	0.000	0.000	0.000	
2	0.000	0.000	0.000	0.000	0.000	0.000	
3	0.000	0.000	0.000	0.000	0.000	0.000	
4	0.000	0.001	0.000	0.000	0.000	0.000	
5	0.003	0.004	0.000	0.000	0.000	0.000	
6	0.004	0.005	0.000	0.000	0.000	0.000	
7	0.008	0.008	0.000	0.001	0.000	0.000	
8	0.011	0.014	0.000	0.002	0.000	0.000	
9	0.018	0.020	0.001	0.003	0.000	0.000	
10	0.027	0.030	0.004	0.008	0.000	0.000	
11	0.039	0.042	0.008	0.013	0.000	0.000	
12	0.056	0.060	0.015	0.021	0.001	0.001	
13	0.092	0.099	0.034	0.042	0.008	0.008	Max
14	0.102	0.141	0.103	0.131	0.051	0.048	Max + 1
15	0.250	0.331	0.157	0.220	0.092	0.094	
16	0.268	0.317	0.197	0.298	0.123	0.135	
17	0.271	0.575	0.265	0.324	0.188	0.153	
0							

Table 4.7:
Data From Series 3EA77

Column	L, left R, right	Rebar Slip					
		30 ksi			42 ksi		
		top	mid	bot	top	mid	bot
9	3EA77aL		0	0		0.001	0.001
10	3EA77bL	0.002	0	0	0.007	0.001	0
11	3EA77cL	0.003	0	0	0.009	0.001	0
12	3EA77dL	0.006	0	0	0.013	0.001	0
13	3EA77eL	0	0	0	0	0	0
14	3EA77fL	0.003	0	0	0.008	0.001	0
15	3EA77gL	0.003	0	0	0.011	0	0.002
9	3EA77aR	0	0	0	0	0.001	0
10	3EA77bR	0	0	0	0.001	0.001	0
11	3EA77cR		0	0		0.001	0
12	3EA77dR		0	0		0	0
13	3EA77eR	0	0	0	0	0	0
14	3EA77fR		0	0		0.001	0.001
15	3EA77gR	0.001	0	0	0.007	0	0
	mean	0.0018	0	0	0.0056	0.0006	0.0003
	stdev	0.00199	0	0	0.00495	0.00050	0.00061
	Low	0	0	0	0	0	0
	High	0.006	0	0	0.013	0.001	0.002
	Range	0.006	0	0	0.013	0.001	0.002

Column	L, left R, right	60 ksi			bot		bot	
		top	mid	bot	max load		max load +1 step	
					ksi	slip	ksi	slip
9	3EA77aL		0.007	0.001	77.54	0.011	77.69	0.015
10	3EA77bL	0.027	0.01	0	71.62	0.004	75.15	0.032
11	3EA77cL	0.027	0.009	0.001	77.62	0.011	76.09	0.041
12	3EA77dL	0.041	0.011	0	71.72	0.009	71.03	0.054
13	3EA77eL	0	0	0	71.13	0	68.95	0
14	3EA77fL	0.029	0.007	0	77.51	0.006	75.85	0.007
15	3EA77gL	0.03	0.007	0.003	71.93	0.061	69.47	0.096
9	3EA77aR	0.001	0.007	0.001	76.71	0.1	76.78	0.115
10	3EA77bR	0.008	0.007	0	71.44	0.002	75.23	0.02
11	3EA77cR		0.006	0	77.23	0.008	75.85	0.034
12	3EA77dR		0.004	0	71.51	0.011	70.85	0.052
13	3EA77eR	0	0	0	70.92	0	68.04	0
14	3EA77fR		0.011	0.001	77.23	0.012	75.50	0.013
15	3EA77gR	0.024	0.01	0	71.47	0.067	68.35	0.132
	mean	0.0187	0.0069	0.0005	73.97	0.0216	73.20	0.0436
	stdev	0.01500	0.00353	0.00085	3.02	0.03089	3.52	0.04254
	Low	0	0	0	70.92	0	68.04	0
	High	0.041	0.011	0.003	77.62	0.1	77.69	0.132
	Range	0.041	0.011	0.003	6.69	0.1	9.64	0.132

Table 4.8:
Summary Of Statistics Across All Series

	30 ksi			42 ksi			60 ksi		
	top	mid	bot	top	mid	bot	top	mid	bot
3EA77aL									
mean	0.0018	0	0	0.0056	0.0006	0.0003	0.0187	0.0069	0.0005
stdev	0.00199	0	0	0.00495	0.00050	0.00061	0.01500	0.00353	0.00085
n	10	14	14	10	14	14	10	14	14
3EA73aL									
mean	0.0039	0.0003	0.0001	0.0097	0.0006	0.0002	0.0306	0.0045	0.0004
stdev	0.00173	0.00047	0.00027	0.00330	0.00074	0.00058	0.00490	0.00210	0.00084
n	10	14	14	10	14	14	10	14	14
3EA97aL									
mean	0.0044	0.0004	0	0.0110	0.0009	0	0.0322	0.0074	0
stdev	0.00108	0.00065	0	0.00229	0.00083	0	0.00385	0.00238	0
n	14	14	14	14	14	14	14	14	14
3EA93aL									
mean	0.0039	0	0	0.0112	0.0005	0	0.0335	0.0042	0
stdev	0.00141	0	0	0.00236	0.00052	0	0.00663	0.00283	0
n	14	14	14	14	14	14	14	14	14
3B_7aL									
mean	0.0025	0	0	0.0083	0.0002	0	0.0248	0.0027	0
stdev	0.00105	0	0	0.00121	0.00041	0	0.00271	0.00052	0
n	6	6	6	6	6	6	6	6	6
3B_3aL									
mean	0.0028	0	0	0.0078	0	0	0.0235	0.0017	0
stdev	0.00117	0	0	0.00214	0	0	0.00373	0.00103	0
n	6	6	6	6	6	6	6	6	6

Sample Statistical Analysis from Series 3EA77 and 3EA73:

Data set 3EA73	30ksi, Top Gage	Data set 3EA77
$x1 := 0.0039$	mean	$x2 := 0.0018$
$s1 := 0.00173$	standard deviation	$s2 := 0.0020$
$n1 := 10$	number of data points	$n2 := 10$

Variances are unknown and possibly unequal

T-test hypothesis:

Ho: $\mu_1 - \mu_2 = 0$

Ha: $\mu_1 - \mu_2 > 0$

$\alpha_{t_test} := 0.05$ for a two tailed t-test

$\alpha_{f_test} := 0.10$

σ_1^2 and σ_2^2 are unknown

$$F_{S1} := \frac{s1^2}{s2^2} \quad F_{S1} = 0.748$$

$$F_{S2} := \frac{s2^2}{s1^2} \quad F_{S2} = 1.336$$

The larger of $s1$ and $s2$ should be the numerator, so...

$$F_S := \text{if}(F_{S1} > F_{S2}, F_{S1}, F_{S2}) \quad F_S = 1.336$$

F-test Hypothesis:

Ho: $\sigma_1^2 = \sigma_2^2$

Ha: $\sigma_1^2 \neq \sigma_2^2$

Fb	$\alpha / 2$	0.05		
	n2-1	9	over	
	n1-1	9	down	
			F-test table =>	$F_b := 3.18$
Fa	$1 - (\alpha / 2)$	0.95	F-test table	
	n1-1	9	over	
	n2-1	9	down	
			F-test table =>	$\text{output_a} := 3.18$
			$F_a := \frac{1}{\text{output_a}}$	$F_a = 0.314$

Is F_S between F_a and F_b ?

$$F_a = 0.314 \quad F_b = 3.18$$

$$F_S = 1.336$$

$$F_{\text{decision}} := \text{if}(F_S > F_a, \text{if}(F_S < F_b, \text{"YES"}, \text{"NO"}), \text{"NO"}) \quad F_{\text{decision}} = \text{"YES"}$$

If **YES**, accept H_0 and assume $\sigma_1^2 = \sigma_2^2$

$$t_{\text{test_number}} := n_1 + n_2 - 2$$

$$t_{\text{test_number}} = 18$$

$$s_{\text{squared}} := \frac{(n_1 - 1) \cdot s_1^2 + (n_2 - 1) \cdot s_2^2}{t_{\text{test_number}}}$$

$$s_{\text{squared}} = 0.000003496$$

$$t_{\text{test_value}} := \frac{(x_1 - x_2) - 0}{\sqrt{\left(\frac{s_{\text{squared}}}{n_1}\right) + \left(\frac{s_{\text{squared}}}{n_2}\right)}}$$

$$t_{\text{test_value}} = 2.511$$

$$\begin{array}{cc} \text{t-test} & \alpha \\ & n_1 + n_2 - 2 \end{array} \quad \begin{array}{cc} 0.05 \\ t_{\text{test_number}} = 18 \end{array}$$

$$\text{t-test table} \Rightarrow \quad t := 1.734$$

Is $t_{\text{test_value}}$ greater or less than $t(\alpha, n_1 + n_2 - 2)$?

$$t_{\text{decision}} := \text{if}(t_{\text{test_value}} < t, \text{"Less than"}, \text{"Greater than"}) \quad t_{\text{decision}} = \text{"Greater than"}$$

If $t_{\text{test_value}}$ is "Less than" t
Accept H_0 : $\mu_1 = \mu_2$
the means are the same

If $t_{\text{test_value}}$ is "Greater than" t
Reject H_0 : $\mu_1 \neq \mu_2$
Accept H_a : $\mu_1 - \mu_2 > 0$
the means are different

If **NO**, reject H_0 , accept H_a : $\sigma_1^2 \neq \sigma_2^2$

$$t_{\text{test_value}} := \frac{x_1 - x_2}{\sqrt{\left(\frac{s_1^2}{n_1}\right) + \left(\frac{s_2^2}{n_2}\right)}}$$

$$t_{\text{test_value}} = 2.511$$

$$v := \frac{\left[\left(\frac{s_1^2}{n_1}\right) + \left(\frac{s_2^2}{n_2}\right)\right]^2}{\frac{\left(\frac{s_1^2}{n_1}\right)^2}{n_1 - 1} + \frac{\left(\frac{s_2^2}{n_2}\right)^2}{n_2 - 1}}$$

$$v = 17.634$$

$$t_{\text{test_number}} := v$$

```

t-test    alpha      0.05
          n1+n2-2    t_test_number = 18
          t-test table =>    t := 1.734

```

Is t_test.value greater or less than t(alpha, v)?

```

t_decision := if(t_test_value < t, "Less than" , "Greater than" )    t_decision = "Greater than"

```

<p>If t_test.value is "Less than" t</p> <p>Accept Ho: $\mu_1 = \mu_2$</p> <p>the means are the same</p>	<p>If t_test.value is "Greater than" t</p> <p>Reject Ho: $\mu_1 = \mu_2$</p> <p>Accept Ha: $\mu_1 - \mu_2 > 0$</p> <p>the means are different</p>
--	--

END CALCULATION

Table 4.9:
Statistical Analysis Output For All Series

Combinations	30 ksi			42 ksi			60 ksi		
	top	mid		top	mid		top	mid	
		Variance	mean		Variance	mean		Variance	mean
3EA73	3EA77	Same	not	na	not	same	not	not	not
3B_3	3EA93	Same	same	na	not	same	Same	same	same
	3B_3	Same	same	na	not	not	not	Same	not
3EA77	3EA97	not	not	na	not	same	not	Same	same
3B_7	3B_7	not	same	na	not	not	not	not	not
	3EA97	Same	same	na	not	same	not	not	not
3EA93	3EA97	Same	same	na	not	same	not	Same	not
3B_3	3B_3	Same	same	na	not	same	not	Same	not
	3B_7	Same	not	na	not	not	Same	not	not
3B_3	3B_7	Same	same	na	not	same	Same	Same	not

Combinations	30 ksi			42 ksi			60 ksi		
	top	mid		top	mid		top	mid	
		Variance	mean		Variance	mean		Variance	mean
3EA73	3EA77	3EA73	3EA77	3EA73	3EA77		3EA73	3EA77	3EA77
3EA93		3EA73	3EA93						
3B_3		3EA73	3B_3				3EA73	3B_3	3B_3
3EA77	3EA97	3EA77	3EA97	3EA77	3EA97		3EA77	3EA97	
3B_7									
3EA93		3EA93	3EA97					3EA77	3B_7
3B_3				3EA93	3B_3		3EA93	3B_3	3B_3
3EA97	3B_7	3EA97	3B_7	3EA97	3B_7		3EA97	3B_7	3B_7
3B_3								3B_3	3B_7

Higher mean slip value is shaded. Blank spaces indicate series are statistically the same.

The left table is a summary of statistical analysis performed for comparing each pair of series. The tests showed the series to be the same, not the same, or NA when zeros were present in the incoming data.

The right table indicates which series need to have ratios calculated and which series has the higher mean value. Blank spaces indicated the compared series were statistically the same.

Table 4.10:
Full Set Of Series Ratios

		(Coated / Uncoated),		(A9 / A7),		(7db / 3db)			
Combinations		30 ksi		42 ksi		60 ksi		mean slip ratio	
		top	mid	top	mid	top	mid	top	mid
3EA73	3EA77	0.46	0	0.58	1	0.61	1.52	0.55	0.85
	3EA93	1	0	1	1	1	1	1.00	0.68
	3B_3	1	29	1	64	1.30	2.70	1.10	31.85
3EA77	3EA97	2.42	43	1.96	1	1.72	1	2.04	14.95
	3B_7	1	1	1	3.86	1	2.57	1.00	2.48
3EA93	3EA97	1	43	1	1	1	1.76	1.00	15.21
	3B_3	1	1	1.43	50	1.43	2.53	1.29	17.84
3EA97	3B_7	1.74	43	1.32	5.57	1.30	2.79	1.45	17.07
3B_3	3B_7	1	1	1	1	1	1.60	1.00	1.20

In the first run of calculating ratios all the values were included. The shaded values were ratios where one or both of the series had a zero value. A significantly small number was used in place of an actual zero to keep the automatic-calculations running without errors. The shaded ratios are then removed so that the data is not skewed by the presence of a zero. For the purpose of comparing ratios, series identified as being statistically the same receive a one.

Table 4.11:
Reduced Set Of Series Ratios

		(Coated / Uncoated),		(A9 / A7),		(7db / 3db)			
Combinations		30 ksi		42 ksi		60 ksi		mean slip ratio	
		top	mid	top	mid	top	mid	top	mid
3EA73	3EA77	0.46		0.58	1	0.61	1.52	0.55	1.26
	3EA93	1		1	1	1	1	1.00	1.00
	3B_3	1		1		1.30	2.70	1.10	2.70
3EA77	3EA97	2.42		1.96	1	1.72	1	2.04	1.00
	3B_7	1	1	1	3.86	1	2.57	1.00	2.48
3EA93	3EA97	1		1	1	1	1.76	1.00	1.38
	3B_3	1	1	1.43		1.43	2.53	1.29	1.76
3EA97	3B_7	1.74		1.32	5.57	1.30	2.79	1.45	4.18
3B_3	3B_7	1	1	1	1	1	1.6	1.00	1.20

The mean slip ratios for each set of compared series here are then put to graphical form for an easier visual comparison. The graphs can be found in Chapter 4: Results.

4.3.4 Effect of Tie Spacing

This section is broken into two parts: first will be a comparison of tie spaces using only Phase 2 specimens, and second will be a comparison using only Phase 3 specimens.

4.3.4.1 Phase 2

In Phase 2 specimens with variable tie spacings and black hooked bars were compared at various rebar stress levels. The data analysis method used in Phase 2 is different from that used in Phase 3 due to an insufficient sample size, data lost due to malfunctions within the experimental setup, and the irrational results of the analysis when the Phase 3 approach was attempted.

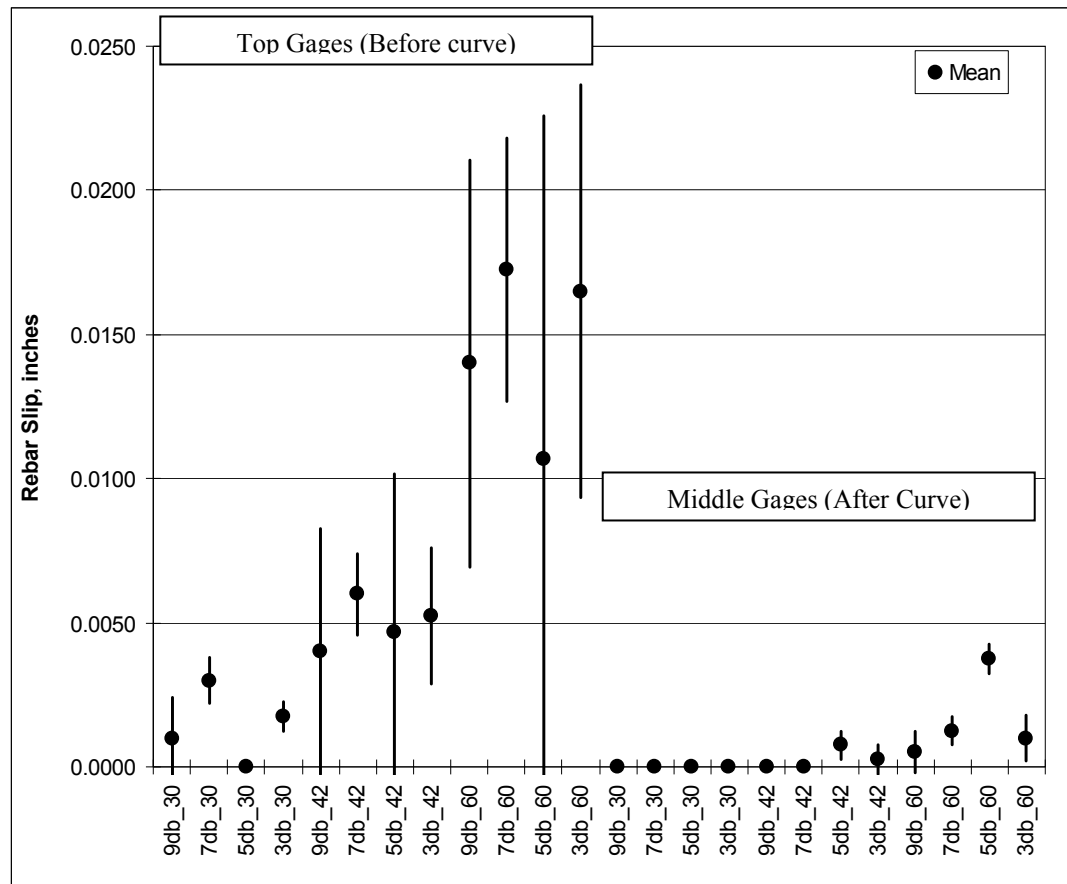


Figure 4.17: +/- One standard deviation from mean for the top & mid gage

Figure 4.17 and Figure 4.18 use +/- one standard deviation from the data series mean to provide a way to compare the series. This method leaves out statistical comparisons that help to reduce false conclusions and instead relies on the raw data

without modification. The mean values shown in Figure 4.17 can be found in Table 4.5. The 30, 43, and 60 designations denote which level of kips per square inch (ksi) the value is related to. Additional figures using the standard deviation and confidence interval about the mean can be found in the appendix.

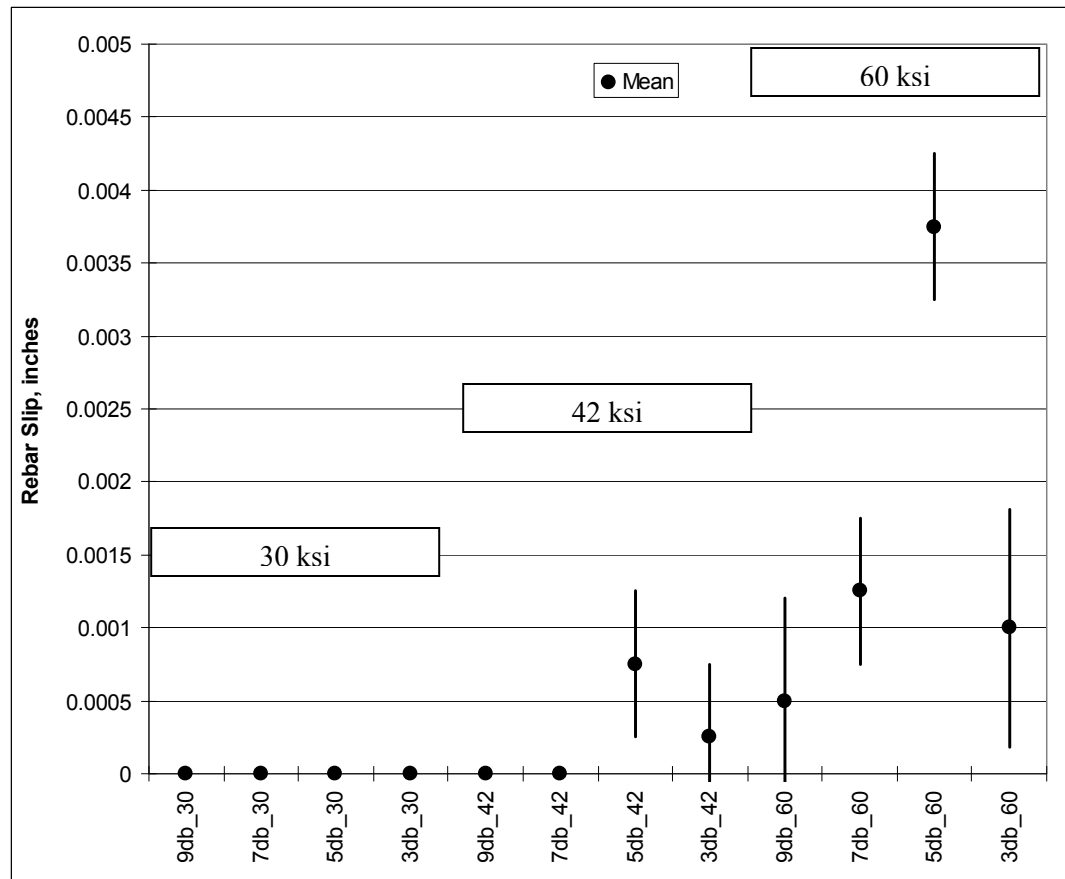


Figure 4.18: +/- One standard deviation from mean for the mid gage

Figure 4.18 is an enlarged view of the same data found in Figure 4.17 regarding the Mid gage. There are only a couple of items of value to note from these figures. The first item is that across all four values of tie spacing, as the stress level increases in the hooked rebar from low to high, the value of the recorded slip increases as well. The second item is that across all four values of tie spacing (with consideration of the raw nature of the data), as the tie spacing increases, the value of the recorded slip does not increase. This seems to indicate that the tie spacing, across the values used, has little

effect on slip values. Instead, the level of stress by itself controls the level of slip experienced by the rebar.

The relationship between stress and slip is well known, but the idea that decreased tie spacing does not correlate to a decrease in slip is contradictory to common tie reinforcement theory and practice. Normally it is believed that a higher joint strength, hook capacity, and joint stiffness can be achieved by reducing the tie spacing (which is also increasing the reinforcement ratio of steel to concrete). The number of specimens used in Phase 2 is small though and so seems very likely the cause of some misdirection. If the data that was collected happened to be the outliers of a hypothetical larger sample size then the observations made could be very different. At this point there is no way to know for sure. Phase 3 of this research program uses many more specimens and these ideas will be revisited for a reduced scope of two tie spaces, $3*d_b$ and $7*d_b$.

4.3.4.2 Phase 3

In an early attempt to utilize the vast amount of data in a meaningful way, a set of figures were created which show all the separate series using standard deviations and confidence intervals as range values from the series mean. It quickly became apparent that a more in-depth analysis would be needed to make definitive comparisons because the series mean values and the improvised series range values often didn't clearly show which series had higher values. The very wide coverage of the range values is caused by the shortage of data points and the inconsistent nature of reinforced concrete when analyzed precisely. The figures for both Phase 2 and Phase 3 of the program can be found in the appendix.

The statistical analysis consisted of checking to see if each comparable series had the same variability and the same means. An F-test was performed first, using alpha equal to 0.05 to compare the variability. If the F-test showed that the two series being compared had the same variability, then a two sided T-test, with alpha equal to 0.05, was used to compare the means. When the F-test showed different variability existed between two series, then the degrees of freedom for the T-test were estimated. A more detailed description of where the values used for the figures in this chapter came from can be found in the Sample Calculations previously presented.

Because the ACI Code (318-05) requires the tie spacing to be $3*d_b$ if the standard reduction factors are to be used, the comparison in Figure 4.19 and Figure 4.20 use the $3*d_b$ spacing as the base value for establishing the slip ratios.

In Figure 4.19 all three stress values (30ksi, 42ksi, and 60ksi) are used for comparing slip ratios. According to the Top gages there is no difference between the Uncoated (3B_) rebar and the A934 (3EA9) coated rebar, but the A775 (3EA7) coated rebar has almost half as much slip as the other two. The Mid gages show a different picture. All three sets at the Mid gage have slip ratios between 1.2 and 1.4, which is fairly tightly grouped and shows a more uniform reaction to the applied load than seen at the Top gage.

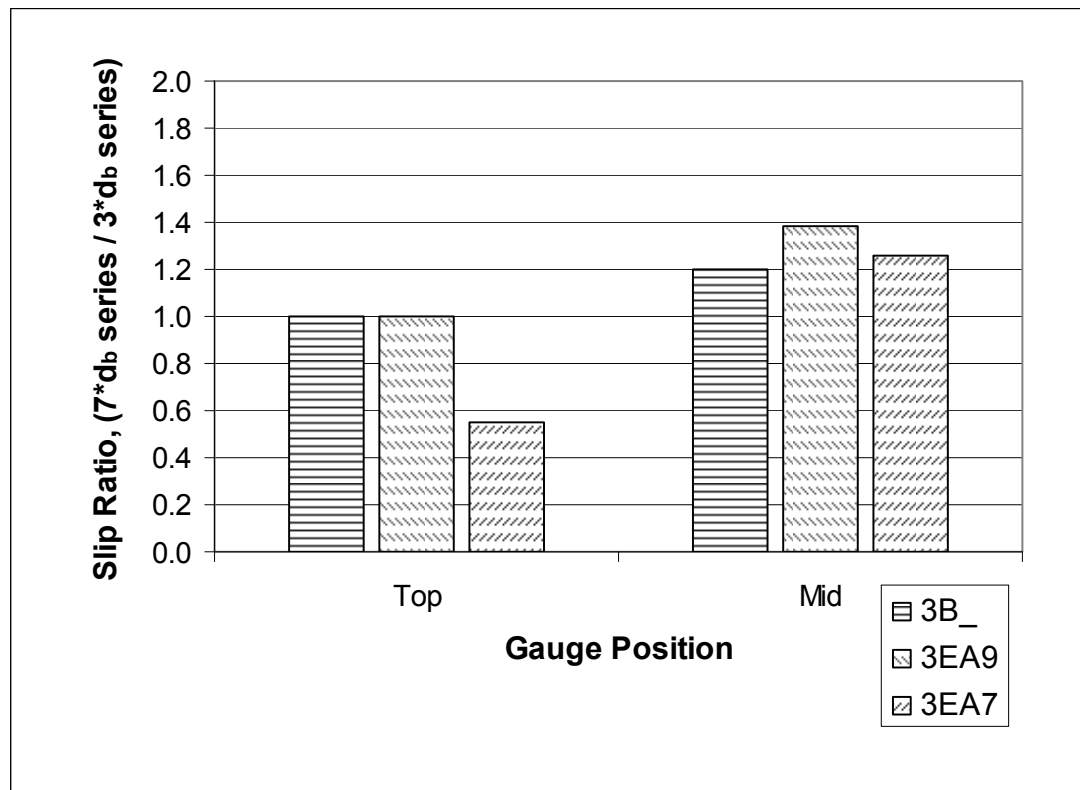


Figure 4.19: Slip ratios for tie spacing for all stress values

In Figure 4.20, the 60ksi bar stress has been separated from the other stress levels. At the Top gage there is no change from the results in Figure 4.19, but at the Mid gages the value of the ratios have risen. The 60ksi level also shows that the A775 bars experienced less relative slip than the A934 bars at higher stress levels.

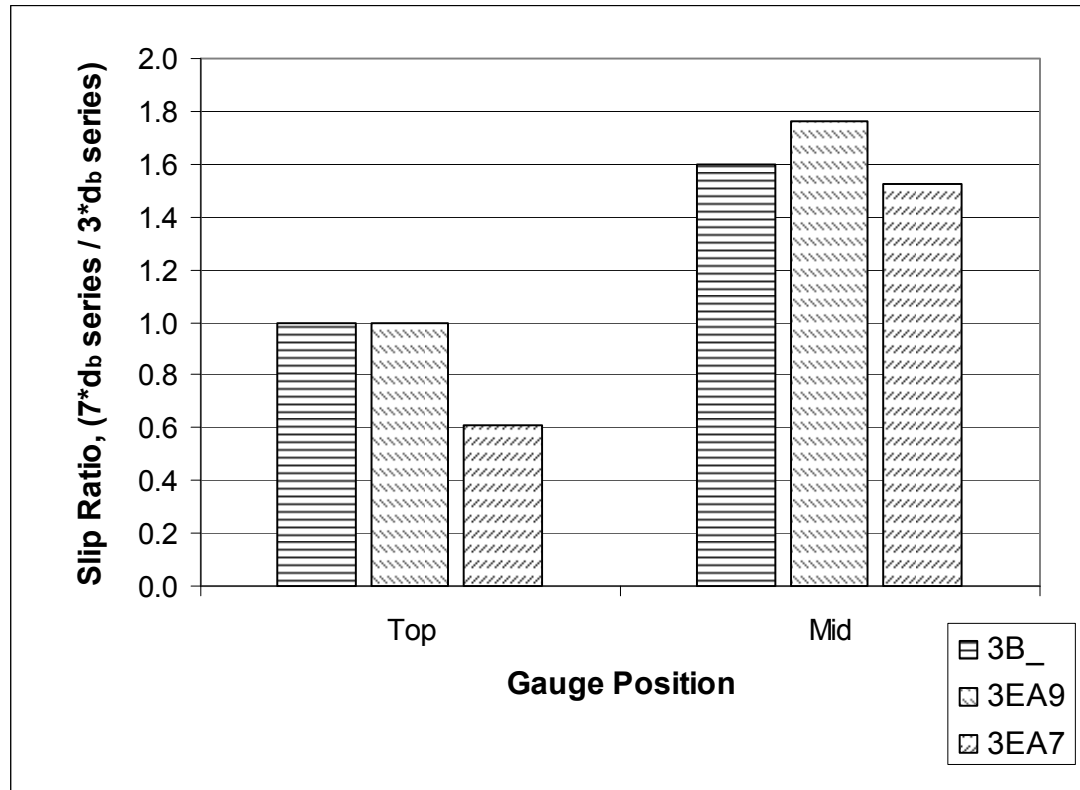


Figure 4.20: Slip ratios for ties spacing at the 60 ksi stress level

Returning to the issues raised previously in Phase 2 regarding tie spacing and stress levels in relation to the amount of slip recorded; in Phase 3 there was more relative slip recorded for the higher tie spacing and even more relative slip recorded for the higher level of stress.

4.3.5 Effect of Coating Hooked Rebar

The Coated series are compared to the Uncoated series using the Uncoated series as the standard base for Figure 4.21 and Figure 4.22. The Uncoated slip value is not set to 1.0, instead it is the recorded value from the testing data of the similar series. This means that the 3*d_b and 7*d_b series have differing values to compare against, but it also means that the values that are being compared are from specimens set up in the most similar manner. As before, the first figure uses all three stress levels and the second figure segregates the data for the 60 ksi level of rebar stress.

There are many combinations for comparisons that can be made in Figure 4.21 so only generalizations will be made here. At the Top gage, the A775 rebar seems to slip similarly to the Uncoated rebar, but the A934 rebar has 25% to almost 50% more slip. At the Mid gage the slip values have significantly increased and both Coating types are slipping more than the Uncoated bar. The situation is exacerbated for the A934 bar where a large difference exists between the 3*db and 7*db tie spacing. This appears to indicate that when the A934 bar is well confined it performs closer to the Uncoated bar, but with a small adjustment to the tie spacing towards less confinement then the A934 bar slips much more than the Uncoated bar. At the Mid gage, the A775 bar has unexpectedly high values of relative slip, but is fairly consistent between the two tie spacings. Previous research programs had indicated that only a 1.2 factor would be needed to correct for having Coated rebar verses Uncoated rebar. The values in this figure for A775 rebar, which is the same type of rebar tested by Hamad et al. 93, suggest a factor closer to 2.5 may be needed.

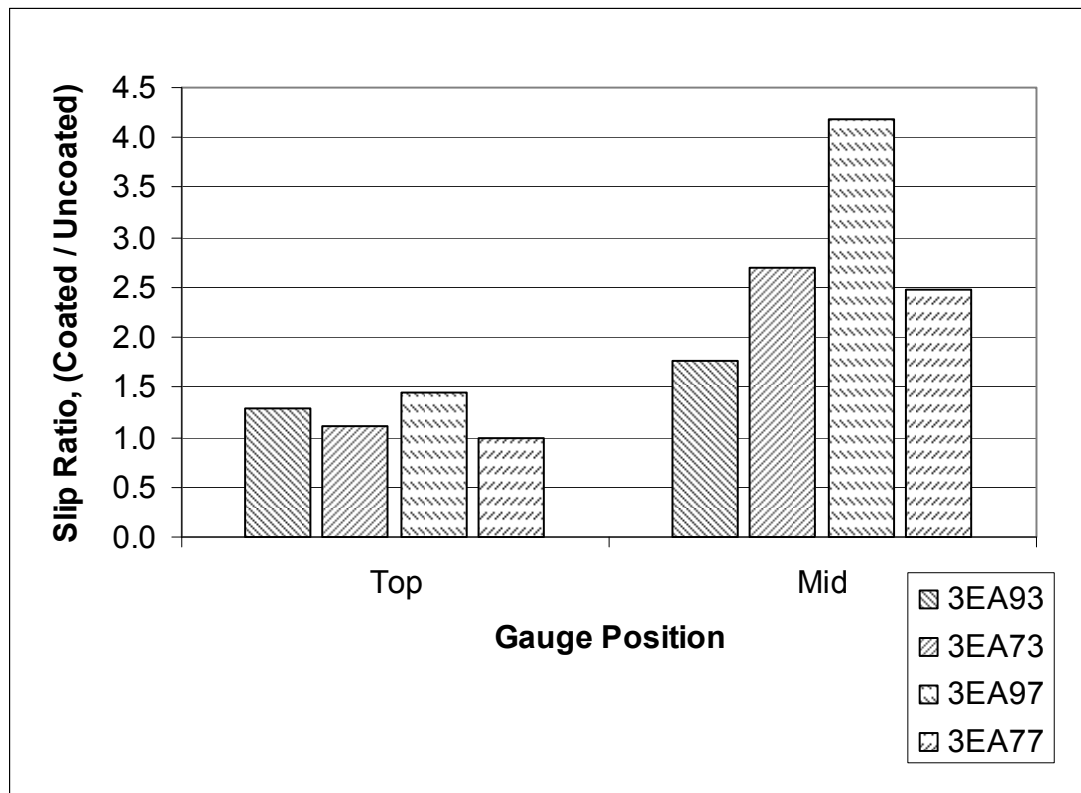


Figure 4.21: Slip ratios against black bar across all stress values

In Figure 4.22, only data at the 60 ksi level of rebar stress is compared. The Top gage values are not very different from those seen using all three stress levels. Even at the Mid gage the slip values are not much different for the A775 series. The real change is how the A934 rebar behaves at the 60ksi level. There is still more slip when the ties are at $7 \cdot d_b$ compared to $3 \cdot d_b$, but the spread between the two series has closed greatly. For higher confinement (3EA93) this means that the A934 bars have less relative slip at lower stresses and then have more relative slip at higher stresses. The opposite appears to be true for lower confinement (3EA97) where more relative slip is seen at lower stresses instead of higher stresses. The relative slip values for A934 bars are also close to those found for the A775 bars on average.

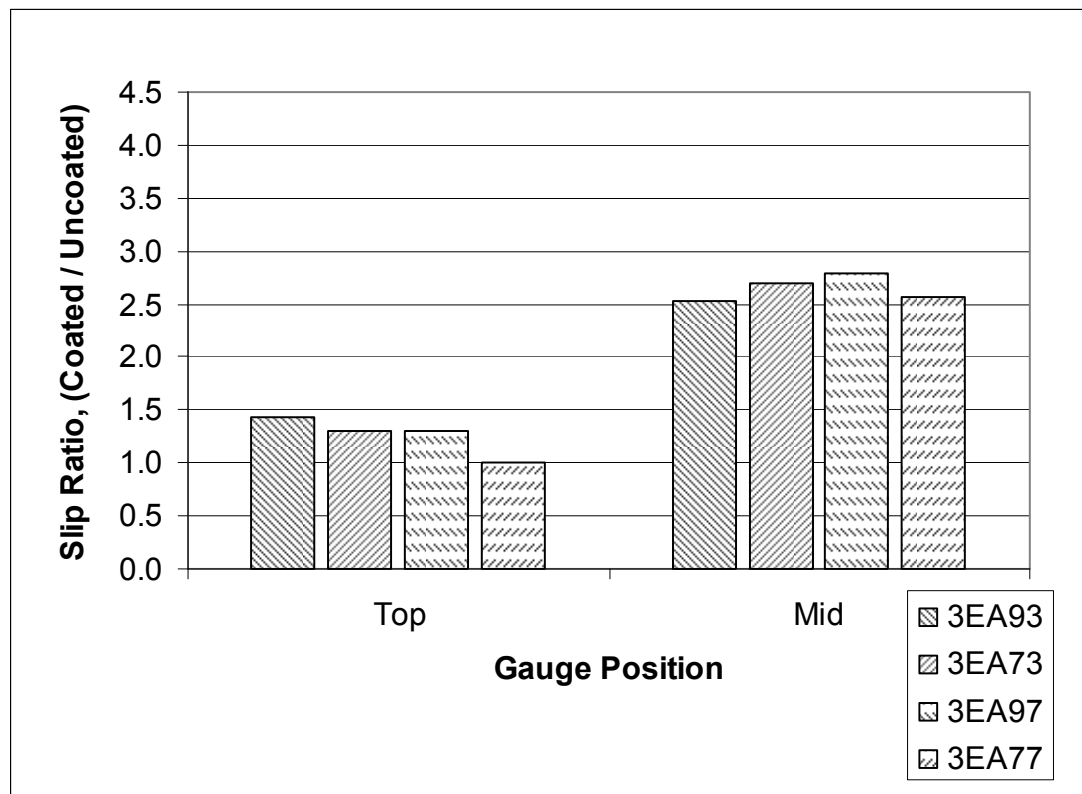


Figure 4.22: Slip ratios against black bar for 60 ksi stress level

The Top gage showed that the Coated rebar performed similar to the Uncoated rebar, but at the Mid gage it becomes apparent that the Coated rebar is not resisting the applied stress as well as the Uncoated rebar is. In general, Figure 4.22 reinforces the idea

that coated hooked rebar have about a 2.5 times higher slip ratio than the uncoated rebar, independent of the tie spacing.

From the figures above comparing tie spacing and coating type there is a general relationship that becomes apparent; in all cases the Mid gages recorded higher relative slip values than the Top gages. This indicates that the part of the rebar considered as the straight embedment length has less impact on the pullout load versus slip than does the coating type and confinement used on the tail of the hooked rebar. The similar slip experienced between Coated and Uncoated bar at the Top gage shows that the surface condition for the straight embedment is not significantly important. The higher slip experienced by the Coated bar at the Mid gage shows that the coating and confinement did not allow the tail to anchor the bar nearly as well as for the Uncoated bar. As described in Chapter 3, the embedment length was purposely reduced from the ACI Code (318-05) recommended length in order to ensure the rebar pulled out versus having the rebar rupture. The question that now arises is how much can the embedment be reduced and still achieve 60 ksi of rebar stress in light of the data in this study that shows that the hook's tail is mostly responsible for the pullout capacity, not the straight embedment?

Further proof that the strength is in the tail comes from the data from the Bottom gage which was located at the end of the hooks' tail. In almost all cases during testing the Bottom gage only just began to show movement of the rebar when the entire joint reached the ultimate capacity. In Figure 4.23 the slip values are fairly tightly grouped between 0 and 0.02 inches for whichever load increment happened to be the last increment for that specimen. Post-ultimate load slip values for the Bottom gage show a speedy degradation of the joint. Figure 4.24 shows the same information, but includes the rebar slip values for one load increment past ultimate load. Here the values are mostly scattered from 0 to 0.08 inches of slip, but retain a fairly high level of stress, all above the critical threshold of 60 ksi.

The retention of load while slip occurs is a good quality to see here when recalling the reinforced concrete theory that the system should show ductility, and show damage, before it reaches the point of critical failure. Unfortunate to see is that, if the load is not reduced from the ultimate value, then the slip values would be even higher and the joint would likely totally come apart in a violent manner rather than simply receive a

widespread pattern of spiderwebbing cracks. It is worth reiterating that the rebar stress levels recorded at ultimate load for the joint were in many cases very close to the ultimate load capacity for the rebar itself. If the joint were made stronger and capable of a higher ultimate load, then rebar ruptures would be expected to begin to appear in the data.

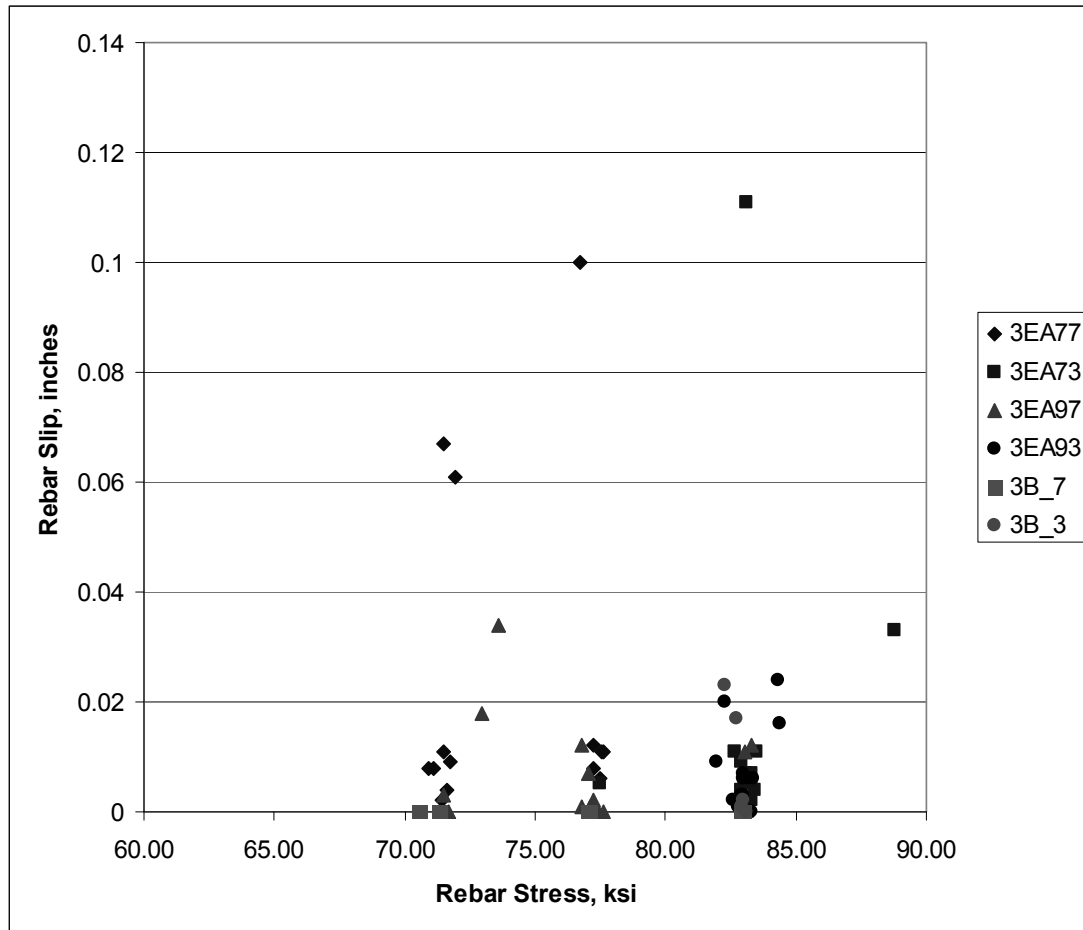


Figure 4.23: Bottom gage at max stress

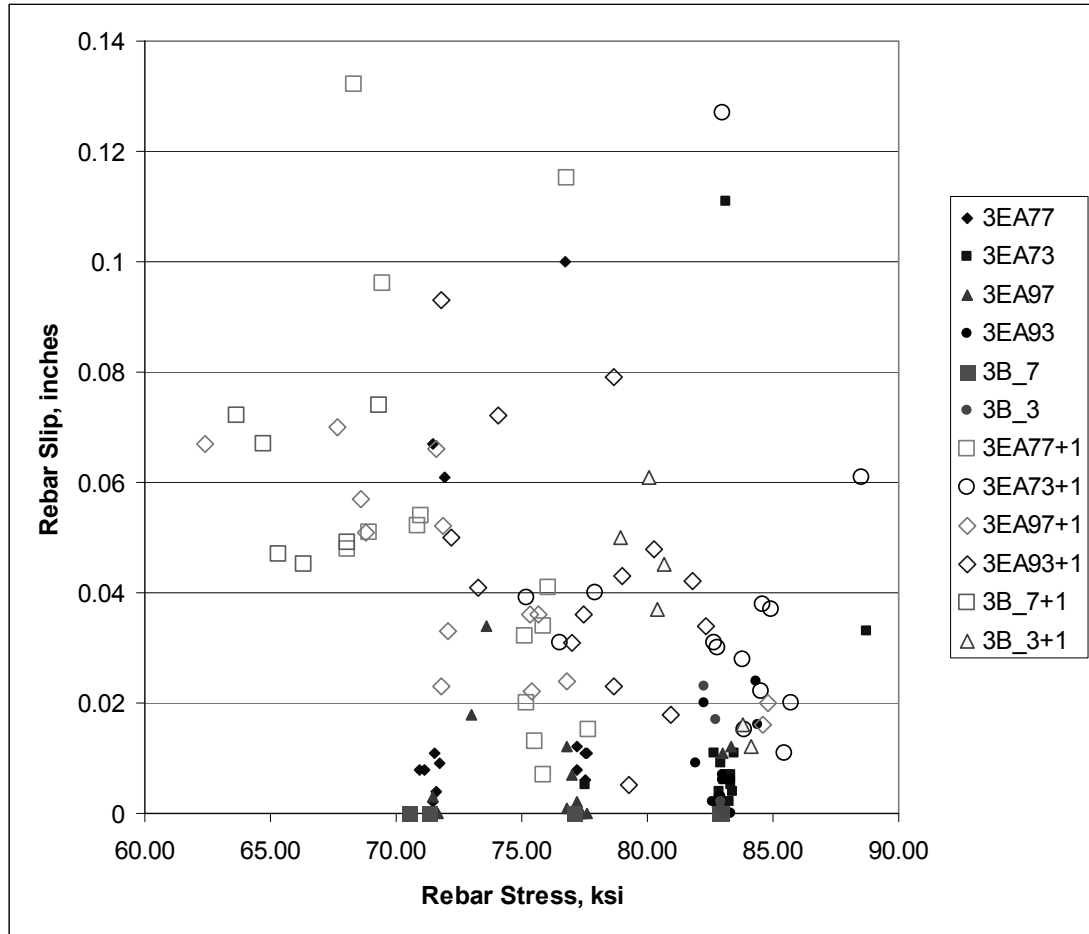


Figure 4.24: Bottom gage at max stress plus one load increment

4.3.6 Effect of Coating Type

The A775 coating type was tested in previous work (Hamad et al. 93) so it is used as the base value for computing slip ratios on the following Figure 4.25 and Figure 4.26. Except for the 200% higher relative slip found at the Top gage for the 7*db tie spacing, the two coating types appear to be equal for Mid gages independent of tie spacing. This is a similar picture to that seen in the previous comparisons.

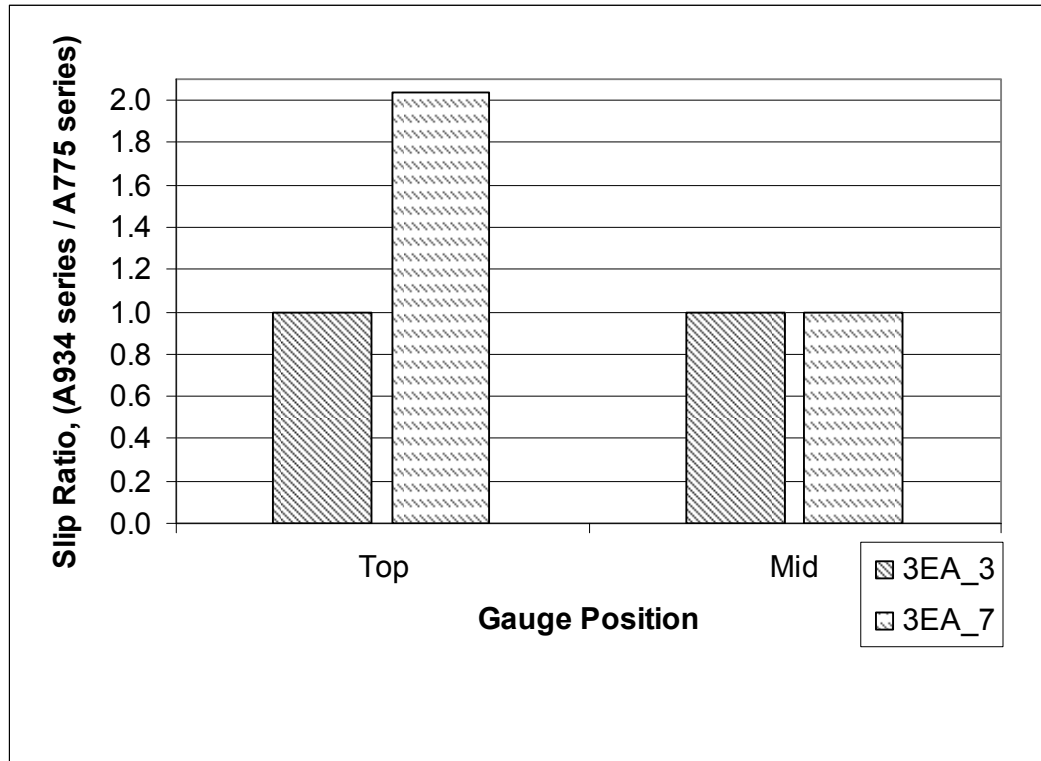


Figure 4.25: Slip ratios for coating type across all stress values

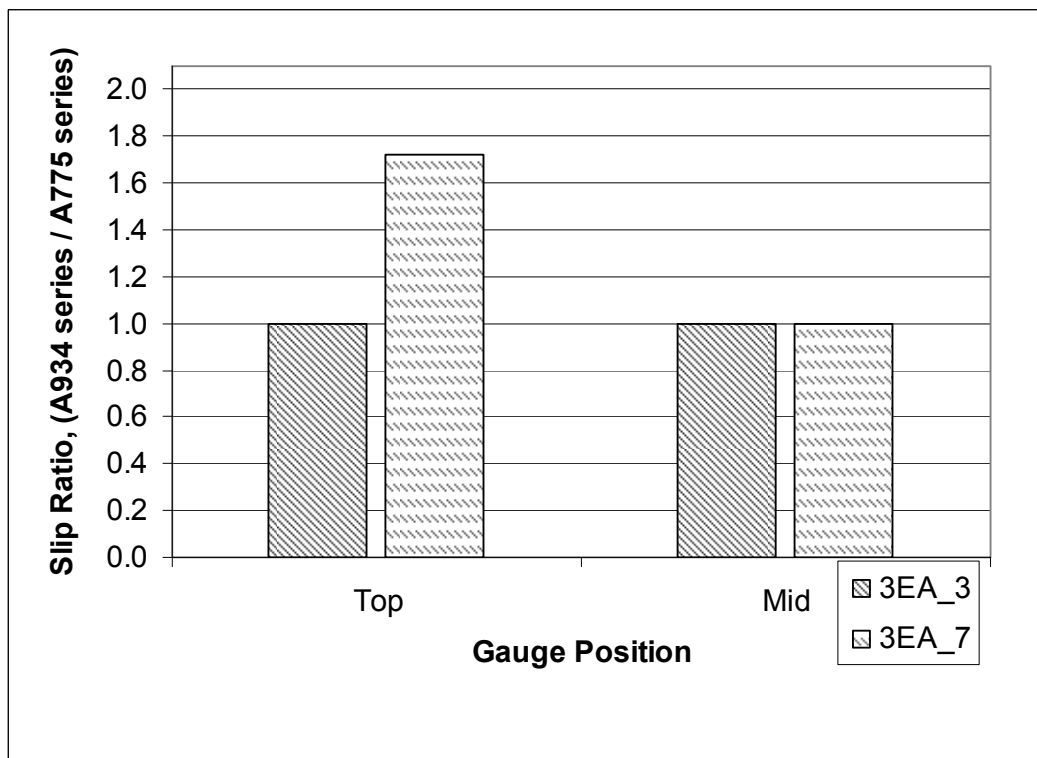


Figure 4.26: Slip ratios for coating type for 60 ksi stress level

The six bar graph figures, Figure 4.19 through Figure 4.26, presented previously for comparisons, are based on the results of the statistical analysis and so through the data reduction method there was some loss of information. To get a feel for how this data loss affected the statistical figures, data from all of the exact values was used regardless if the two series being compared were statistically the same or not. Recall, if the data points were found to be statistically equal, the slip ratios were set equal to one. Figure 4.27 was created using the same raw data as Figure 4.26 except that statistics are ignored. In just this one sample figure it is possible to see that the A934 series did not perform exactly the same as the A775 series, but that the results between the two series are still similar. Other figures created using the exact values had more or less the same effect of indicating slight variations from the statistical values, but the overall picture is unchanged.

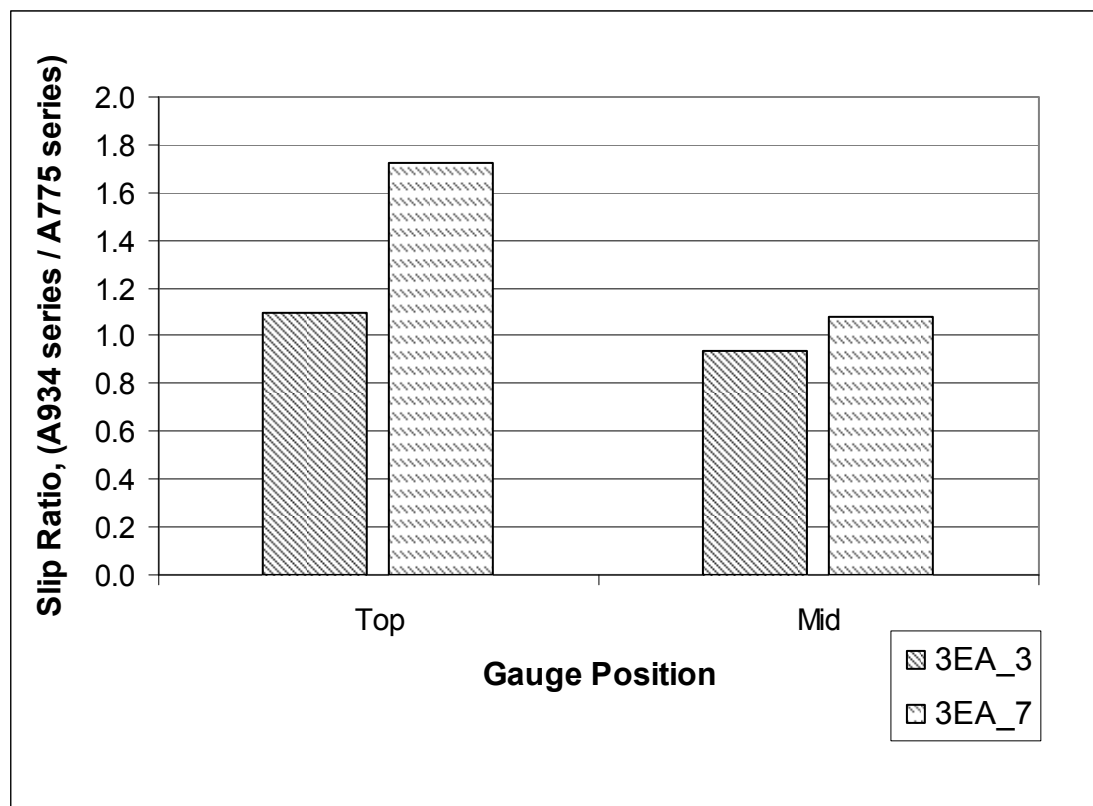


Figure 4.27: Exact (raw) slip ratios for coating type for 60 ksi level

5 Conclusions

5.1 Review of Program

This program tested to failure forty two (42) full size reinforced concrete beam-column joints to explore rebar coating type (ASTM A775, ASTM A934) and joint tie spacing ($3d_b$, $5d_b$, $7d_b$, and $9d_b$) effects which contribute to the pullout strength of hooked rebar. Each specimen had two hooked bars and was measured for relative displacement at three points along the embedded portion of the hook (Figure 3.5). This allowed for two hundred and fifty two (252) sets of load verses displacement data over the three phases of the program. Three lines were extracted from each data set corresponding to the loaded hooked rebar stress levels of 30 ksi, 42 ksi, and 60 ksi. The data was statistically compared, when possible, in pairs to determine if the two mean values were the same. Data groups were then set to graphical form for broad comparisons used to gain insight into the program objectives outlined in Chapter 1.

A summary of physical proprieties is as follows:

- By rebar coating type, the yield stress and tensile stress was on average:

Uncoated (Black)	72 ksi and 97 ksi
A775 Coated	79 ksi and 102 ksi
A934 Coated	68 ksi and 101 ksi
- The tensile fracture plane was the same for Black and A775 rebar at a jagged 45 degrees, but was different for A934 rebar at a smooth 90 degrees.
- The coating thicknesses were found to be very different than as reported by the manufacturer.
- The coating thickness for A775 rebar was found to mostly follow ASTM requirements, but the A934 rebar coating thickness was highly scattered and was very often thicker than ASTM maximum thickness limits.
- The A934 coating method can produce locations that never receive a coating, while the A775 method is more susceptible to loss of coating continuity on the outside of bends.

- The average concrete strength was 4.05 ksi and 5.83 ksi for Phase 2 and 3, respectively, with the Phase 3 cylinders showing a larger range of compressive strengths overall. In general, concrete which was emptied from the ready-mix truck later during each casting session produced somewhat higher strengths than the earlier portion of the same batch.

5.2 General Discussion

Data comparisons between current research and historical research were much less useful than was originally hoped and planned. Inconsistencies over time regarding every part of how the research was carried out causes diverse data output. This leads to little possibility of using older data to supplement new data for direct analysis of the impact of individual variables on the integrated structure of reinforced concrete.

The full combination of parameters that created the test specimens and test setup in the current program was capable of producing repeatable results. This does not mean that there were no unexpected results within a single series, but when viewing the data curves for a series they were usually quite similar from one specimen to the next. The largest variances in the data curves occurred near, and post, ultimate load.

Significant post ultimate load capacity exists within the joint, even with a sustained applied load. Only after many times more rebar slip than that experienced at ultimate load does the internal stress redistribution system fully begin to fail. This contrasts with the failure mechanism reported by Marques and Jirsa (1975), in which “failure was fairly sudden...” The key difference between the two programs was application of an axial load to the column specimens in the 1975 study.

The previous ACI Code (318-05) provision which requires a modification factor of 1.2 for epoxy coated rebar may not be adequate. Instead the factor may need to be closer to 2.5. The problem though is that the factor is used to adjust the lead embedment length in order to increase pullout capacity. The current program has discussed many aspects to confinement which indicate that a larger lead length may not be the most effective method to adjust capacity. Research has not been thoroughly performed on the affects of changing other confinement variables and the code does not address the issue in

Chapter 12. The result is that the practicing engineer does not have clear alternatives for configuration changes within the beam column joint.

Using all recorded data for comparisons produces the same general relationships as found when using the statistically comparable data. The statistically non-comparable data was removed though for formulating conclusions in order to help add some consistency to relationships that are not as straightforward as desired.

5.3 Discussion Regarding Objectives

There were three main objectives outlined in Chapter 1 which guided the current program. Discussion around these objectives can now be conveyed.

The first objective was to compare the A934 and A775 coating methods to help determine if the newer A934 method produces the same pullout strength results as the previously tested A775 method. The outcome is that the A934 coating type produced roughly the same relative slip values as found for the A775 hooked rebar.

The second objective was to compare both the A775 and A934 coating methods against the alternative of having no coating. Generally, the coated rebar slipped through the concrete more than uncoated rebar. It is difficult to quantify the difference that exists, but a factor of 2.5 may be appropriate based on the 60 ksi stress level ratios. The section “Effect of Coating Hooked Rebar” in Chapter 4 provides a more in-depth analysis where the levels of load, as well as the position where the relative slip is being measured, both affect the Coated vs. Uncoated Slip Ratio.

The third objective was to explore the effects of changing the level of confinement within the joint. This was accomplished by altering the spacing of the rebar acting as ties within the joint from $3*d_b$ to $9*d_b$.

The Phase 2 results seem to show that decreased tie spacing does not increase the level of hooked bar slip. Instead, only the level of stress applied to the hook controls the slip experienced. This is only a preliminary idea though as too few specimens were tested to make a definitive conclusion.

The Phase 3 results showed that decreased tie spacing had about the same impact on the Coated and the Uncoated hooked bar slip with the larger tie spacing causing slip of about 1.6 times larger, as measured on the back side of the curve (Mid gage).

5.4 Suggestions For Future Work

An extensive program should be conducted to explore the idea that less lead embedment length is needed because the tail of the hooked bar is holding the applied load, not the lead embedment length. Included should be variations of each of the relevant variables by which beam column joints are formed.

ASTM based testing parameters, or maybe a specified testing setup, would be beneficial for future research programs so that variables can be more systematically explored and new materials can be more readily verified by direct comparison to historical data.

It is often assumed when performing load based destructive testing that a displacement controlled load application system is preferred. While this method can often lead to greater safety in the event of catastrophic failure of the test specimen, the real world effect of gravity applied loads can be missed. The loading system used in the current program was load controlled, with minor losses to the load level incurred as creeping displacement continued to occur. Using this system has allowed for capture of a limited amount of the post-ultimate load capacity of the specimen, which has not been reported in previous research on the topic.

5.4.1 Data Gathering

Using synchronized digital cameras to record the load and all dial gages was a useful and cost effective means of gathering data. There was usually little question as to whether or not a single data point within a set was valid or if it was caused by a glitch of some kind. The real benefit of the pictures was the ability to identify visually what caused the error in the data so that the source of the error could be corrected when testing the next specimen.

Shortfalls of the system included: unsteady pictures producing slightly blurry images which could be difficult to enlarge, the necessity for additional personnel, the painstaking task of viewing the photos to record every data point, and having a limited number of data points which could effectively be recorded. Entering each data point by hand has mixed benefits though. It allowed the researcher to become more intimately

familiar with the data for understanding interactions within the tests and pinpointing data errors which could be corrected rather than simply excluded.

Limiting the number of data points which could be collected was also a mixed benefit. With advances in technology it is possible to record data at intervals of fractions of a second, but a high percentage of all that data is smoothed over during further analysis when the extra data points are deemed less useful than originally envisioned. Having fewer data points for each specimen reduced the effort required when manipulating the data within spreadsheets and even then a large portion of the data was not utilized to form conclusions.

5.4.2 Program Setup

Quality control for the many individual components of reinforced concrete is extremely difficult as a whole. One way to help reduce variability would be to have an overly large quantity of straight reinforcement bars delivered to the laboratory and do all the rebar cutting and bending on site. In this way many of the rebar related issues can be minimized through selective usage of the rebar pieces available. On the concrete side of variability it is suggested that crushed quarried rock is used instead of glacier or river gravels. The gravels contain possibly dozens of different types of rock and in many shapes and sizes. In particular, the pieces of sandstone found within the concrete while testing the cylinders was an unfortunate discovery. The sandstone was not more prevalent than other rock varieties, but the possibility of a random gathering of the sandstone stones within either a cylinder or a specimen is enough to cause speculation that inconsistent concrete strength exists, i.e. the normal assumption that concrete is homogeneous is more incorrect than preferred for believing the assumption to be true.

One of the research program design decisions that must be made is whether the program will be adhering to strict laboratory practices, attempting to control every variable, and essentially try to test pristine samples with clearly repeatable results. Or, whether the program will be creating real world samples using materials as they are created through normal manufacturing processes, using tolerances with formwork and rebar placement as would be found on construction sites, and test samples with varied results, but results which show a little more clearly the full range of variability that can

exist without conducting extensive testing programs. The current program is closer to the latter, though it attempted at times to be closer to the former.

Future programs should use more than seven specimens. Seven specimens was chosen a little arbitrarily as being better than three or four, but less costly than 10 or 15. This number of specimens was also less oppressive to handle as the size and weight (700 Lbs) of the specimens was an issue within the laboratory. Considering the high variability of reinforced concrete, the amount of data that gets lost to experimental errors, and the further loss of data due to statistical non-comparability, no less than 10 specimens should be used in the future when testing any one variable. This is still an arbitrary value, but it comes from more experience with the particular test regime. Within a new testing program (using the current programs specimen arrangement and setup) it can be assumed that at least the first four specimens created will not yield quality results during testing and that number will increase if the same crew of testers is not used for each subsequent test. In the current program a crew of four testers were present for an early smooth operation, but was refined to three testers during the latest tests as the tasks and procedures became more familiar to the crew.

Placing the concrete forms on pallets which can be pallet jacked around the lab on casting day (as well as prior to and later on) was an extremely successful exercise. The forms must be restrained such that they don't burst their sides during slight bumps or jolts, but this was fairly easily and cheaply accomplished. The base of each standing form was restrained with scrap blocks of wood 2x4s. At the middle and top of the form restraints were created using 5/16" threaded rods straddling a pair of forms, and through sticks of wood 2x2s, similar to a post-tensioned system. In the current program, the pallets were second hand from a local lumberyard and largely mismatched, but this didn't cause any significant problems and it did help in reducing costs.

The full loading system is discussed in Chapter 3. It is noteworthy to mention though that while the rebar chucks adequately gripped the rebar for the duration of testing, the wedges used within the chucks did have a fairly short useful life. Within each chuck were 2 equally spaced large-toothed wedges. Generally, each set of wedges would last 6 to 8 full loading cycles before needing replacement.

A safety note on the loading setup: do not allow anyone to walk past the end of a loaded rebar. The large tensile forces exerted into the rebar cause them to elastically stretch to a large degree. If and when the rebar unexpectedly breaks it uses all of the stored potential energy to launch itself out of the load frame at great speed and with great force. It is folly to believe this force can be adequately contained by anything less than a masonry or steel wall. The best approach is to fully deny access for all personnel (researchers included) to the danger zone.

6 References

- American Concrete Institute. 1977. Building Code Requirements for Structural Concrete (ACI 318) and Commentary (ACI 318R). Farmington Hills(MI).
- American Concrete Institute. 1989. Building Code Requirements for Structural Concrete (ACI 318) and Commentary (ACI 318R). Farmington Hills(MI).
- American Concrete Institute. 1995. Building Code Requirements for Structural Concrete (ACI 318) and Commentary (ACI 318R). Farmington Hills(MI).
- American Concrete Institute. 1999. Building Code Requirements for Structural Concrete (ACI 318) and Commentary (ACI 318R). Farmington Hills(MI).
- American Concrete Institute. 2002. Building Code Requirements for Structural Concrete (ACI 318) and Commentary (ACI 318R). Farmington Hills(MI).
- American Concrete Institute. 2005. Building Code Requirements for Structural Concrete (ACI 318) and Commentary (ACI 318R). Farmington Hills(MI).
- American Society for Testing and Materials. 2006. Standard Specification for Epoxy-Coated Steel Reinforcing Bars (A775/A 775M –06). ASTM International: Pennsylvania.
- American Society for Testing and Materials. 2004. Standard Specification for Epoxy-Coated Prefabricated Steel Reinforcing Bars (A934/A 934M –04). ASTM International: Pennsylvania.
- American Society for Testing and Materials. 2001. Standard Specification for Fabrication and Jobsite Handling of Epoxy-Coated Steel Reinforcing Bars (D3963/D 3963M –01). ASTM International: Pennsylvania.
- American Society for Testing and Materials. 2006. Standard Specification for Deformed and Plain Carbon-Steel Bars for Concrete Reinforcement (A615/A 615M –06a). ASTM International: Pennsylvania.
- American Society for Testing and Materials. 2005. Standard Test Methods and Definitions for Mechanical Testing of Steel Products (A370 –05). ASTM International: Pennsylvania.
- American Society for Testing and Materials. 1997. Standard Test Method for Specific Gravity and Absorption of Fine Aggregate (C128 –97). ASTM International: Pennsylvania.
- American Society for Testing and Materials. 2001. Standard Test Method for Sieve Analysis of Fine and Coarse Aggregates (C136 –01). ASTM International: Pennsylvania.
- American Society for Testing and Materials. 1988. Standard Test Method for Specific Gravity and Absorption of Coarse Aggregate (C127 –88). ASTM International: Pennsylvania.

- American Society for Testing and Materials. 2005. Standard Test Method for Temperature of Freshly Mixed Hydraulic-Cement Concrete (C1064/C 1064M – 05). ASTM International: Pennsylvania.
- American Society for Testing and Materials. 2004. Standard Test Method for Air Content of Freshly Mixed Concrete by the Pressure Method (C231 –04). ASTM International: Pennsylvania.
- American Society for Testing and Materials. 2006. Standard Test Method for Making and Curing Concrete Test Specimens in the Field (C31/C 31M –06). ASTM International: Pennsylvania.
- American Society for Testing and Materials. 2005. Standard Test Method for Compressive Strength of Cylindrical Concrete Specimens (C39/C 39M –05). ASTM International: Pennsylvania.
- American Society for Testing and Materials. 2005. Standard Test Method for Slump of Hydraulic-Cement Concrete (C143/C 143M –05a). ASTM International: Pennsylvania.
- Ayyub BM and McCuen RH. 2003. Probability, Statistics, and Reliability for Engineers and Scientists, Second Edition. Chapman & Hall/CRC: New York.
- Hamad BS, Al Hammoud R, and Kunz J. 2006. Evaluation of Bond Strength of Bonded-in or Post-Installed Reinforcement. ACI Structural Journal. 103(2):207-218.
- Hamad BS, Jirsa JO, and D’Abreu de Paulo N. 1993. Anchorage Strength of Epoxy-Coated Hooked Bars. ACI Structural Journal. 90(2):210-217.
- Hamad BS, Jirsa JO, and D’Abreu de Paulo N. 1990. Effect of Epoxy Coating on Bond and Anchorage of Reinforcement in Concrete Structures. Center for Transportation Research: The University of Texas at Austin, Research Report 1181-1F December
- International Federation for Structural Concrete. 2000. Bond of reinforcement in concrete. State-of-art-report Bulletin 10. p. 217-267.
- Jirsa JO, Lutz LA, and Gergely P. 1979. Rationale for Suggested Development, Splice, and Standard Hook Provisions for Deformed Bars in Tension. Concrete International. 1(7):47-61.
- Minor J and Jirsa JO. 1975. Behavior of Bent Bar Anchorages. ACI Journal Proceedings. 72(4):141-149.
- Marques JLG and Jirsa JO. 1975. A Study of Hooked Bar Anchorages in Beam-Column Joints. ACI Journal Proceedings. 72(5):198-209.
- Pinc RL, Watkins MD, and Jirsa JO. 1977. Strength of Hooked Bar Anchorages in Beam-Column Joints. CESRL Report No. 77-3 November

Appendix A. Aggregate Distribution

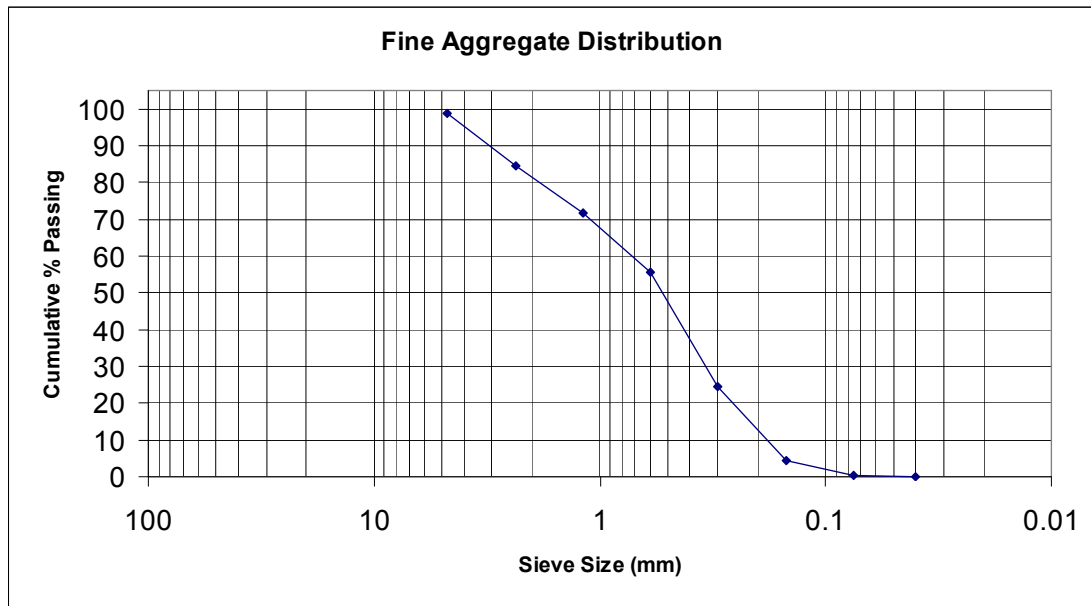


Figure A.1: Fine aggregate Distribution

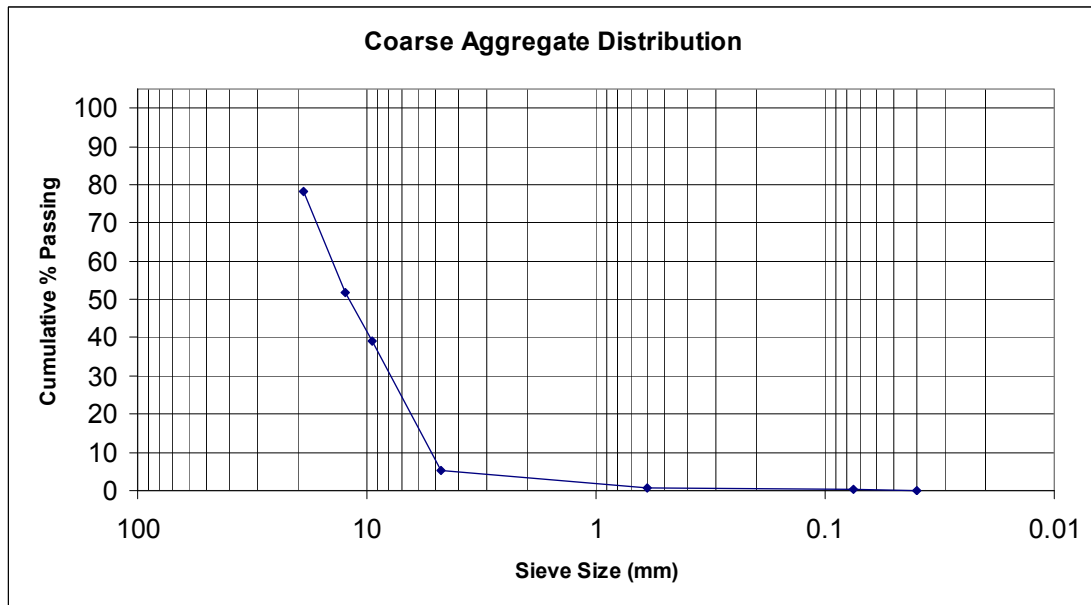


Figure A.2: Coarse aggregate distribution

Appendix B. Additional Rebar Information

Series	Column No.	Bar No.	Rib	
			Angle	Spacing
3EA77 Coated A775	9	2	60	1/4
	9	5	60	1/4
	10	8	56	3/8
	10	1	56	3/8
	11	10	60	3/8
	11	3	60	3/8
	12	9	60	3/8
	12	4	60	3/8
	13	17	56	3/8
	13	12	56	3/8
	14	13	56	3/8
	14	15	56	3/8
	15	11	60	3/8
	15	20	60	3/8
	16	16	60	3/8
	16	18	56	3/8
3EA73	17	22	60	3/8
	17	29	60	3/8
	18	28	60	3/8
	18	25	60	3/8
	19	19	60	1/4
	19	23	60	1/4
	20	30	56	3/8
	20	24	60	3/8
	21	17	56	3/8
	21	27	60	3/8
	22	21	56	3/8
	22	26	56	3/8
3EA97 Coated A934	23	9	66	3/8
	23	10	66	3/8
	24	19	66	3/8
	24	29	66	3/8
	25	13	66	3/8
	25	15	66	3/8
	26	16	66	3/8
	26	17	66	3/8
	27	1	66	3/8
	27	6	66	3/8
	28	4	66	3/8
	28	8	66	3/8
	29	5	66	3/8
	29	2	66	3/8
	30	12	66	3/8
	30	14	66	3/8
3EA93	31	7	66	3/8
	31	3	66	3/8
	32	18	66	3/8
	32	11	66	3/8
	33	25	66	3/8
	33	27	66	3/8
	34	21	66	3/8
	34	20	66	3/8
	35	22	66	3/8
	35	24	66	3/8
	36	30	66	3/8
	36	28	66	3/8

Series	Column No.	Bar No.	Rib	
			Angle	Spacing
3B_7 Uncoated	37	12	56	1/4
	37	11	66	1/4
	38	10	60	1/4
	38	9	66	3/8
	39	8	74	1/4
	39	7	60	1/4
3B_3	40	6	66	1/4
	40	5	56	1/4
	41	2	60	1/4
	41	1	66	3/8
	42	4	74	1/4
	42	3	60	1/4

Figure B.1: Rib angle and spacing for all specimens

Appendix C. Data Plots

The figures within this appendix are created from the raw data. No statistical analysis has been applied. These figures were created in the hopes that using a simple range of one standard deviation or one confidence interval from the mean of the data would be adequate to form firm relationships between series. Figures are presented first from Phase 2 and then from Phase 3. A couple of similar figures have already been presented within the Results chapter and so are included in this set as duplicate.

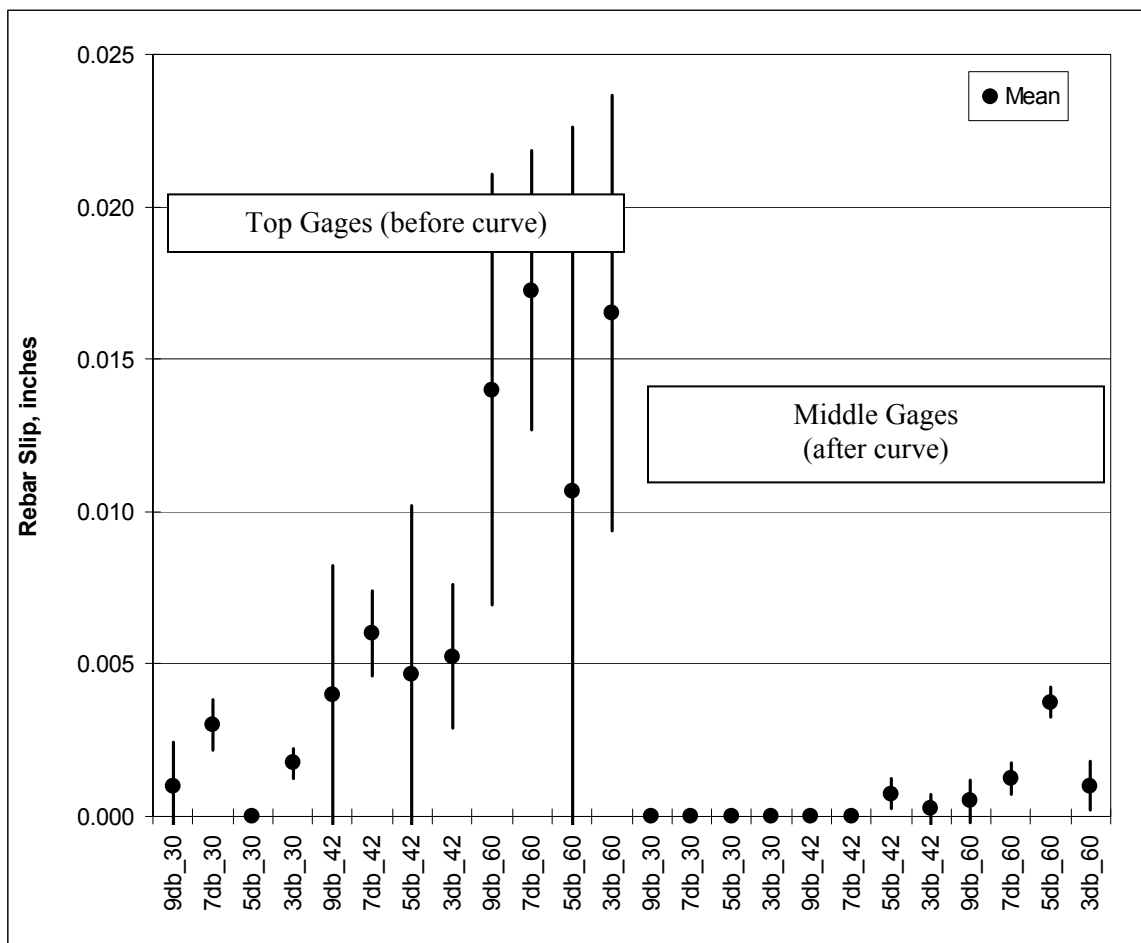


Figure C.1: Phase 2 +/- one standard deviation from mean for the top & mid gage

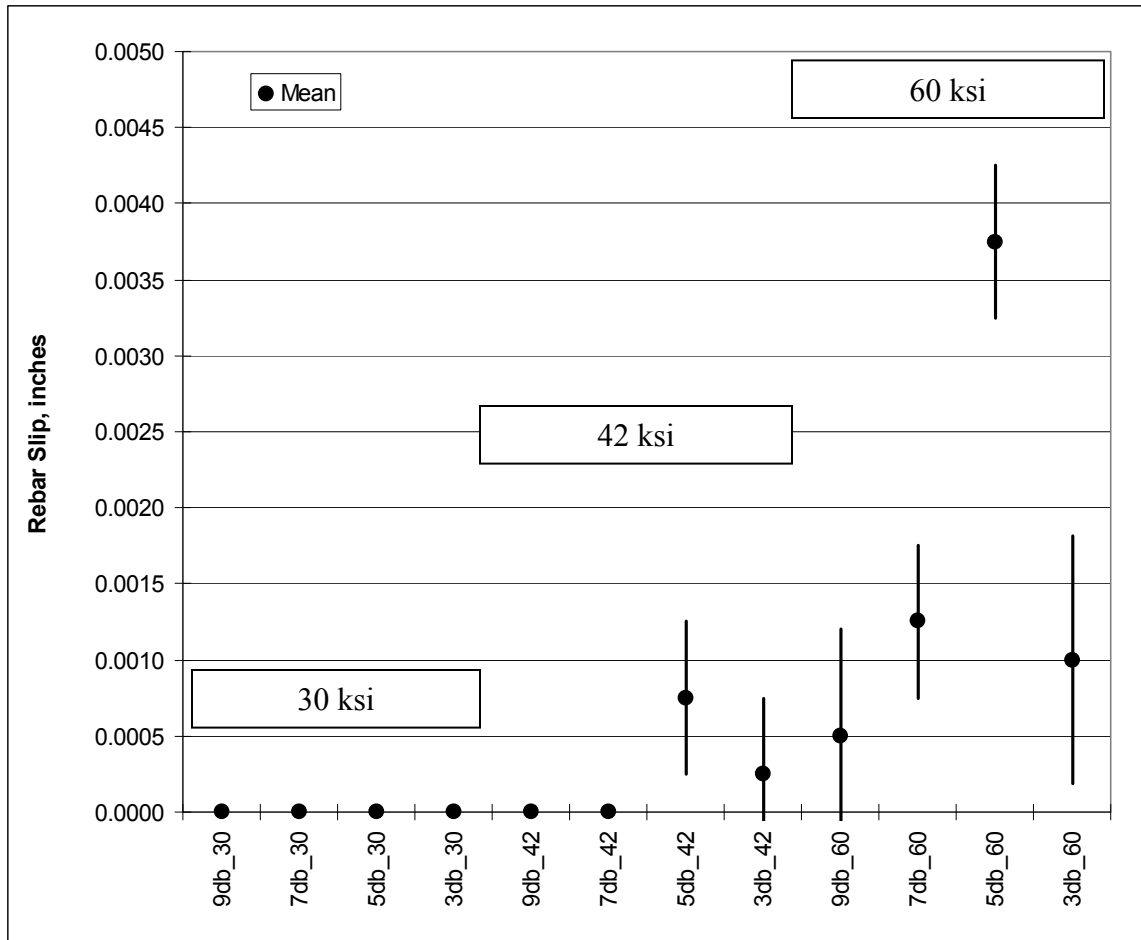


Figure C.2: Phase 2 +/- one standard deviation from the mean for the mid gage

The middle gages are presented here to provide a higher resolution on the Y-axis.

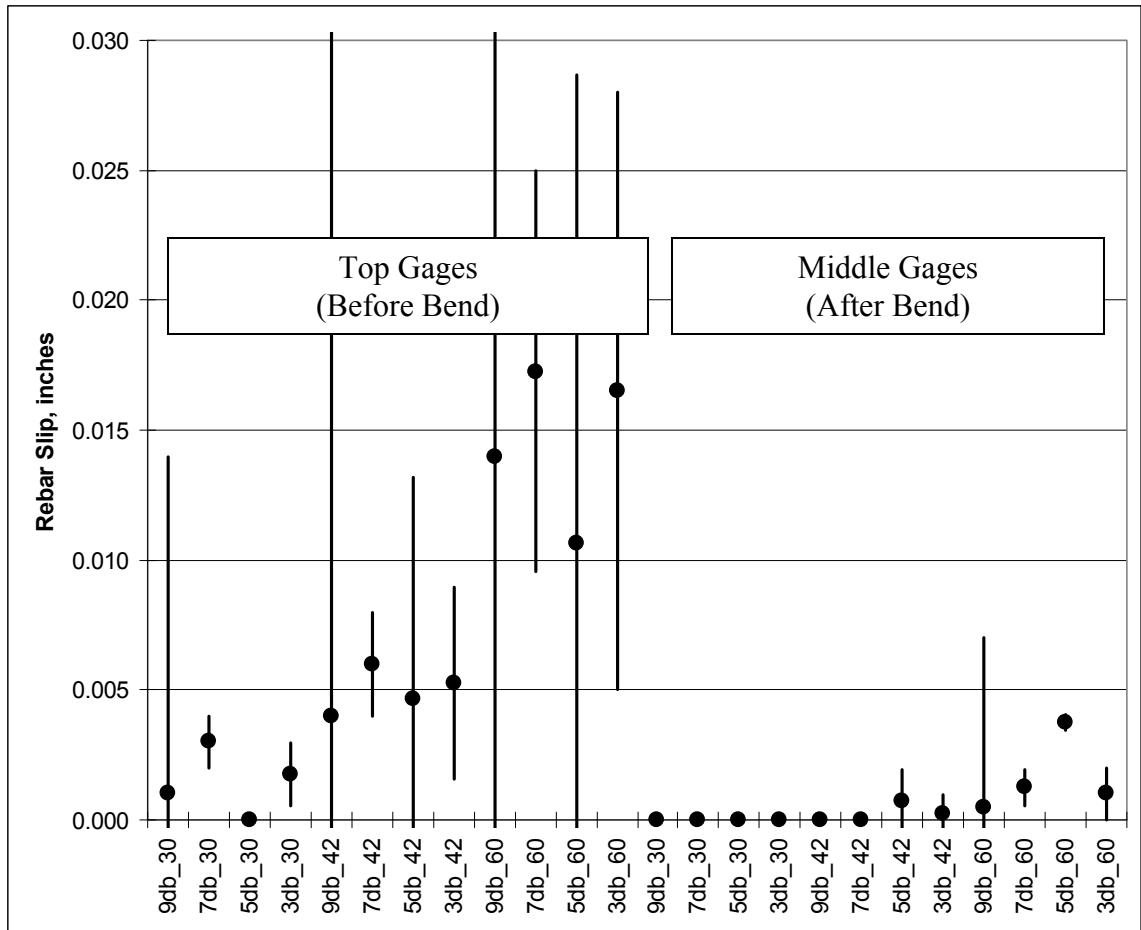


Figure C.3: Phase 2 \pm one confidence interval from the mean for the top and mid gage

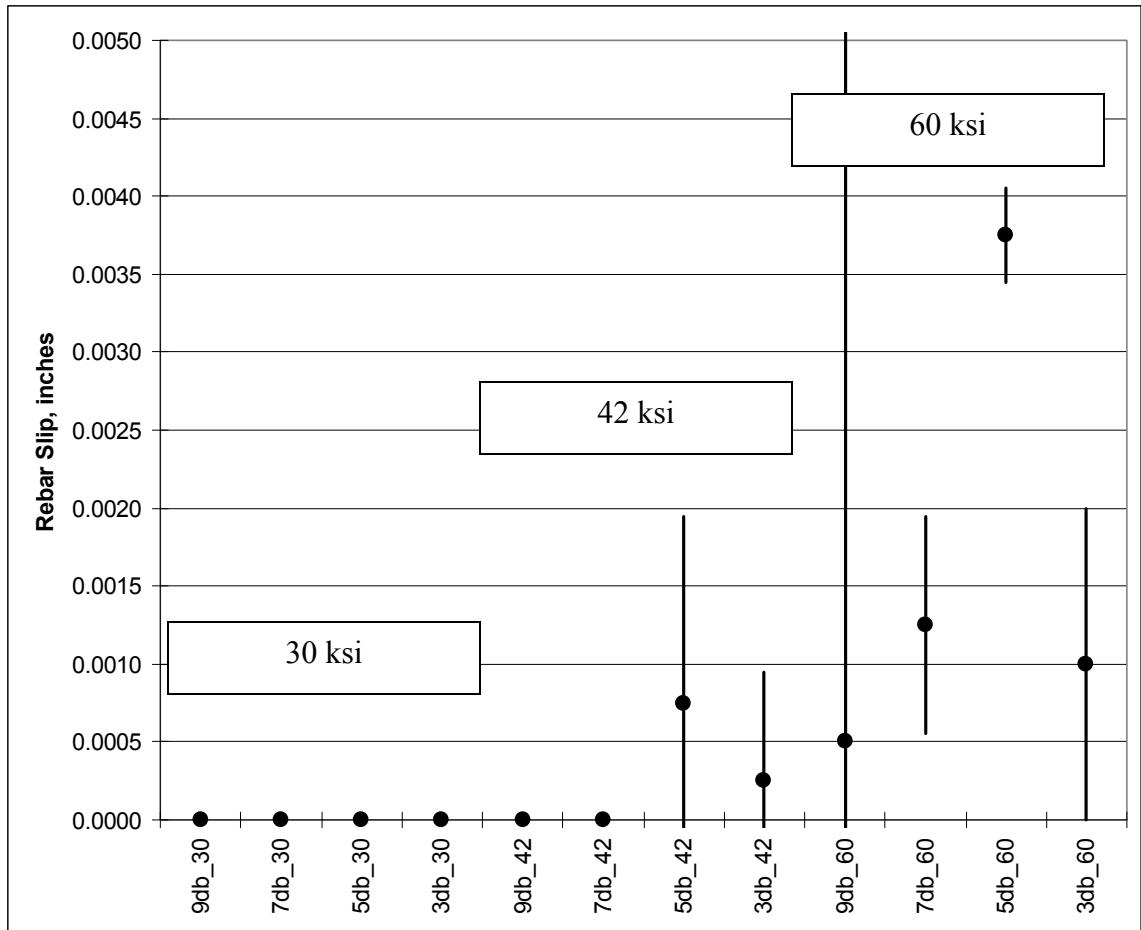


Figure C.4: Phase 2 +/- one confidence interval from the mean for the mid gage

The middle gages are presented here to provide a higher resolution on the Y-axis.

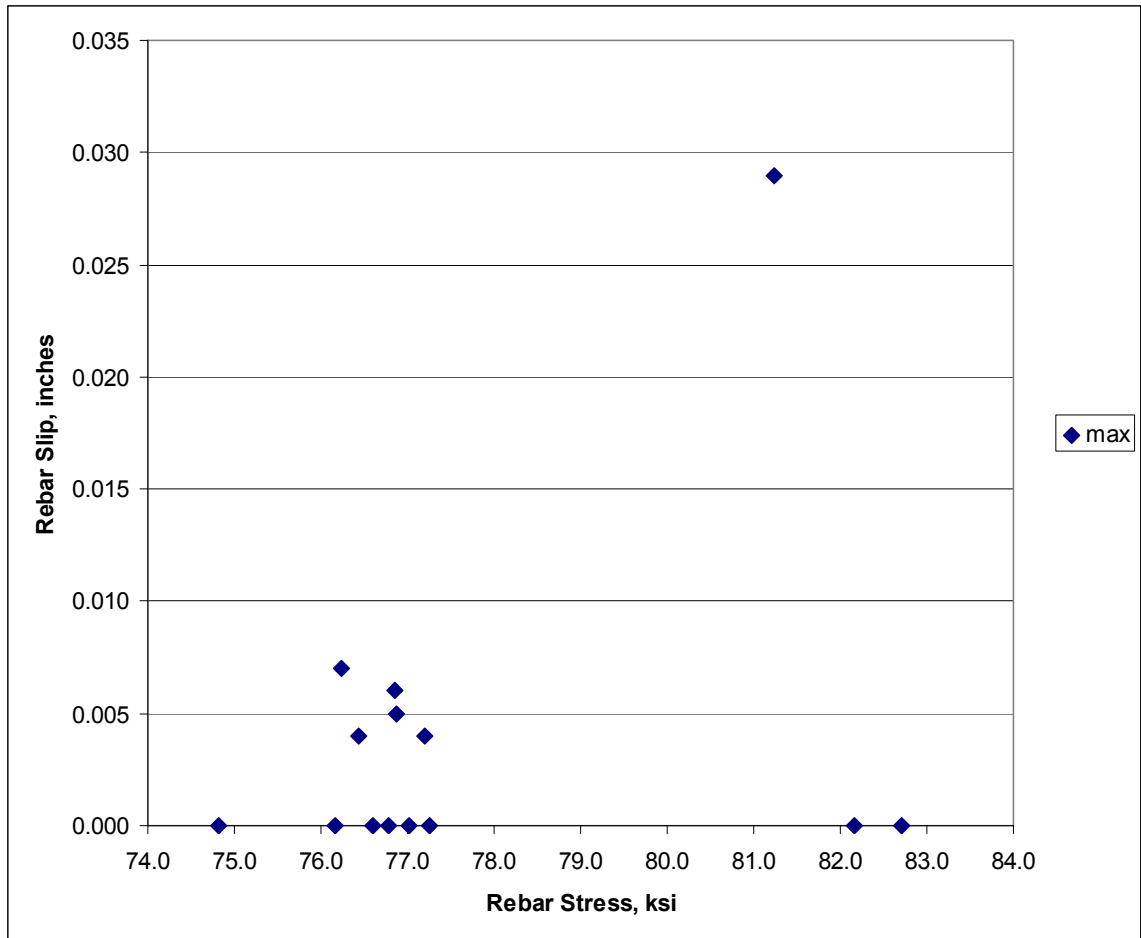


Figure C.5: Phase 2 raw data for rebar slip at max rebar stress as recorded at the bot gage

Two figures have been included here to show how the bottom gage presents the same general activity in Phase 2 as in Phase 3. Similar Phase 3 figures were previously presented in the Results chapter.

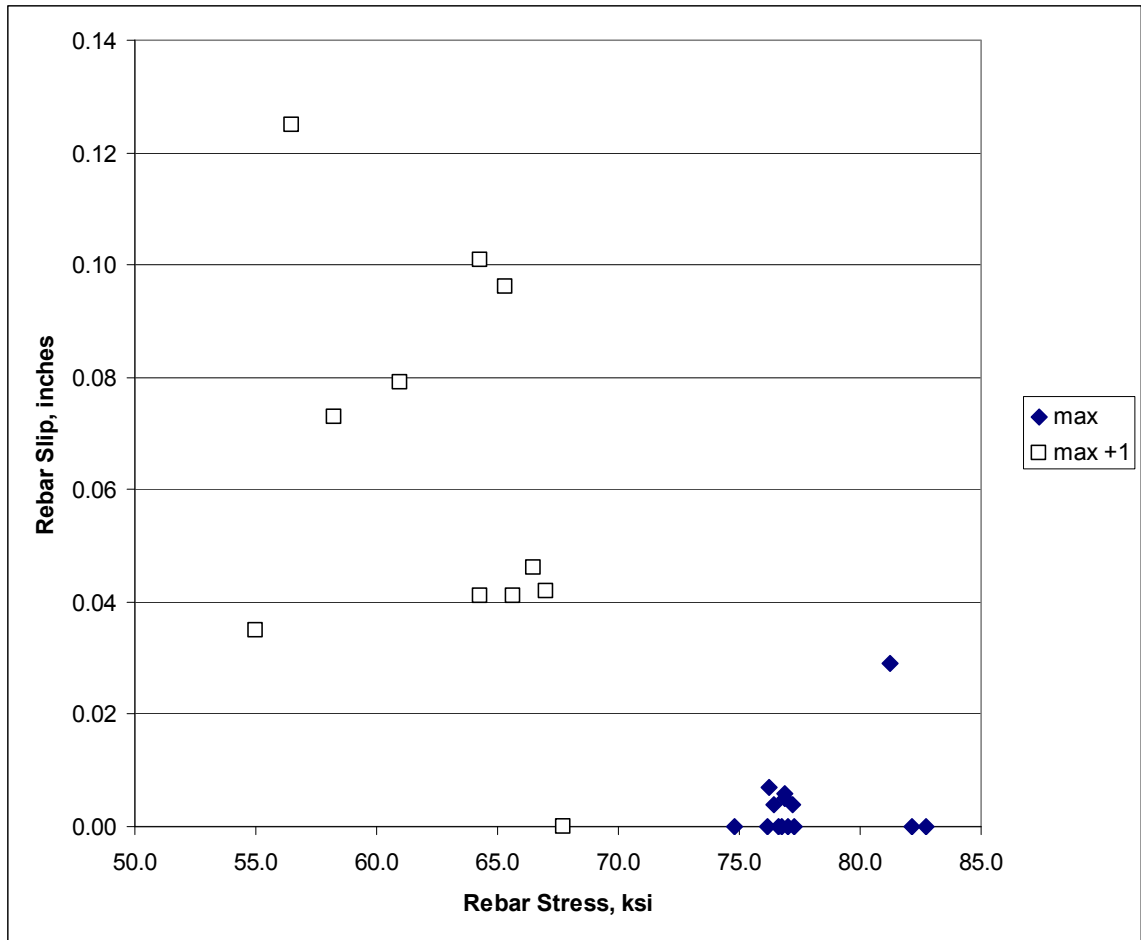


Figure C.6: Phase 2 raw data for rebar slip at maximum rebar stress plus one load step as recorded at the bottom gage

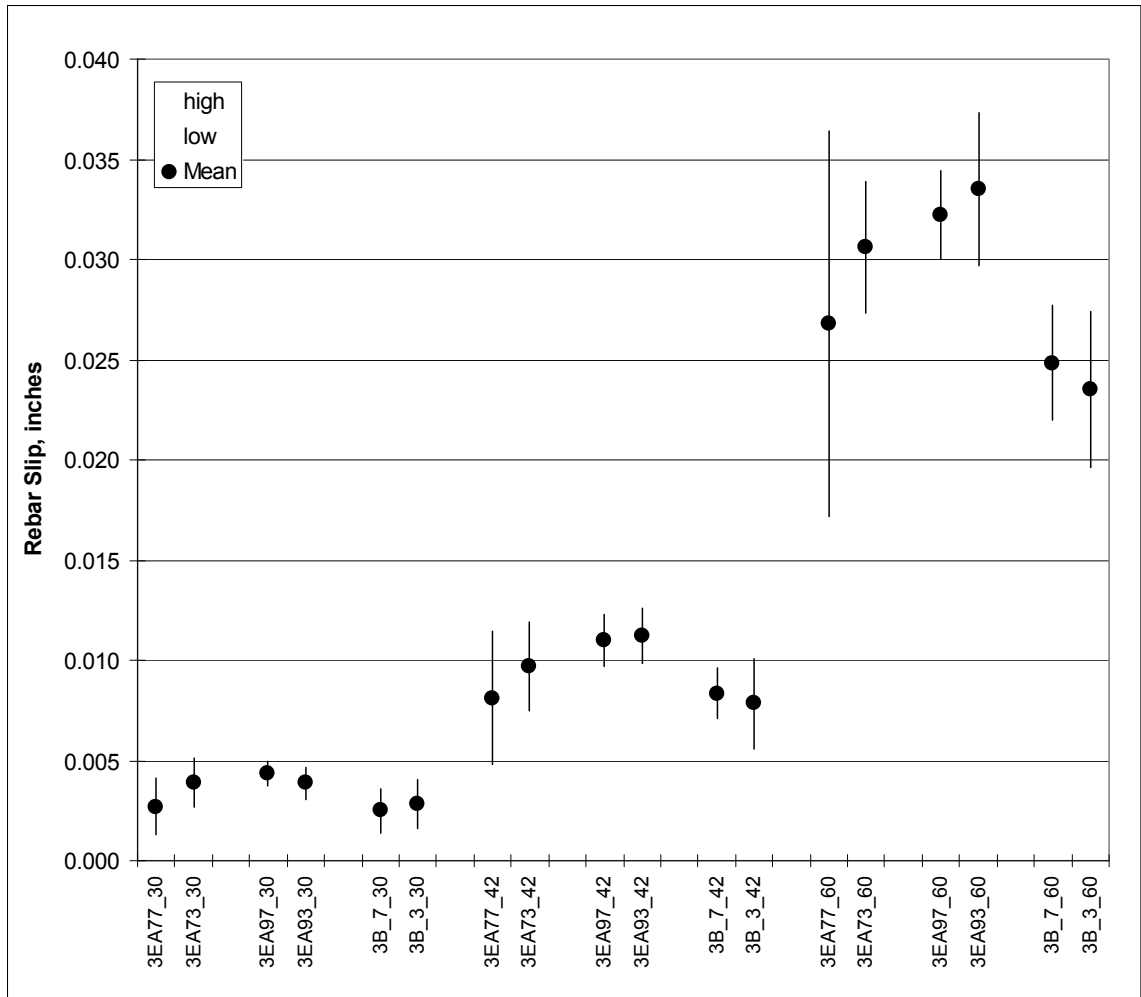


Figure C.7: Phase 3 95% confidence interval from mean for effect of tie spacing at the top gage (7db & 3db in pairs)

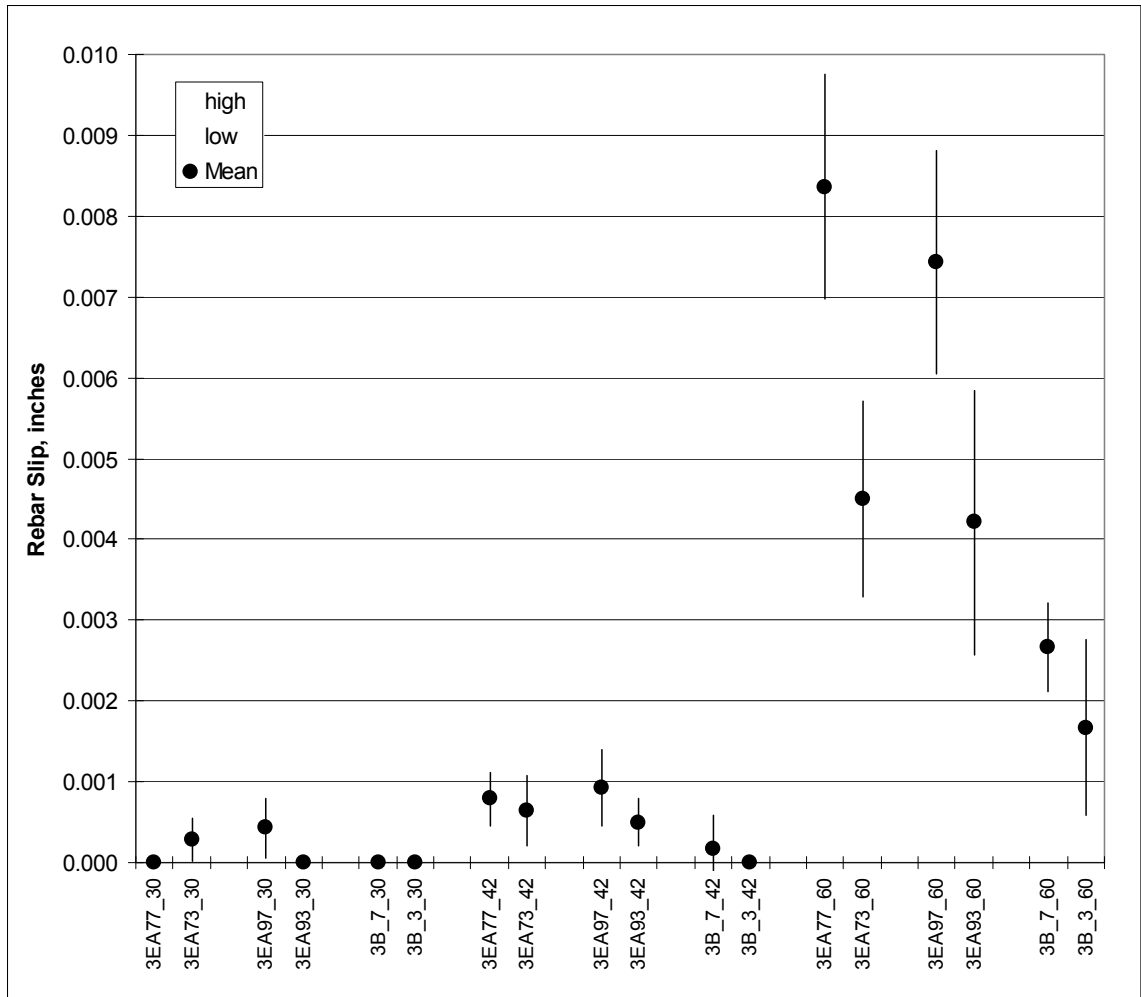


Figure C.8: Phase 3 95% confidence interval from mean for effect of tie spacing at the mid gage (7db & 3db in pairs)

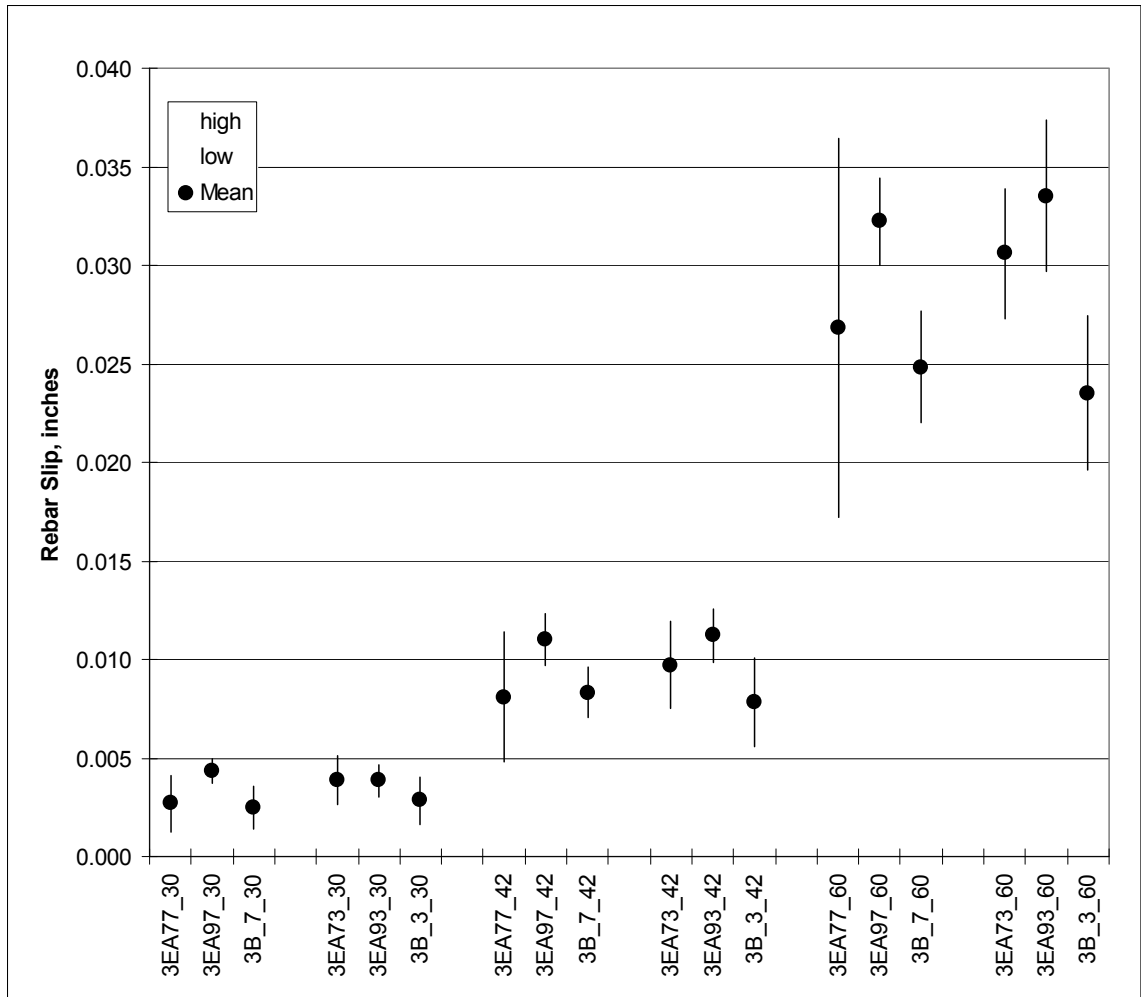


Figure C.9: Phase 3 95% confidence interval from mean for effect of tie spacing at the top gage (775, 934 & uncoated in sets)

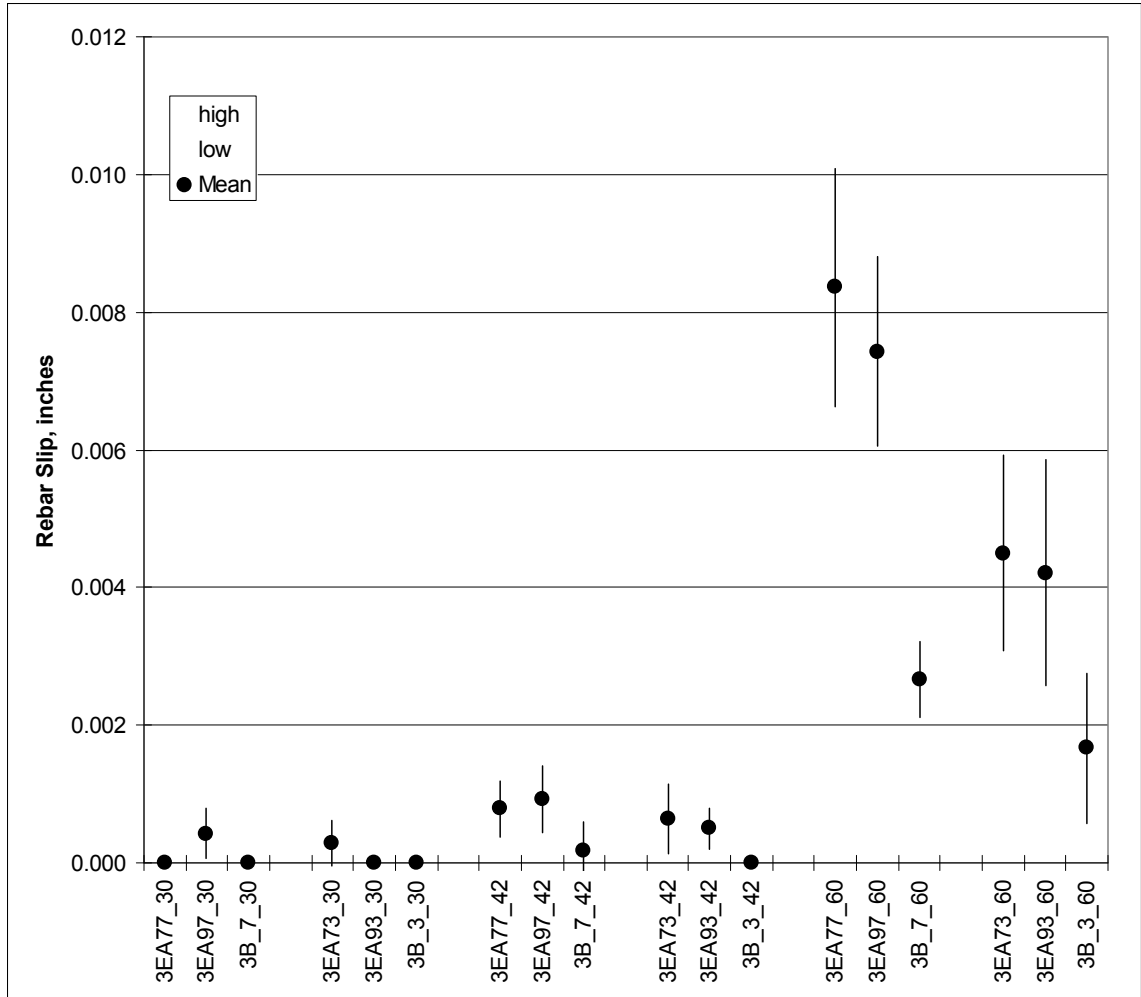


Figure C.10: Phase 3 95% confidence interval from mean for effect of tie spacing at the mid gage 9775, 934, & uncoated in sets)

Appendix D. Crack Patterns

During testing of the beam column specimens the progression of the surface cracks was marked during the resting period when the load was held steady. At lower levels of load there may be only a couple cracks forming, but then at the highest loads there were many small cracks spiderwebbing in different directions. The cracks were marked as best as possible using black felt tip markers. The furthest extent of the largest cracks identified were marked with a perpendicular line and the current level of load (in kips). Within the next few days, after testing, each specimen was given a more thorough review to mark every stress related crack that could be found, this time with a green felt tip marker. On every specimen there were numerous additional cracks.

The most informative was the horizontal crack that formed across the back side of the concrete at almost the same exact height on every specimen. The crack had only been identified a couple times during testing and it had only appeared in the minutes after the load was released, never before. Though unconfirmed, this crack is believed to be caused by the straightening out of the column which was bent under load. The longitudinal tension steel retained some elastic potential energy and wants to close the tension face cracks in the concrete. Debris within the cracks prevents them from closing, but the tensile stress in the steel still exists. The result is that the previous compression face of the concrete receives a tensile load which is high enough to cause a crack.

There are many other ideas that could be explored using the many cracks recorded as evidence. As an example, matching up the crack patterns across series of specimens the internal stresses could be modeled and examined to identify how applied loads are redistributed. This could then lead to direction as to what variables need to be adjusted to more efficiently create a beam column joint that resists various applied loads.

For whatever purpose a future researcher chooses, two sets of photos are provided for 41 of the specimens (the original 1st specimen was not recorded). The first photo in each set is in Grayscale so that the difference between black and green markings may be discernable, as well as greater detail in surface textures. The second photo is in Black and White which may be easier for computer programs to identify between the white

background surface and black cracks. The second photo may also retain the crack structure more precisely for lower quality printers and reproductions.

Each photo from Phase 2 has a label of 3db, 5db, 7db, or 9db. These relate to the spacing of the column ties within the joint region. Each photo from Phase 3 has a label showing the exact column number. The column numbers may be used to find further information about the rebar that was included in that column and may be traced through the spreadsheet files/calculations which have the specific load and relative slip values.

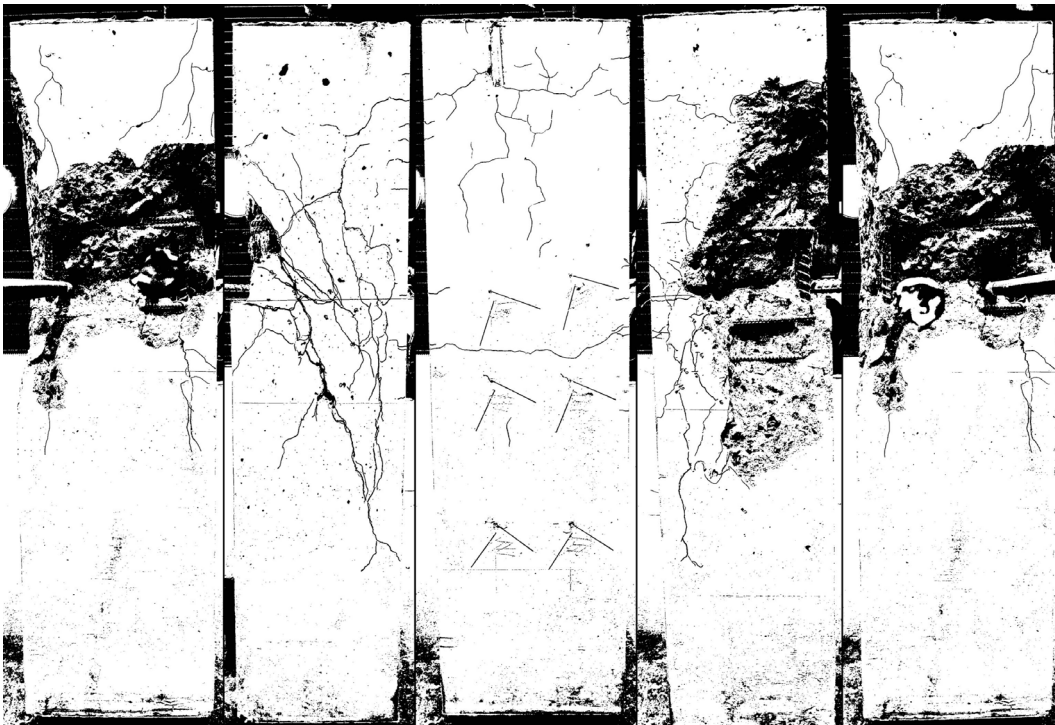
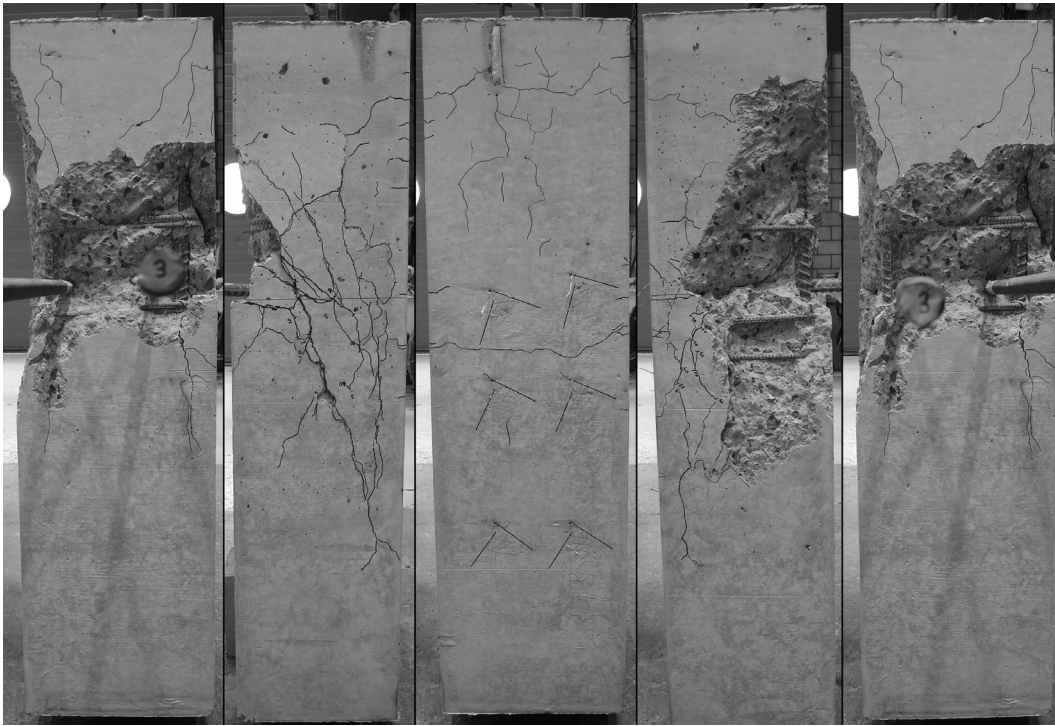


Figure D.1: Phase 2 specimen 3db_a

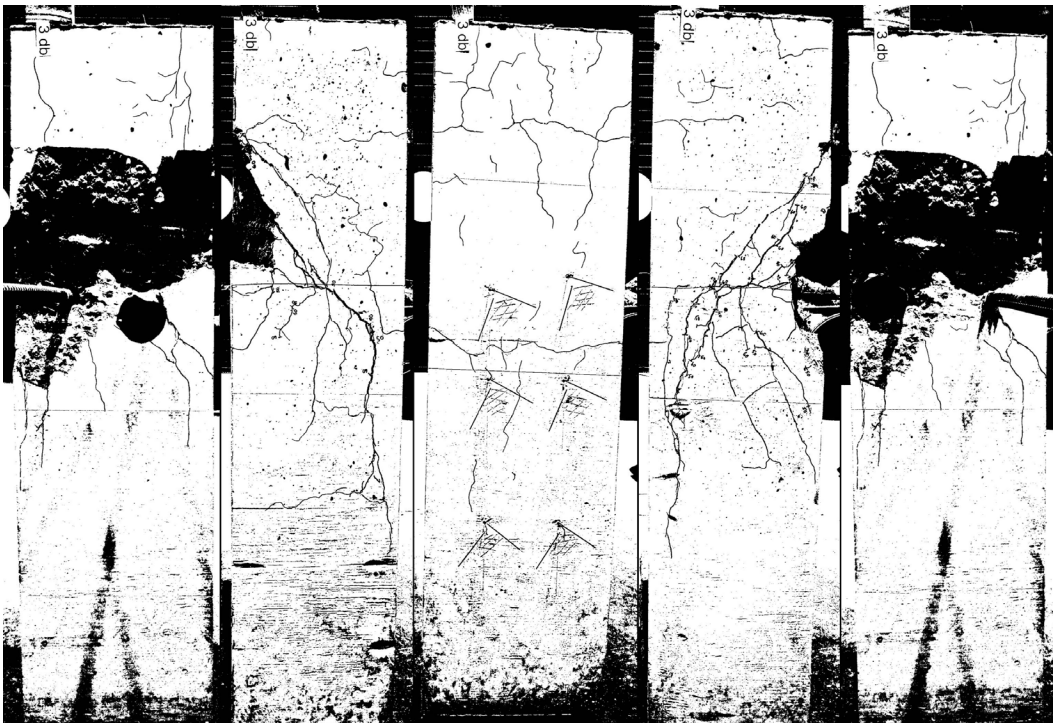
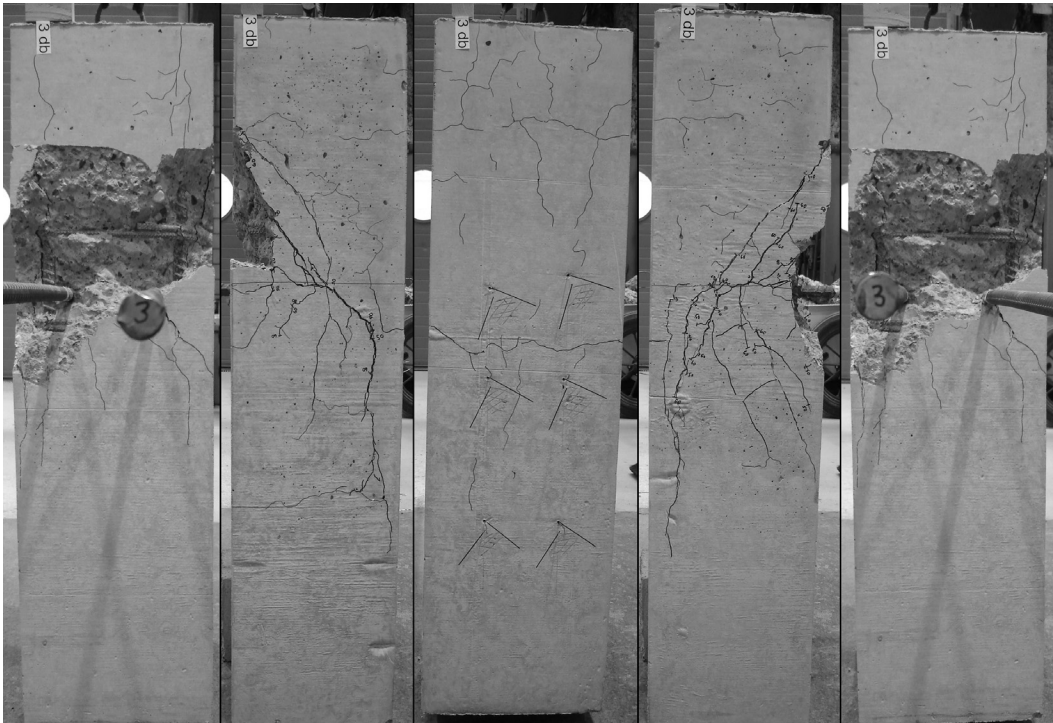


Figure D.2: Phase 2 specimen 3db_b



Figure D.3: Phase 2 specimen 5db_a

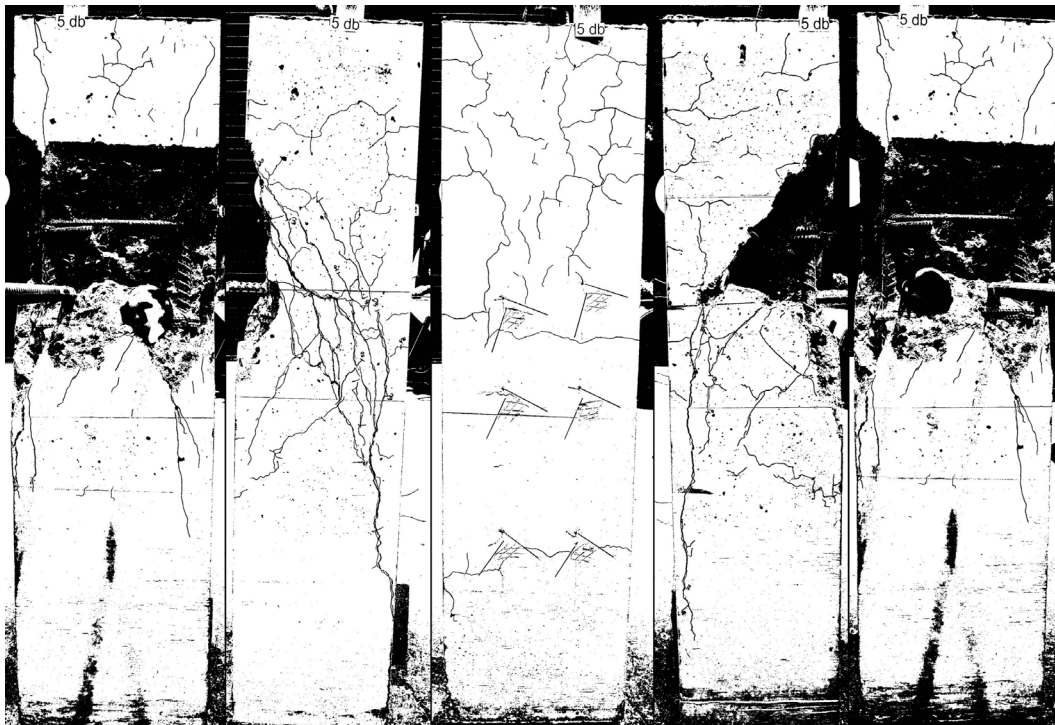
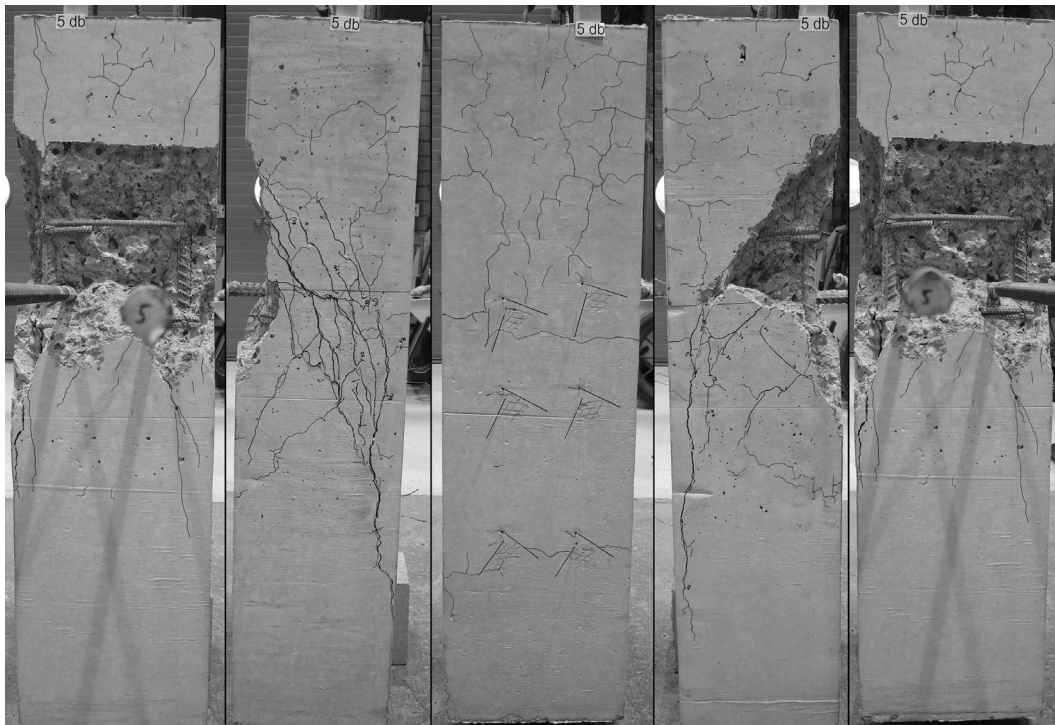


Figure D.4: Phase 2 specimen 5db_b

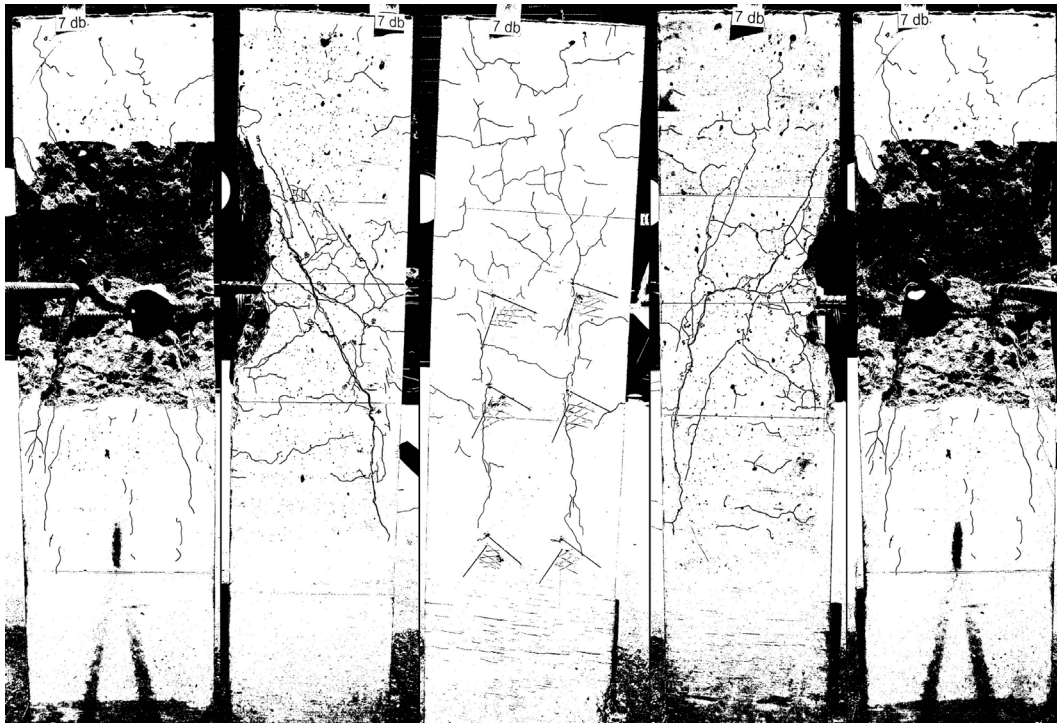
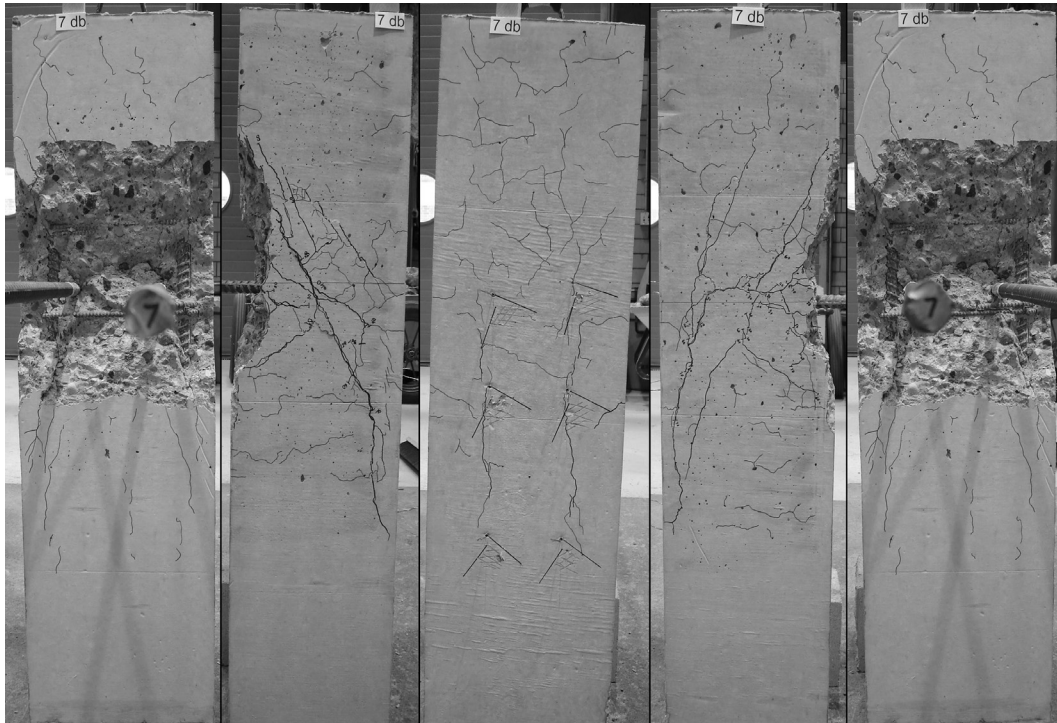


Figure D.5: Phase 2 specimen 7db_a

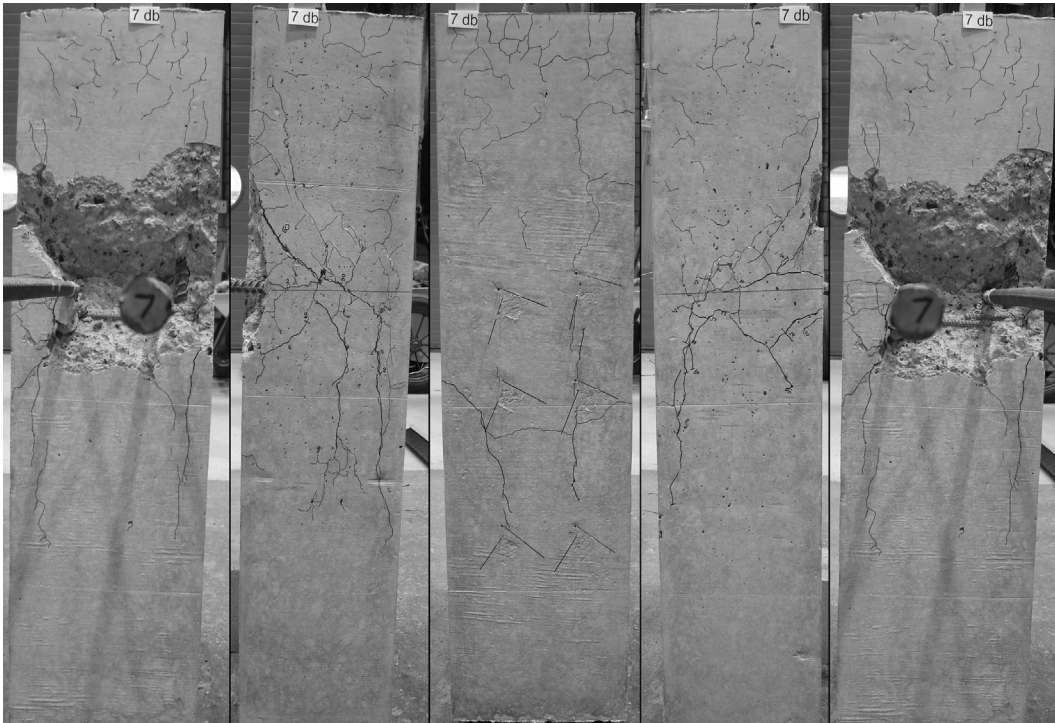


Figure D.6: Phase 2 specimen 7db_b

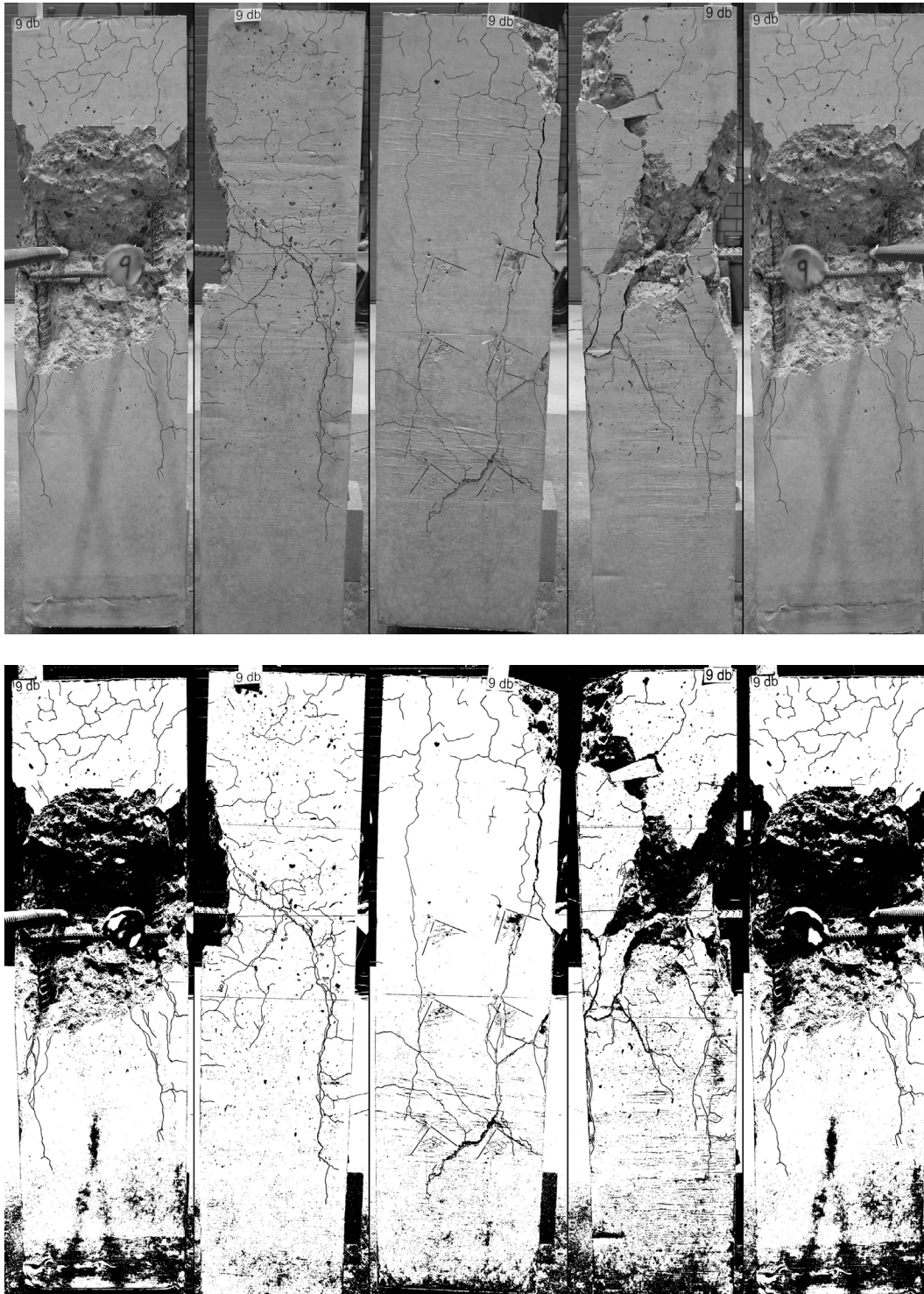


Figure D.7: Phase 2 specimen 9db

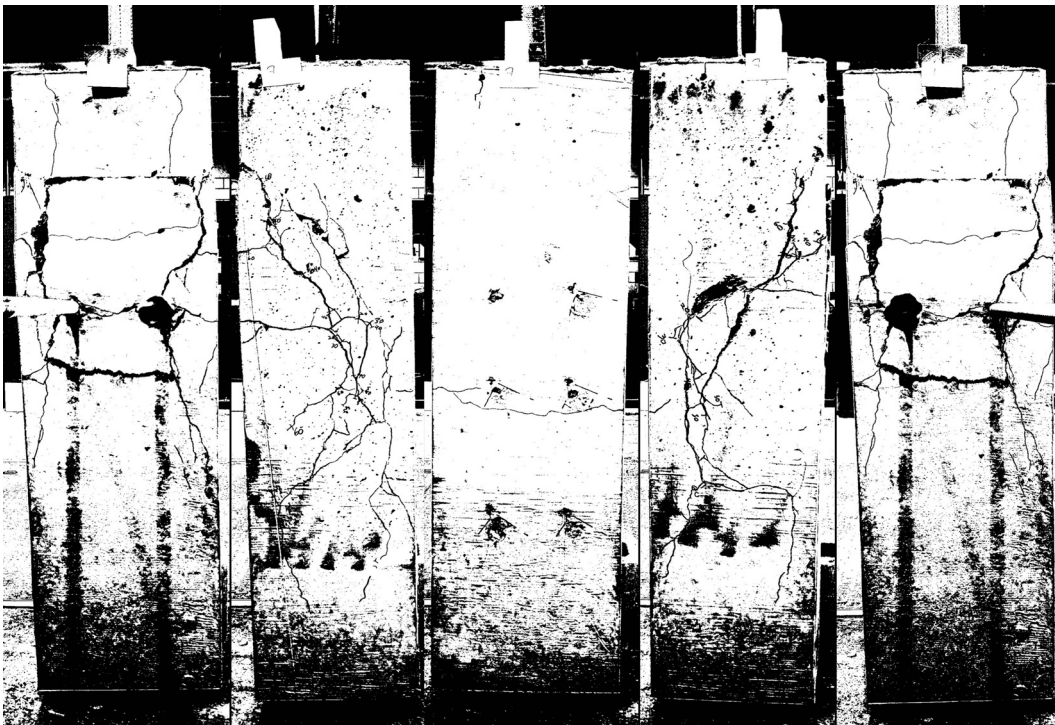
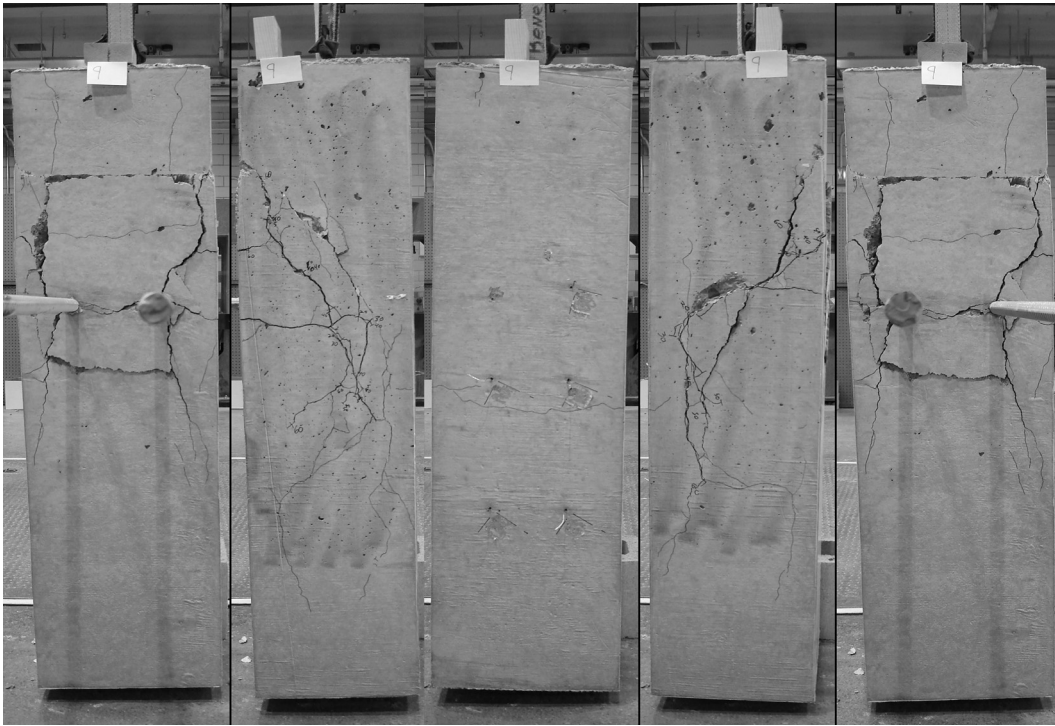


Figure D.8: Phase 3 specimen 9

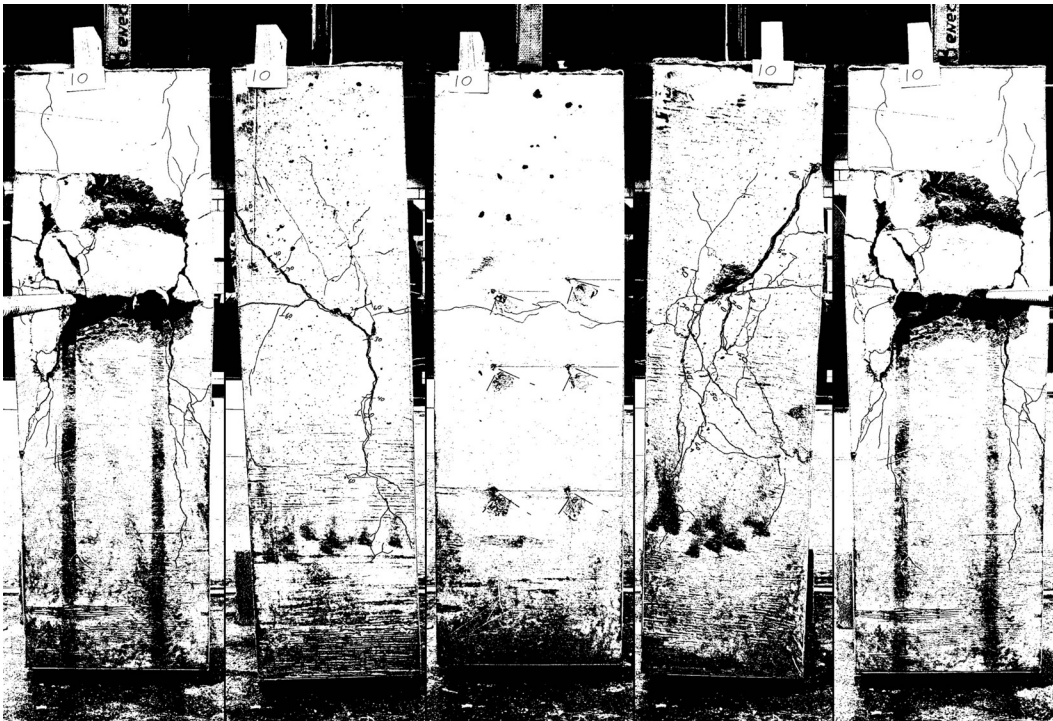
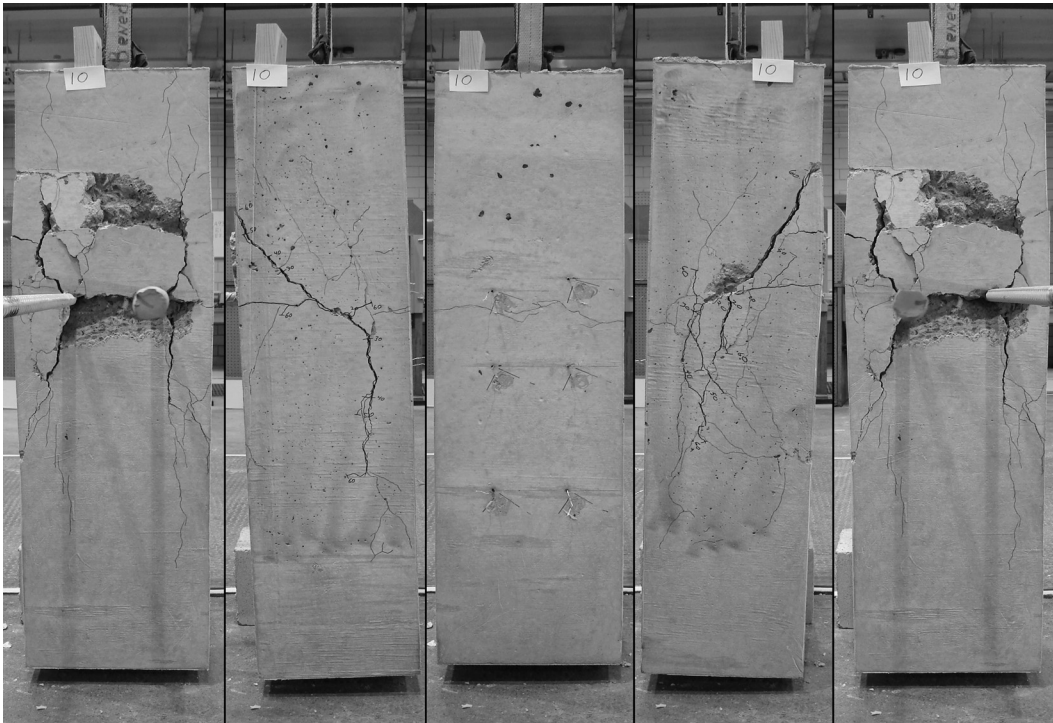


Figure D.9: Phase 3 specimen 10

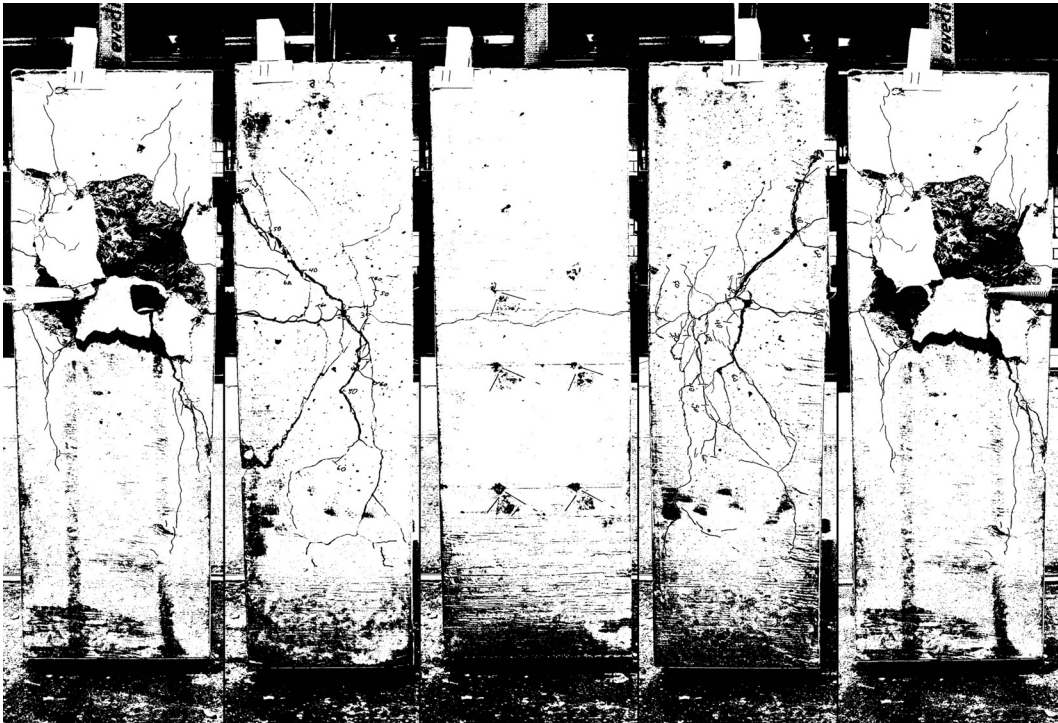
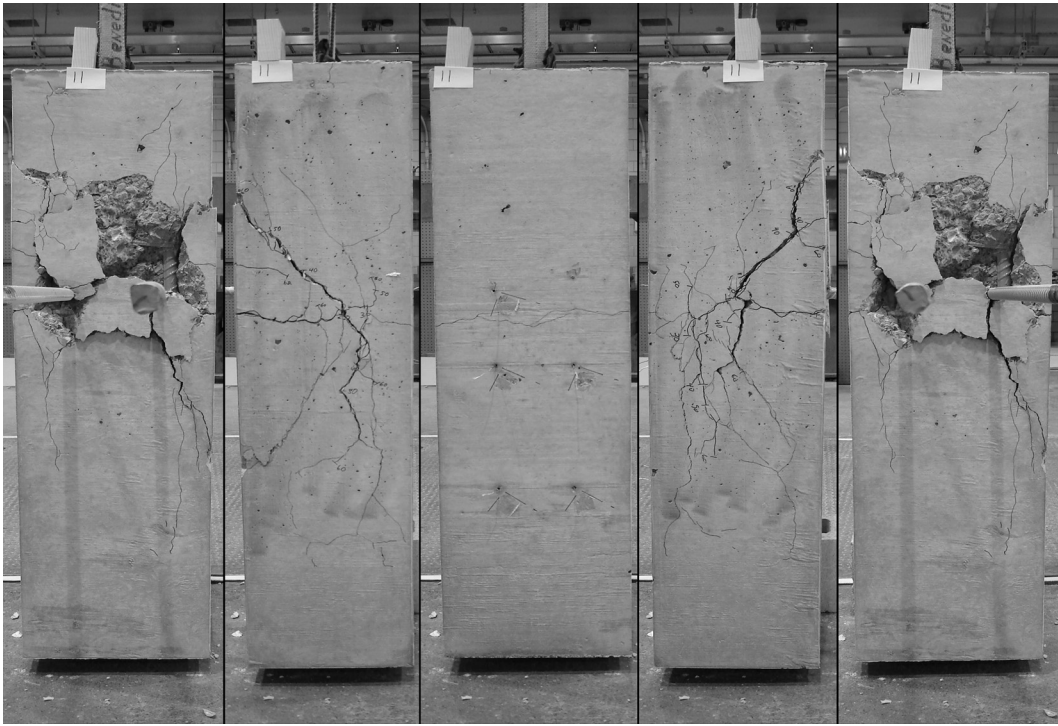


Figure D.10: Phase 3 specimen 11

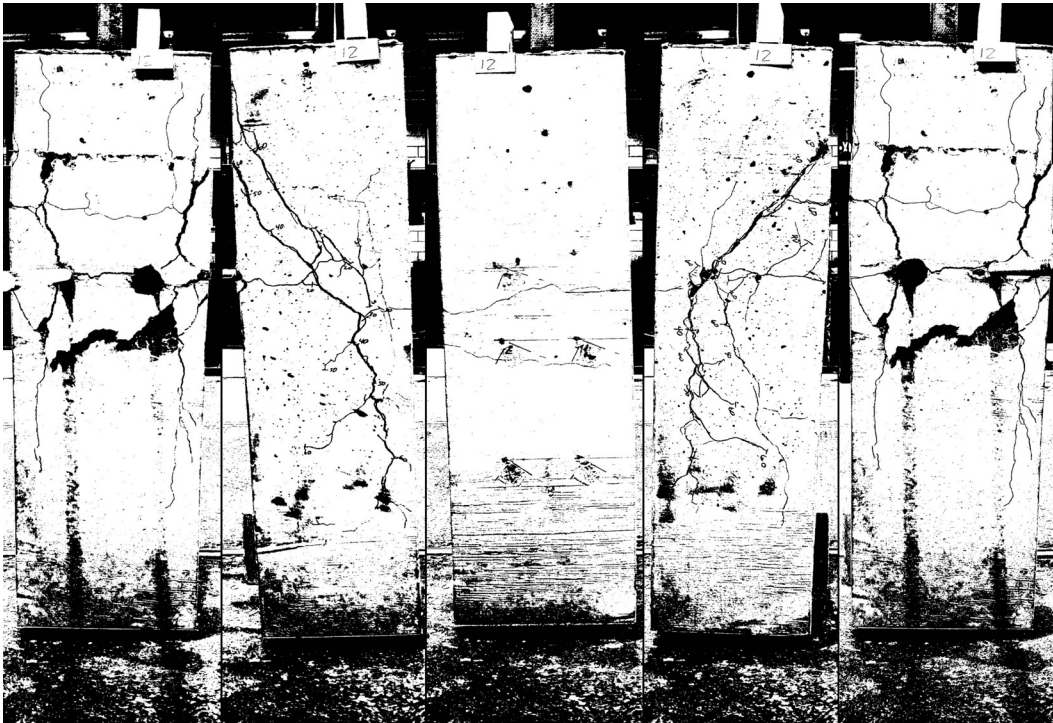
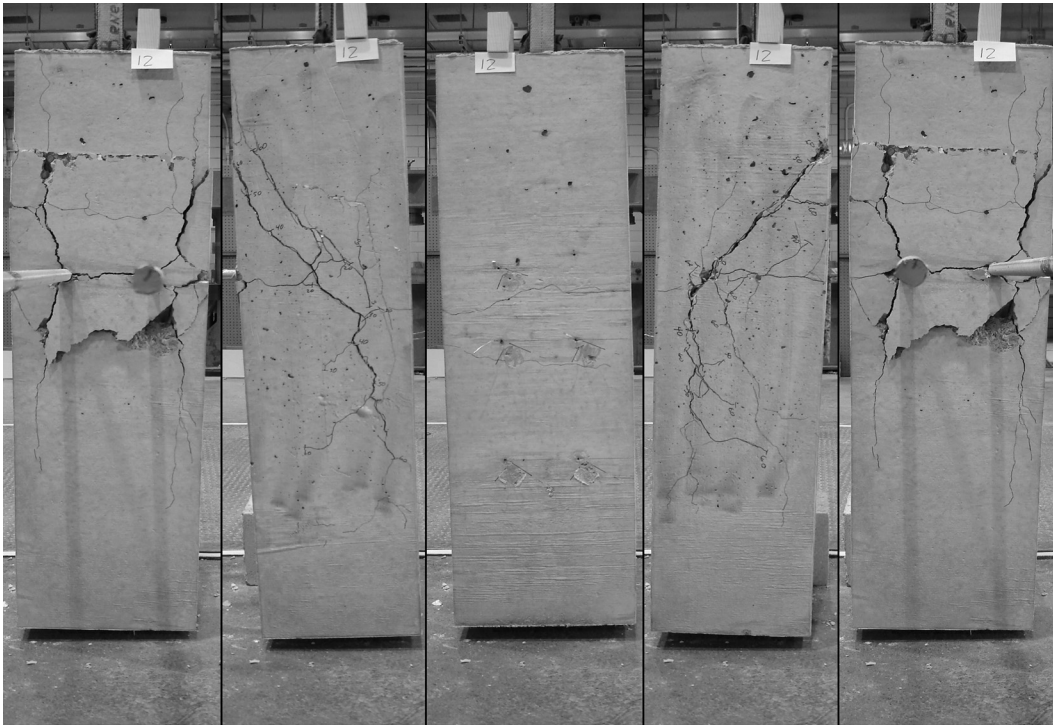


Figure D.11: Phase 3 specimen 12

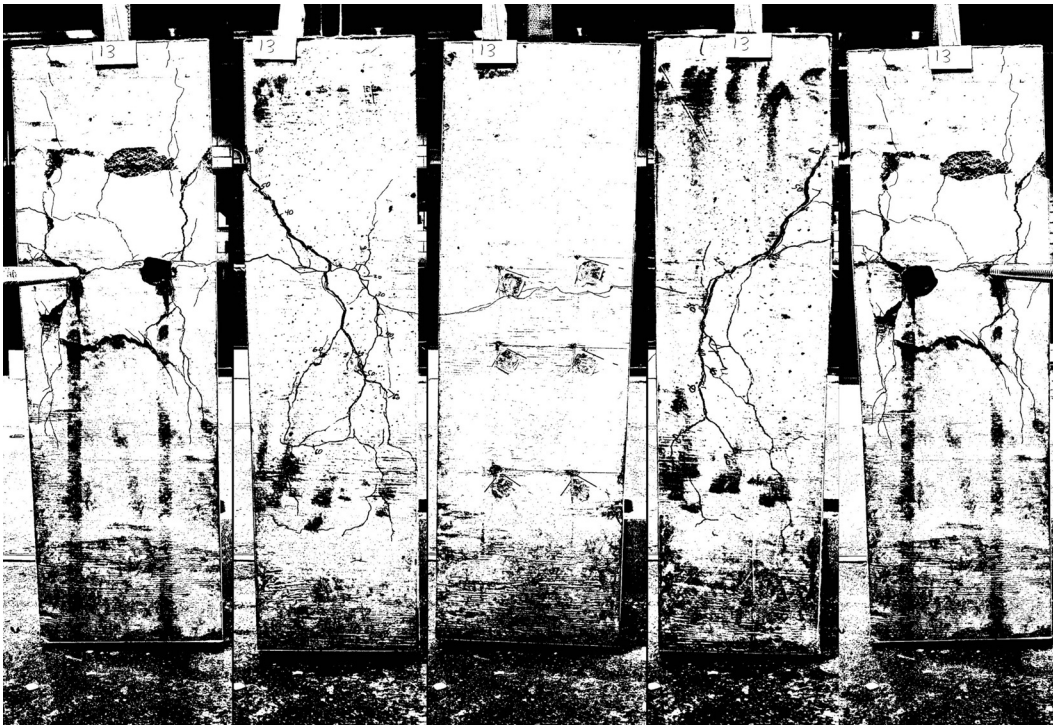
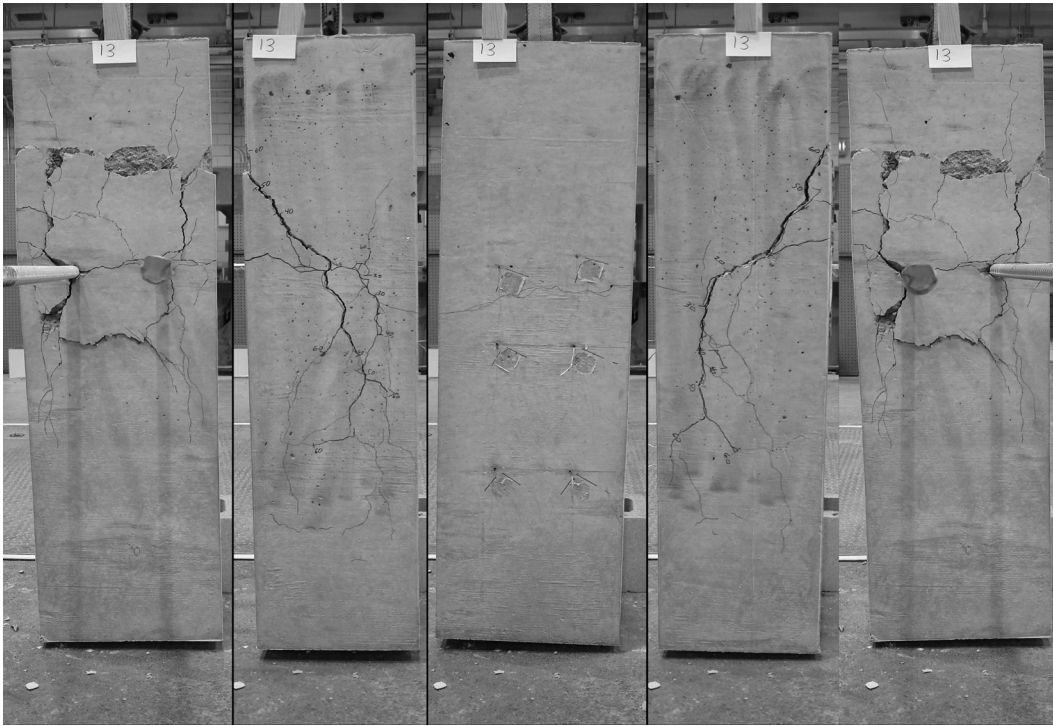


Figure D.12: Phase 3 specimen 13

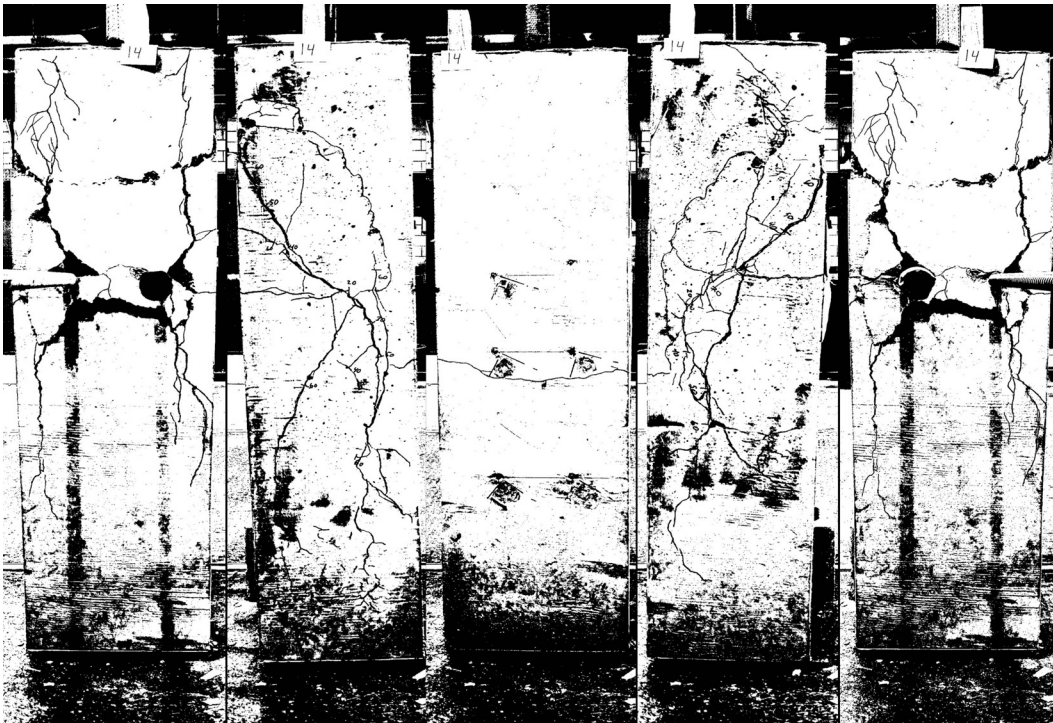
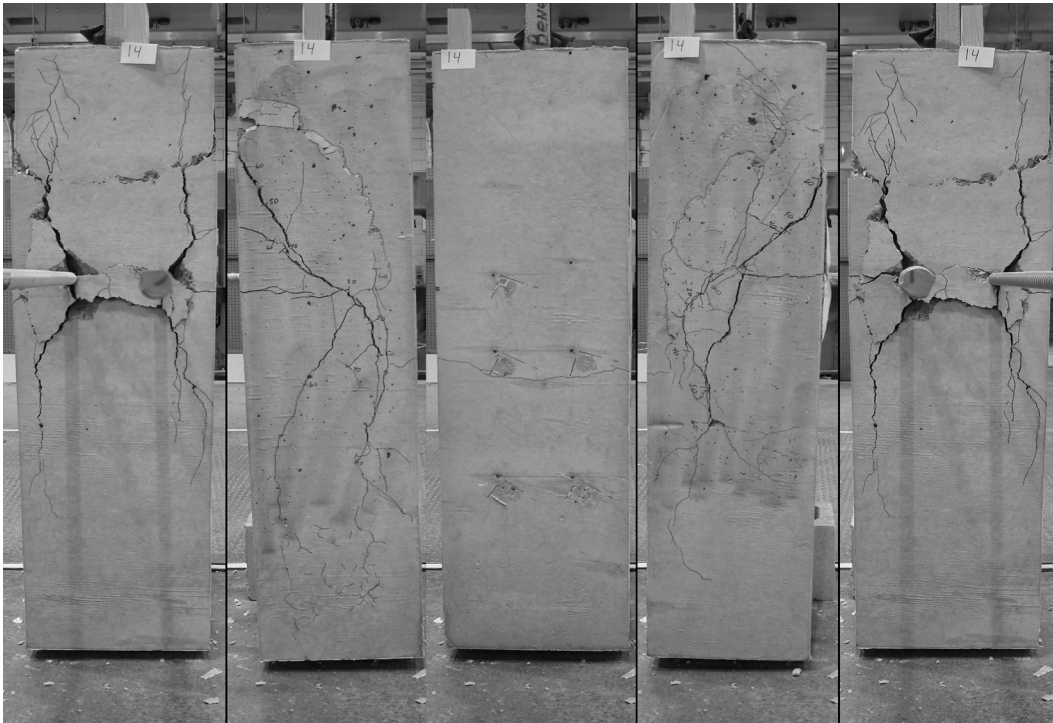


Figure D.13: Phase 3 specimen 14

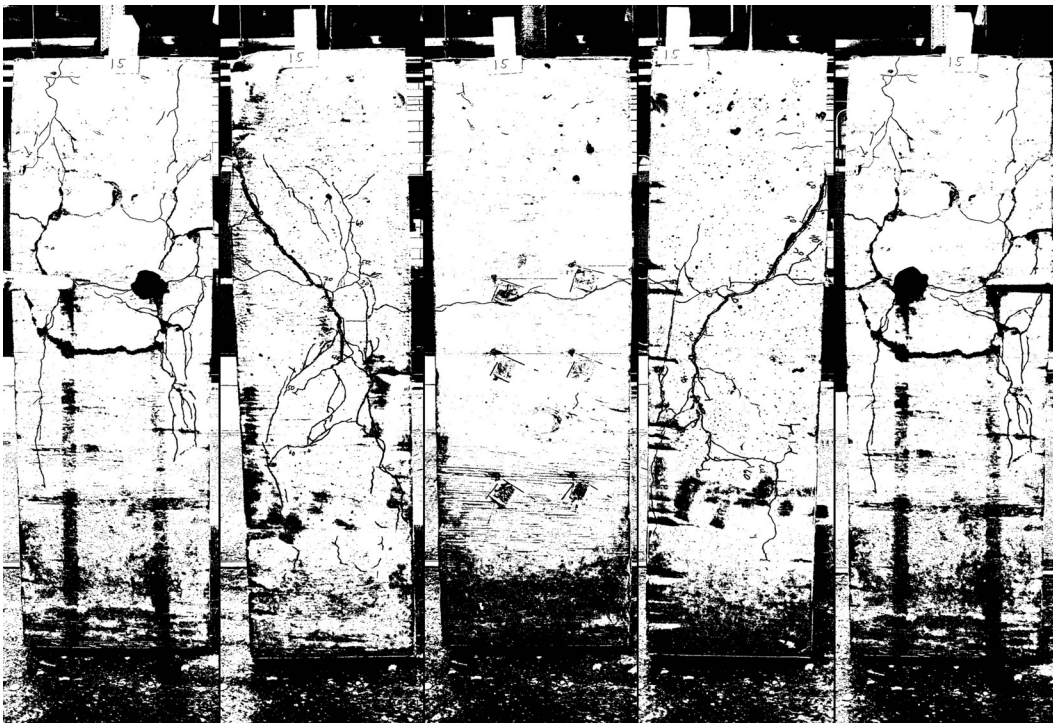
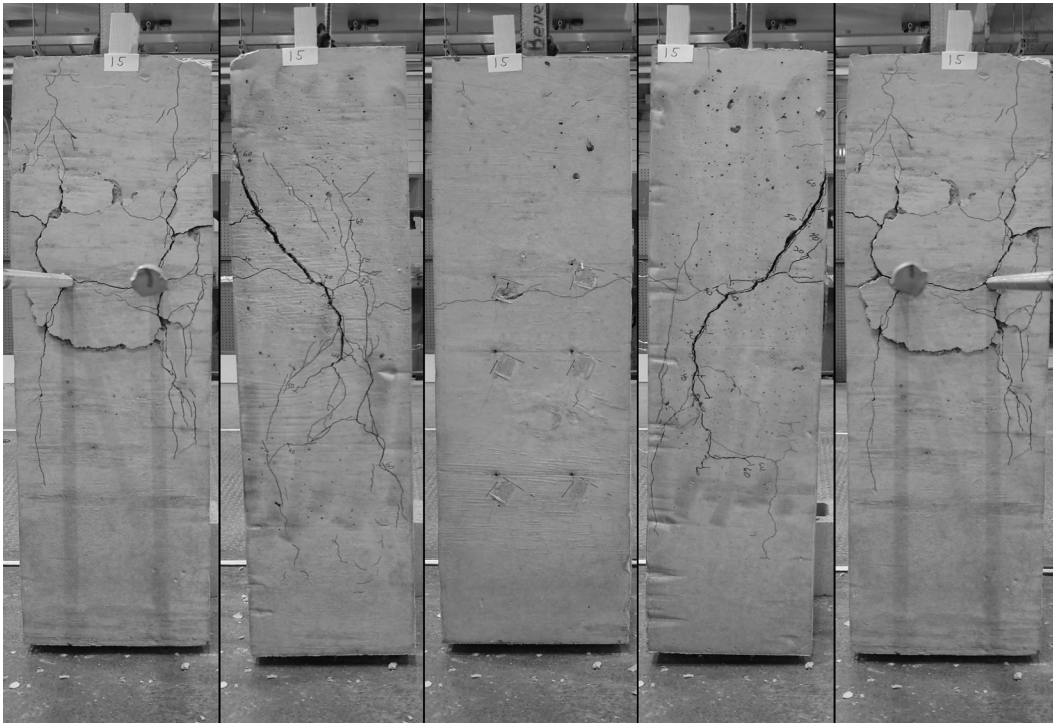


Figure D.14: Phase 3 specimen 15

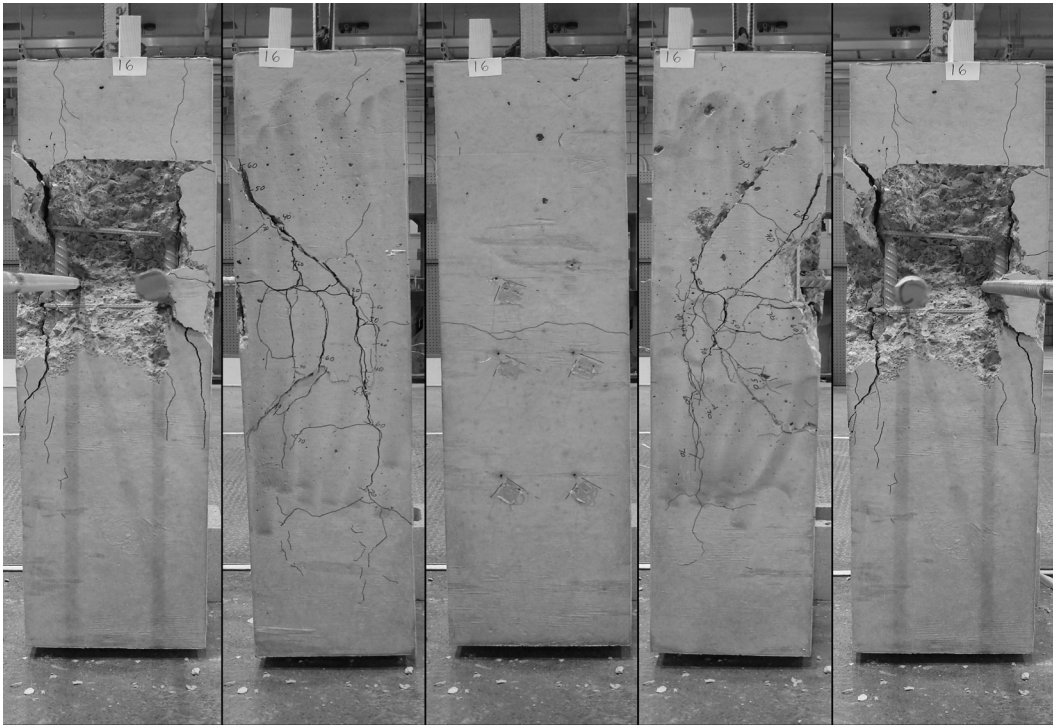


Figure D.15: Phase 3 specimen 16

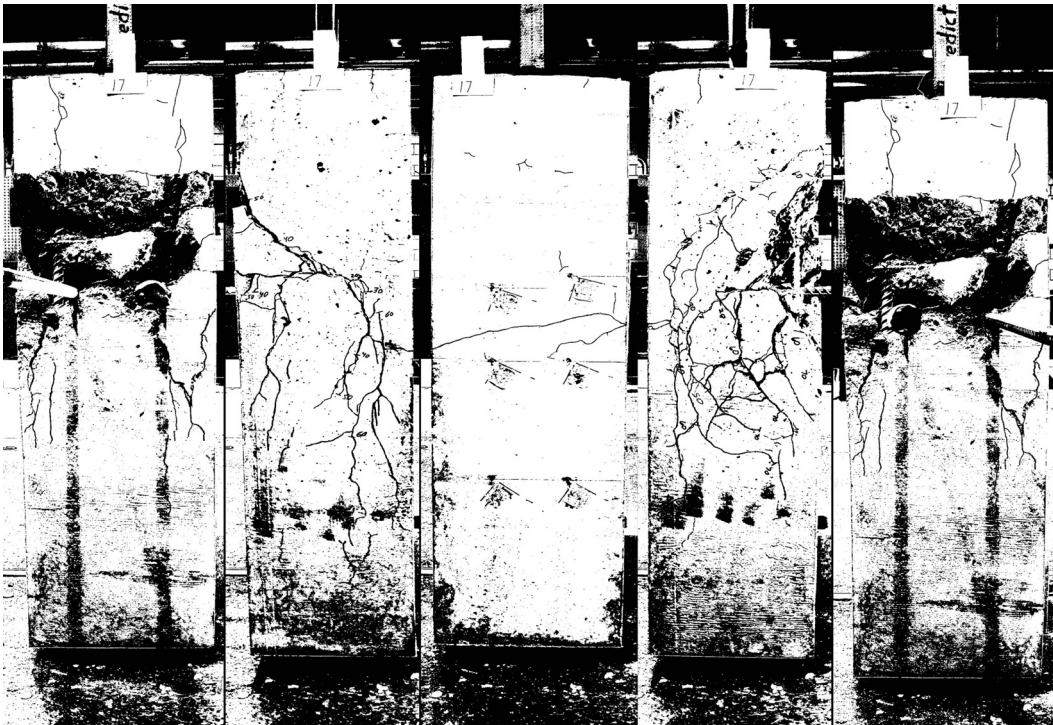
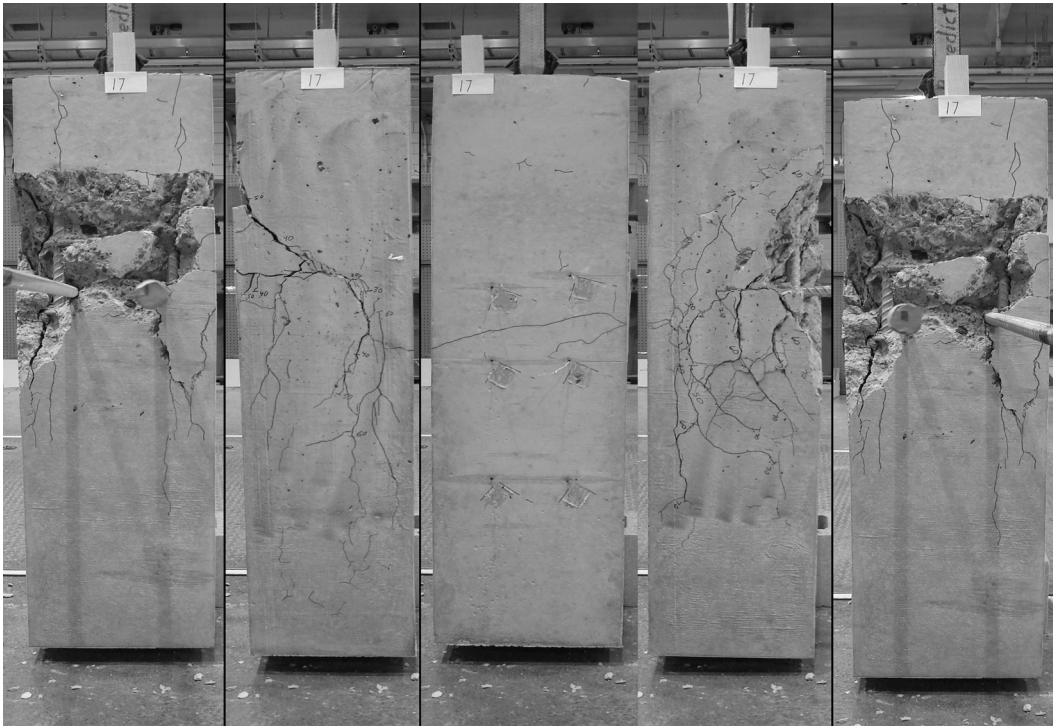


Figure D.16: Phase 3 specimen 17

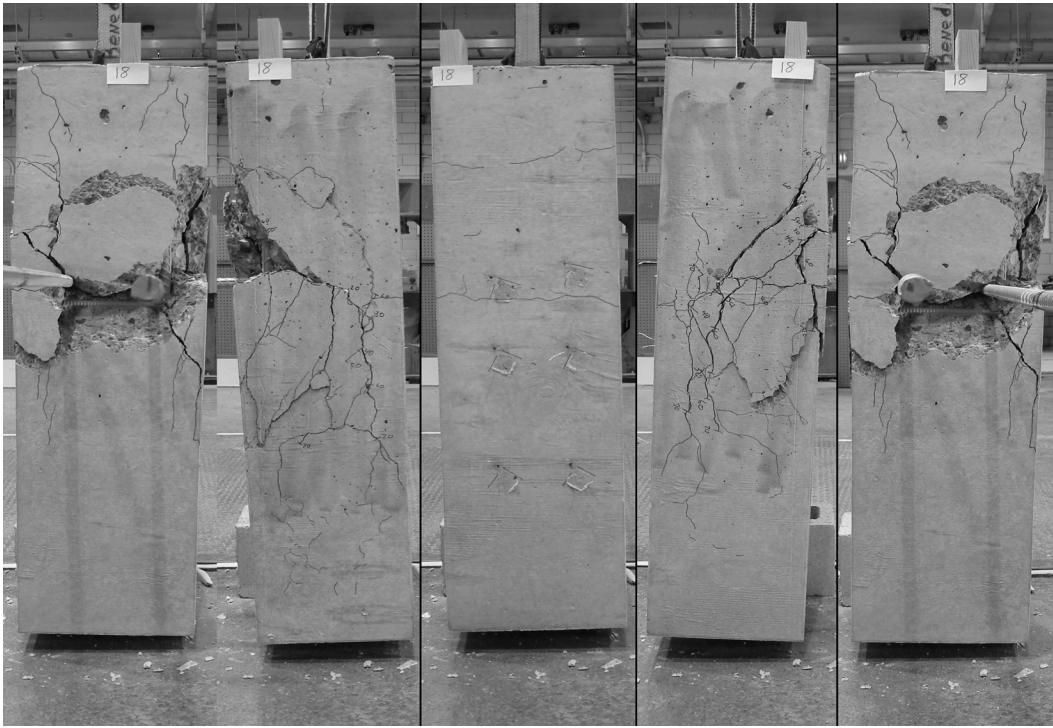


Figure D.17: Phase 3 specimen 18

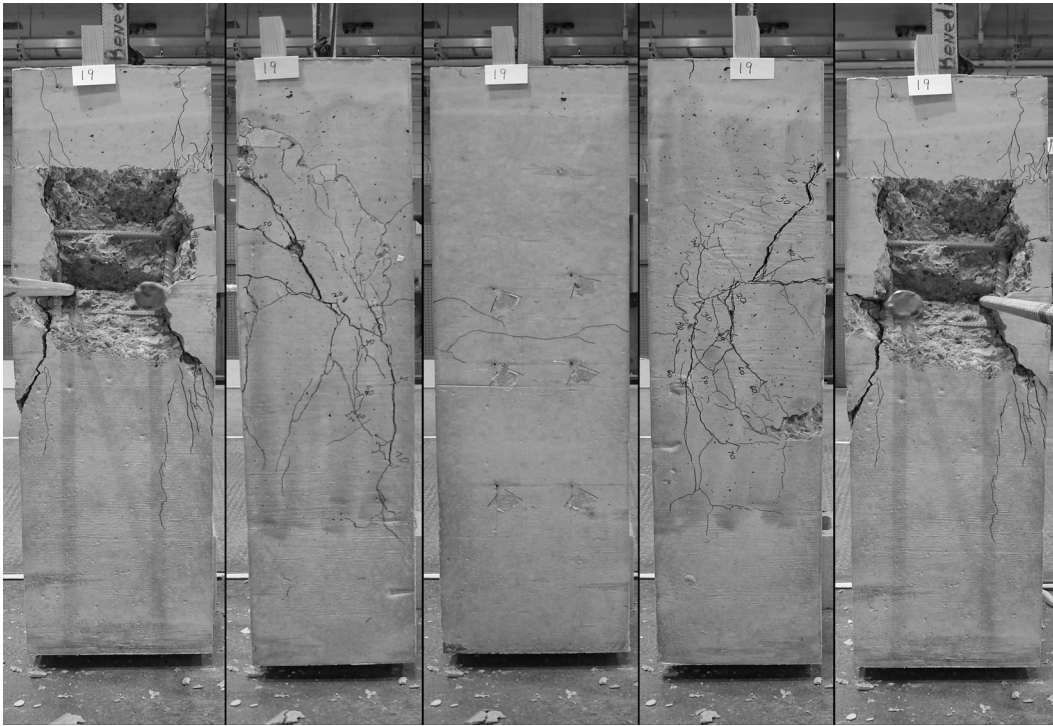


Figure D.18: Phase 3 specimen 19

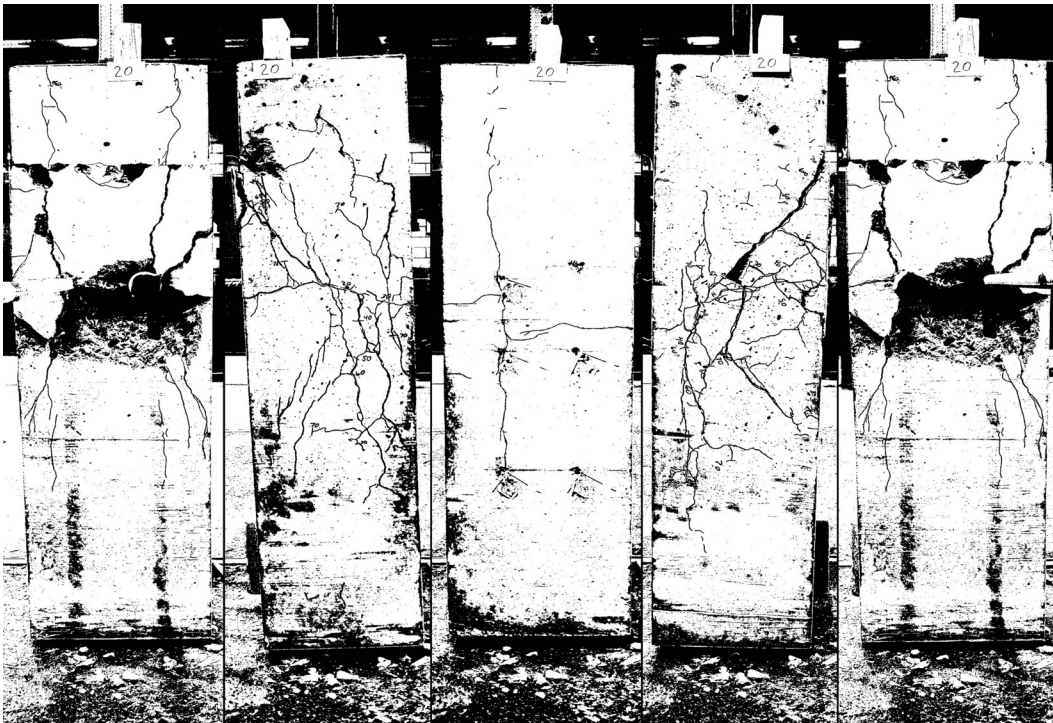
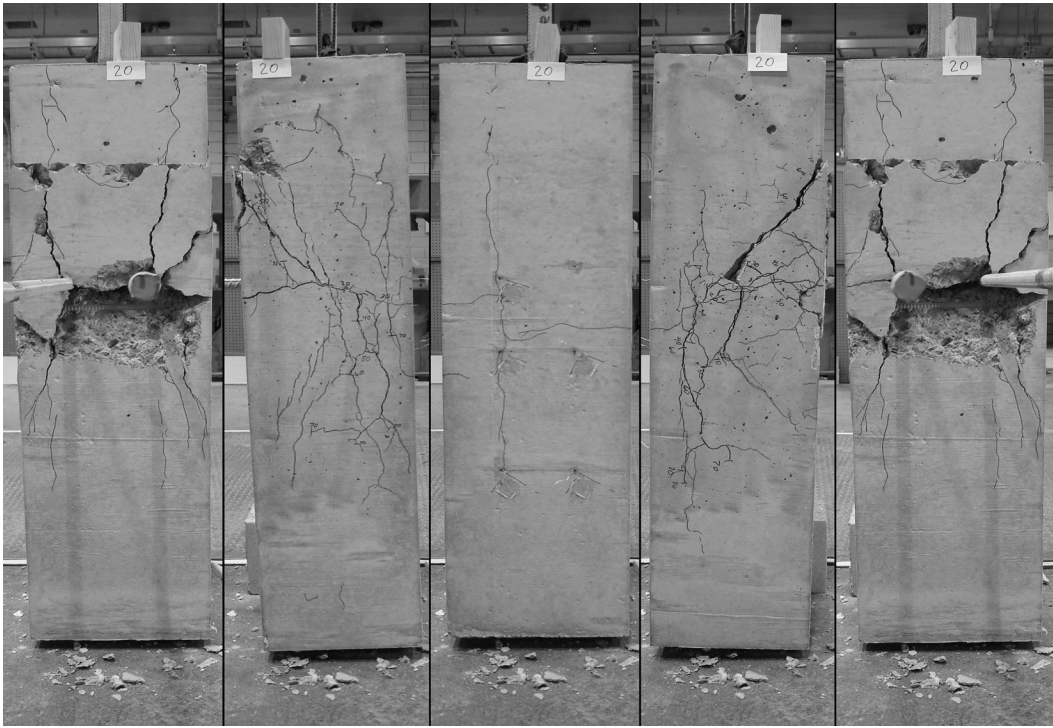


Figure D.19: Phase 3 specimen 20

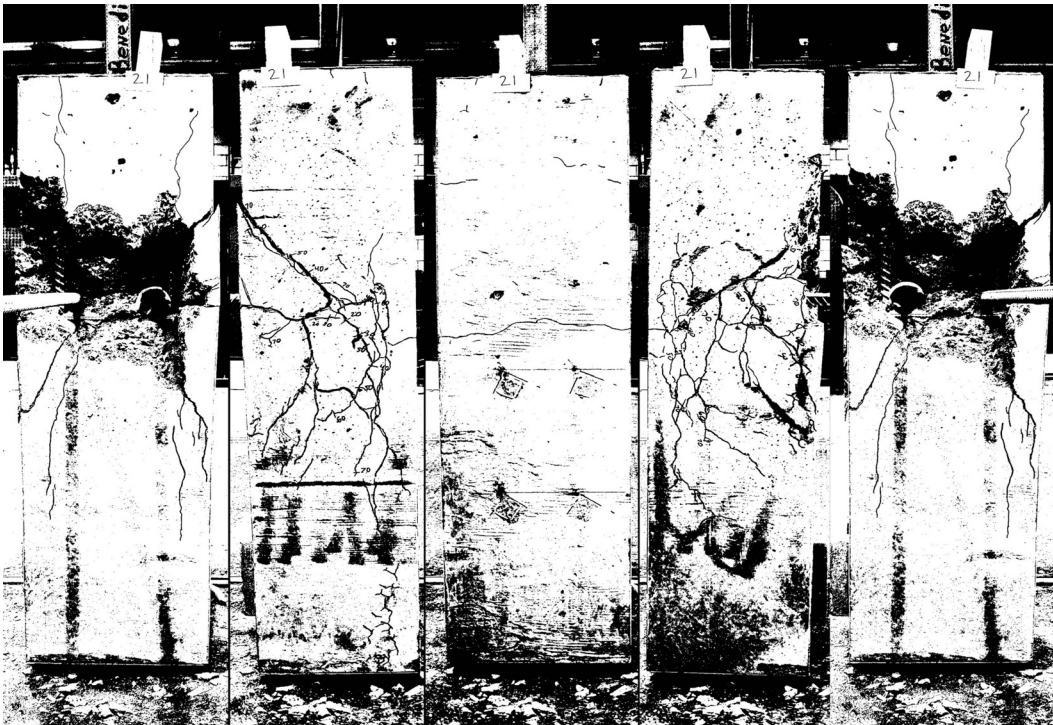
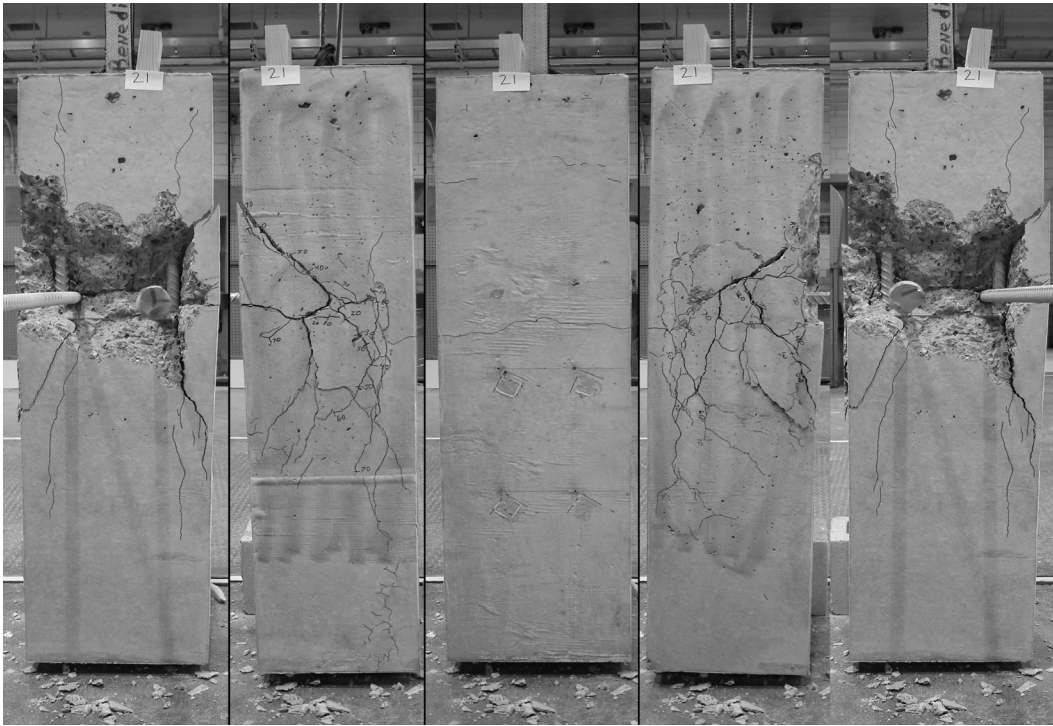


Figure D.20: Phase 3 specimen 21



Figure D.21: Phase 3 specimen 22

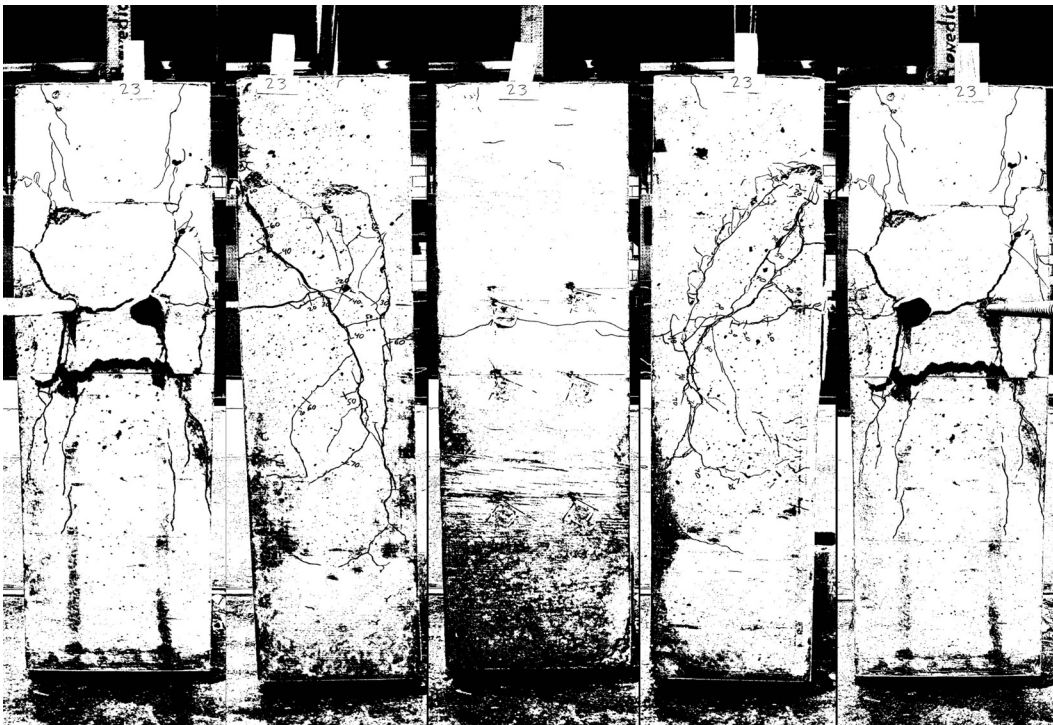
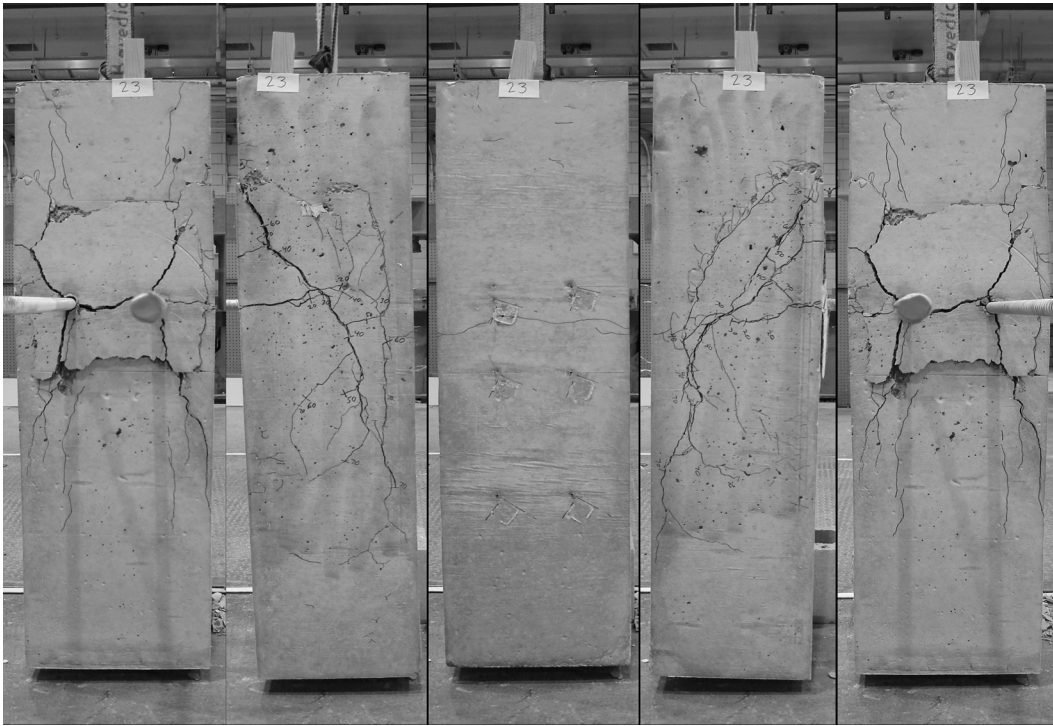


Figure D.22: Phase 3 specimen 23

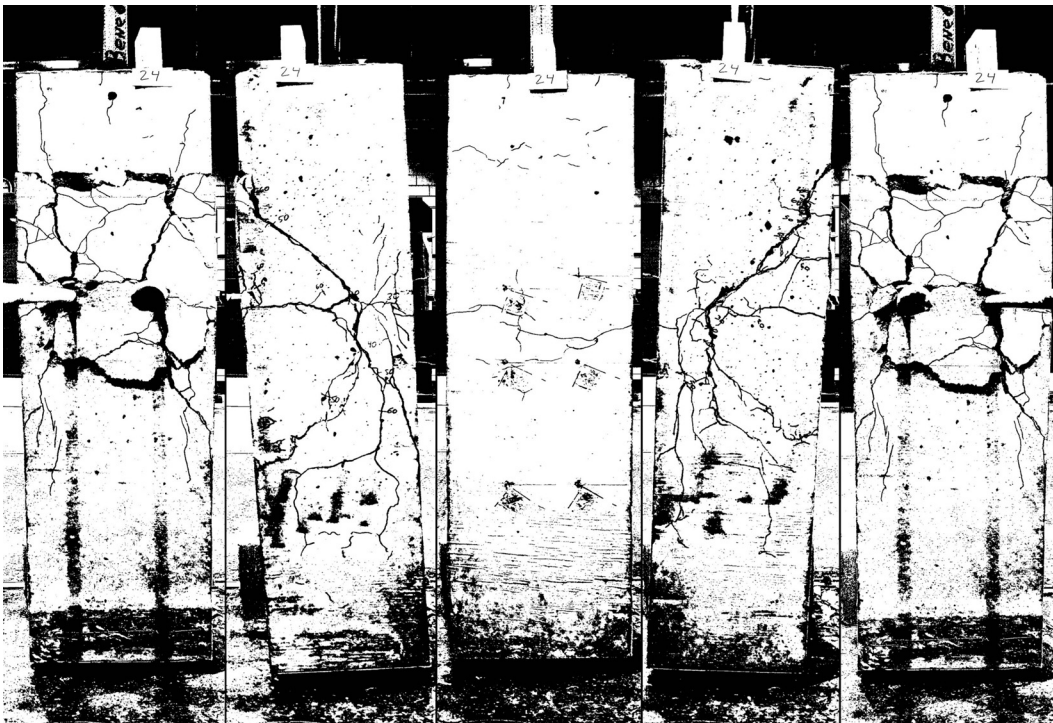
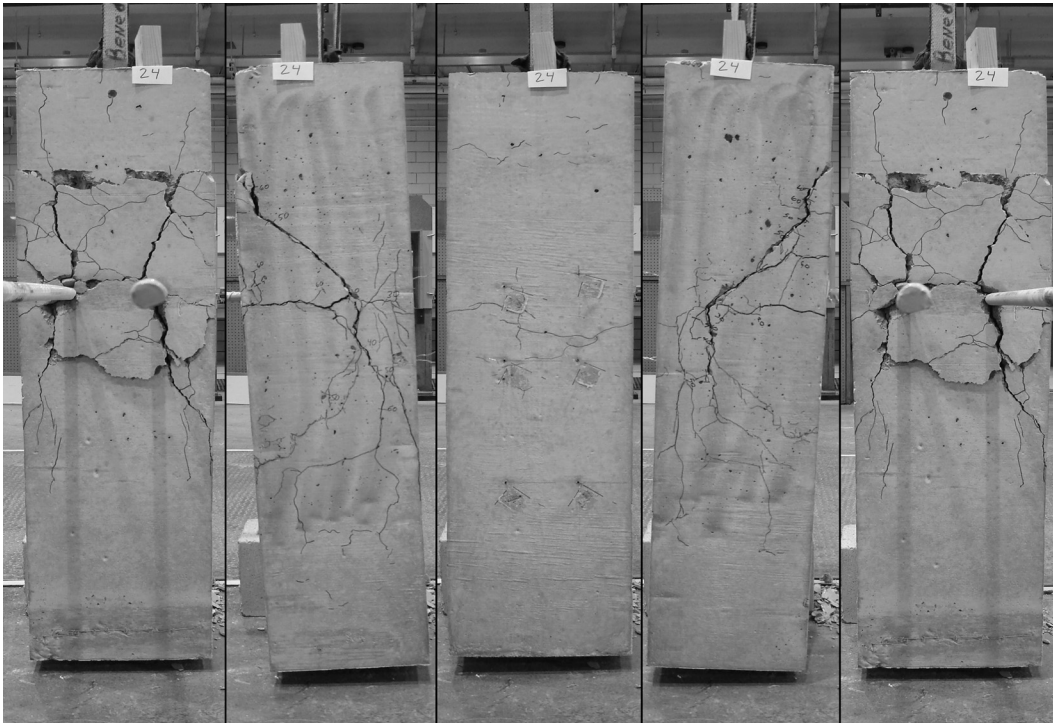


Figure D.23: Phase 3 specimen 24

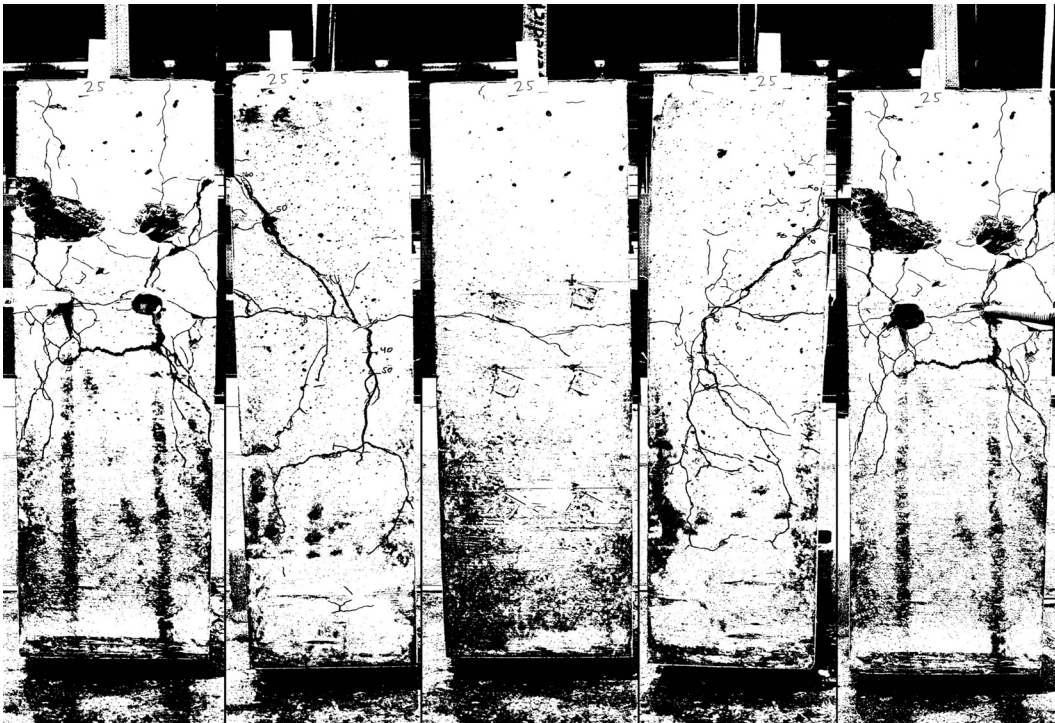
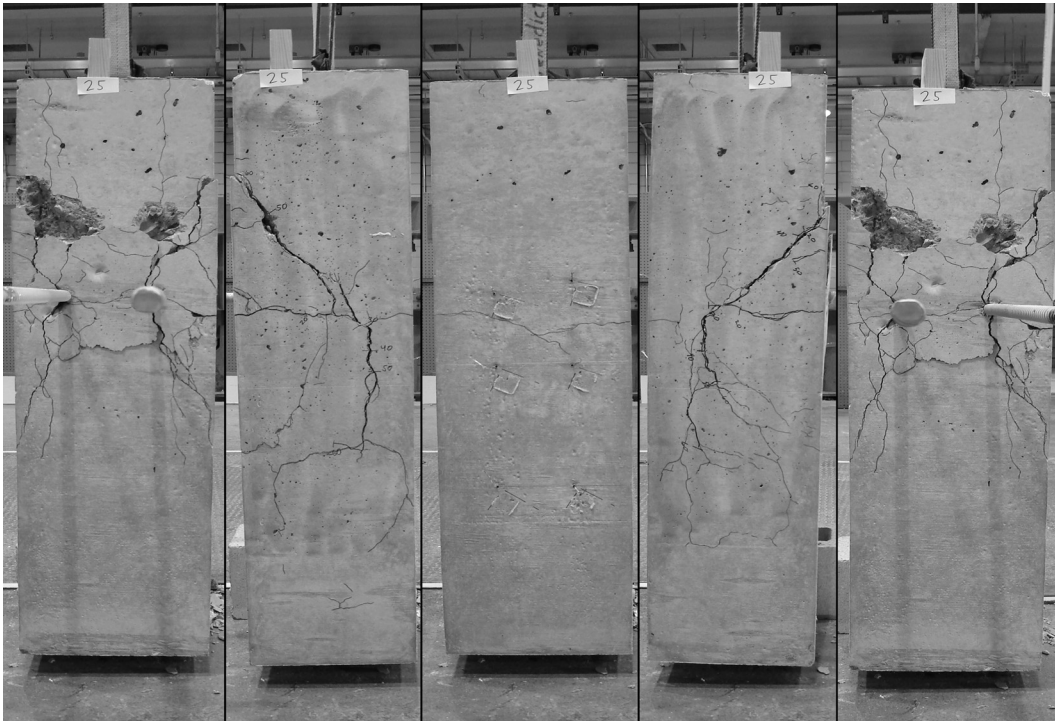


Figure D.24: Phase 3 specimen 25

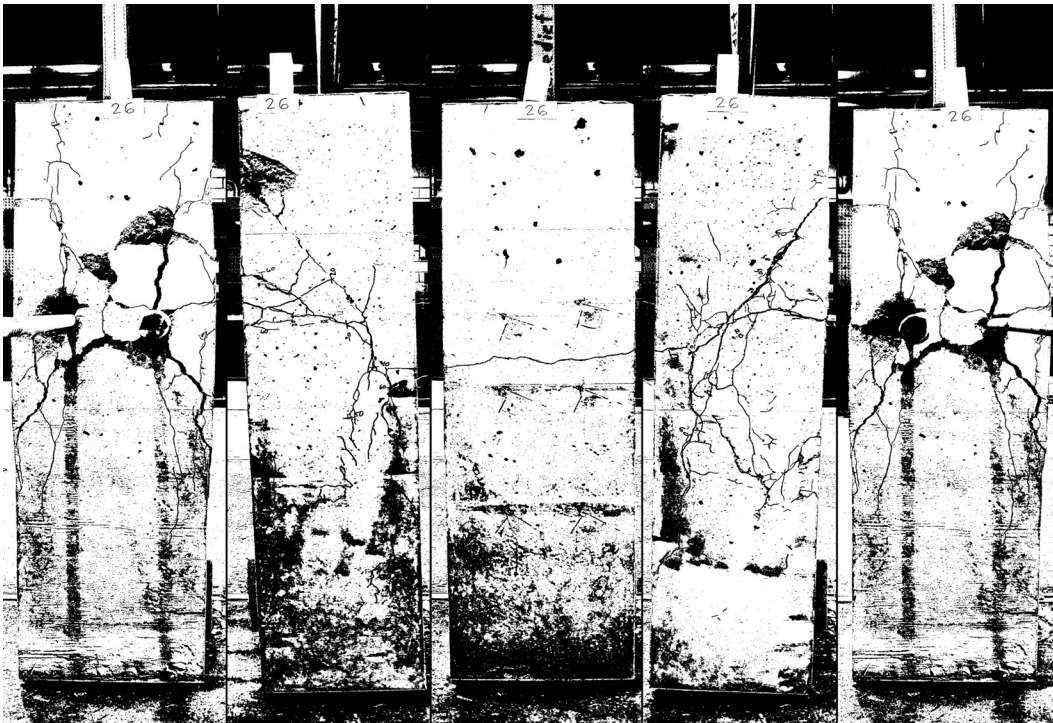
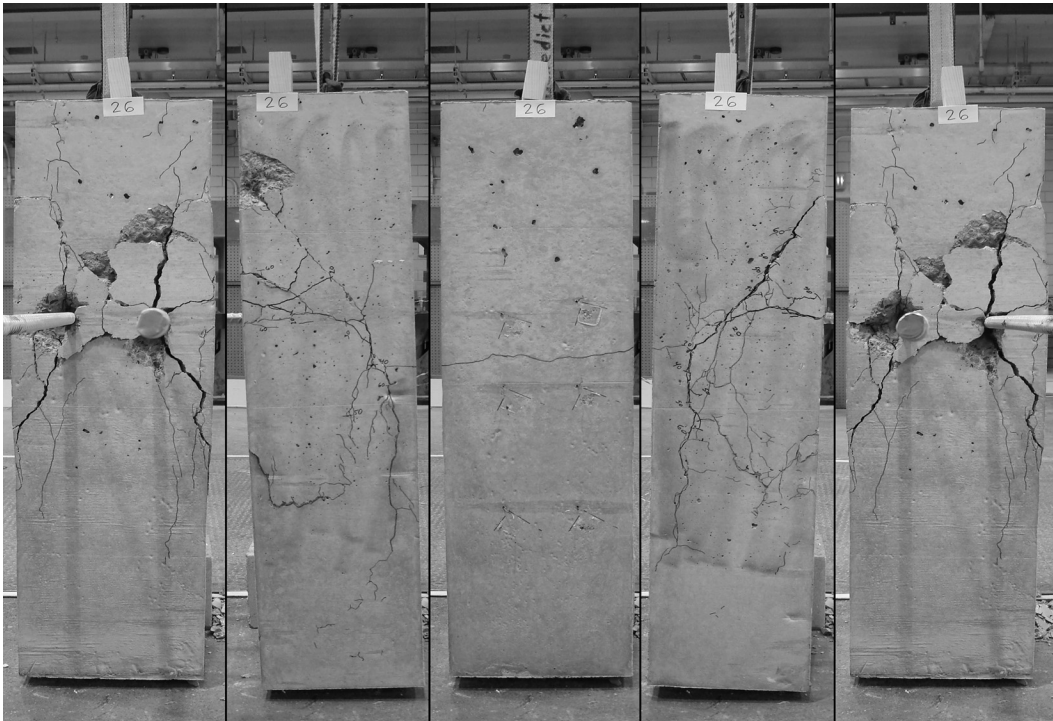


Figure D.25: Phase 3 specimen 26

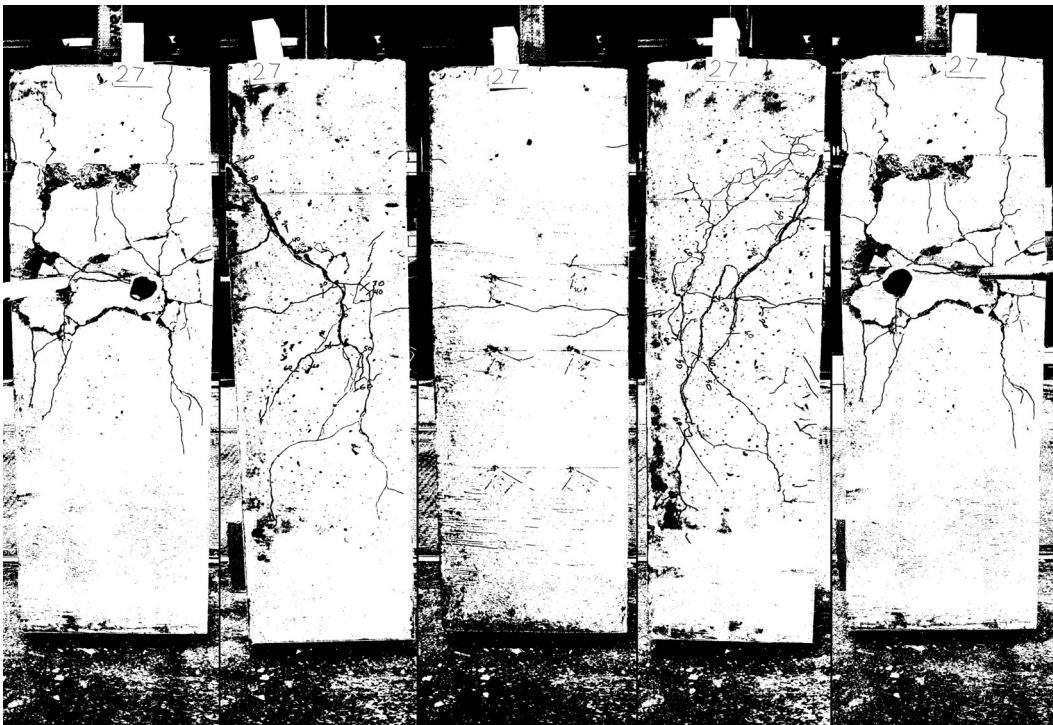
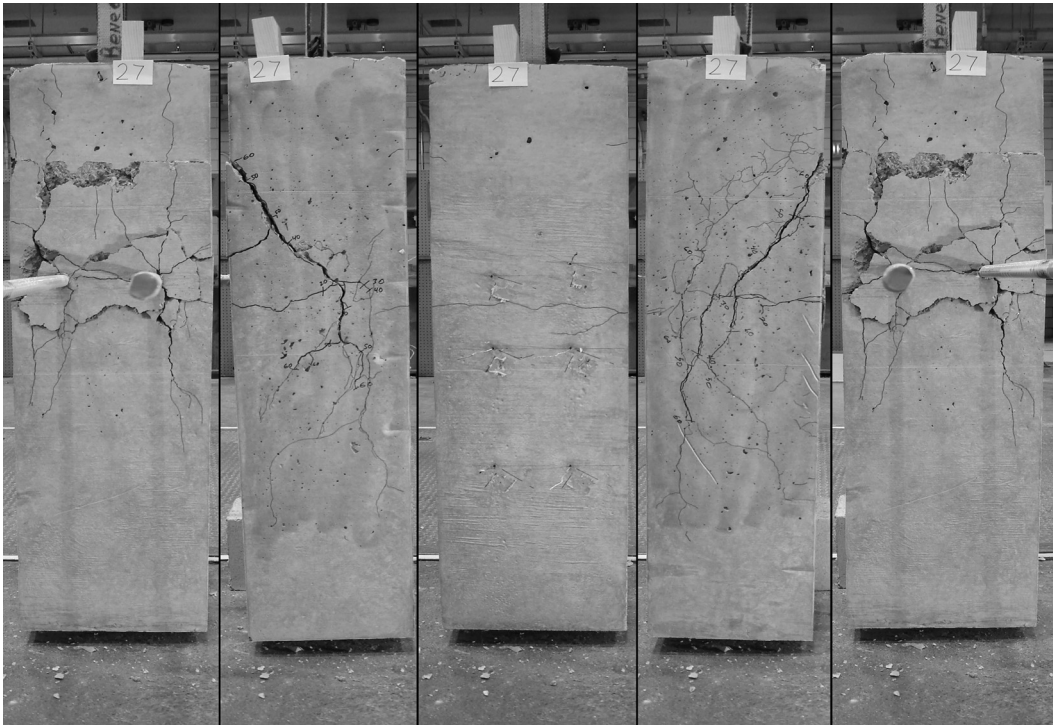


Figure D.26: Phase 3 specimen 27

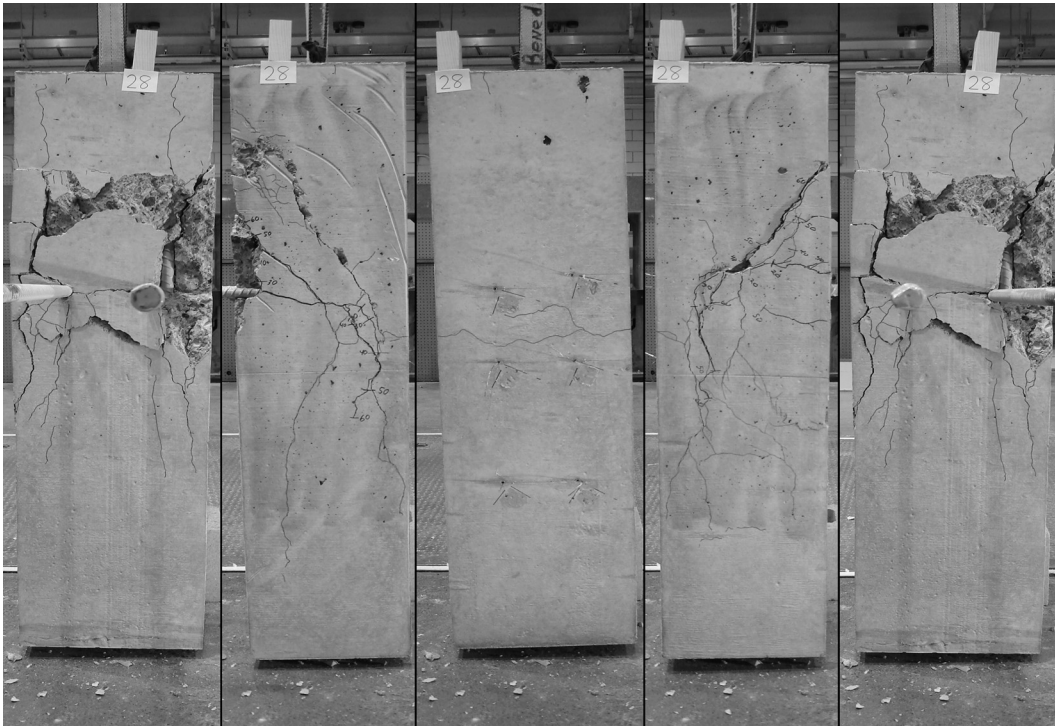


Figure D.27: Phase 3 specimen 28

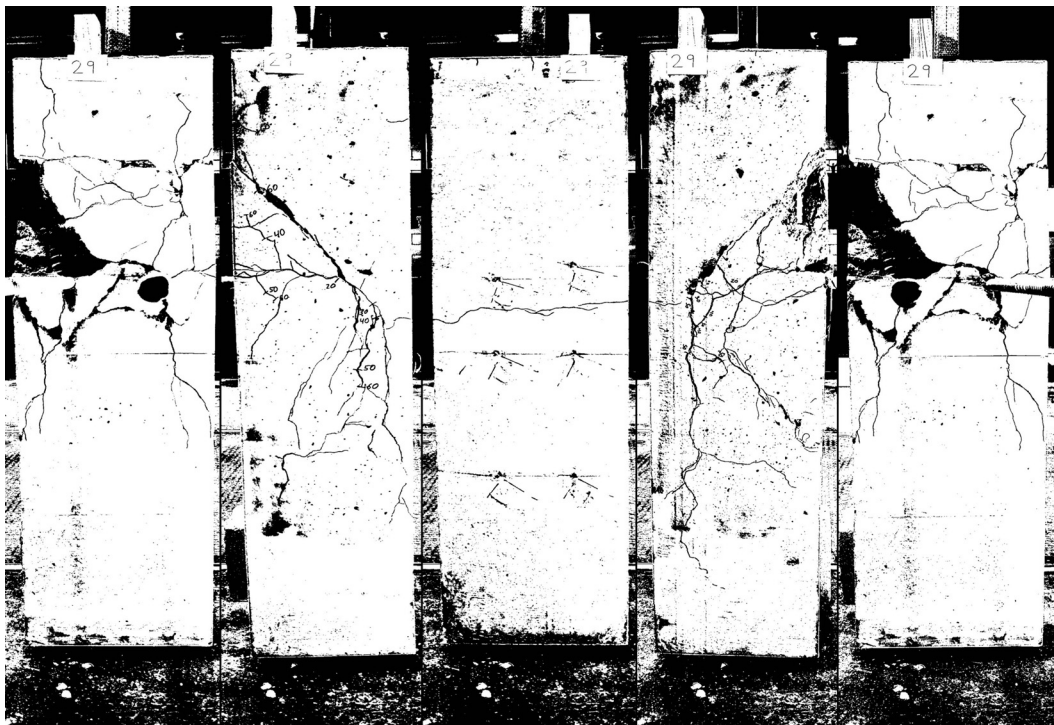
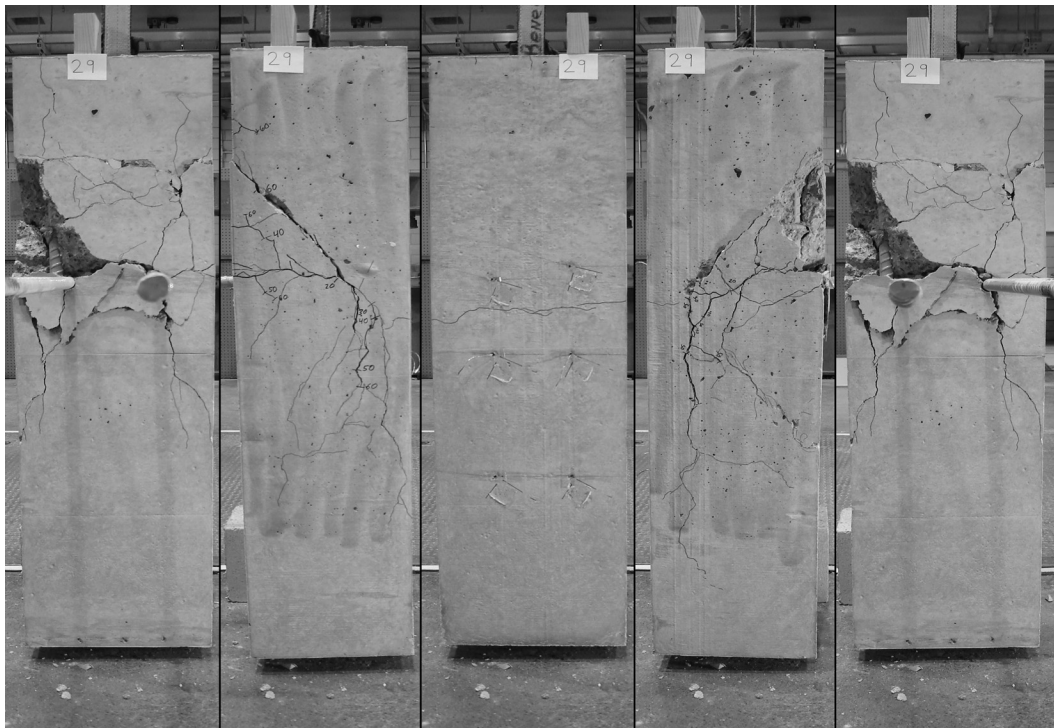


Figure D.28: Phase 3 specimen 29

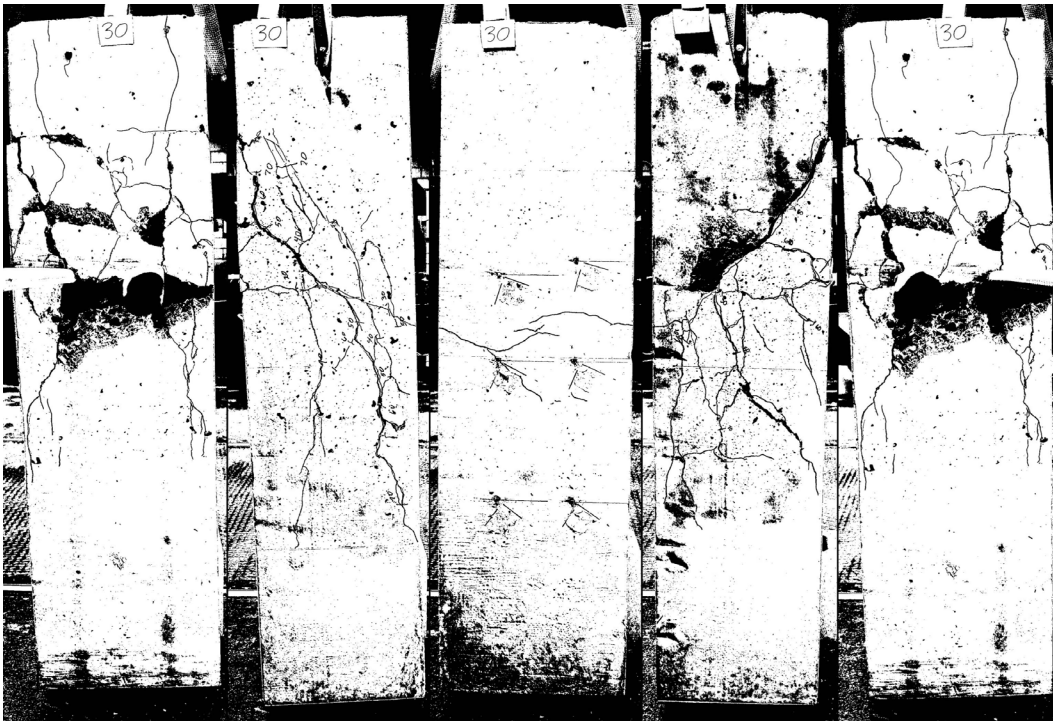
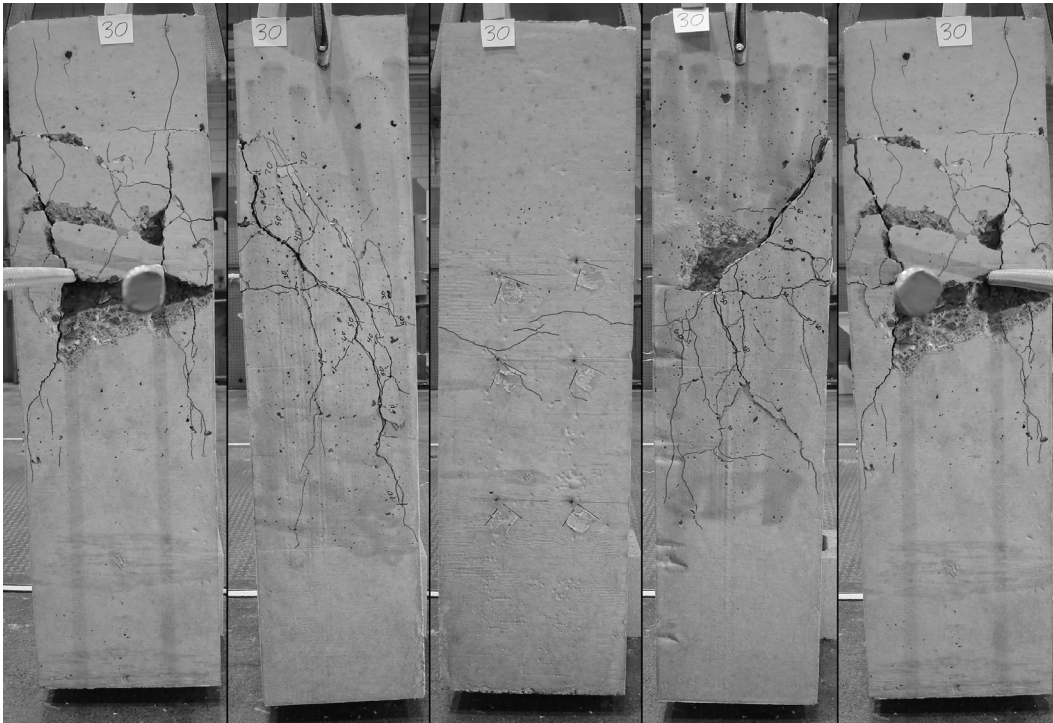


Figure D.29: Phase 3 specimen 30

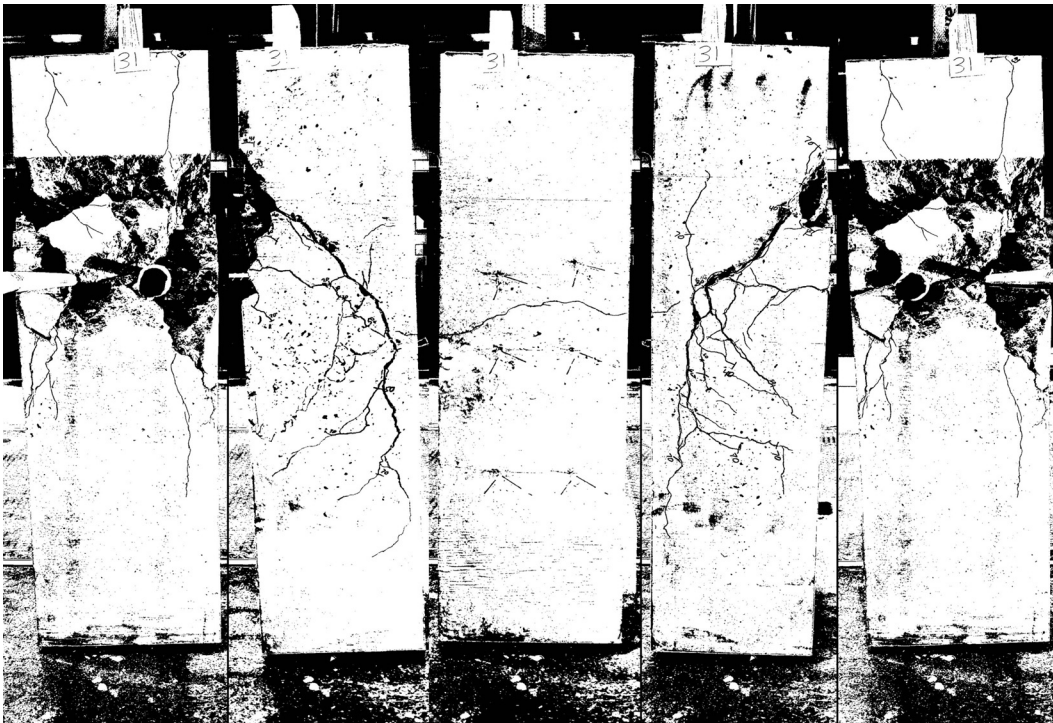
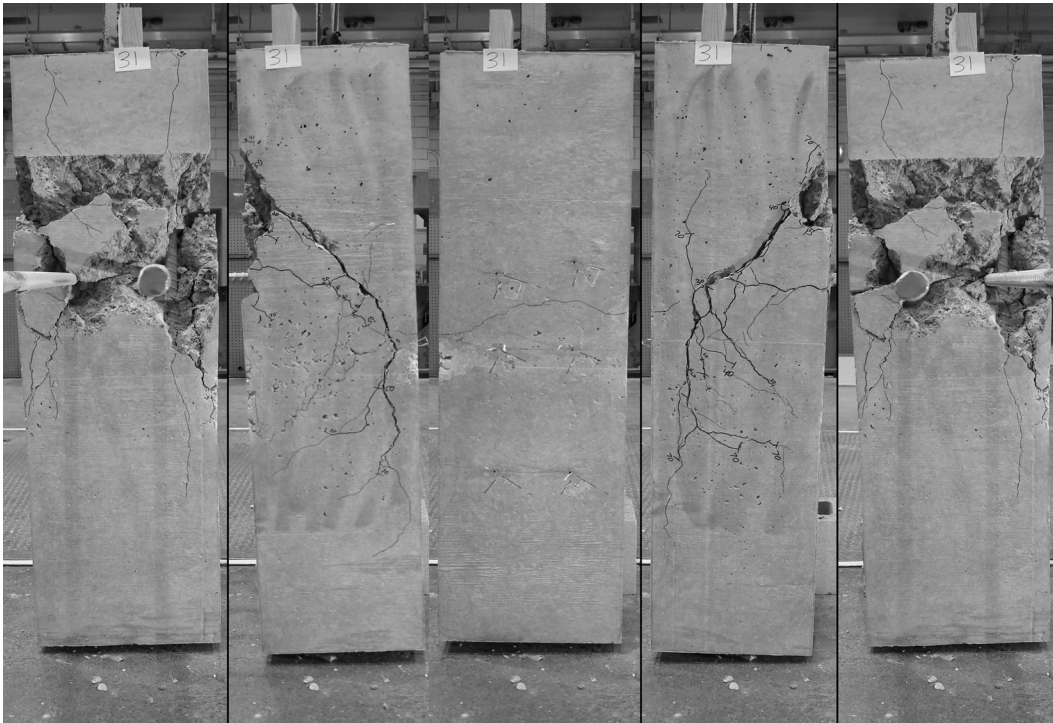


Figure D.30: Phase 3 specimen 31

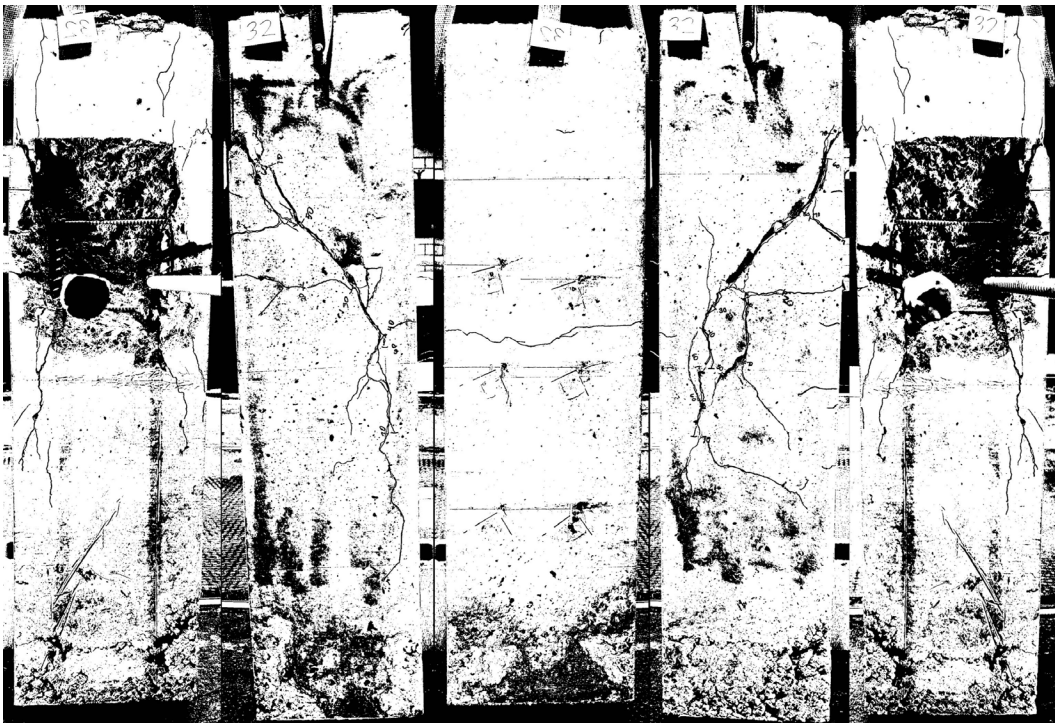
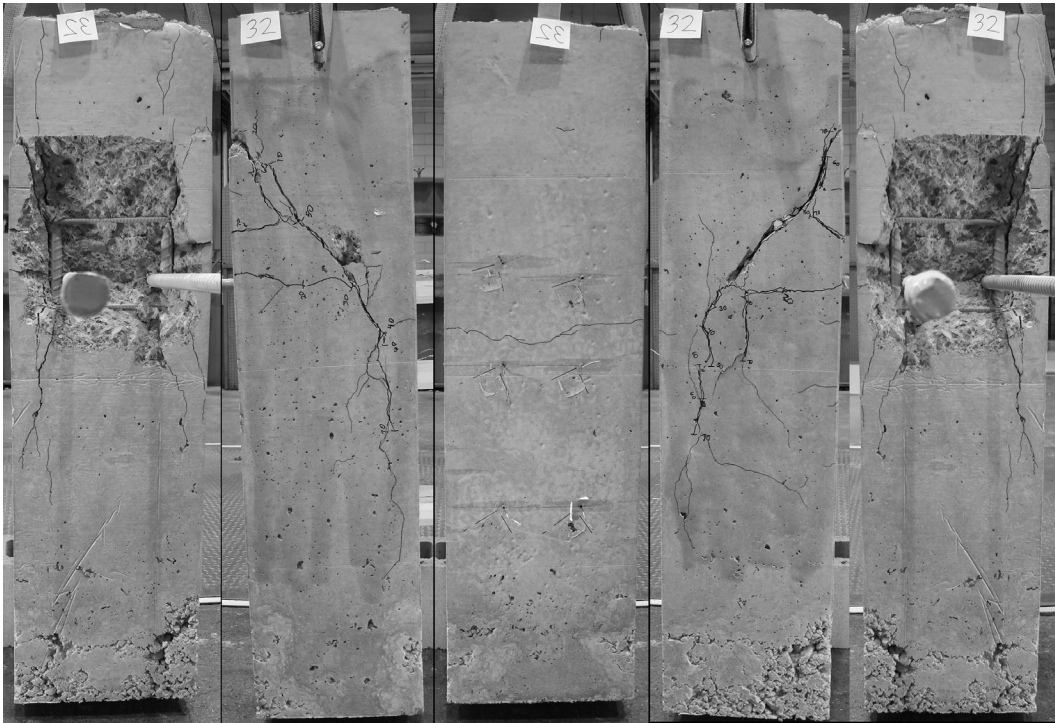


Figure D.31: Phase 3 specimen 32

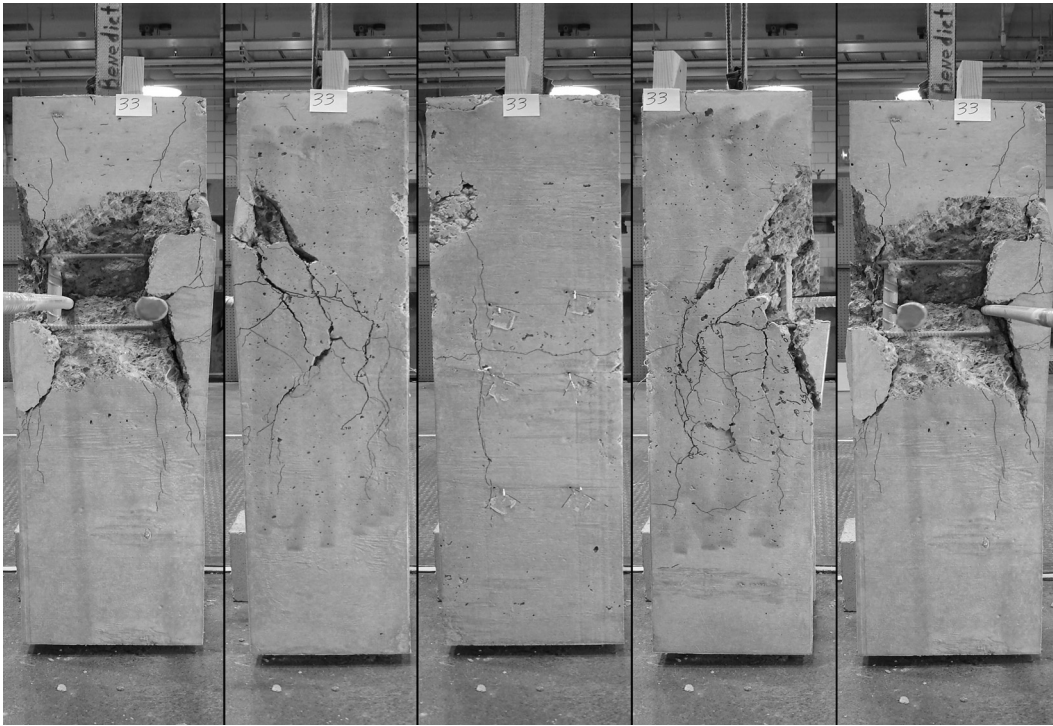


Figure D.32: Phase 3 specimen 33



Figure D.33: Phase 3 specimen 34

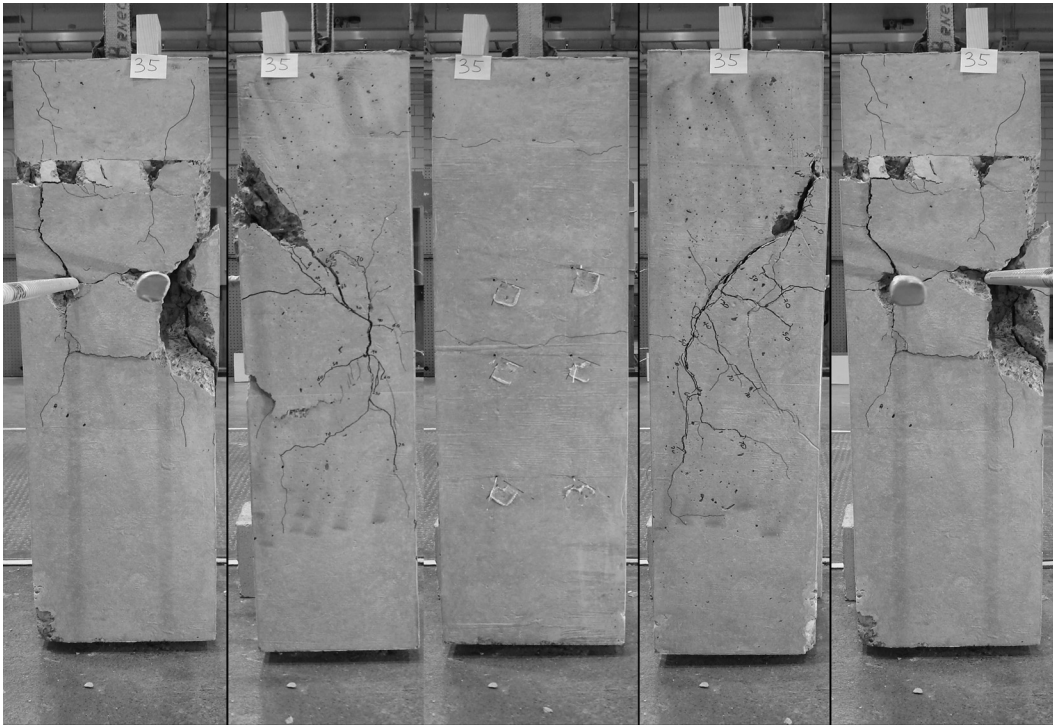


Figure D.34: Phase 3 specimen 35

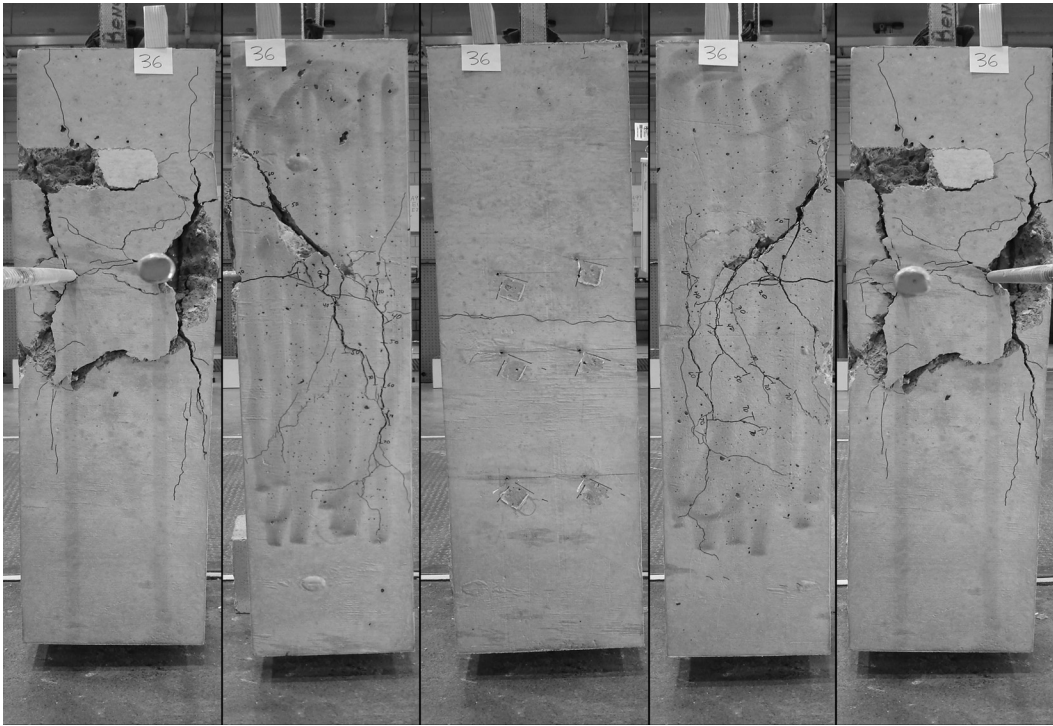


Figure D.35: Phase 3 specimen 36

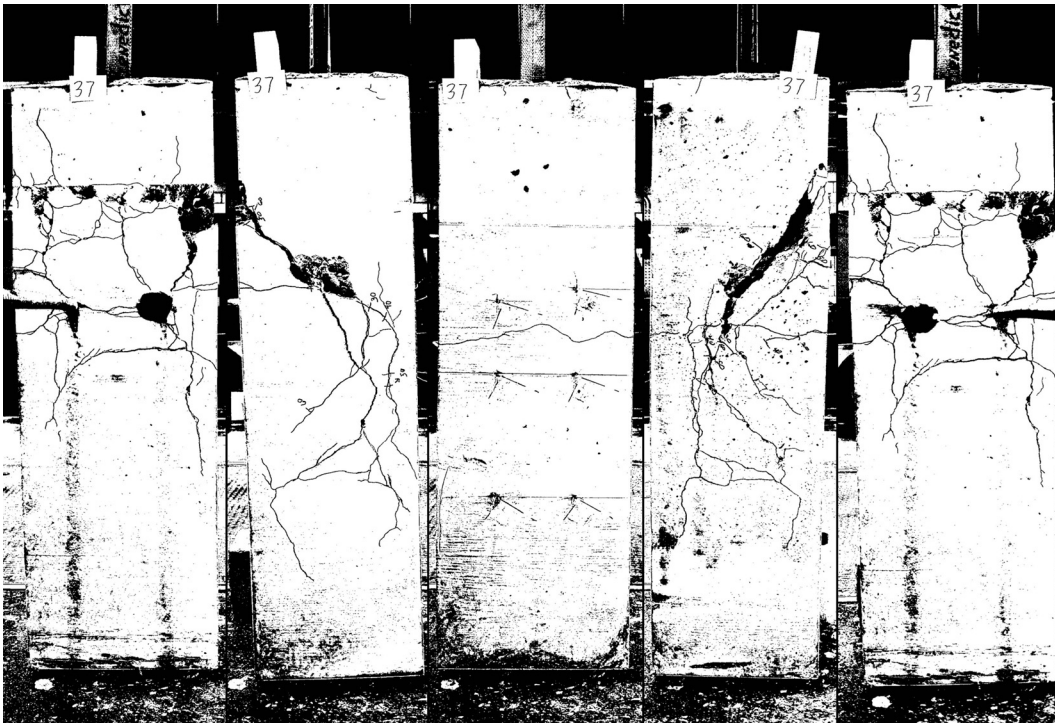
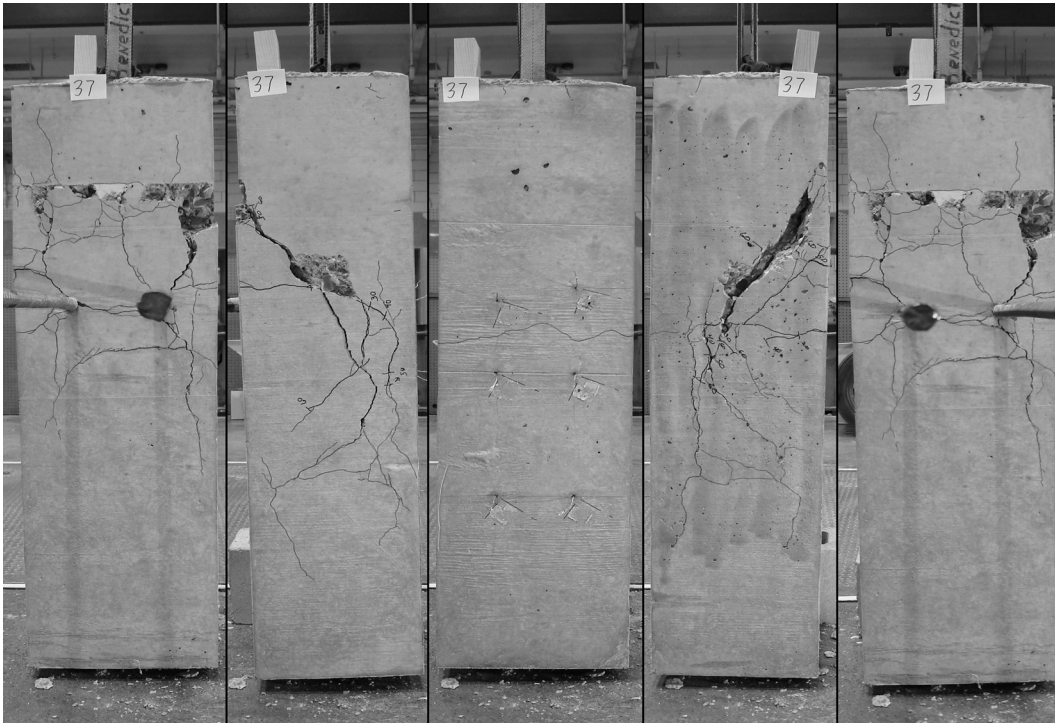


Figure D.36: Phase 3 specimen 37

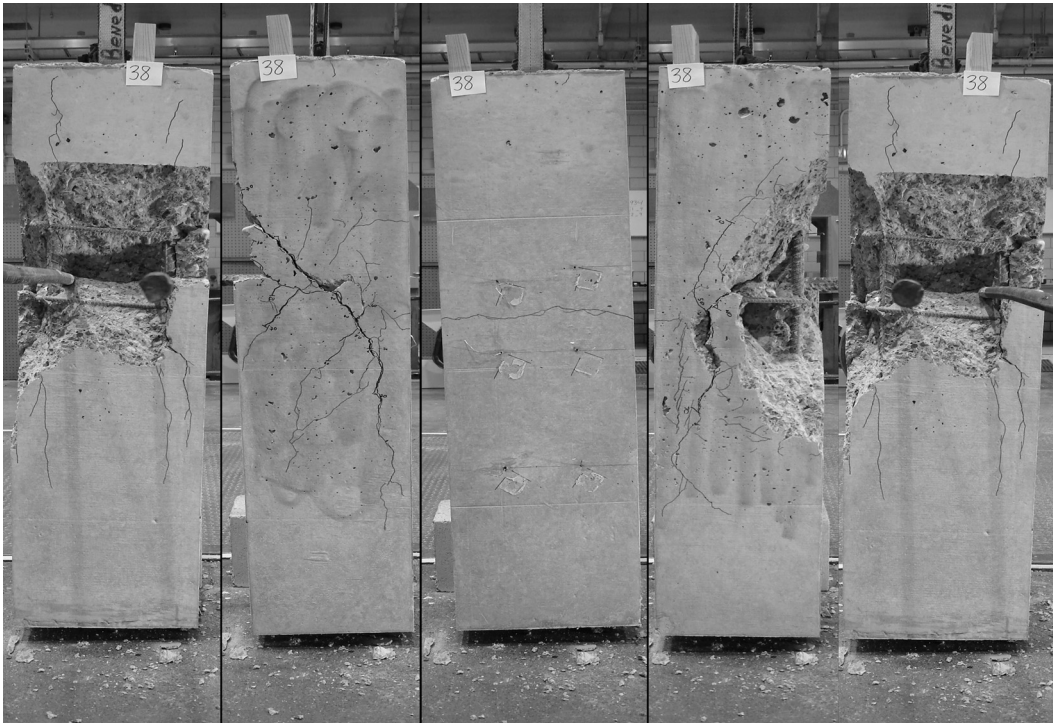


Figure D.37: Phase 3 specimen 38

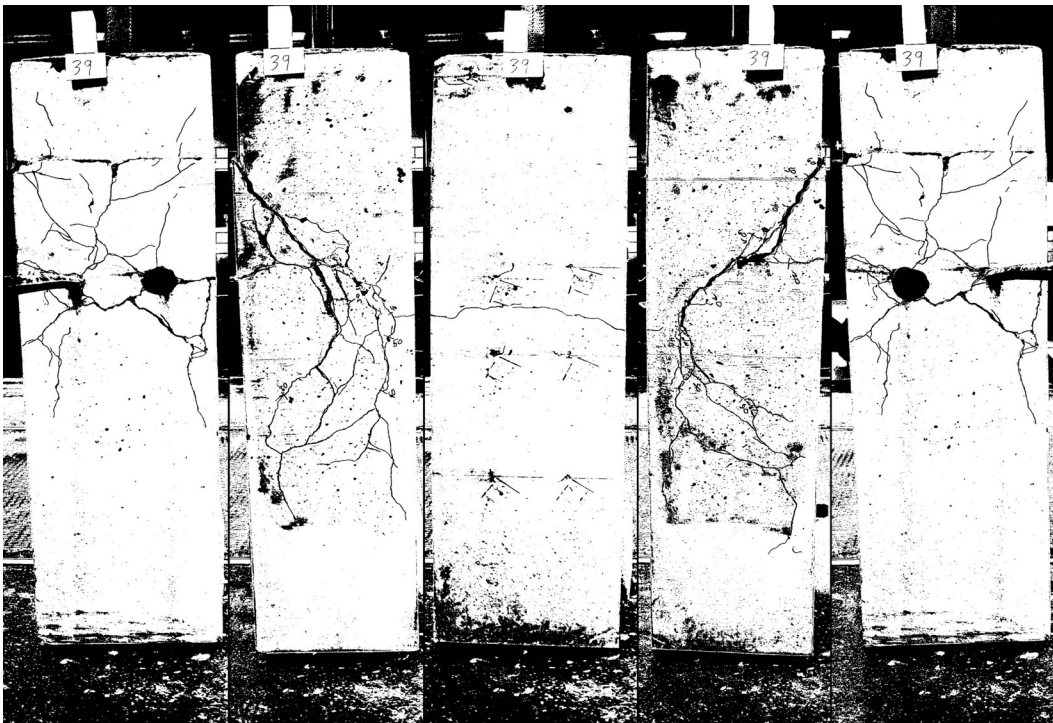


Figure D.38: Phase 3 specimen 39

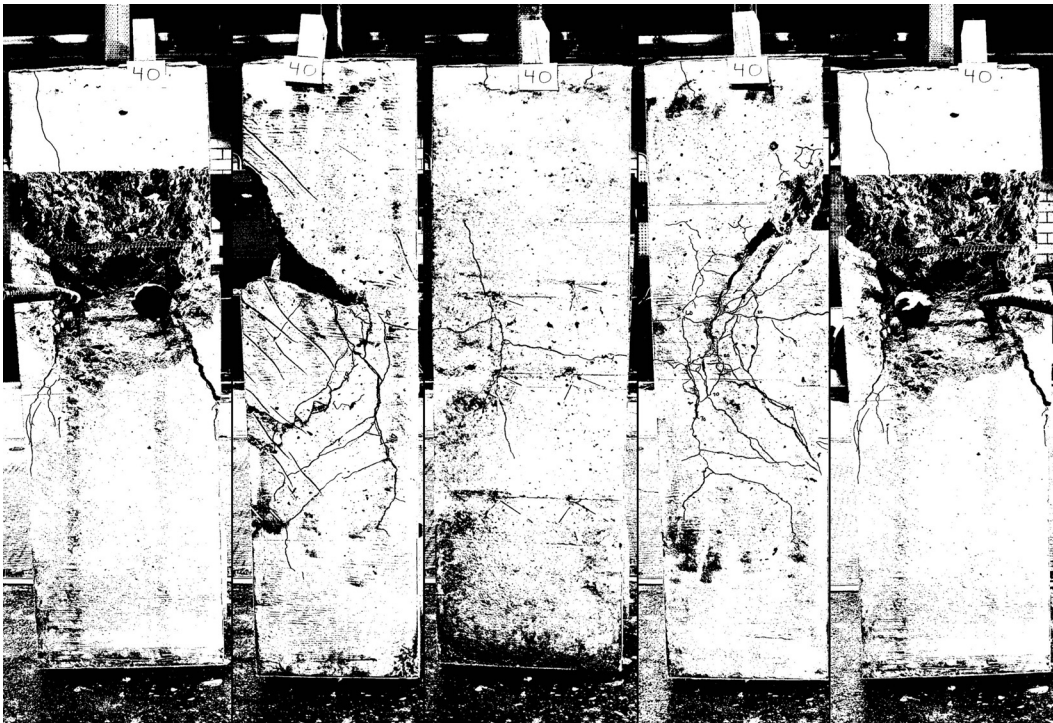
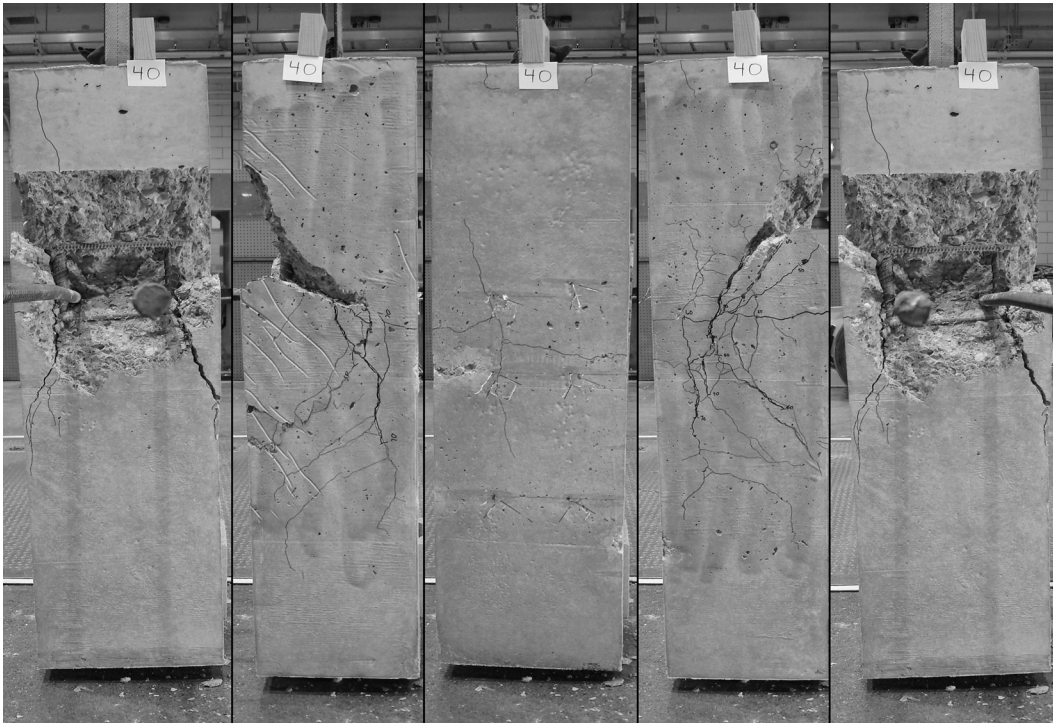


Figure D.39: Phase 3 specimen 40



Figure D.40: Phase 3 specimen 41

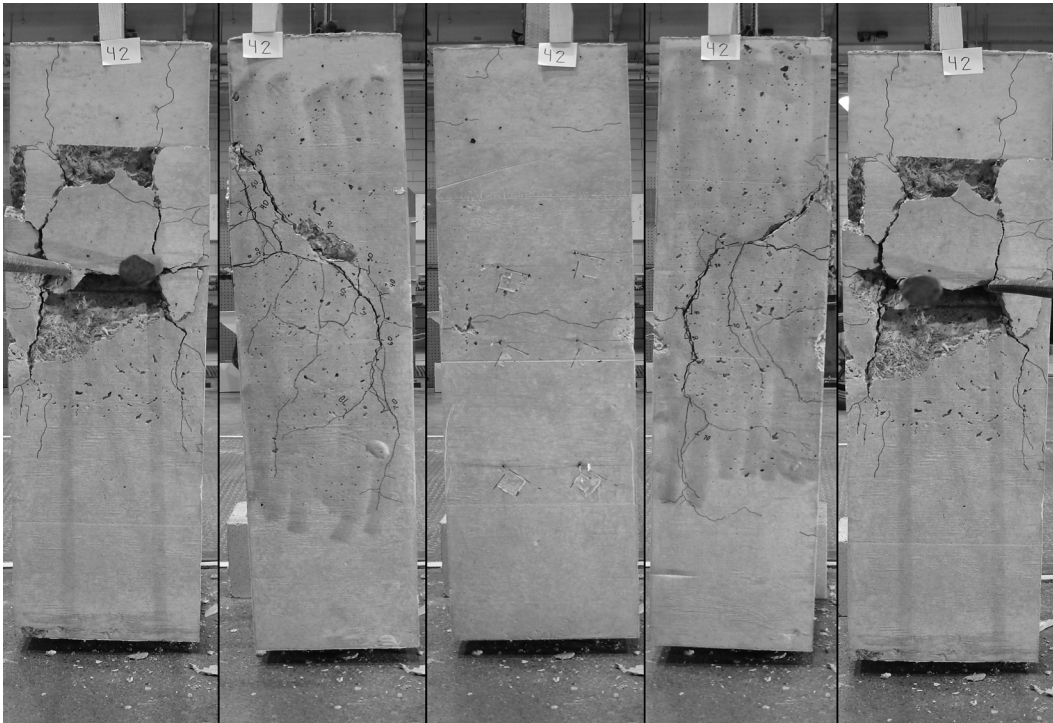


Figure D.41: Phase 3 specimen 42